A THEORETICAL INVESTIGATION OF DISLOCATION DISTRIBUTIONS IN TWO PHASE SYSTEMS

By

David M. Barnett

March, 1967

SU-DMS-Report No. 67-7

A THEORETICAL INVESTIGATION OF DISLOCATION DISTRIBUTIONS IN TWO-PHASE SYSTEMS

A DISSERTATION

SUBMITTED TO THE DEPARTMENT OF MATERIALS SCIENCE

AND THE COMMITTEE ON THE GRADUATE DIVISION

OF STANFORD UNIVERSITY

IN PARTIAL FULFILLMENT OF THE REQUIREMENTS

FOR THE DEGREE OF

DOCTOR OF PHILOSOPHY

NSG-622 29ACV

By

David Morton Barnett

9 March, 1967

ABSTRACT

The interactions between dispersed second phase particles or inclusions and slip dislocations exert a large influence upon the strength and ductility of crystalline solids. An important example of such interactions may be represented by a planar array of slip dislocations which has been blocked by, and thus has piled up against, the second phase. The present study is an examination of the effects of second phase size and rigidity upon the stresses associated with such blocked dislocation arrays.

Using the method of continuously distributed dislocations, exact analytical solutions are obtained for the stress fields associated with

(1) a screw dislocation pileup at a rigid circular inclusion

(2) a screw dislocation pileup at a semi-infinite second phase of finite rigidity

(3) a screw dislocation pileup at a circular inclusion of finite rigidity.

The local stresses near the pileup tip are shown to be of the form

$$\tau_{ij} \sim \tau \sqrt{\frac{L}{4R}} \left(\frac{4R}{\rho}\right)^{g}, \qquad \frac{L}{R} > 2$$

$$\tau_{ij} \sim \tau \left(\frac{2L}{\rho}\right)^{g}, \qquad \frac{L}{R} < 2$$

where L is the slip line length, R is the radius of the second phase, ρ is the radial distance from the pileup tip, and τ is the effective applied longitudinal shear stress. g, the strength of the pileup tip stress singularity, is a function of the elastic constants and is given by

$$0 < g = \frac{2}{\pi} \sin^{-1} \sqrt{\frac{G_1}{G_1 + G_2}} < 1 ,$$

where G_2 and G_1 are the second phase and matrix shear moduli, respectively. The physical significance of the above results is discussed in terms of image dislocation forces induced by the presence of a second phase ahead of a slip band.

An exact solution for the stresses generated by an infinite sequence of parallel screw dislocations piled up against an elastic half-plane of finite rigidity is also presented. The local stresses near the pileup tips are given by

$$\tau_{ij} \sim \tau\left(\frac{2h}{\pi\rho}\right)^g , \qquad \frac{h}{L} < 2$$

$$\tau_{ij} \sim \tau\left(\frac{2L}{\rho}\right)^g , \qquad \frac{h}{L} > 5$$

where h is the separation distance between the slip bands. In addition, the more difficult plane strain problem involving an edge dislocation pileup against an elastic half-plane is formulated, and a method for determining the pileup tip stress singularity is discussed.

The results obtained from the above calculations are used to discuss relaxation of the pileup stresses by fracture initiation in the second phase and by cross-slip of the leading array dislocations around the second phase. Fracture initiation in a second phase which is harder than the matrix $(G_2 > G_1)$ can only be predicted by an atomistic modification of the Griffith-Irwin-Stroh criterion used in single phase elasticity. It is shown that cross-slip should be the more favorable relaxation mode when $L/R > 2$, and that fracture initiation should be possible only when $L/R < 2$. In typical two-phase systems this analysis predicts that fracture initiation in the second phase should be possible only when the inclusion diameter is greater than about one micron.

ACKNOWLEDGMENTS

The author wishes to express his appreciation and gratitude to:

Dr. A. S. Tetelman, his thesis advisor, not only for his constant support and encouragement throughout the course of this research, but also for his efforts to introduce the author to new areas of scientific endeavor;

Professors W. A. Tiller and J. N. Goodier, his dissertation readers, for their interest and their efforts to stimulate critical thinking;

Dr. J. Dundurs of Northwestern University, for drawing the author's attention to the available solutions for single dislocations near elastic inclusions;

Dr. A. K. Head of the Tribophysics Division, CSIRO, Australia, for a stimulating discussion on current topics in dislocation theory and for suggesting that the author attempt the problem of a screw dislocation array at an elastic half-plane of finite rigidity;

Dr. Y. T. Chou of the E. C. Bain Laboratories, U. S. Steel Corporation, whose earlier work provided the stimulus for attacking inhomogeneous elasticity problems using the method of continuously distributed dislocations, and with whom the author was privileged to have several friendly, informative discussions.

Professors H. E. Levine, G. E. Latta, and M. M. Schiffer, whose courses in mathematics and mathematical physics proved to be invaluable during the course of this investigation;

Dr. K. P. Horn of the Aerospace Corporation and Mr. A. L. Robinson of the Stanford Materials Science Department, with whom the author enjoyed many relaxing evenings sampling fine cuisine and engaging the laws of probability;

Miss Rosemarie Stampfel, for typing this dissertation as well as three previous technical reports by the author;

The Ford Foundation, whose fellowship the author held during the first year of his graduate tenure at Stanford, and the National Aeronautics and Space Administration for supporting this investigation under contract NSG-622;

Miss Vaiva Pukite and Miss Diana Butler for their assistance in performing the necessary computations on the Burroughs B5500 computer at the Stanford Computation Center.

One special acknowledgment has been reserved for last, for no amount of words is sufficient to truly indicate the debt of gratitude the author owes his parents. Aside from the tremendous encouragement they always provided, they taught him that the only real failure was the failure to try.

TABLE OF CONTENTS

TABLE OF CONTENTS Cont.

TABLE OF CONTENTS Cont.

LIST OF ILLUSTRATIONS

LIST OF ILLUSTRATIONS CONT.

LIST OF ILLUSTRATIONS CONT.

LIST OF ILLUSTRATIONS CONT.

LIST OF ILLUSTRATIONS CONT.

CHAPTER I

INTRODUCTION

1. Purpose of the Investigation

Dispersed second phase particles and non-metallic inclusions exert a large influence upon the mechanical properties of materials. In addition to increasing the yield strength by raising the stress necessary to move dislocations through the matrix, the presence of dispersed phases and inclusions affects the fracture behavior of these materials by providing sites for void formation via particle or particle-interface cracking at the tip of a blocked slip band. Under applied stresses these voids grow and coalesce, causing fracture at large plastic strains.

Any detailed analysis of the mechanical properties of real materials must therefore include a study of the interactions between slip bands (and cracks) and hard particles, since these interactions play an important role in determining strength and ductility. To a first approximation the slip band--particle interaction may be represented by a planar array of dislocations which has been blocked by, and thus piled up against, the barrier.

Before one can investigate the interesting problems of particle fracture, particle interface fracture, or cross slip of the piled up dislocations over the barrier, one must first determine the stress

distribution associated with such blocked arrays of dislocations as a function of particle shape, size, and rigidity. An analytical treatment of this problem requires, in turn, the selection of an inhomogeneity shape which allows a mathematical solution to be obtained and is at the same time a reasonable physical choice. Having chosen the shape, the effect of the remaining variables, size and rigidity (elastic constants), can then be examined. This examination is the subject of the present investigation.

The technique which shall be used to examine the stress fields associated with distributions of dislocations in two phase materials is the method of continuously distributed dislocations. As a means of introduction to this technique, the following two sections will present certain features of the theory of isolated elastic dislocations in single and two phase media; the continuous distribution technique is then reviewed in the latter sections of this chapter. Specific problems involving arrays of screw and edge dislocations in heterogeneous materials are presented in Chapters II through VI.

2. The Dislocation as the Green's Function for Internal Stress

The concept of a dislocation, as presented in elementary texts on elasticity and plasticity of solids, is one of a solid body which has been cut along some interior surface Σ ; the two new surfaces formed by the cutting process are then displaced relative to one another by a rigid body motion[1] (if we wish to speak of crystal dislocations) and

then welded together, leaving the body in a state of residual or internal stress in the absence of applied external tractions and body forces. One may, however, give an alternate, more compact definition of a dislocation. Such a definition proves to be quite advantageous, since it allows us to easily see the one-to-one correspondence between an electrostatic line charge in a dielectric medium and a stationary screw dislocation in an elastic medium.[2] Therefore, let us define a dislocation in the following manner:

"A dislocation is the Green's function for internal stress."

In order to show that the above statement constitutes an adequate definition of a dislocation, consider an infinitely long, straight, non-radiating line of charge $-q$ per unit length in free space. Orient a right-hand x-y-z Cartesian frame in this space so that the z-axis coincides with the line charge. Translational invariance in the z-direction dictates that the electrostatic potential ϕ be a function only of x and y. Thus, ϕ satisfies

$$\nabla^2\phi = \frac{\partial^2\phi}{\partial x^2} + \frac{\partial^2\phi}{\partial y^2} = q\delta(\vec{r}) \ , \qquad \text{(I.2-1)}$$

where $\vec{r}$ is the polar radius vector from the line source to any field point, and $\delta(\vec{r})$ is the Dirac delta function. If we stipulate that the applied electric field is zero, then the solution ϕ is the familiar logarithmic potential or Green's function for the two dimensional Laplace equation:

$$\phi = \frac{q}{2\pi} \ln|\vec{r}| \ . \qquad \text{(I.2-2)}$$

The associated internal electric field, $\vec{E}$, is radial and evidences radial symmetry about the line source, i.e.,

$$\vec{E} = - \frac{q}{2\pi} \frac{\vec{r}}{|\vec{r}|^2} \quad . \tag{I.2-3}$$

Thus, even in the absence of an applied electric field, an internal field exists due to the presence of the singular line source.

That a dislocation displays the character of a Green's function for internal stress is now obvious. A solid containing a dislocation possesses an associated internal stress field even though external surface tractions and gravity forces are absent. The electrostatic line charge-elastostatic screw dislocation analogy is most easily seen by considering the complex Green's function, $G^*(\zeta)$, for the two dimensional Laplace equation:

$$G^*(\zeta) = \frac{q}{2\pi} \ln \zeta \ , \tag{I.2-4}$$

where ζ denotes a field point in complex notation, i.e.,

$$\left.\begin{aligned} \zeta &= x + iy = re^{i\theta} \\ |\vec{r}| &= \sqrt{x^2 + y^2} \\ 0 \leq \theta &= \arg(\zeta) \leq 2\pi. \end{aligned}\right\} \tag{I.2-5}$$

Separating $G^*(\zeta)$ into its real and imaginary parts,

$$G^*(\zeta) = \phi(x,y) + iw(x,y) = \frac{q}{2\pi} \{\ln|\vec{r}| + i\theta\} \ . \tag{I.2-6}$$

Hence, the real part of $G^*(\zeta)$ corresponds to the electrostatic potential of a singular line source in free space, and the imaginary part of $G^*(\zeta)$ represents the elastostatic displacement field of a screw dislocation of strength q at the origin in an infinite isotropic medium;[1] these two fields are thus conjugate harmonic functions. One will note that the branch of the logarithmic function given in Eq. (I.2-5) is an arbitrary choice. Any branch

$$\theta_0 \leq \theta = \arg(\zeta) \leq \theta_0 + 2\pi \qquad \text{(I.2-7)}$$

could have been taken to make the logarithm a single-valued function. This freedom in the choice of branch cut is the mathematical equivalent of the physical statement that the screw dislocation may be defined independent of the cutting surface Σ.

The two dimensional form of Gauss' Law of electrostatics is implicit in Eq. (I.2-1). Integrating both sides of (I.2-1) over a two-dimensional domain pierced by the line singularity and applying Green's Theorem, one finds that

$$\oint_C \frac{\partial \phi}{\partial n} \, ds = q \, . \qquad \text{(I.2-8)}$$

$\partial/\partial n$ denotes differentiation with respect to the outward normal to a closed curve C encircling the line source, and ds is an elemental arc of C. Considering $G^*(\zeta)$, one notes that

$$\oint_C \frac{\partial w}{\partial s} \, ds = q \, ; \qquad \text{(I.2-9)}$$

$\partial/\partial s$ denotes the tangential derivative along a closed curve C encircling the line singularity. Equation (I.2-9) is the familiar law of the Burgers' circuit in dislocation theory.

One could equally well have chosen to identify the screw dislocation as the elastostatic analog of a vortex line in fluid flow, in which case ϕ and w, the real and imaginary parts of the Green's function $G^*(\zeta)$, would be identified as the potential and stream functions, respectively, for the vortex.[3] The Burgers' circuit law then becomes the analog of the circulation integral taken around the vortex.

The edge dislocation is likewise a Green's function for internal stress. However, the stress field associated with a straight edge dislocation is derived from an Airy stress function satisfying a bipotential, not a potential, equation. The bipotential Green's function is interpreted physically as a concentrated force. Consequently, edge dislocation monopoles, dipoles, quadrupoles, and higher order multipoles are equivalent to concentrated forces, couples, double couples, etc. in the interior of an elastic solid.

The electrostatic analogy is useful when discussing screw dislocations in inhomogeneous elastic media. If one can find a solution or method of solution in the literature for an electrostatic line charge (or point charge in two dimensions) in an inhomogeneous dielectric medium (and many such solutions are available), the corresponding boundary value problem involving a screw dislocation in an inhomogeneous elastic medium may be solved in a straightforward manner, since the displacement field of the screw is merely the conjugate harmonic function corresponding to the appropriate electrostatic potential. Often the conjugate harmonic function is easily constructed by the method of images, provided the boundaries involved in the problem are simple geometric shapes (circular arcs and/or straight lines).

3. Previous Treatments of Single Dislocations in Elastic Media

a. Screw Dislocations

Consider a bimetallic medium (Figure I-1) composed of two elastic half-planes welded together at $x = 0$. The shear modulus is G_1 if $x > 0$ and is G_2 if $x < 0$. Let a single right-hand screw dislocation of Burgers' vector b (parallel to the z-direction) be situated in $x > 0$ at $(t,0)$. Assuming perfect bonding at the weld, so that τ_{xz} and the z-component of the displacement field are continuous at $x = 0$, A. K. Head[4] in 1953 found the stress field of the screw to be given by:

$$\left.\begin{aligned}
\tau_{xz} &= -\frac{G_1 b}{2\pi}\frac{y}{(x-t)^2+y^2} - \frac{G_1 b}{2\pi}\kappa\frac{y}{(x+t)^2+y^2} \quad ; && x > 0 \\
&= -\frac{G_1 b}{2\pi}(1+\kappa)\frac{y}{(x-t)^2+y^2} \quad ; && x < 0 \\
\tau_{yz} &= \frac{G_1 b}{2\pi}\frac{x-t}{(x-t)^2+y^2} + \frac{G_1 b}{2\pi}\kappa\frac{x+t}{(x+t)^2+y^2} \quad ; && x > 0 \\
&= \frac{G_1 b}{2\pi}(1+\kappa)\frac{x-t}{(x-t)^2+y^2} \quad ; && x < 0
\end{aligned}\right\} \quad (I.3\text{-}1)$$

where

$$\kappa = \frac{G_2 - G_1}{G_2 + G_1} \, . \qquad (I.3\text{-}2)$$

The solution may be constructed by referring to the analogous electostatic problem.[5] In the region $x > 0$ the stress field is the same as that in an infinite medium of shear modulus G_1 containing

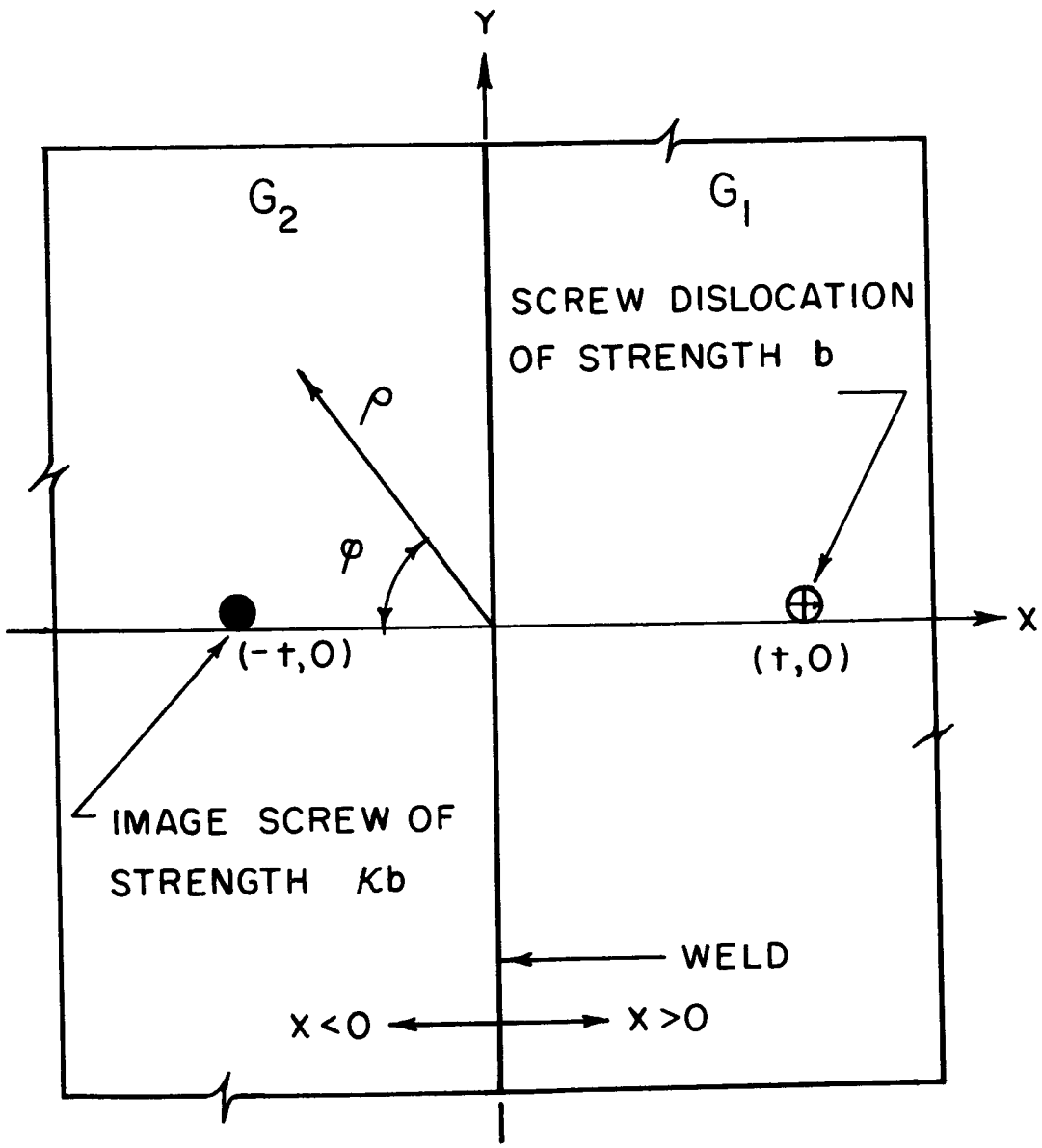

Figure I-1: Schematic illustration of a screw dislocation in a bimetallic elastic medium and its induced image.

the real screw dislocation at $(t,0)$ and a virtual or image screw dislocation of Burgers' vector κb located at $(-t,0)$. When $\kappa > 0$ $(G_2 > G_1)$, the screw dislocation is repulsed from the boundary $x = 0$ by this "image force". If $\kappa < 0$ $(G_2 < G_1)$, the image force attracts the dislocation toward the weld. Head presented the above solution as a model for the interaction of a grain boundary with a dislocation; two adjacent grains in a polycrystalline sample may appear to have different shear moduli because of crystallographic orientation differences with respect to the direction of imposed deformation (in a tensile test, the specimen tensile axis).

The more general case of a screw dislocation exterior to a circular cylindrical inclusion has been treated by Dundurs.[6] Consider the infinite two-phase elastic medium depicted in Figure I-2. Region 2 is a circular cylindrical inclusion of radius R and shear modulus G_2 which is imbedded in a matrix of shear modulus G_1. The cylinder is infinitely long in the z-direction with the z-axis coinciding with the cylinder axis. Since the problem to be formulated will be independent of z, only the x-y plane section in Figure I-2 need be considered. The elastic displacement field $w(x,y)$ of a straight screw dislocation of Burgers' vector b (parallel to the z-axis) located at $(t,0)$ in the matrix is:

$$\left.\begin{aligned} w &= \frac{b}{2\pi}\{\theta_1 + \kappa(\theta_2 - \theta)\} \quad ; \quad x^2 + y^2 \geq R^2 \\ &= \frac{b}{2\pi}\{(1-\kappa)\theta_1 + \pi\kappa\} \quad ; \quad x^2 + y^2 \leq R^2 \end{aligned}\right\} \qquad (I.3\text{-}3)$$

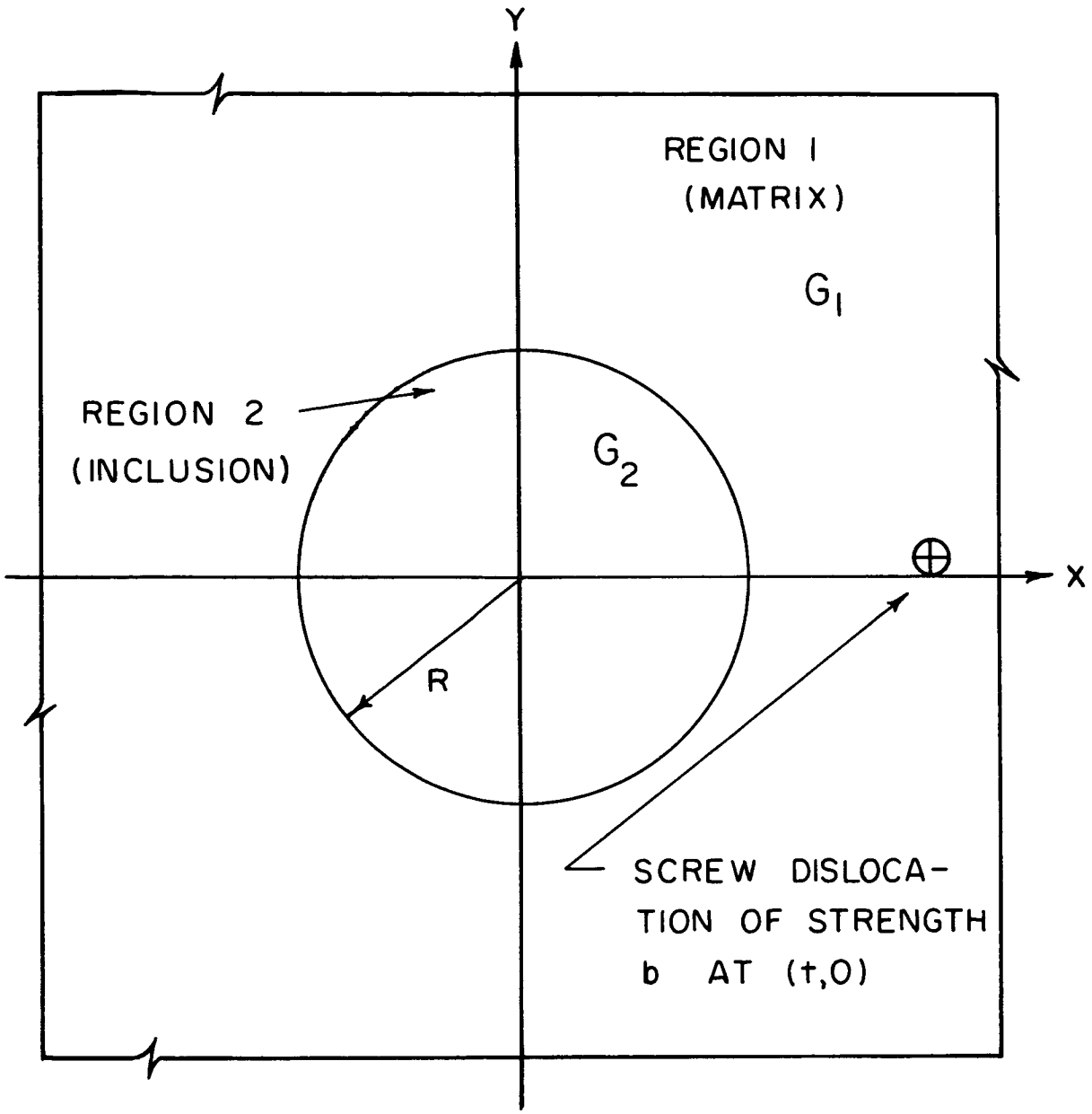

Figure I-2: Schematic illustration of a screw dislocation exterior to a circular inclusion of shear modulus G_2 imbedded in a matrix of shear modulus G_1.

where

$$\left.\begin{aligned} \kappa &= \frac{G_2 - G_1}{G_2 + G_1} \\ \theta &= \tan^{-1}\frac{y}{x} \\ \theta_1 &= \tan^{-1}\frac{y}{x-t} \\ \theta_2 &= \tan^{-1}\frac{y}{x - (R^2/t)} \end{aligned}\right\} \quad (I.3\text{-}4)$$

The associated stress field of the dislocation is then:

$$\left.\begin{aligned} \tau_{xz} &= -\frac{G_1 b}{2\pi}\left\{\frac{y}{(x-t)^2 + y^2} + \kappa\left[\frac{y}{(x-R^2/t)^2 + y^2} - \frac{y}{x^2 + y^2}\right]\right\}, \\ &\qquad\qquad (x^2 + y^2 > R^2) ; \\ &= -\frac{G_1 b}{2\pi}(1+\kappa)\frac{y}{(x-t)^2 + y^2}, \qquad (x^2 + y^2 < R^2) ; \\ \tau_{yz} &= \frac{G_1 b}{2\pi}\left\{\frac{x-t}{(x-t)^2 + y^2} + \kappa\left[\frac{x - R^2/t}{(x-R^2/t)^2 + y^2} - \frac{x}{x^2 + y^2}\right]\right\}, \\ &\qquad\qquad (x^2 + y^2 > R^2) ; \\ &= \frac{G_1 b}{2\pi}(1+\kappa)\frac{x-t}{(x-t)^2 + y^2}, \qquad (x^2 + y^2 < R^2) . \end{aligned}\right\} \quad (I.3\text{-}5)$$

Perfect interface bonding has been assumed so that τ_{rz} and w are continuous across the interface $x^2 + y^2 = R^2$. With these boundary conditions the stress field in the matrix is equivalent to the stress

field in an infinite homogeneous medium of shear modulus G_1 containing the real dislocation at $(t,0)$ and two image dislocations at $(R^2/t,0)$ and the origin whose Burgers' vectors are κb and $-\kappa b$, respectively (Figure I-3). The dislocation is attracted to the inclusion by the image forces when $\kappa < 0$ and repelled when $\kappa > 0$. As $R \to \infty$, the second phase becomes a half-plane, and the distance between the image dislocation at the origin and the interface becomes infinite. Thus, the dislocated half-plane problem is characterized by only a single image dislocation (Eq. I.3-1).

The need for a pair of image dislocations of opposite strength is most easily seen by considering the Burgers' circuits depicted in Figure I-4. The Burgers' circuit C_1 yields a closure failure b as required, since C_1 encircles only the real dislocation; the circuit C_2 yields zero closure failure since the closure failures of the two image dislocations cancel one another. Similar reasoning shows that the circuit C_3 yields closure failure b as required. When formulating more general problems involving a dislocated elastic matrix containing inclusions of finite size, one can expect that the image dislocation systems will involve pairs of opposite strength monopoles and even order multipoles, since these types of image systems automatically insure that Burgers' circuits taken in the multiply-connected matrix will yield the correct closure failures.

Knowing the solution for the screw dislocation exterior to the circular inclusion, the solution for the dislocation inside the inclusion may be obtained by conformal mapping. The inversion mapping

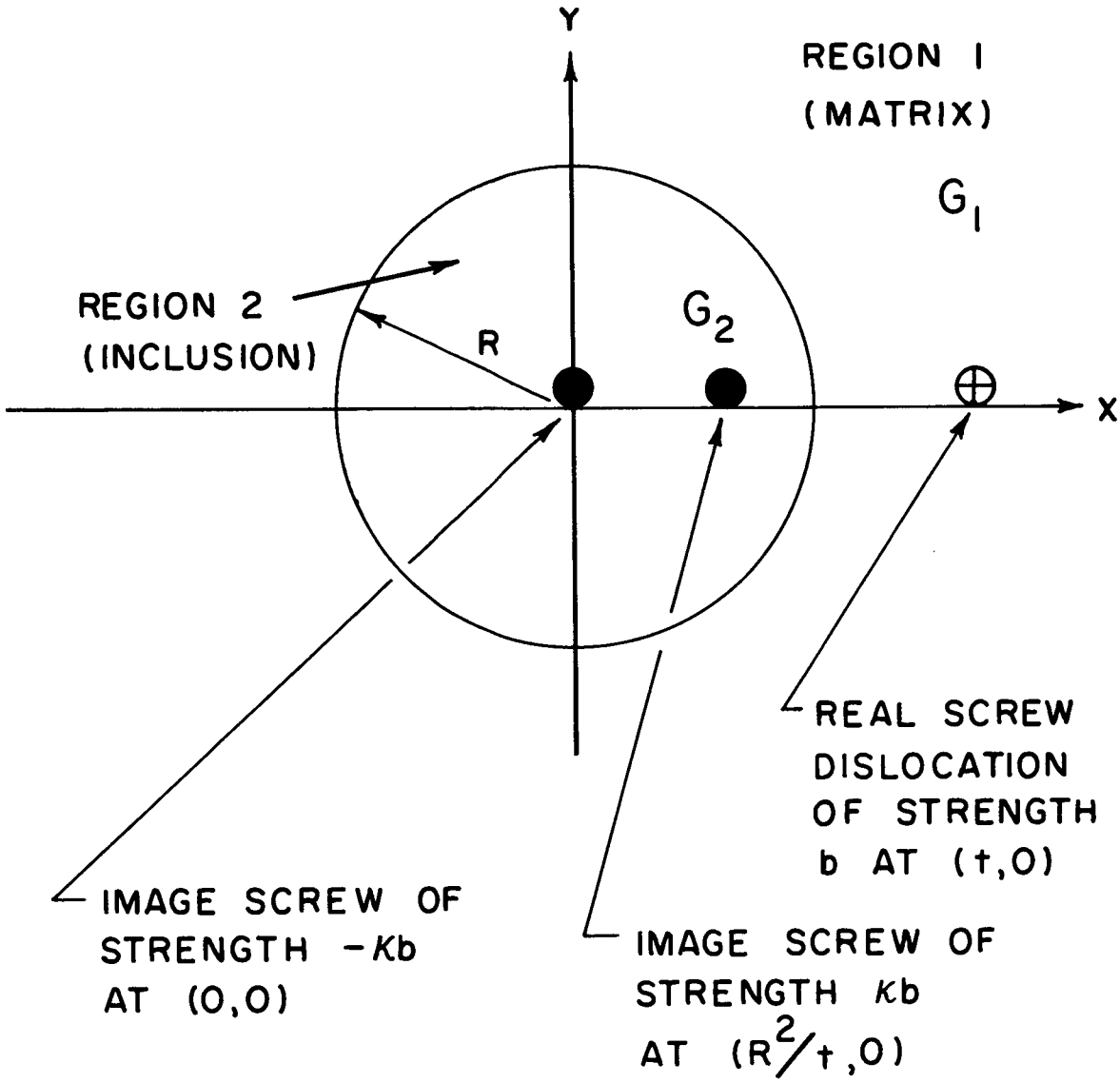

Figure I-3: The equivalent image system representing the stress field in a dislocated matrix containing a circular inclusion.

$\zeta = R^2/\alpha$, where $\alpha = x + iy$, maps the inclusion into the matrix and vice-versa. The necessary calculations are summarized in Appendix A. For the screw dislocation located at $(t,0)$ inside a circular inclusion of shear modulus G_1 imbedded in a matrix of shear modulus G_2 the displacement field is

$$\begin{aligned} w &= \frac{b}{2\pi}\{\theta_1 + \kappa\theta_2\} \quad , && x^2 + y^2 \le R^2 \ ; \\ &= \frac{b}{2\pi}\{(1-\kappa)\theta_1 + \kappa\theta + \kappa\pi\} && x^2 + y^2 \ge R^2 \ , \end{aligned} \tag{I.3-6}$$

and the corresponding stresses are

$$\left.\begin{aligned} \tau_{xz} &= -\frac{G_1 b}{2\pi}\left\{\frac{y}{(x-t)^2 + y^2} + \frac{\kappa y}{(x-R^2/t)^2 + y^2}\right\}, \quad x^2 + y^2 \le R^2 \ ; \\ &= -\frac{G_2 b}{2\pi}\left\{(1-\kappa)\frac{y}{(x-t)^2 + y^2} + \frac{\kappa y}{x^2 + y^2}\right\} \quad , \quad x^2 + y^2 \ge R^2 \ ; \\ \tau_{yz} &= \frac{G_1 b}{2\pi}\left\{\frac{x-t}{(x-t)^2 + y^2} + \kappa\frac{x - R^2/t}{(x-R^2/t)^2 + y^2}\right\} \quad , \quad x^2 + y^2 \le R^2 \ ; \\ &= \frac{G_2 b}{2\pi}\left\{(1-\kappa)\frac{x-t}{(x-t)^2 + y^2} + \kappa\frac{x}{x^2 + y^2}\right\} \quad , \quad x^2 + y^2 \ge R^2 \ , \end{aligned}\right\} \tag{I.3-7}$$

where

$$\left.\begin{aligned} \theta_1 &= \tan^{-1}\frac{y}{x-t} \\ \theta_2 &= \tan^{-1}\frac{y}{x - R^2/t} \\ \theta &= \tan^{-1}\frac{y}{x} \ . \end{aligned}\right\} \tag{I.3-8}$$

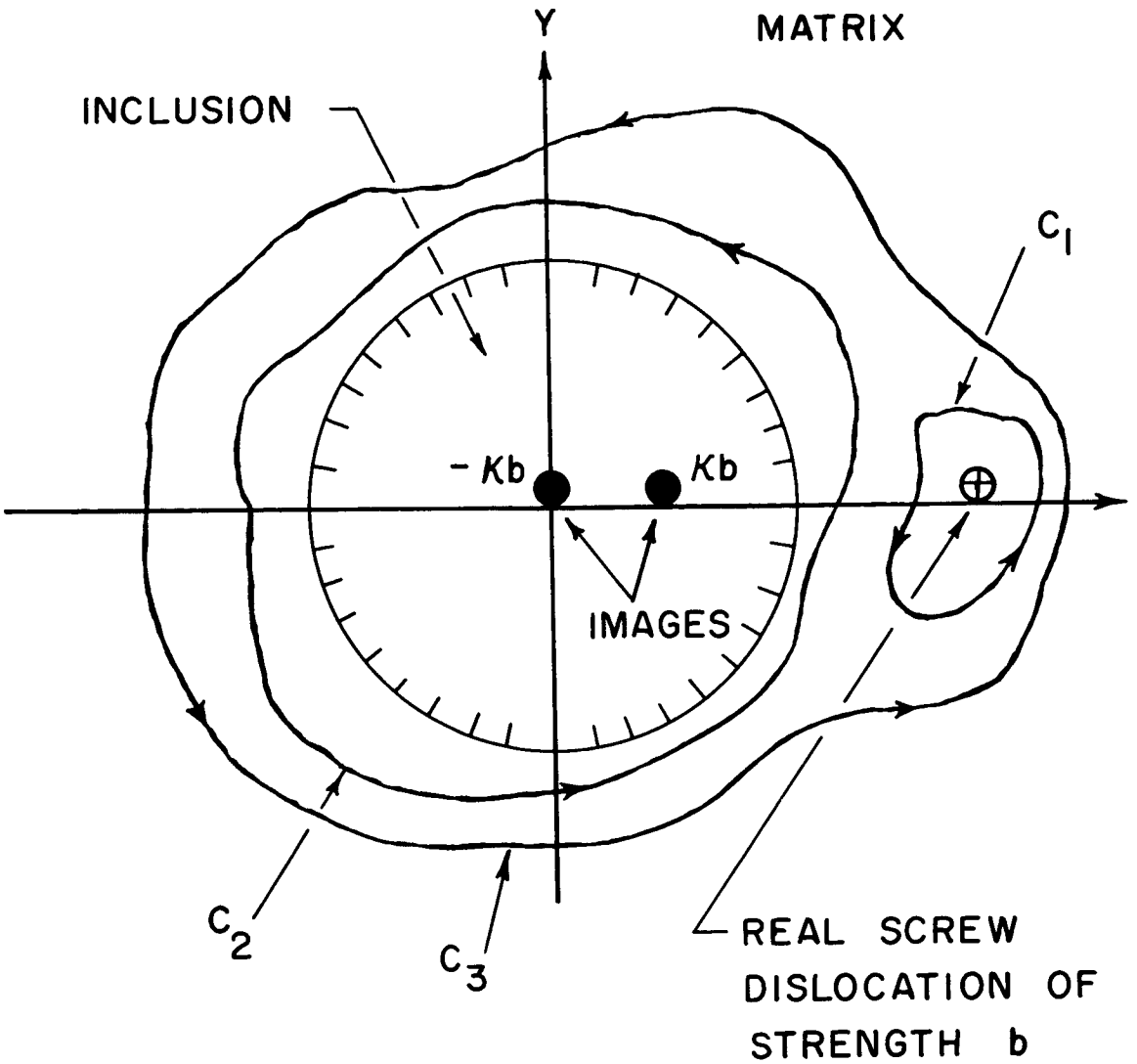

Figure I-4: Burgers' circuits in a multiply-connected dislocated matrix containing a circular inclusion.

Hence, the stress field in the dislocated inclusion is equivalent to the stress field in an infinite medium of shear modulus G_1 containing the real dislocation at $(t,0)$ and an image dislocation of strength Kb at the inverse point $(R^2/t,0)$ (Figure I-5).

The problem of a tri-metal (Figure I-6) containing a screw dislocation has been treated by Head,[4] Chou,[7] and the author.[8] The results are quite lengthy and shall not be reproduced here. It is worth noting that the tri-metallic problem (of which a surface oxide layer on a metal[4] is a special case) differs from the previously discussed solutions in that infinite sets of image dislocations are required to describe the internal stress state. Chou[9] has also treated the case of a screw dislocation in a wedge-shape medium (Figure I-7) by a conformal mapping technique. When the wedge angle is equal to $2\pi/k$, where k is integral, $k-1$ image dislocations are sufficient to describe the stress state. When k is non-integral, it is probable that the stress state can be described either by a contour integral or by a technique attributed to Sommerfeld[10] (an infinite set of images situated on Riemann surfaces above and below the plane of physical interest).

b. Edge Dislocations

The problems involving edge dislocations in two phase media are more complicated than their screw counterparts for two reasons:

(1) The screw dislocation represents a state of anti-plane strain so that the only one displacement and two shear stresses, τ_{xz} and

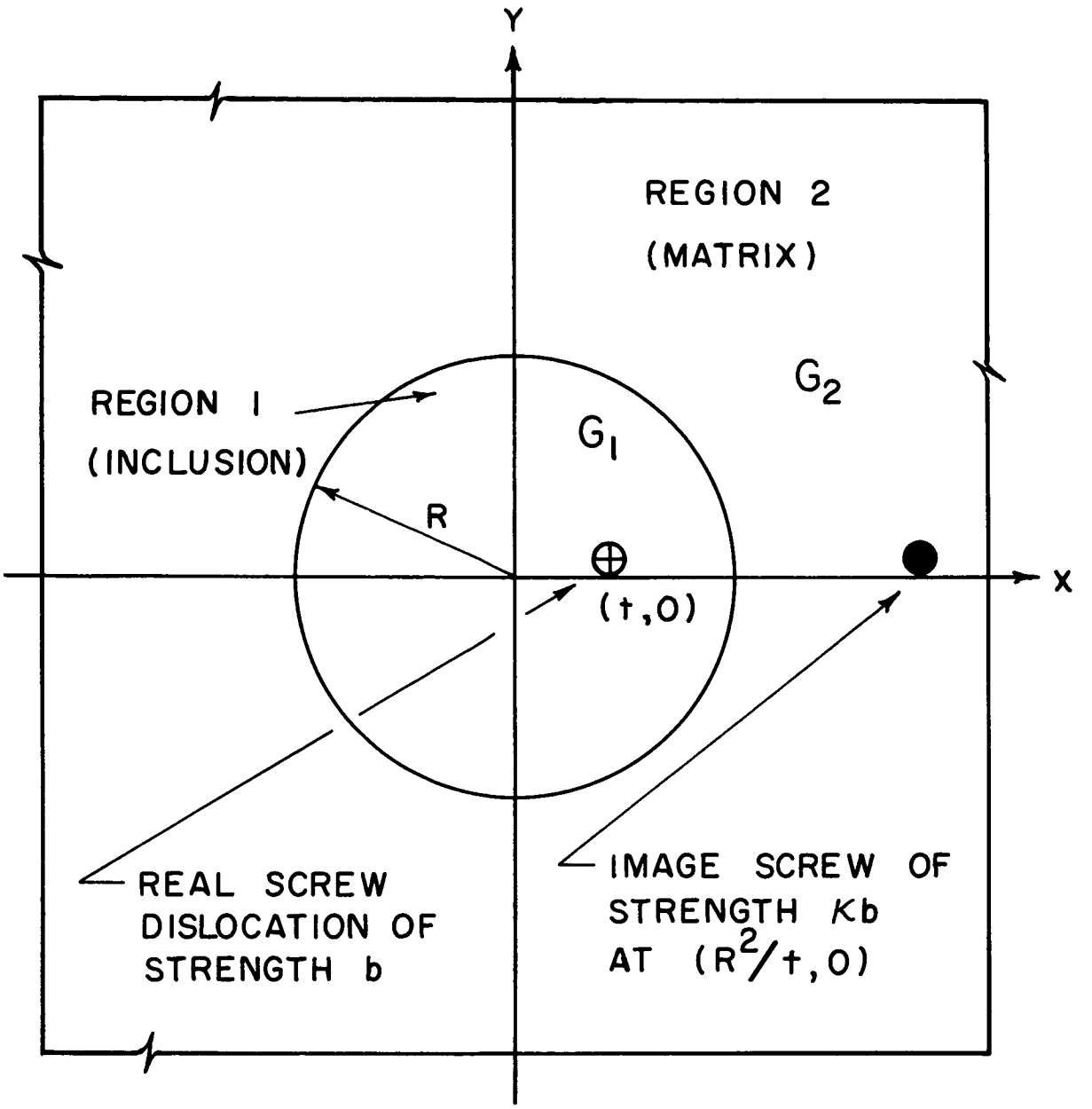

Figure I-5: The equivalent image system representing the stress field inside a dislocated circular inclusion of shear modulus G_1 imbedded in a matrix of shear modulus G_2.

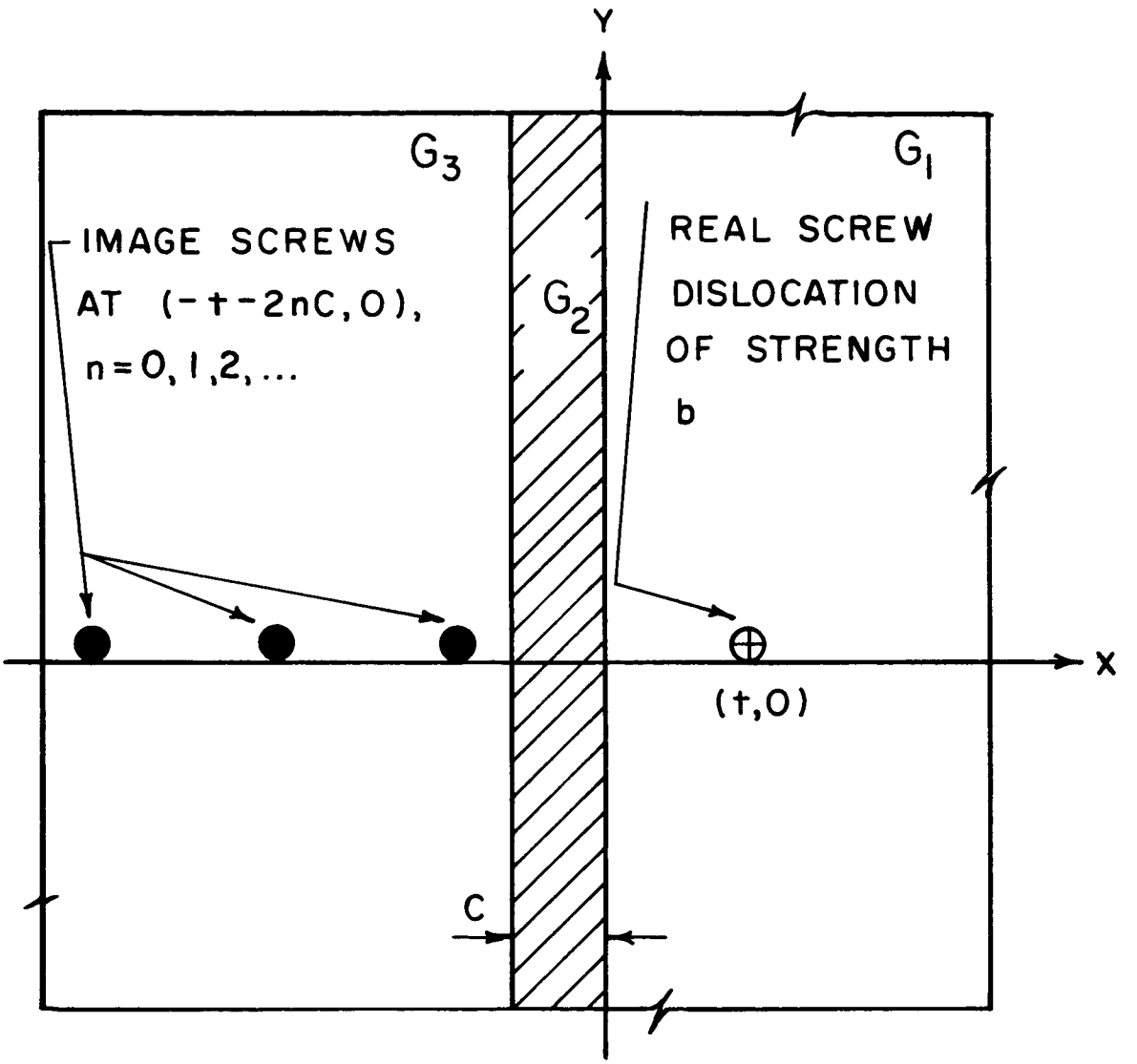

Figure I-6: The equivalent image system representing the stress field in the dislocated region ($x > 0$) of a tri-metallic elastic medium.

τ_{yz}, are non-vanishing. Plane strain edge dislocation problems normally involve two displacements and four stresses, σ_{xx}, σ_{yy}, σ_{zz} and τ_{xy}.

(2) The screw dislocation has no associated dilatation, so that Poisson's ratio effects are of no importance; this is not the case when edge dislocation solutions are sought. The strengths of the various image dislocations used to describe the edge solutions depend upon complex combinations of the respective shear moduli and Poisson's ratios of the two phases.[11,12]

Head[11] first treated the single edge dislocation in a bimetallic elastic medium by reducing the original bipotential problem to a pair of potential problems. His solutions include cases in which the junction $x = 0$ (Figure I-1) is a free surface, a perfect weld, and a slipping boundary. In general the image dislocation system needed to describe the stress state in the dislocated half of the bimetal consists of an image edge monopole, an image edge dipole, and an image edge quadrupole, all located at the reflected point $(-t,0)$. The image strengths are complex functions of the bimetallic elastic constants, so that numerical calculations are required to determine the attractive or repulsive nature of the net image force on the real dislocation. Dundurs and Sendeckyj[12] also solved the "perfect weld" bimetal problem in such a manner that the dependence of the net image force upon the elastic constants is in a form more tractable than that given by Head.

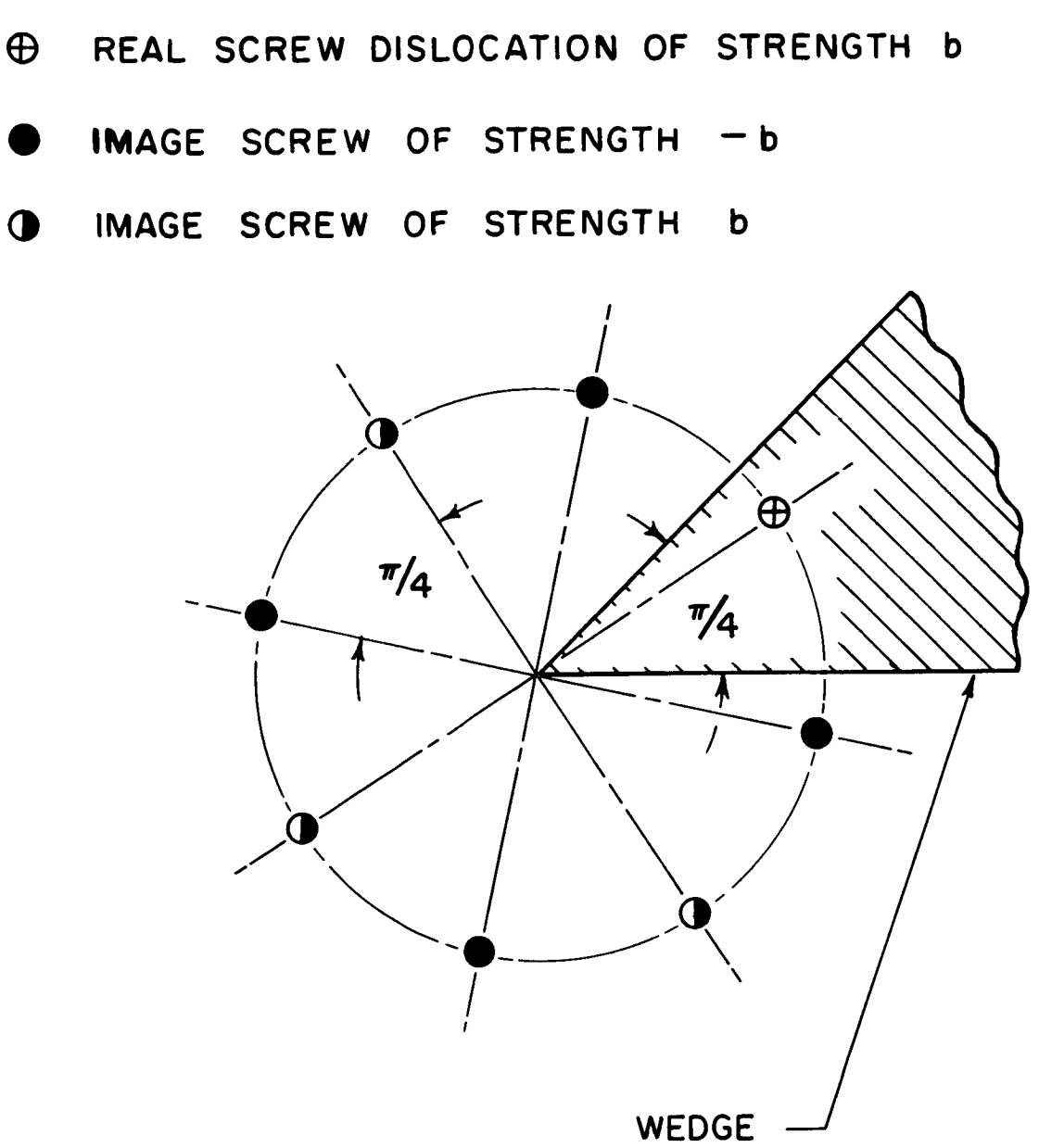

Figure I-7: The equivalent image system representing the stress field in a dislocated wedge of angle $\pi/4$.

Dundurs and Mura[13] and Dundurs and Sendeckyj[14] have treated the edge dislocation inside and exterior to a circular inclusion. Again the results depend upon complicated combinations of the elastic constants. The image system describing the matrix stress state for the exterior problem consists of an image monopole, dipole, and quadrupole at each of the image points $(R^2/t, 0)$ and the origin (Figure I-3).

4. Previous Treatments of Arrays of Dislocations in Elastic Media

a. General Remarks

The most natural extension of the solutions for single dislocations in elastic media is the consideration of arrays of such line defects. This dissertation will concern itself only with dislocation arrays of the following class:

(1) The arrays will exist in an infinite three dimensional elastic medium (not necessarily single phase).

(2) Only two dimensional problems involving these arrays will be considered. All dislocation lines in the arrays will be parallel to the z-axis of an x-y-z Cartesian frame fixed in the medium, and any second phases (inhomogeneities) present will be considered infinite in the z-direction. Thus, translational invariance along the z-direction will insure that the stress and displacement fields of the arrays are independent of z.

(3) The array dislocations will be restricted to lie upon lines parallel to the x-axis of the Cartesian frame. Hence, we shall speak of linear or planar dislocation arrays.

The stress field associated with an array of dislocations is merely the sum of the stress fields of the dislocations in the array. The evaluation of such sums requires knowledge of the position of each dislocation in the array. At static equilibrium the array dislocations must be positioned so that each dislocation experiences zero net force, i.e., the force upon any one dislocation due to all other dislocations in the array must be balanced by the component of the effective applied stress tending to move the dislocation. In general the determination of the distribution of array dislocations is not an easy task.

As a means of introduction to the techniques available for treating dislocation array problems, the following three sections will illustrate three different analytical treatments of the same problem--a pileup of screw or edge dislocations in a single phase material. This is the simplest array problem which may be treated analytically in closed form, and the results may be favorably compared with elasticity calculations of stress concentrations near crack tips in a single phase medium.

b. The Discrete Dislocation Formulation

Eshelby, Frank, and Nabarro[15] in 1951 considered a pileup of screw or edge dislocations in an infinite, single phase, isotropic elastic material (Figure I-8). Physically, the picture is that of a planar slip band of right-hand screw or positive edge dislocations (on the slip plane $y = 0$) moving to the left under the action of an effective applied shear stress τ ($= -\tau_{yz}$ for the case of right-hand screws, $= -\tau_{xy}$ for the case of positive edge dislocations). The leading

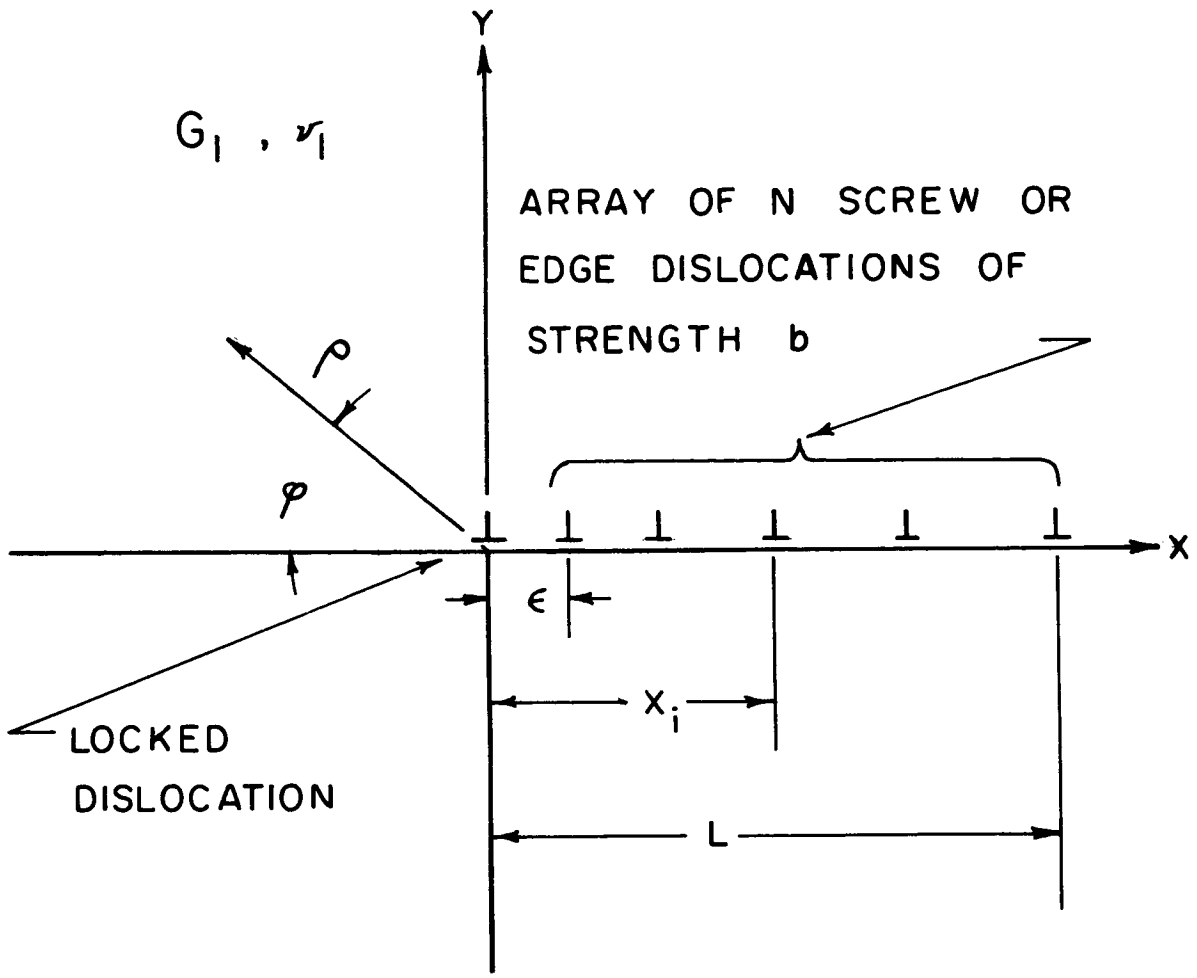

Figure I-8: A screw (or edge) dislocation pileup in a single phase, isotropic elastic medium (Eshelby, Frank, and Nabarro).

dislocation has become locked at the origin by an unspecified short range force proportional to δ' $(x = 0)$, the derivative of Dirac's delta function, and the remaining N dislocations in the array have piled up behind the locked dislocation. The condition of static equilibrium requires that the positions x_j of the array dislocations be determined from:

$$A\left\{ \sum_{\substack{i=1 \\ i\neq j}} \frac{1}{x_j - x_i} + \frac{1}{x_j} \right\} - \tau = 0 \; ; \quad j = 1,2, \ldots , N \; . \qquad \text{(I.4-1)}$$

where

$$A = \frac{Gb}{2\pi} \qquad \text{for a screw array}$$

$$= \frac{Gb}{2\pi(1-\nu)} \qquad \text{for an edge array}$$

G = shear modulus

b = Burgers' vector

ν = Poisson's ratio .

In Eq. (I.4-1) the first term on the left represents the stress on a dislocation at x_j due to all other array dislocations (the term $i = j$ has been deleted from the sum because the j^{th} dislocation exerts no force upon itself). The second term in (I.4-1) is the stress on the dislocation at x_j due to the locked dislocation at the origin, and the third term is the effective applied shear tending to move the dislocations along the slip plane $y = 0$.

The Eshelby, Frank and Nabarro[15] (hereafter referred to as EFN) solution for the dislocation positions x_j utilizes a technique discussed by Stieltjes[16] in 1885 in connection with the analogous problem of electrostatic line charges distributed in a linear array. Stieltjes' method is the following. If we regard the x_j's as the zeroes of a polynomial $f(x)$ of degree N, then

$$f(x) = \prod_{i=1}^{N} (x-x_i) \quad . \tag{I.4-2}$$

The logarithmic derivative of $f(x)$ is

$$\frac{d(\ln f(x))}{dx} = \frac{f'(x)}{f(x)} = \sum_{i=1}^{N} \frac{1}{x-x_i} \quad . \tag{I.4-3}$$

The equilibrium condition (I.4-1) may then be written as

$$A \lim_{x \to x_j} \left\{ \frac{f'(x)}{f(x)} - \frac{1}{x-x_j} \right\} + \frac{A}{x_j} - \tau = 0 \; ; \quad j = 1,2,\ldots,N \; . \tag{I.4-4}$$

Using L'Hospital's rule twice, one may show that

$$\lim_{x \to x_j} \left\{ \frac{f'(x)}{f(x)} - \frac{1}{x-x_j} \right\} = \frac{f''(x_j)}{2f'(x_j)} \; , \tag{I.4-5}$$

so that the equilibrium condition may be expressed as

$$f''(x_j) + 2 \left\{ \frac{1}{x_j} - \frac{\tau}{A} \right\} f'(x_j) = 0; \qquad j = 1,2,\ldots,N \tag{I.4-6}$$

with the auxiliary condition

$$f(x_j) = 0; \qquad j = 1,2,\ldots,N . \tag{I.4-7}$$

Letting $\zeta_j = (2\tau x_j)/A$, Eq. (I.4-6) may be written as

$$\zeta_j f''(\zeta_j) + (2 - \zeta_j) f'(\zeta_j) = 0 ; \qquad j = 1,2,\ldots,N . \tag{I.4-8}$$

Now suppose we consider the differential equation

$$\zeta f''(\zeta) + (2-\zeta) f'(\zeta) + q(N,\zeta) f(\zeta) = 0 . \tag{I.4-9}$$

If we can choose a function $q(N,\zeta)$ such that (I.4-9) has as a solution a polynomial of the N^{th} degree, all of whose roots are real and distinct, and if $q(N,\zeta)$ has no poles at these roots, then the problem is solved. The EFN choice for $q(N,\zeta)$ was

$$q(N,\zeta) = N-1 , \tag{I.4-10}$$

so that $f(\zeta)$ satisfies

$$\zeta f''(\zeta) + (2-\zeta) f'(\zeta) + (N-1) f(\zeta) = 0 . \tag{I.4-11}$$

The desired solution is [17]

$$f(\zeta) = L_N'(\zeta) = L_N'\left(\frac{2\tau x}{A}\right) , \tag{I.4-12}$$

where L_N' is the derivative of the N^{th} Laguerre polynomial. Thus, the spacing of the array dislocations is essentially the spacing of the radial nodes of a hydrogen atom wave function for an Ns state.[17]

Knowing the distribution of the array dislocations the EFN calculations showed that

(1) $\frac{\tau}{A}\frac{L}{N} \approx 1.84$; $L = x_N - x_1$, the slip line length.

(2) $\epsilon \approx L/N^2$, where ϵ is the separation distance between the locked dislocation and the nearest array dislocation.

(3) Ahead of the pileup tip $(x < 0,\ L/|x| \gg 1)$ the shear stress on the slip plane $y = 0$ is

$$\frac{\tau_{ij}}{\tau} \approx -\sqrt{\frac{L}{|x|}} ,$$

where $ij = xy$ for an edge array and $ij = yz$ for a screw array. Using the asymptotic (large N) properties of the Laguerre polynomials, Stroh[18] extended the EFN solution by deriving approximate expressions for the local stress field near the pileup tip as part of a discussion of the criterion for crack initiation at the tip of a blocked slip band. Both the local stresses given by the EFN and Stroh calculations are a factor of $\sqrt{2}$ higher than the local stresses near the tips of elastic cracks in single phase media.[19] This is not unexpected, since the EFN slip band evidences a stress singularity only at its leading edge $(x = 0)$. The stress concentration factors given by Paris and Sih[19] apply to symmetric cracks, i.e., cracks with singularities at both ends.

Although it is a beautiful analytical technique, the method of Stieltjes' is not well-suited for treating more complex dislocation array problems, in particular those involving dislocation arrays in two phase media or opposite sign arrays in single phase media. Indeed, one might view the EFN solution as a very fortitious one, since a $q(N,\zeta)$ could be chosen to yield the desired $f(\zeta)$, and the polynomial $f(\zeta)$ turned out to be a function whose asymptotic (large N) properties and roots were known.

c. The Continuously Distributed Dislocation Formulation

A means of circumventing the difficulties inherent in the discrete dislocation formulation is the method of continuously distributed dislocations. Credit for the introduction of this technique is generally given to Eshelby and Leibfried.[20] A rigorous presentation of the method has also been discussed by Bilby, Bullough, and Smith.[21] As its name implies, the method of continuously distributed dislocations is the replacement of a discrete dislocation arrangement by a continuous distribution of dislocations of infinitesimal Burgers' vectors, such that the total Burgers' vector of the continuous distribution is the same as that of the discrete dislocation configuration. Physically speaking, we have "smeared out" the discrete dislocations so that we may describe the dislocation arrangement by a continuously varying scalar function (in one-dimensional problems involving linear arrays). Near the tip of a blocked dislocation array where the dislocation spacing is of the magnitude of the Burgers' vector (or interatomic

spacing), such a description seems quite appropriate, e.g., if two dislocations on a common slip plane are separated by only 2-5Å, it makes little sense to speak of two discrete dislocations, since the separation distance is comparable to the width of the dislocations. The EFN calculation showed that the leading pileup dislocations were separated by a distance $\epsilon \approx L/N^2$. For a typical slip line length, $L \approx 10^{-4}$ cm, the two leading dislocations in a pileup of 100 dislocations are separated by only about 1Å!

If we now reformulate the EFN problem using the continuous distribution approximation, we are left with two choices for treating the dislocation locked at the origin. We can consider this dislocation as part of the smeared out array, or we may treat it as a discrete line defect, separate from the remainder of the array. In this section we shall treat the locked dislocation as being incorporated into the continuous distribution; the following section will treat the EFN problem assuming the locked dislocation to be discrete.

When N is large enough to invoke the approximation of continuously distributed dislocations, the equation of static equilibrium (I.4-1) is recast as a singular integral equation

$$\int_0^L \frac{f(t)\,dt}{x-t} = \frac{\tau}{A}\,; \qquad 0 < x \leq L\,, \tag{I.4-13}$$

which must be solved for the unknown dislocation distribution function, $f(t)$. x is a source point, t a field point, and the integral in (I.4-13) is understood to be a Cauchy principal value integral, i.e.,

$$\int_0^L \frac{f(t)\,dt}{x-t} = \lim_{\delta \to 0} \left\{ \int_0^{x-\delta} \frac{f(t)\,dt}{x-t} + \int_{x+\delta}^{L} \frac{f(t)\,dt}{x-t} \right\} \quad . \tag{I.4-14}$$

Mathematically, we have deleted a small neighborhood about the field point x in the distribution. This is analogous to deleting the term $i = j$ in the sum in Eq. (I.4-1). The Cauchy principal value, or symmetrical deletion, is chosen to avoid ambiguity. One normally employs a similar symmetrical deletion when speaking of the core of a dislocation, i.e., the core is pictured as the region inside a circle of radius r_0 drawn about the dislocation line as a center.[1]

The end conditions for $f(t)$ are that:

(1) $f(L) = 0$, since there are no dislocations at the trailing end of the pileup.

(2) $f(t)$ is unbounded with a weak singularity ($tf(t) \to 0$ as $t \to 0$) at $t = 0$, since we expect a stress intensification at the leading edge of the pileup.

The solution for the dislocation distribution function $f(t)$ is (see Appendix B):

$$f(t) = \frac{\tau}{\pi A} \sqrt{\frac{L-t}{t}} \quad . \tag{I.4-15}$$

N, the number of dislocations in the array is given by

$$\frac{\tau}{A} \frac{L}{N} = 2 \quad , \tag{I.4-16}$$

which compares favorably with the EFN relation

$$\frac{\tau}{A} \frac{L}{N} = 1.84 \quad . \tag{I.4-17}$$

The utility of the continuous distribution approach is apparent when one calculates the pileup stress field. Excluding the external applied shear component, τ, the stress field of the array is given by the superposition integral

$$\tau_{ij}(x,y) = \int_0^L \tau_{ij}(x,y,t)\, f(t)\, dt \ . \qquad \text{(I.4-18)}$$

Close to the pileup tip $(L/\rho \gg 1)$ the stress field of a screw array is approximately

$$\left.\begin{aligned} \tau_{xz} &\approx -\tau \sqrt{\frac{L}{\rho}} \quad \sin\frac{\varphi}{2} \ , \\ \tau_{yz} &\approx -\tau \sqrt{\frac{L}{\rho}} \quad \cos\frac{\varphi}{2} \ , \end{aligned}\right\} \qquad \text{(I.4-19)}$$

where ρ and φ are the polar coordinates depicted in Figure (I-8). As noted previously, Eqs. (I.4-19) are higher, by a factor of $\sqrt{2}$, than the Mode III stress fields reported by Paris and Sih.[19]

d. The Modified Continuous Distribution Approach

The technique described in this section is a modification suggested to the author by A. D. Brailsford[22] of the Ford Scientific Laboratories. The essential difference between the modification and the treatment outlined in the previous section is that the locked dislocation at the origin is allowed to remain discrete; the remainder of the array dislocations are smeared out in a continuous distribution, $f(t)$, which is bounded (zero) at its end-points $t = L$ and $t = \epsilon$, where ϵ is the separation distance between the two leading pileup

dislocations (Figure I-8). Static equilibrium is satisfied provided that $f(t)$ satisfies

$$\int_{\epsilon}^{L} \frac{f(t)\,dt}{x-t} = \frac{\tau}{A} - \frac{1}{x} ; \qquad \epsilon \leq x \leq L . \tag{I.4-20}$$

Equation (I.4-20) is soluble provided (see Appendix B) that

$$\sqrt{L\epsilon} = \frac{A}{\tau} ; \tag{I.4-21}$$

the appropriate modified distribution function is

$$f(t) = \frac{\tau}{\pi A} \frac{\sqrt{(L-t)(t-\epsilon)}}{t} . \tag{I.4-22}$$

One notes that in the limit as ϵ tends to zero (when the locked dislocation is incorporated into the continuous distribution), the modified $f(t)$ given by (I.4-22) reduces to the unmodified form (Eq. (I.4-15)).

N, the number of pileup dislocations is given by

$$N = \int_{0}^{L} f(t)\,dt = \frac{\tau}{A}(L + \epsilon) - 1 . \tag{I.4-23}$$

Combining Eqs. (I.4-23) and (I.4-21) yields

$$L + \epsilon = (N+1)\sqrt{L\epsilon} , \tag{I.4-24}$$

so that when $N > 10$

$$\epsilon \approx \frac{L}{N^2 + 2N - 1} = \frac{L}{N^2} , \tag{I.4-25}$$

which is the EFN result deduced from knowledge of the asymptotic (large N) properties of the Laguerre polynomials.

Of the three methods presented for treating the problem of the pileup in a single phase material, the method of section (c) presents the least computational difficulty. The technique of section (c) seems more suitable for computations than the modified method outlined in this section, partly because the integral equation for $f(t)$ is somewhat simpler, and partly because one need not worry about the auxiliary solubility condition associated with a distribution function bounded at both its end-points. Therefore, the calculations in this dissertation will utilize the continuous distribution approach treating the leading array dislocation as part of the "smeared out" distribution. It will be seen that the continuous distribution technique provides a profitable analytical technique for treating in closed form problems involving screw dislocation arrays in simple two phase systems. Knowing the solution for a single dislocation in a two phase medium, this method permits the immediate formulation of a rather complicated boundary value problem in terms of an integral equation which has already incorporated within it the appropriate boundary values and the static equilibrium condition. This incorporation is important in two phase problems where the boundary (interface) conditions are of the dielectric variety, i.e., continuity of the displacement field and linear combinations of its derivatives across the phase boundaries.

e. The Method of Johnson and Webster

There exists yet an alternative method introduced by Johnson and Webster[23,24] for treating screw dislocation array problems. The method is equivalent to that of the continuous dislocation distribution, and it avoids the need for computing the array stress field by evaluating the superposition integral. However, the use of the method appears to be restricted (on a practical basis) to treatments of screw dislocation arrays in single phase media.

This technique recognizes the screw dislocation--vortex line analogy, and, since the displacement field of a screw is harmonic, uses conformal mapping as part of the method of solution. Basically, the technique involves solving for a complex stress potential in much the same manner as described by Muskhelishvili[48] in the case of plane stress or plane strain elastostatic problems. Conformal transformation of the plane curves over which dislocations are distributed to segments of either the unit circle or the real axis allows the transformed complex stress function to be obtained by standard techniques. Normally this requires solution of a Riemann-Hilbert problem for the sectionally holomorphic complex stress function. This step in the procedure is fully equivalent to finding the dislocation distribution function from the integral equation of static equilibrium. Inversion of the mapping and differentiation of the stress function yield the array stress field, and the discontinuity in tangential shear stress across the plane curves threaded by the dislocations is related to the dislocation distribution function.

The limitation of the applicability of the complex stress potential analysis to dislocation arrays in single phase systems is due to the dielectric type of boundary conditions associated with the multiphase problems. Conformal mapping usually does not prove to be a useful tool in such cases; the more straightforward continuous distribution approach is preferable because of the built-in boundary values. In single phase problems the great merit of the Johnson-Webster approach is apparent in the treatment of configurations of non-colinear planar screw arrays--e.g., the case of the interaction of two parallel slip bands (Figure I-9). A Schwartz-Christoffel transformation can be used to map the lines of the arrays onto segments of the real axis, and the transformed stress potential can be calculated. Usually, however, inversion of the mapping and subsequent expression of the stresses is a numerical calculation. The standard continuous distribution approach to this type of problem requires numerical calculations to solve the integral equation (or equations) of static equilibrium and to evaluate the superposition integral for the stresses.

f. Dislocation Arrays at a Rigid Half-Plane

There exist in the literature numerous other treatments of continuous distributions of dislocations in single phase materials, the most notable being those by Leibfried,[20] Head,[26] Louat,[27] Head and Louat,[28] Smith,[29,30] Bilby, Cottrell and Swinden,[31] and Weertman.[32] Because any single phase elastostatic dislocation array problem will involve solving a singular integral equation with only a

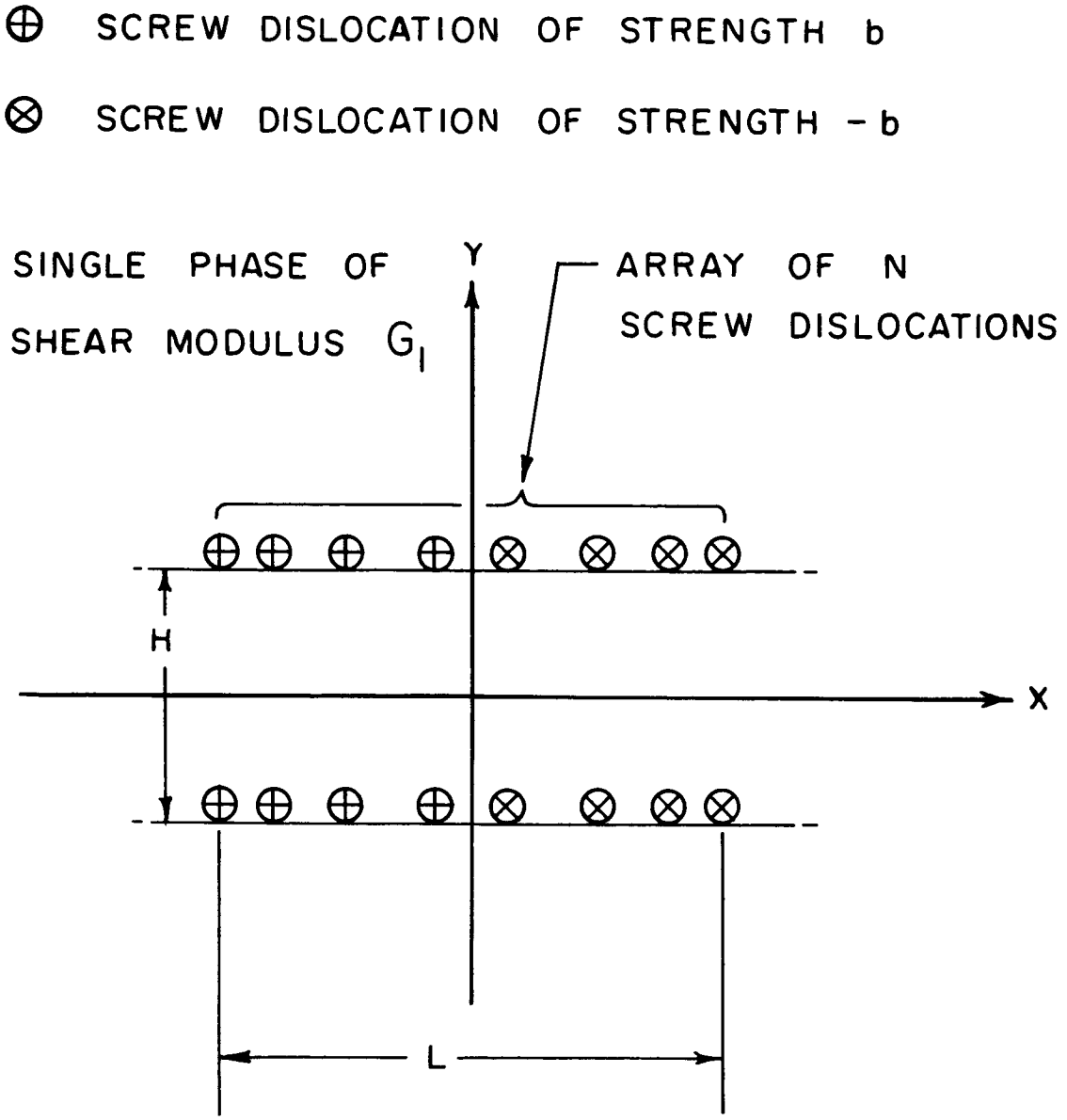

Figure I-9: Two screw dislocation pileups on parallel slip planes in a single phase, isotropic elastic medium (Johnson and Webster).

simple Cauchy kernel,[25] the mathematical treatments of such problems are adequately described by Appendix B. However, as we shall see, the presence of second phases near dislocation arrays generates additional terms in the kernel of the integral equation of static equilibrium. These extra terms in the kernel arise from the previously discussed image forces produced by the inhomogeneity and lead to a class of integral equations which, to the author's knowledge, have not been investigated.

Chou[33] in 1965 considered the application of the method of continuously distributed dislocations to the problem of a screw pileup against a rigid semi-infinite second phase. Consider N right-hand screw dislocations, each with Burgers' vector b, in a slip band of length L which is blocked by a semi-infinite second phase ($x < 0$) whose shear modulus, G_2, is much greater than the matrix ($x > 0$) shear modulus G_1 (Figure I-10). The applied stress is $\tau_{yz} = -\tau$. If the weld $x = 0$ is perfect, then using Head's solution for the single screw dislocation in a bimetal, noting that $\kappa \to 1$ when $G_2 \gg G_1$, and invoking the distributed dislocation approximation, static equilibrium requires that

$$\int_0^L \frac{f(t)\,dt}{x-t} + \int_0^L \frac{f(t)\,dt}{x+t} = \frac{2\pi\tau}{G_1 b}, \qquad 0 < x \leq L \qquad \text{(I.4-26)}$$

where $f(t)$ is the dislocation distribution function.

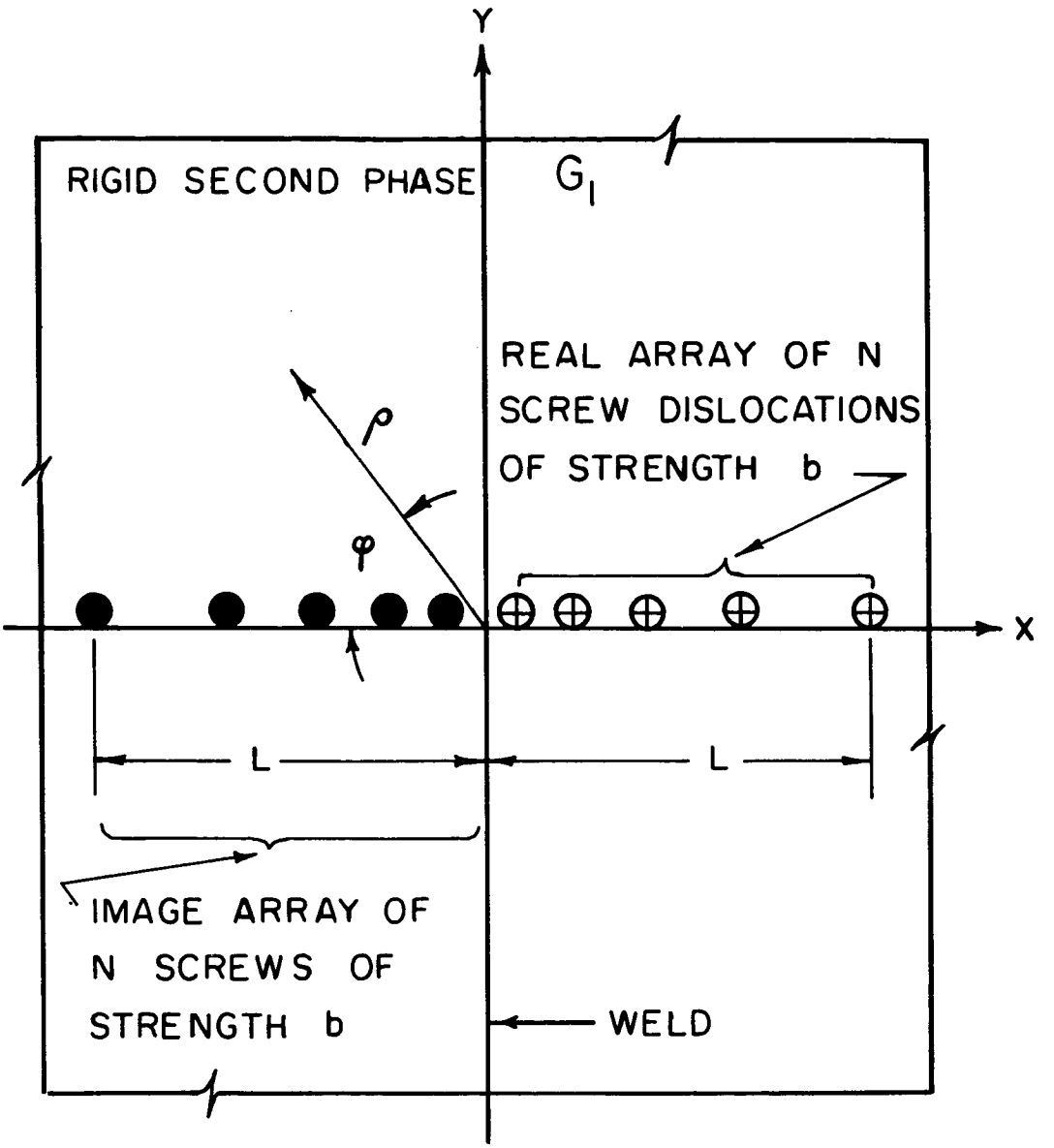

Figure I-10: A screw dislocation pileup at a rigid elastic half-plane and its induced image array.

The first term in (I.4-26) contains the usual Cauchy kernel common to single phase problems; the second term containing the "image kernel" $1/x+t$ may be interpreted as the stress at a field point x in the real pileup due to an image screw array of total Burgers' vector Nb, distributed on the interval $[-L,0)$. Combining terms on the left side of (I.4-26) yields

$$\int_0^L \frac{f(t)\,dt}{x^2-t^2} = \frac{\pi\tau}{G_1 bx} , \qquad 0 < x \leq L , \qquad (I.4\text{-}27)$$

whereupon the substitutions $\lambda = x^2$, $\zeta = t^2$ reduce Eq. (I.4-27) to a singular integral equation with a simple Cauchy kernel. Inverting according to the techniques outlined in Appendix B, the dislocation distribution function is found to be

$$f(t) = \frac{4\tau}{\pi G_1 b} \cosh^{-1}\left(\frac{L}{t}\right) , \qquad (I.4\text{-}28)$$

and N, the number of piled-up dislocations is given by

$$\frac{2\pi\tau}{G_1 b}\frac{L}{N} = \pi . \qquad (I.4\text{-}29)$$

Barnett and Tetelman[34] have evaluated the superposition integral and found the stresses in the second phase $(x < 0)$ to be given by

$$\begin{aligned} \tau_{xz} &= -\frac{4\tau}{\pi^2}\,\mathrm{sgn}(y)\;\omega_0\Omega_0 \\ \tau_{yz} &= -\frac{2\tau}{\pi^2}\left\{\omega_0^2 + \frac{\pi^2}{4} - \Omega_0^2\right\} , \end{aligned} \qquad (I.4\text{-}30)$$

$$\begin{aligned} \text{sgn}(y) &= 1, && y > 0 \\ &= -1, && y < 0 \\ &= 0, && y = 0 \end{aligned}$$

where

$$\left.\begin{aligned} \sinh^2 \omega_0 &= \frac{1}{2}\left\{\left(\frac{L}{\rho}\right)^2 - 1 + \sqrt{\left\langle\left(\frac{L}{\rho}\right)^2 - 1\right\rangle^2 + \left\langle\frac{2L}{\rho}\sin\varphi\right\rangle^2}\right\} \\ \sin^2 \Omega_0 &= \frac{1}{2}\left\{1 - \left(\frac{L}{\rho}\right)^2 + \sqrt{\left\langle\left(\frac{L}{\rho}\right)^2 - 1\right\rangle^2 + \left\langle\frac{2L}{\rho}\sin\varphi\right\rangle^2}\right\} . \end{aligned}\right\} \qquad (I.4\text{-}31)$$

ρ and φ are polar coordinates in the second phase (Figure I-10). Close to the pileup tip in the second phase $(L/\rho \gg 1)$, the local stresses are

$$\left.\begin{aligned} \tau_{xz} &\approx -\frac{4\tau}{\pi^2}\varphi \ln\left(\frac{2L}{\rho}\right) , \\ \tau_{yz} &\approx -\frac{2\tau}{\pi^2}\left\{\left\langle\ln\left(\frac{2L}{\rho}\right)\right\rangle^2 + \frac{\pi^2}{4} - \varphi^2\right\} . \end{aligned}\right\} \qquad (I.4\text{-}32)$$

Chou[33] has noted that the same analysis holds for a pileup of edge dislocations at a rigid half-plane when the weld $x = 0$ cannot support shear stresses. The local stresses of the edge pileup are then approximately[34]

$$\left.\begin{aligned} \tau_{xx} &\approx -\frac{8\tau}{\pi^2}\left\{\varphi + \frac{1}{2}\sin 2\varphi\right\} \ln\left(\frac{2L}{\rho}\right) \\ \tau_{yy} &\approx -\frac{8\tau}{\pi^2}\left\{\varphi - \frac{1}{2}\sin 2\varphi\right\} \ln\left(\frac{2L}{\rho}\right) \\ \tau_{xy} &\approx -\frac{8\tau}{\pi^2}\cos^2\varphi \ln\left(\frac{2L}{\rho}\right) . \end{aligned}\right\} \qquad (I.4\text{-}33)$$

The maximum normal tensile stress occurs across a plane inclined to the slip plane at an angle $\varphi = -66.15°$. For an edge pileup in a single phase material Stroh[18] found that the maximum normal tensile stress occurs across a plane inclined at $\varphi = -70°$.

Two noteworthy results of the rigid half-plane problem are:

(1) The stress singularity at the pileup tip is a logarithmic one as opposed to the inverse square root singularity predicted by single phase elasticity calculations (Eq. (I.4-19)).

(2) The number of dislocations, N, in the pileup is less than that predicted by single phase calculations (Eq. (I.4-16)). In fact Chou surmised that the relation

$$\frac{2\pi\tau}{G_1 b}\frac{L}{N} = 2 + (\pi-2)\kappa , \qquad 0 \leq \kappa \leq 1 , \qquad \text{(I.4-34)}$$

should hold for a screw array blocked at a half-plane of finite rigidity.

Both observations indicate a lowering of the local stresses generated by the pileup due to the presence of the rigid second phase, since the logarithmic singularity is less severe than the inverse square root singularity, and a lesser number of dislocations in the array will lower the local stress intensification.

In a real material, of course, the second phases present are of finite size and finite rigidity. In order to examine the effects of inclusion size and rigidity upon the local stress field of a blocked slip band, the following three chapters will treat the problems of:

(1) a screw dislocation array blocked by a rigid circular inclusion (Chapter II).

(2) a screw dislocation array blocked by a semi-infinite second phase of finite rigidity (Chapter III).

(3) a screw dislocation array blocked by a circular inclusion of finite rigidity (Chapter IV).

Obviously (3) is the completely general problem which includes (1) and (2) as special cases, but the general problem is most readily treated using the experience gained from first solving the special cases. Chapter V will treat the problem of an infinite sequence of screw dislocation arrays (on parallel slip planes) stacked against a half-plane of finite rigidity; this might be taken as a simple model appropriate for a work-hardened material, since the slip dislocations are no longer confined to a single slip band. In Chapter VI the problem of an edge dislocation array blocked by a semi-infinite second phase will be formulated. All of the above problems will be treated by the continuous distribution approximation subject to the restriction that no relaxation of the array stresses will be allowed during pileup formation.

Applications of the results obtained in Chapters II-V will be discussed in Chapter VII. The effect of the presence of second phases upon a derivation of a Hall-Petch type relation for the grain size dependence of the yield stress of a polycrystal will be examined. Finally, the following possible modes for relaxation of the pileup stresses will be considered:

(1) Yielding near the second phase.

(2) Fracture of the second phase or of the second phase-matrix interface.

(3) Cross slip of the leading array dislocations around the second phase.

Approximate static criteria for relaxation by either (1), (2) or (3) will then be formulated.

CHAPTER II

A SCREW DISLOCATION PILEUP AT A RIGID CIRCULAR INCLUSION

1. Analysis

Let us now relax Chou's condition of a semi-infinite second phase[33] in order to examine the effect of a finite size rigid inclusion upon the distribution of dislocations in and the local stresses associated with a blocked slip band. Consider the two-phase medium depicted in Figure I-2 (a circular inclusion imbedded in an infinite matrix). Let a planar array of N right hand screw dislocations, each of Burgers' vector b, distributed over a length L on the slip plane $y = 0$, be piled against the inclusion due to a shear stress $\tau_{yz}\ (y = 0) = -\tau(x)$; the leading dislocation is blocked by the inclusion at the point $(R,0)$ (Figure II-1). When the inclusion is rigid, so that $\kappa = (G_2-G_1)/(G_2+G_1) \to 1$, the use of eq. (I.3-5) to formulate the static equilibrium condition yields

$$\frac{G_1 b}{2\pi}\left\{\sum_{\substack{j=1\\ j\neq i}}^{N}\frac{1}{x_i-x_j}+\sum_{j=1}^{N}\frac{1}{x_i-R^2/x_j}-\frac{N}{x_i}\right\}=\tau(x_i),\qquad i=1,2,\ldots,N\ . \tag{II.1-1}$$

These N equations determine the position of each discrete dislocation in the array. The first sum on the left side of (II.1-1) is the stress on a pileup dislocation at x_i due to the other $N-1$ pileup dislocations at positions x_j; the second sum may be interpreted as the

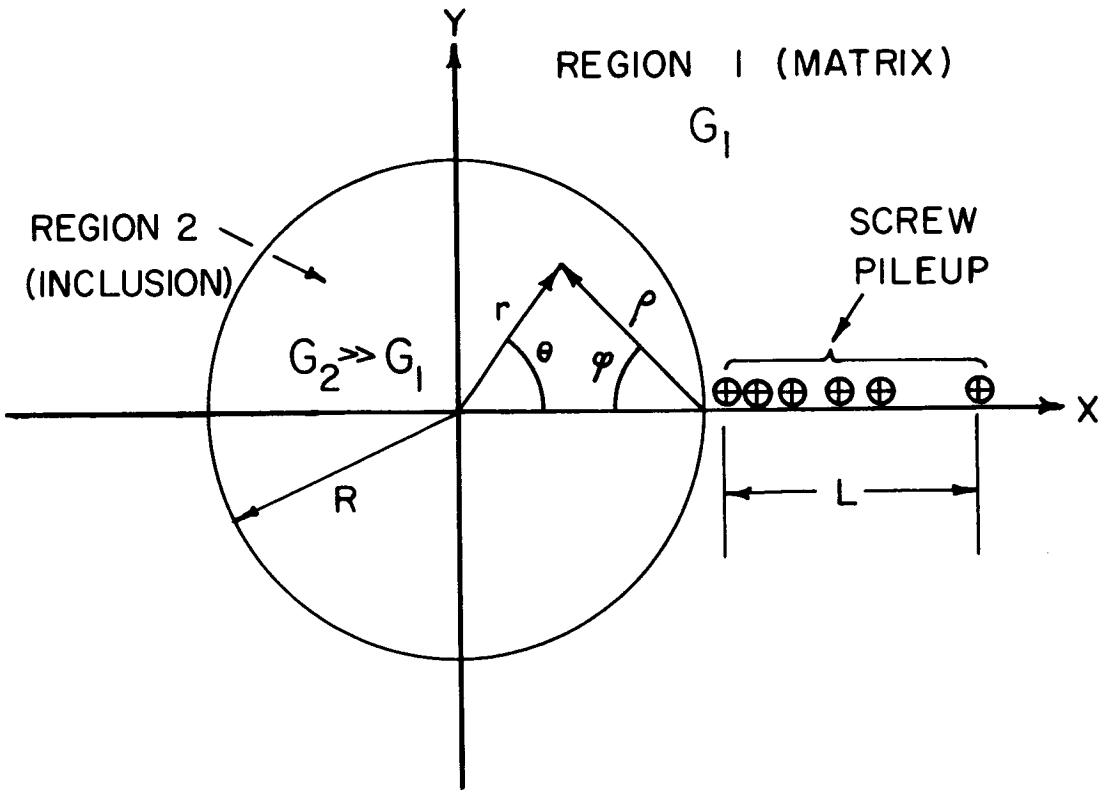

Figure II-1: Schematic illustration of a screw dislocation pileup at a rigid circular inclusion.

retarding stress on the dislocation at x_i due to a pileup of N dislocations of strength b at positions R^2/x_j, the image positions of the N real dislocations at x_j; the third term represents the attractive stress acting on the dislocation at x_i due to a giant left-hand image screw of strength Nb at the origin (Figure II-2). Defining the dimensionless parameters $t_j = x_j/R$ and replacing the discrete dislocations in the array by a continuously distributed dislocation array, the equilibrium condition is recast as the singular integral equation

$$\int_1^\beta \frac{f(t)\,dt}{\lambda - t} + \int_1^\beta \frac{f(t)\,dt}{\lambda - 1/t} = \frac{N}{\lambda} + \frac{2\pi R}{G_1 b}\,\tau(\lambda); \quad 1 < \lambda \leq \beta\,, \tag{II.1-2}$$

where

$$\beta = \frac{L}{R} + 1\,. \tag{II.1-3}$$

λ (= x/R) is a field point in the array, t a source point, and f(t) is the unknown dislocation distribution function.

At this point in the analysis it is appropriate to comment on the exact form of $\tau(\lambda)$, the component of applied stress acting on the slip plane in the matrix. Consider an infinite elastic medium of shear modulus G_1 in which is imbedded a circular inclusion of radius R and shear modulus G_2. If a shear $\tau_{yz} = -\tau$ is applied at infinity, and if one demands continuity of the displacement field and the tangential shear τ_{rz} across the inclusion interface, then the solution for the elastic stress field in the matrix is easily shown to be:

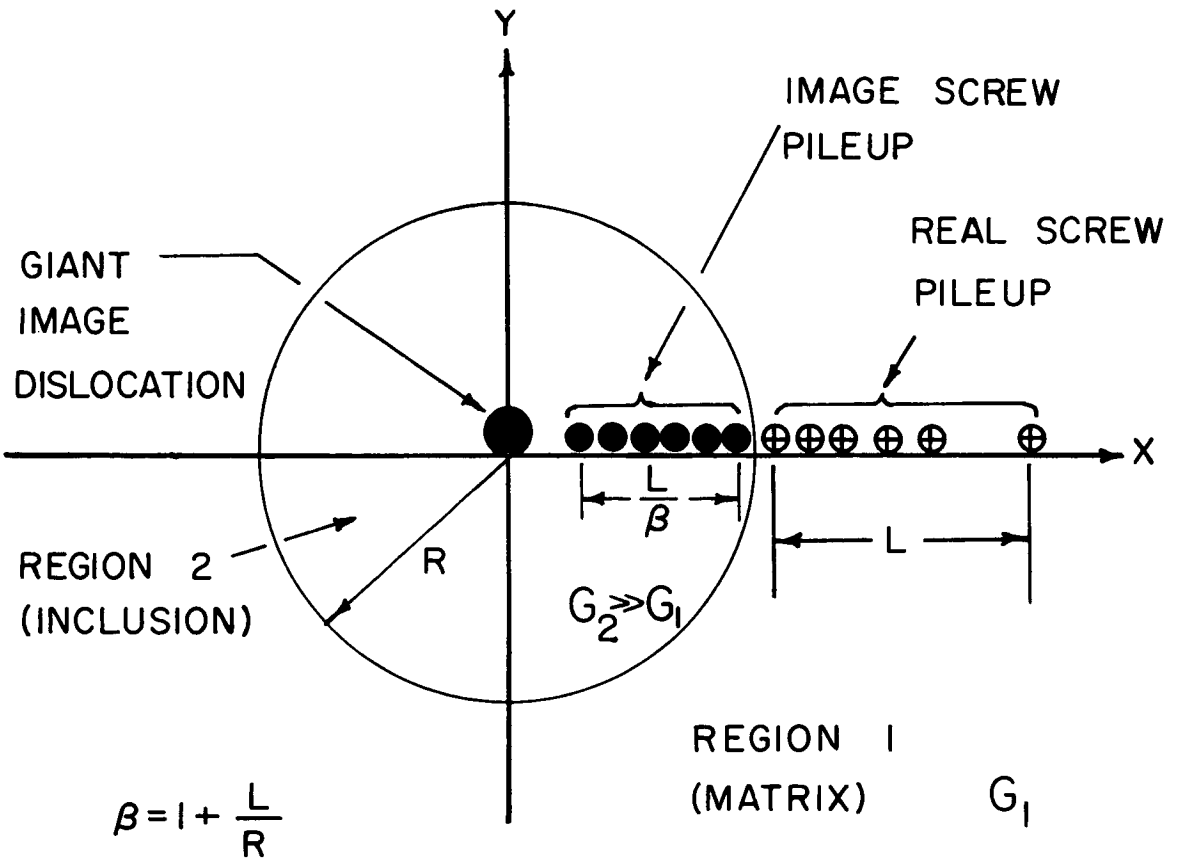

Figure II-2: A screw dislocation pileup at a rigid circular inclusion and its induced image array.

$$\tau_{xz} = -\frac{\kappa\tau R^2}{x^2 + y^2} \sin 2\theta$$

$$\tau_{yz} = -\tau + \frac{\kappa\tau R^2}{x^2 + y^2} \cos 2\theta \qquad \text{(II.1-4)}$$

where

$$\theta = \tan^{-1} \frac{y}{x} ,$$

$$\kappa = \frac{G_2 - G_1}{G_2 + G_1} .$$

Along the slip plane $y = 0$, τ_{xz} vanishes, and

$$\tau_{yz} = -\tau \left\{ 1 - \frac{\kappa R^2}{x^2} \right\} . \qquad \text{(II.1-5)}$$

Hence, in the purely elastic case, the stress $\tau(\lambda)$ in (II.1-2) should be given by (when $\kappa = 1$)

$$\tau(\lambda) = \tau \left\{ 1 - \frac{1}{\lambda^2} \right\} , \qquad \text{(II.1-6)}$$

where $\lambda = x/R$. If, however, we say that the presence of a slip band on the interval $1 < \lambda \leq \beta = L/R + 1$ is indicative of plastic yielding in this region, one may, based upon a yield criterion, wish to say that $\tau(\lambda) = \tau$, the yield stress in pure longitudinal shear. In this chapter we shall identify $\tau(\lambda)$ with the yield stress in anti-plane strain. The integral equation (II.1-2) may be easily solved for either choice of $\tau(\lambda)$; however, it will turn out that by letting $\tau(\lambda) = \tau$, we will gain additional information which will prove useful in constructing

the general solution of Chapter IV (regardless of the choice of $\tau(\lambda)$).

Hence, we seek a solution to

$$\int_1^\beta \frac{f(t)\,dt}{\lambda - t} + \int_1^\beta \frac{f(t)\,dt}{\lambda - 1/t} = \frac{N}{\lambda} + \frac{2\pi R}{G_1 b}\pi \,, \qquad 1 < \lambda \leq \beta \,, \tag{II.1-7}$$

such that $f(1)$ is unbounded with a weak singularity and $f(\beta) = 0$ (there are no dislocations at the trailing end of the pileup). Equation (II.1-7) is not in standard form because only one of the kernels is a standard Cauchy difference kernel. However, one may physically extend the equation to the full interval $[1/\beta, \beta]$ so that only a simple Cauchy kernel appears. This is done in the following manner. Since (II.1-7) can also be regarded as the equilibrium condition describing two planar asymmetric dislocation arrays, each containing N dislocations, piled up against one another in a single phase medium due to a shear $\tau_{yz}(1 < \lambda \leq \beta) = -\{(G_1 b/2\pi R)(N/\lambda) + \tau\}$, then

$$N = \int_1^\beta f(t)\,dt = \int_{1/\beta}^1 g(t)\,dt \,, \tag{II.1-8}$$

where $g(t)$ is the distribution function for dislocations in the image pileup in $[1/\beta, 1)$. Making the substitution $t' = 1/t$, one finds that

$$\frac{1}{t^2} f\left(\frac{1}{t}\right) = g(t) \,, \qquad \frac{1}{t^2} g\left(\frac{1}{t}\right) = f(t) \,. \tag{II.1-9}$$

Thus, one can define a distribution function $f(t)$ for the full interval $[1/\beta, \beta]$ with the property

$$\frac{1}{t^2} f\left(\frac{1}{t}\right) = f(t) \ . \qquad \text{(II.1-10)}$$

Equation (II.1-7) can then be rewritten as

$$\int_{1/\beta}^{\beta} \frac{f(t)\, dt}{\lambda - t} = \frac{N}{\lambda} + \frac{2\pi R\tau}{G_1 b} \ , \qquad 1 < \lambda \leq \beta \qquad \text{(II.1-11)}$$

Letting $\lambda = 1/\lambda'$ in (II.1-7) the integral equation for the full interval $[1/\beta, \beta]$ is obtained.

$$\int_{1/\beta}^{\beta} \frac{f(t)\, dt}{\lambda - t} = \frac{N}{\lambda} + \left\{ \begin{array}{ll} \dfrac{2\pi R\tau}{G_1 b} \ ; & 1 < \lambda \leq \beta \\ - \dfrac{2\pi R\tau}{G_1 b \lambda^2} \ ; & \dfrac{1}{\beta} \leq \lambda < 1 \end{array} \right\} . \qquad \text{(II.1-12)}$$

Since $f(\beta) = 0$, Eq. (II.1-10) implies $f(1/\beta) = 0$, and (II.1-12) is soluble provided (see Appendix B)

$$\frac{G_1 N b}{2\tau L} = \frac{1}{\sqrt{\beta}} + \frac{\beta - 1}{2\beta} \left\{ \frac{\pi}{2} + \sin^{-1} \frac{\beta - 1}{\beta + 1} \right\} . \qquad \text{(II.1-13)}$$

Figure II-3 shows N (in units of $\tau L/G_1 b$) as a function of β. One notes that

$$\frac{G_1 N b}{2\tau L} \to 1 \quad \text{as} \quad R \to \infty \quad \text{(semi-infinite second phase)}$$

$$\qquad \text{(II.1-14)}$$

$$\frac{G_1 N b}{2\tau L} \to \frac{\pi}{2} \quad \text{as} \quad R \to 0 \quad \text{(single phase homogeneous medium)} .$$

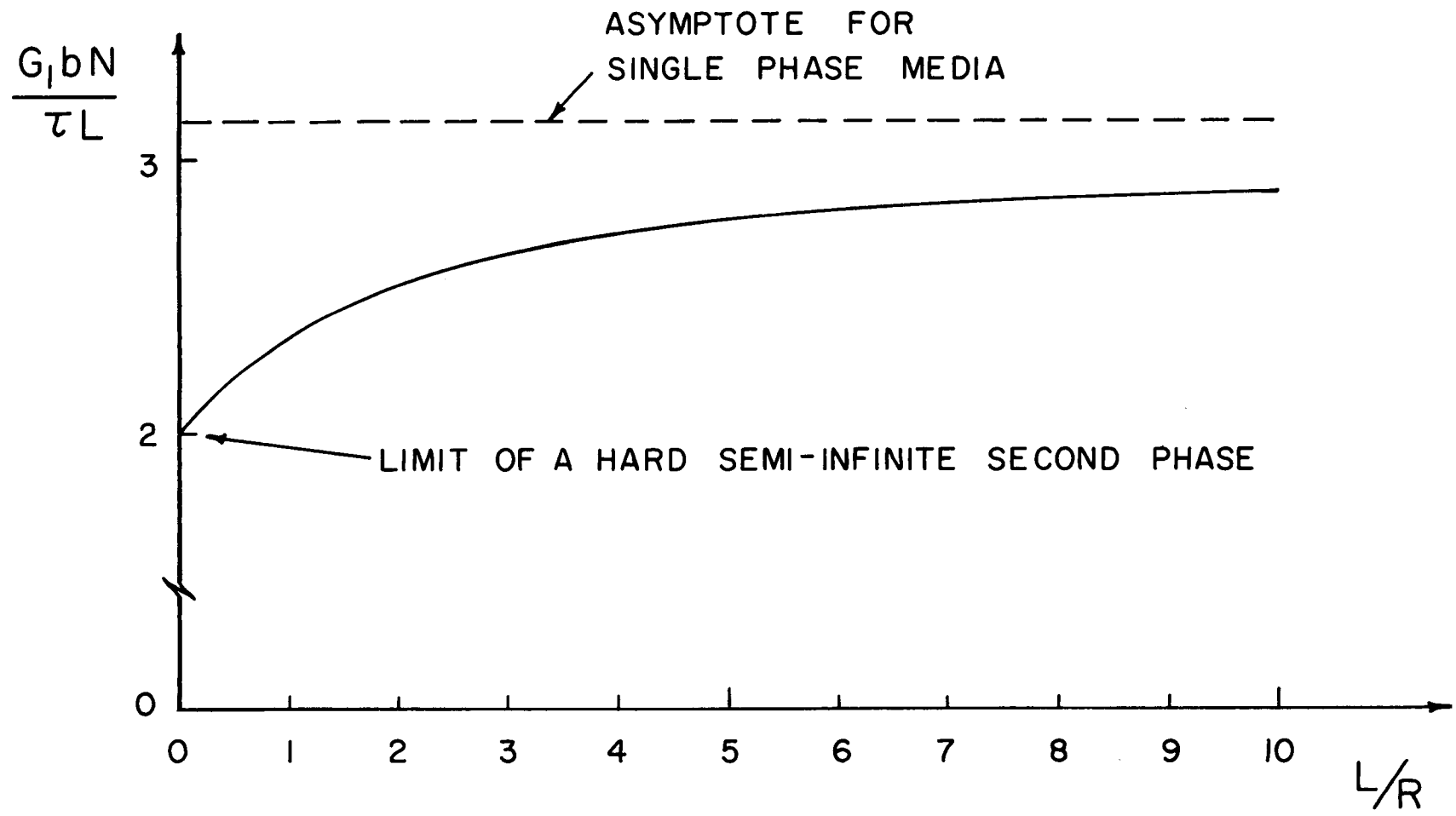

Figure II-3: N, the number of array dislocations, as a function of L/R .

Inversion of the integral equation according to techniques outlined in Appendix B yields

$$f(t) = \frac{2R\tau}{\pi G_1 b}\left[\left(\frac{\pi}{2} + \sin^{-1}\frac{\beta-1}{\beta+1}\right)\left(\frac{1}{t} + \frac{1}{t^2}\right)\sqrt{(\beta-t)(t-1/\beta)}\right.$$

$$\left. + \left(1 + \frac{1}{t^2}\right)\cosh^{-1}\left\langle\frac{\beta-1}{\beta+1}\frac{t+1}{|t-1|}\right\rangle\right] . \qquad \text{(II.1-15)}$$

One notes that $f(t)$ satisfies (II.1-10) as required. Equation (II.1-15) represents the distribution function in dimensionless form. The true distribution on the real interval [R, L+R] is

$$f(\zeta) = \frac{2\tau}{\pi G_1 b}\left[\left(\frac{\pi}{2} + \sin^{-1}\frac{\beta-1}{\beta+1}\right)(\beta-1)\left\{\frac{1}{1+(\beta-1)\zeta} + \left\langle\frac{1}{1+(\beta-1)\zeta}\right\rangle^2\right\}\right.$$

$$\left. \times\sqrt{(1-\zeta)(\zeta+1/\beta)} + \left\{1 + \left\langle\frac{1}{1+(\beta-1)\zeta}\right\rangle^2\right\}\cosh^{-1}\left\langle\frac{2+(\beta-1)\zeta}{(\beta+1)\zeta}\right\rangle\right], \qquad \text{(II.1-16)}$$

where $\zeta = \rho_0/L$, and ρ_0 is the distance from the pileup tip (R,0) to any point in the distribution. $f(\zeta)$ is shown in Figure II-4 for several values of β. Using (II.1-16) one finds agreement with the limiting cases previously studied:

$$f(\zeta) \to \frac{4\tau}{\pi G_1 b}\cosh^{-1}\left(\frac{1}{\zeta}\right) \quad \text{as} \quad R \to \infty \text{ (semi-infinite second phase)}$$

$$f(\zeta) \to \frac{2\tau}{G_1 b}\sqrt{\frac{1-\zeta}{\zeta}} \quad \text{as} \quad R \to 0 \text{ (single phase homogeneous medium)} . \qquad \text{(II.1-17)}$$

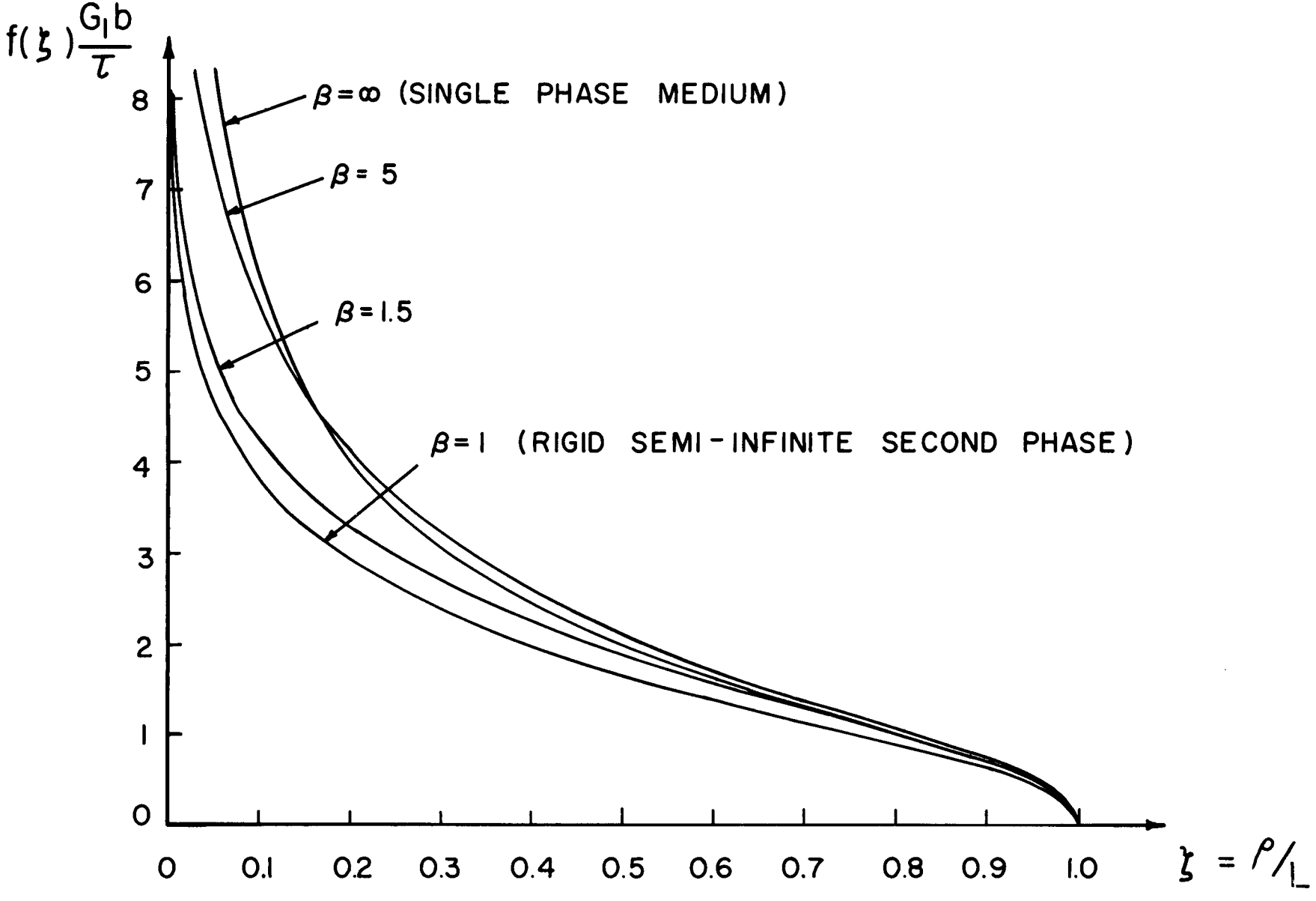

Figure II-4: $f(\zeta)$, the dislocation distribution function, versus ζ for several values of β.

2. The Pileup Stress Field

Evaluation of the superposition integral to yield the stresses associated with the array (excluding the component of the applied stress) is accomplished by contour integrations in the complex plane as outlined in Appendix C. The calculations are somewhat tedious and are most simply performed when (1) $x^2 + y^2 = R^2$, i.e., along the interface, and (2) $y = 0$, along the slip plane.

Interface Stresses

The stress τ_{rz} tending to shear the matrix-inclusion interface is given by

$$\tau_{rz} = -\frac{2\tau}{\pi}\left\{ \left\langle \sinh^{-1}\left(\frac{\beta-1}{\beta+1}\left|\cot\frac{\theta}{2}\right|\right)\right\rangle \cos\theta - \frac{\pi}{2}\sin\theta \right.$$

$$\left. + \left\langle \frac{\pi}{2} + \sin^{-1}\frac{\beta-1}{\beta+1}\right\rangle \cos\frac{\theta}{2}\sqrt{\frac{\beta^2-2\beta\cos\theta+1}{\beta}}\right\} . \quad \text{(II.2-1)}$$

Using the relations

$$\theta = \pi - 2\varphi ,$$

$$\frac{\rho}{L} = \frac{2\cos\varphi}{\beta-1} , \quad \text{(II.2-2)}$$

where θ and φ are polar angles relative to the origin and pileup tip, respectively, and ρ is the vector measured from the pileup tip (Figure II-1), τ_{rz} can be expressed as a function of only ρ/L. The result is shown in Figures II-5a and II-5b for two values of β.

Although the shear τ_{rz} is continuous across the interface, the stress $\tau_{\theta z}$ is not. Approaching the interface from inside the inclusion

$$\tau_{\theta z} = -\frac{2\tau}{\pi^2}\left\{\left[\left(\sinh^{-1}\left(\frac{\beta-1}{\beta+1}\left|\cot\frac{\theta}{2}\right|\right)\right)^2 + \left(\sin^{-1}\frac{\beta-1}{\beta+1}\right)^2\right]\cos\theta\right.$$

$$+\frac{\beta-1}{\sqrt{\beta}}\cos^{-1}\frac{\beta-1}{\beta+1} - \left(\frac{\pi}{2}+\sin^{-1}\frac{\beta-1}{\beta+1}\right)\left[\frac{\beta-1}{\sqrt{\beta}}+\frac{(\beta-1)^2}{2\beta}\cos^{-1}\frac{\beta-1}{\beta+1}\right.$$

$$+2\left(\sin^{-1}\frac{\beta-1}{\beta+1}\right)\cos\theta - 2\cos\frac{\theta}{2}\sqrt{\frac{\beta^2-2\beta\cos\theta+1}{\beta}}$$

$$\left.\left.\times\sinh^{-1}\left(\frac{\beta-1}{\beta+1}\left|\cot\frac{\theta}{2}\right|\right)\right]\right\}. \qquad \text{(II.2-3)}$$

Taking the limit as $R\to\infty$, $\varphi\to\pi/2$, one finds the interface stresses at the semi-infinite second phase.

$$\tau_{rz}(\text{interface}) \to \tau_{xz}(\text{interface}) = -\frac{2\tau}{\pi}\sinh^{-1}\frac{L}{y}$$

$$\tau_{\theta z}(\text{interface}) \to \tau_{yz}(\text{interface}) = -\frac{2\tau}{\pi^2}\left(\sinh^{-1}\frac{L}{y}\right)^2 \qquad \text{(II.2-4)}$$

The interface shear τ_{xz} at a rigid semi-infinite second phase is depicted in Figure II-6.

Shear Stresses on the Slip Plane $y = 0$

Inside the inclusion the stress τ_{yz} on the slip plane $y = 0$ tending to shear the inclusion is

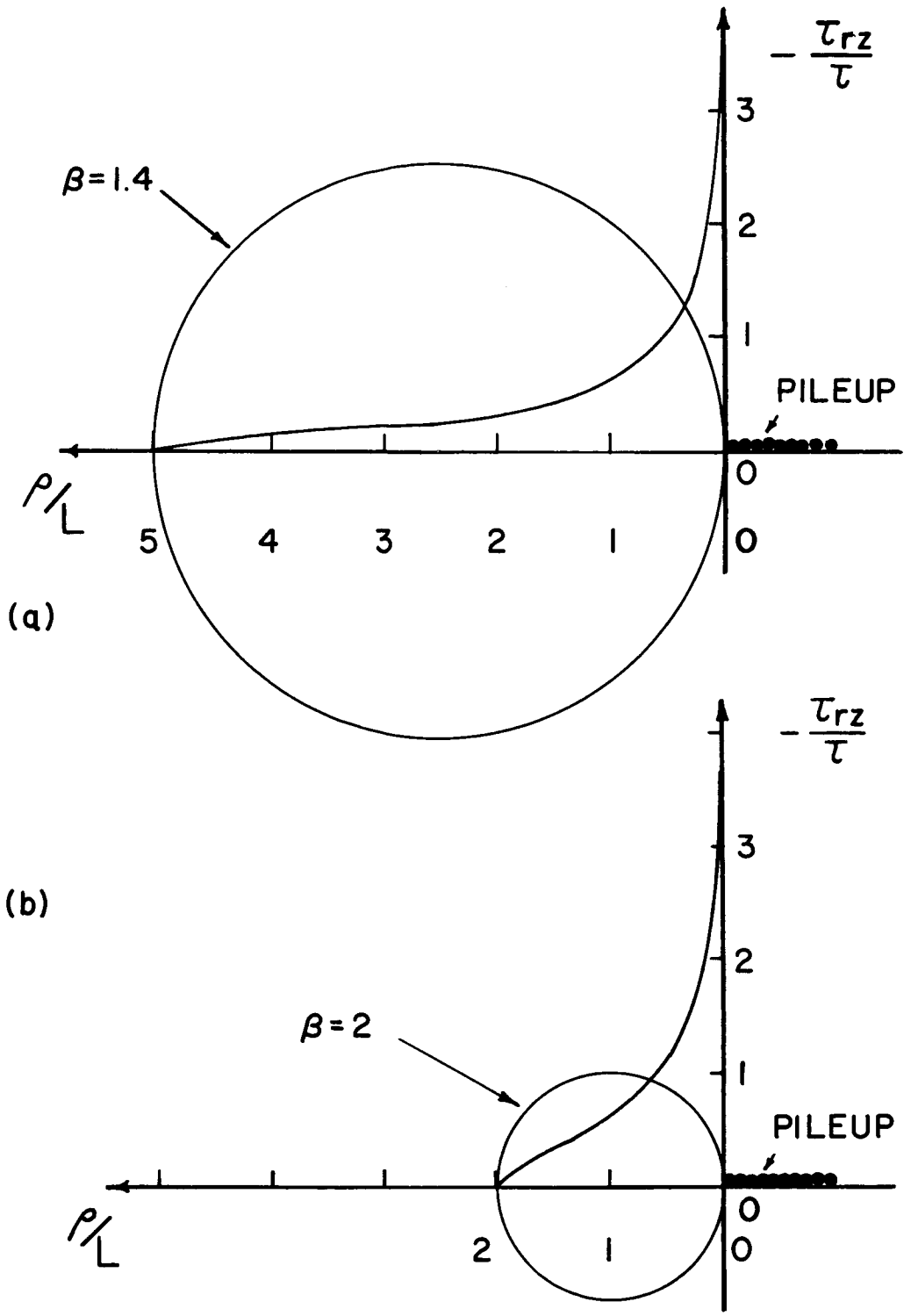

Figure II-5a,b: The shear stress τ_{rz} along the second phase-matrix interface for two values of β. ρ is the distance from the pileup tip to any point along the interface.

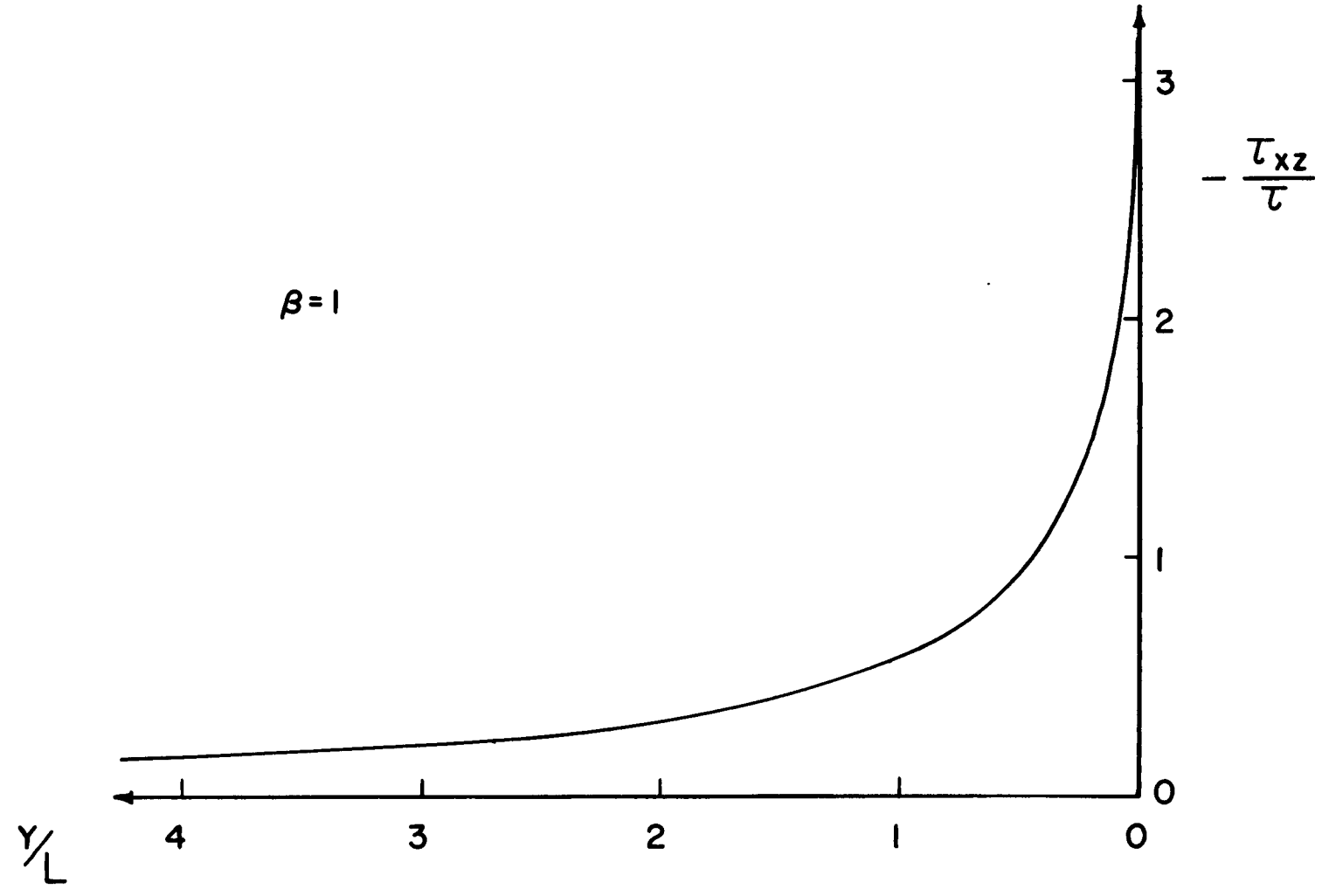

Figure II-6: The shear stress τ_{xz} along the interface of a rigid semi-infinite second phase.

$$\tau_{yz}(y = 0) = -\frac{4\tau}{\pi^2}\left\{\frac{1}{4}\left(1 + \frac{1}{\lambda^2}\right)\left[\left\langle\cosh^{-1}\left(\frac{\beta-1}{\beta+1}\,\frac{1+\lambda}{1-\lambda}\right)\right\rangle^2 + \left(\cos^{-1}\frac{\beta-1}{\beta+1}\right)^2\right]\right.$$

$$-\frac{\beta-1}{2\sqrt{\beta}}\,\frac{\pi}{\lambda} + \frac{\pi}{2}\sin^{-1}\frac{\beta-1}{\beta+1} + \frac{1}{2}\left\langle\frac{\pi}{2} + \sin^{-1}\frac{\beta-1}{\beta+1}\right\rangle$$

$$\times\left[-\left(\frac{\pi}{2} + \sin^{-1}\frac{\beta-1}{\beta+1}\right) + \left(\frac{1}{\lambda} + \frac{1}{\lambda^2}\right)\sqrt{(\beta-\lambda)(\lambda - 1/\beta)}\right.$$

$$\left.\left.\times\cosh^{-1}\left(\frac{\beta-1}{\beta+1}\,\frac{1+\lambda}{1-\lambda}\right) + \left(\frac{1}{\lambda^2} - \frac{(\beta-1)^2}{2\beta}\cdot\frac{1}{\lambda}\right)\cos^{-1}\frac{\beta-1}{\beta+1}\right]\right\},$$

$$1 > \lambda \geq \frac{1}{\beta} \qquad \text{(II.2-5)}$$

where

$$\lambda = \frac{x}{R} \qquad \text{and} \qquad \frac{\rho}{L} = \frac{1-\lambda}{\beta-1}\,.$$

For $-1 \leq \lambda \leq 1/\beta$, τ_{yz} is given by the same expression with

$$\left\langle\cosh^{-1}\left(\frac{\beta-1}{\beta+1}\,\frac{1+\lambda}{1-\lambda}\right)\right\rangle^2 \qquad \text{and} \qquad \cosh^{-1}\left(\frac{\beta-1}{\beta+1}\,\frac{1+\lambda}{1-\lambda}\right)$$

replaced by

$$-\left\langle\cos^{-1}\left(\frac{\beta-1}{\beta+1}\,\frac{1+\lambda}{1-\lambda}\right)\right\rangle^2 \qquad \text{and} \qquad -\cos^{-1}\left(\frac{\beta-1}{\beta+1}\,\frac{1+\lambda}{1-\lambda}\right),$$

respectively.

Outside the inclusion the slip plane shear stress is:

$$\tau_{yz} = \frac{\tau}{\pi}\left\{\frac{\pi}{2}\left(1 - \frac{1}{\lambda^2}\right) + \left(1 + \frac{1}{\lambda^2}\right)\sin^{-1}\left(\frac{\beta-1}{\beta+1}\,\frac{|\lambda|-1}{|\lambda|+1}\right)\right.$$

$$\left.+ \left(\frac{\pi}{2} + \sin^{-1}\frac{\beta-1}{\beta+1}\right)\left(\frac{1}{\lambda} + \frac{1}{\lambda^2}\right)\sqrt{(\beta-\lambda)(1/\beta - \lambda)}\right\};$$

$$\lambda < -1\,. \qquad \text{(II.2-6)}$$

The slip plane shear stress inside and outside the inclusion is shown as a function of ρ/L in Figures II-7a and II-7b for two values of β.

Taking the limit as $R \to \infty$, the slip plane shear stress inside a rigid semi-infinite second phase is seen to be

$$\tau_{yz} = -\frac{2\tau}{\pi^2}\left\{\frac{\pi^2}{4} + \left\langle \cosh^{-1}\frac{L}{|x|}\right\rangle^2\right\}; \quad |x| < L$$

$$= -\frac{2\tau}{\pi^2}\left\{\frac{\pi^2}{4} - \left\langle \cos^{-1}\frac{L}{|x|}\right\rangle^2\right\}; \quad |x| > L \qquad \text{(II.2-7)}$$

in agreement with Chou's earlier calculation.[33] Letting $R \to 0$ in (II.2-6) one recovers the expression for the slip plane shear stress ahead of a pileup in a homogeneous single phase material.

$$\tau_{yz} = \tau\left\{1 - \sqrt{1 + \frac{L}{|x|}}\right\}; \qquad x < 0 \qquad \text{(II.2-8)}$$

Equations (II.2-7) and (II.2-8) are compared graphically in Figure II-8.

Inside the inclusion at distances close to the pileup tip ($L/\rho \gg 1$, $\lambda \approx 1$) the important singular terms contributing to the shear stress on the slip plane are

$$\tau_{yz} = -\frac{2\tau}{\pi^2}\cosh^{-1}\left(\frac{L}{\rho}\left\langle 1 - \frac{L-\rho}{L+2R}\right\rangle\right)$$

$$\times\left[\cosh^{-1}\left(\frac{L}{\rho}\left\langle 1 - \frac{L-\rho}{L+2R}\right\rangle\right) + 2\left(\frac{\pi}{2} + \sin^{-1}\frac{\beta-1}{\beta+1}\right)\frac{\beta-1}{\sqrt{\beta}}\right]. \qquad \text{(II.2-9)}$$

The first term in (II.2-9) is dominant if

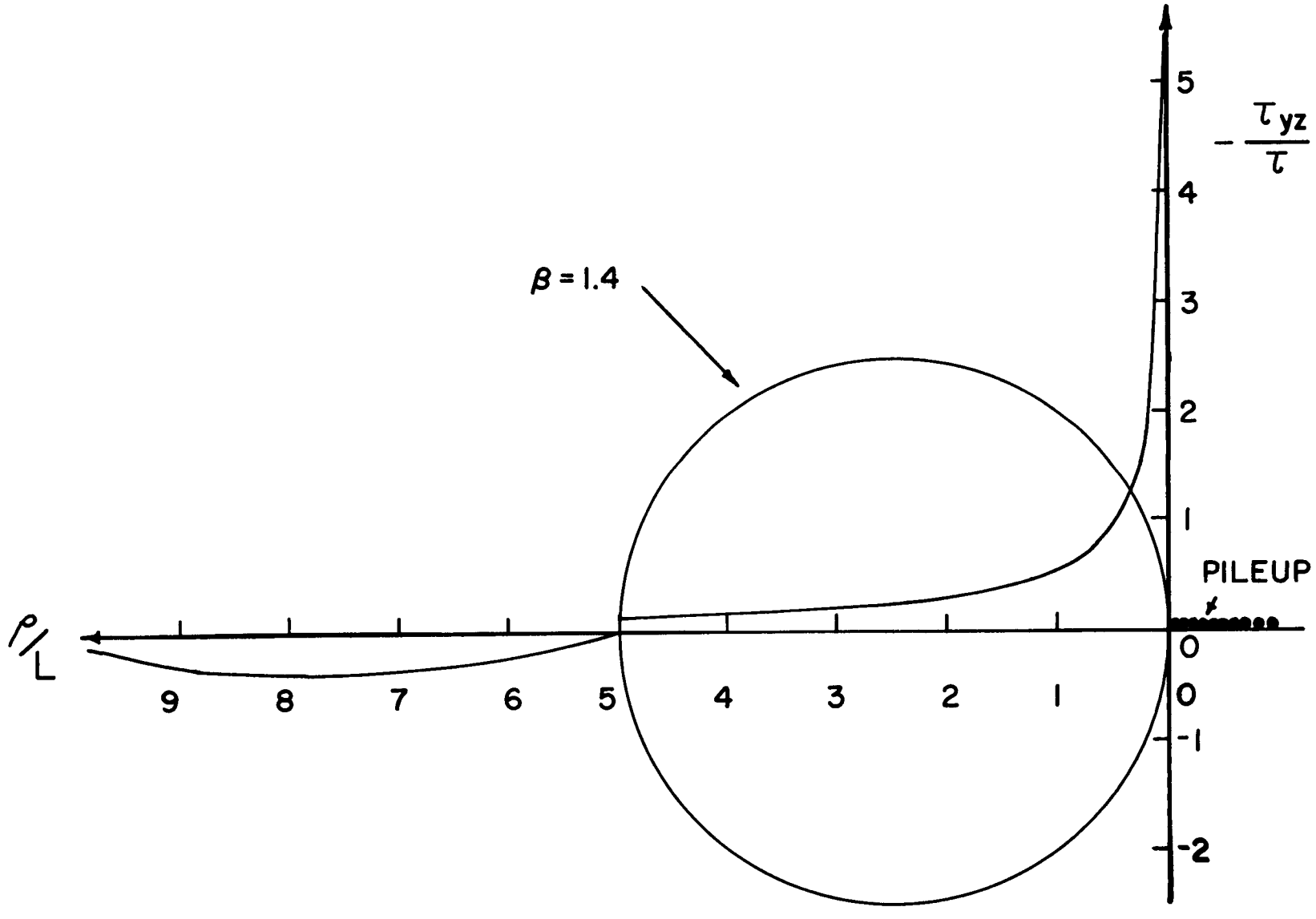

Figure II-7a: The shear stress τ_{yz} on the slip plane $y = 0$ ahead of a screw pileup. $\beta = 1.4$.

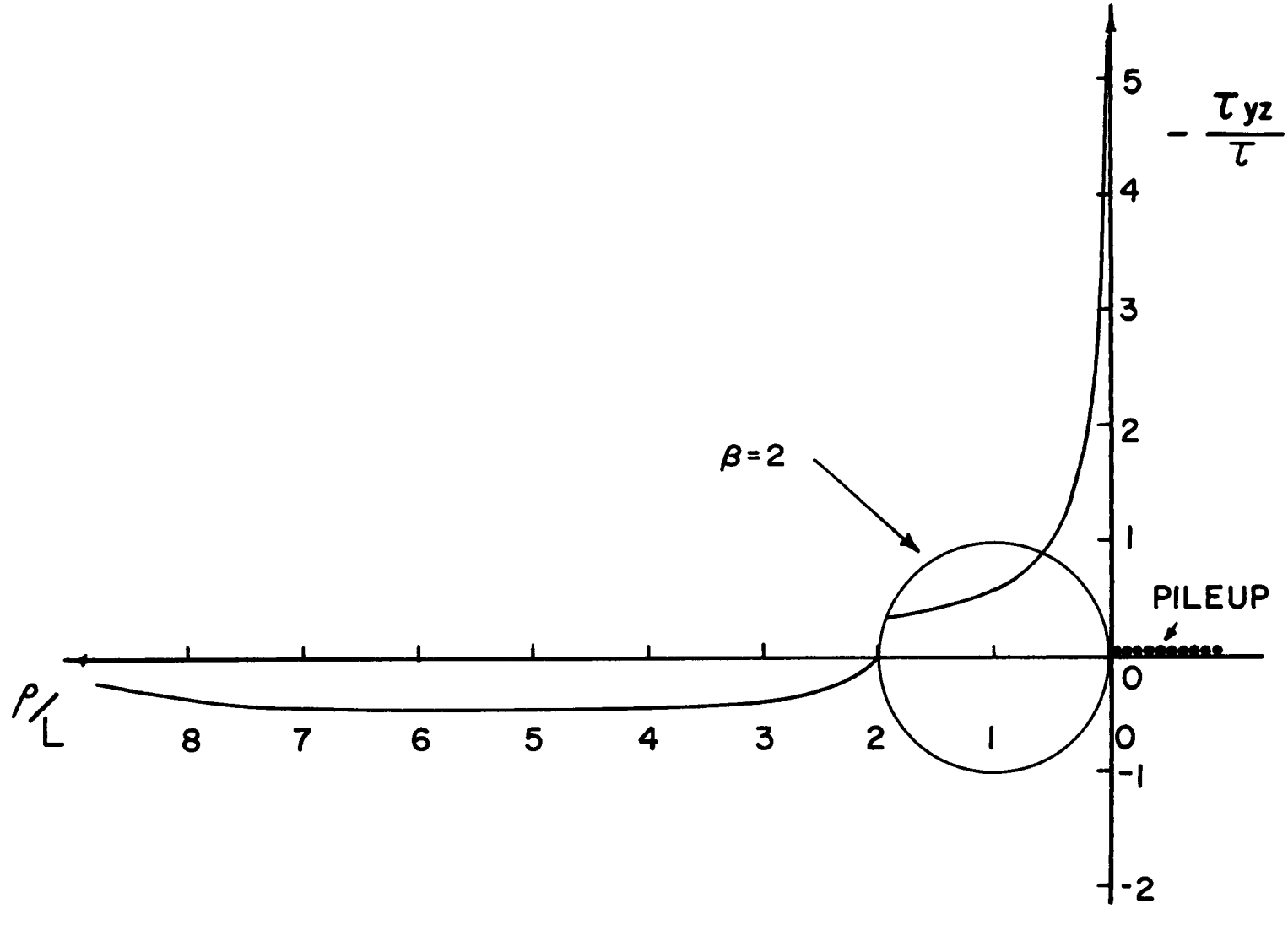

Figure II-7b: The shear stress τ_{yz} on the slip plane $y = 0$ ahead of a screw pileup. $\beta = 2$.

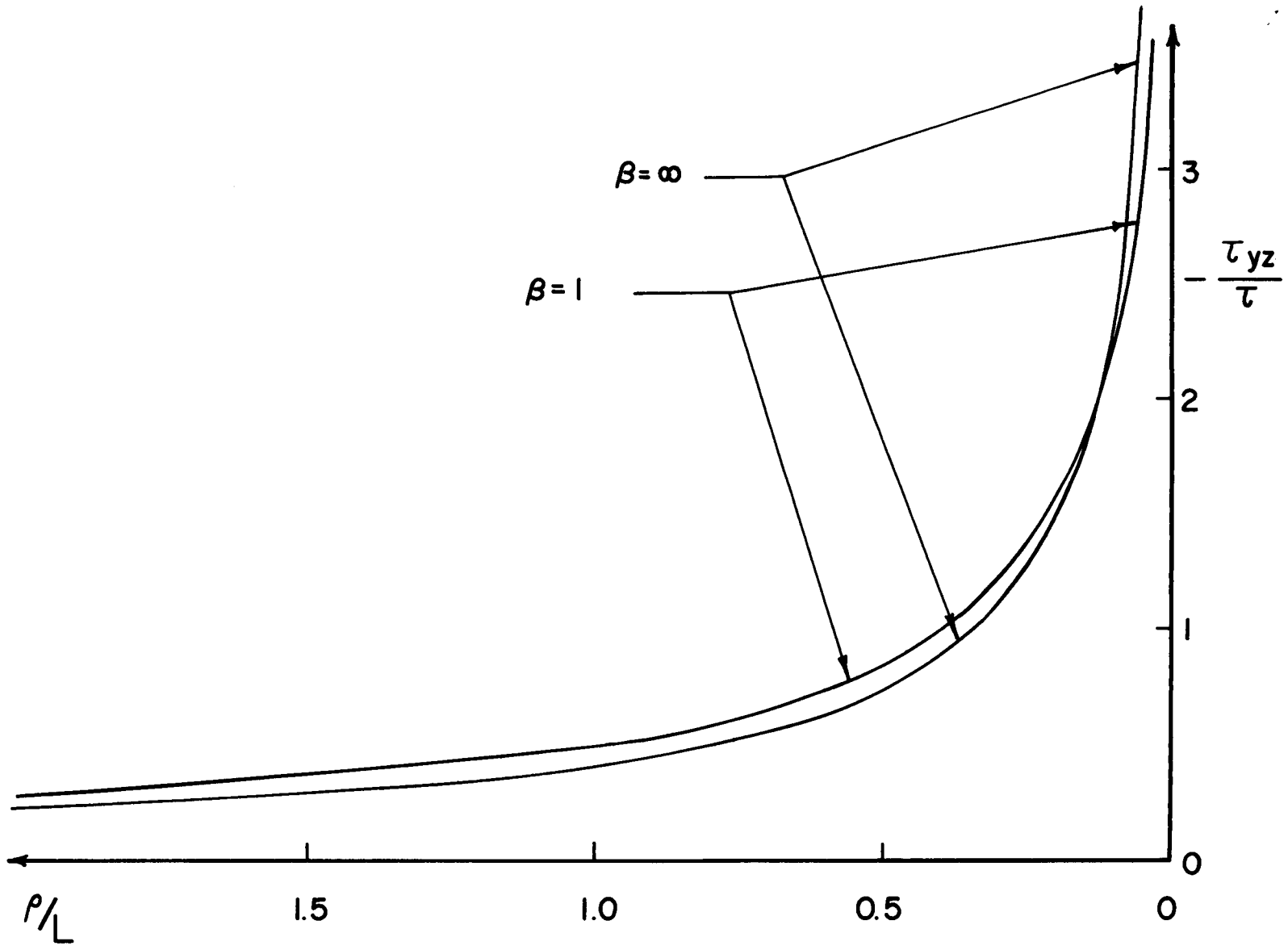

Figure II-8: The shear stress τ_{yz} on the slip plane $y = 0$ ahead of a screw pileup (1) at a rigid half-plane ($\beta = 1$) and (2) in a single phase medium ($\beta = \infty$).

$$\frac{L}{\rho}\left[1 - \frac{L-\rho}{L+2R}\right] > \cosh\left[2\,\frac{\beta-1}{\sqrt{\beta}}\left(\frac{\pi}{2} + \sin^{-1}\frac{\beta-1}{\beta+1}\right)\right]\ ; \quad \text{(II.2-10)}$$

If the inequality is reversed, then the second term in (II.2-9) dominates. Now consider two distinct cases:

Case I. $L/R > 5$

Physically this case might correspond to that of a dispersion hardened material. When $L/R > 5$,

$$\frac{L}{\rho}\left\{1 - \frac{L-\rho}{L+2R}\right\} \approx \frac{L}{\rho}\left\{1 - \left(1 - \frac{\rho}{L}\right)\left(1 - \frac{2R}{L}\right)\right\}$$

$$\approx 1 + \frac{2R}{\rho}\ . \qquad \text{(II.2-11)}$$

Thus (II.2-9) and (II.2-10) combine to yield

$$\tau_{yz} \approx -\frac{4\tau}{\pi}\sqrt{\frac{L}{R}}\cosh^{-1}\left(1 + \frac{2R}{\rho}\right) \qquad \text{(II.2-12)}$$

when

$$\frac{\rho}{2L} > \frac{2R}{L}\ 10^{-0.8\pi\sqrt{L/R}}\ .$$

In this range of ρ, τ_{yz} decreases as R increases (ρ fixed).

If

$$\frac{\rho}{2L} < \frac{2R}{L}\ 10^{-0.8\pi\sqrt{L/R}}\ ,$$

then

$$\tau_{yz} \approx -\frac{2\tau}{\pi^2}\left\langle\cosh^{-1}\left(1 + \frac{2R}{\rho}\right)\right\rangle^2\ , \qquad \text{(II.2-13)}$$

and τ_{yz} increases as R increases (fixed ρ). For $L/R > 5$, (II.2-13) can only apply when $\rho/2L < 2/5 \times 10^{-5}$. Since L, the slip line length, typically varies between 10^{-4} and 10^{-6} cm, (II.2-13) can only apply when ρ is less than one Burgers' vector. Thus, at distances of physical significance, equation (II.2-12) will describe the stress state near the pileup tip in the inclusion.

Case II. $L/R < 0.8$.

This case might correspond to a cermet containing a hard phase volume fraction of about 60% ($L \approx 10^{-4}$ cm, $R \approx 2 \times 10^{-4}$ cm). Proceeding as in Case I, when

$$\frac{\rho}{L} > 10^{-0.4\pi L/R} ,$$

$$\tau_{yz} = -\frac{2\tau}{\pi^2}\frac{L}{R}\cosh^{-1}\left(\frac{L}{\rho}\right) . \qquad \text{(II.2-14)}$$

In this range of ρ, τ_{yz} (at fixed ρ) decreases as R increases. When

$$\frac{\rho}{L} < 10^{-0.4\pi L/R} ,$$

$$\tau_{yz} \approx -\frac{2\tau}{\pi^2}\left(\cosh^{-1}\frac{L}{\rho}\right)^2 , \qquad \text{(II.2-15)}$$

so that the inclusion radius has no effect upon the slip plane shear stress. Again taking typical values for L, the slip line length, Eq. (II.2-15) can apply when ρ is between 10 and 500 Burgers' vectors, a region of considerable physical significance.

Since the case of a perfectly rigid inclusion is never physically realized, little useful information is to be gained from further discussion of the local stresses. The feature of primary interest in this problem is the form of the dislocation distribution function (Eq. (II.1-15)). As mentioned previously, knowledge of the distribution function associated with this problem, when coupled with the solution to be generated in the following chapter, will allow us to construct the exact solution for a screw dislocation pileup at a circular inclusion of finite rigidity.

CHAPTER III

A SCREW DISLOCATION PILEUP AT AN ELASTIC HALF-PLANE OF FINITE RIGIDITY

1. Analysis

Having treated the problem of a screw array blocked at a rigid inclusion of finite size, we shall proceed to the "opposite end of the spectrum" and examine a screw array stopped by a second phase which is semi-infinite in size but of finite rigidity. This is the completely general case of the problem discussed by Chou.[33]

Consider a bimetal composed of two elastic half-planes joined by a perfect weld along $x = 0$. The shear modulus is G_1 if $x > 0$, G_2 is $x < 0$. Let a linear array of length L of N right hand screw dislocations, each of Burgers' vector b, be piled up against the weld under the action of an applied shear $\tau_{yz} = -\tau(x) = -\tau$, a constant (Figure III-1). Using Eqs. (I.3-5), the static equilibrium condition determining the positions x_i of the discrete dislocations becomes

$$\frac{G_1 b}{2\pi}\left\{\sum_{\substack{j=1\\ j\neq i}}^{N}\frac{1}{x_i - x_j} + K\sum_{j=1}^{N}\frac{1}{x_i + x_j}\right\} = \tau,$$

$$i = 1,2,\ldots, N \qquad \text{(III.1-1)}$$

where

$$K = \frac{G_2 - G_1}{G_2 + G_1}.$$

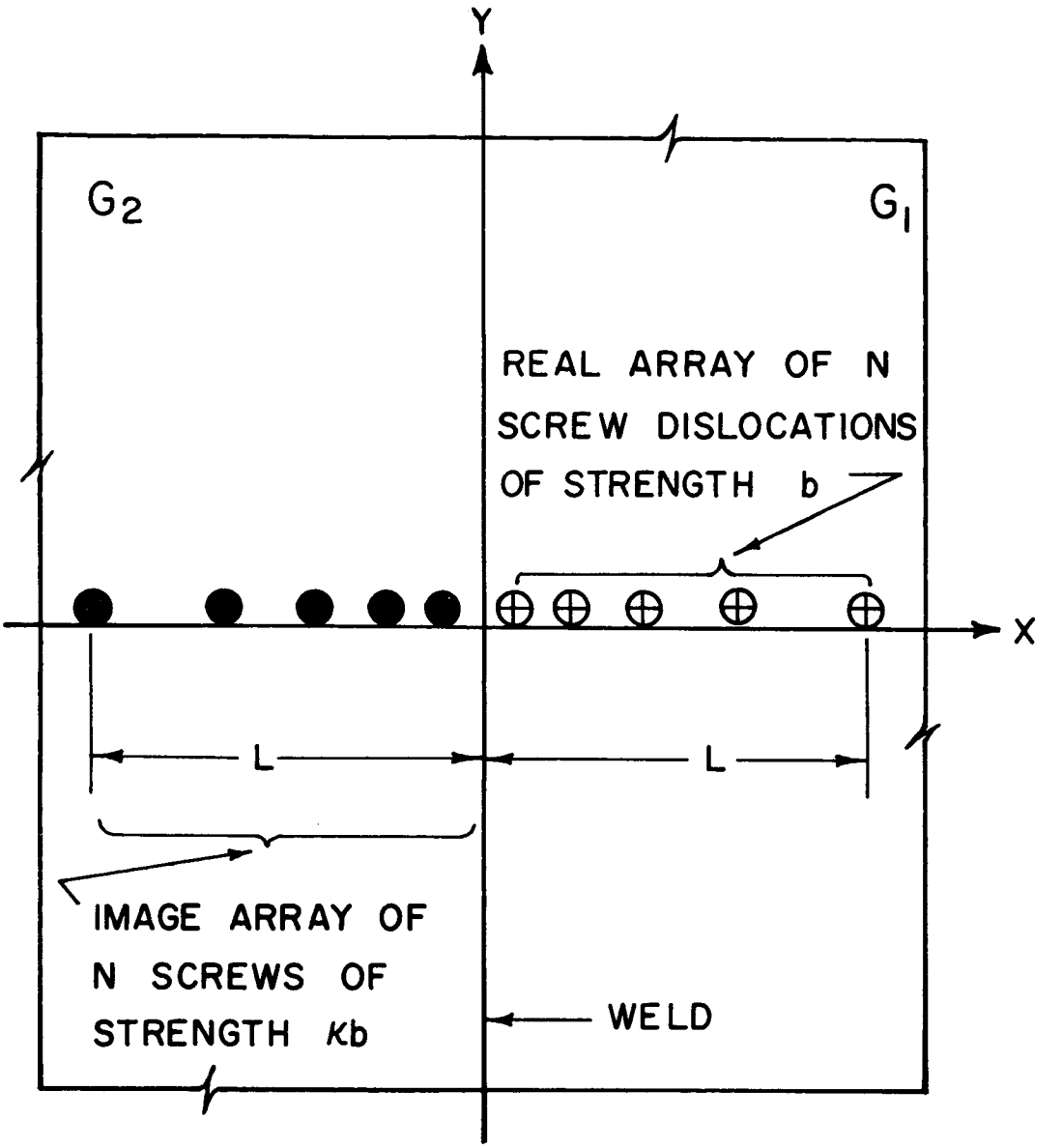

Figure III-1: A screw dislocation pileup at an elastic half-plane of finite rigidity and its induced image pileup.

The second sum in (III.1-1) can be interpreted as the stress on a pile-up dislocation at $(x_i,0)$ due to an image array of N screws, each of strength κb, at positions $(-x_j, 0)$, the image positions of the N real pileup dislocations. The force on the dislocation at $(x_i, 0)$ exerted by the image array is attractive if $\kappa < 0$ (the pileup exists in the harder phase), repulsive if $\kappa > 0$ (the pileup exists in the softer phase). Invoking the continuous distribution approximation, (III.1-1) is transformed into the singular integral equation

$$\int_0^L \frac{f(t)\,dt}{x-t} + \kappa \int_0^L \frac{f(t)\,dt}{x+t} = \frac{2\pi\tau}{G_1 b} \quad ; \qquad 0 < x \leq L \qquad \text{(III.1-2)}$$

with the end conditions $f(L) = 0$; $f(0)$ unbounded with a weak singularity. $f(t)$ is the unknown dislocation distribution function.

No ambiguity in the form of $\tau(x)$, the applied shear, arises in this problem. The elastic solution for the bimetallic medium subjected to an applied shear $\tau_{yz} = -\tau$ at infinity (in $x > 0$) is

$$\left.\begin{aligned} w &= -\frac{\tau}{G_1} y \\ \tau_{xz} &= 0 \\ \tau_{yz} &= -\tau \qquad (x > 0) \\ &= -\frac{G_2}{G_1}\tau \quad (x < 0)\,, \end{aligned}\right\} \qquad \text{(III.1-3)}$$

where w is the displacement field in the z-direction.

Equation (III.1-2) cannot be reduced to a single integral equation with only a Cauchy kernel. However, an exact solution to (III.1-2) can be obtained by considering the appropriate Neumann expansion for $f(t)$. Details of the calculation are given in Appendix D. One finds

$$f(t) = \frac{2\tau}{G_1 b}\sqrt{\frac{2}{1-\kappa}}\sinh\left\{\left(\frac{2}{\pi}\sin^{-1}\sqrt{\frac{1-\kappa}{2}}\right)\cosh^{-1}\left(\frac{L}{t}\right)\right\}, \quad \text{(III.1-4)}$$

which may also be written as

$$f(t) = \frac{\tau}{G_1 b}\sqrt{\frac{2}{1-\kappa}}\left(\frac{L}{t}\right)^g\left\{\left(1+\sqrt{1-(t/L)^2}\right)^g - \left(1-\sqrt{1-(t/L)^2}\right)^g\right\}, \quad \text{(III.1-5)}$$

where

$$g = \frac{2}{\pi}\sin^{-1}\sqrt{\frac{1-\kappa}{2}}\,. \quad \text{(III.1-6)}$$

Equation (III.1-4) is the most convenient form to use when computing integrals involving $f(t)$. Considering the two limiting cases $\kappa \to 1$ and $\kappa \to 0$,

$$f(t) \to \frac{4\tau}{\pi G_1 b}\cosh^{-1}\left(\frac{L}{t}\right) \quad \text{as} \quad \kappa \to 1 \quad \text{(rigid, semi-infinite second phase)}$$

$$f(t) \to \frac{2\tau}{G_1 b}\sqrt{\frac{L-t}{t}} \quad \text{as} \quad \kappa \to 0 \quad \text{(single phase, homogeneous medium)} \quad \text{(III.1-7)}$$

in agreement with previous results. Figure III-2 depicts $f(t)$ for different values of κ.

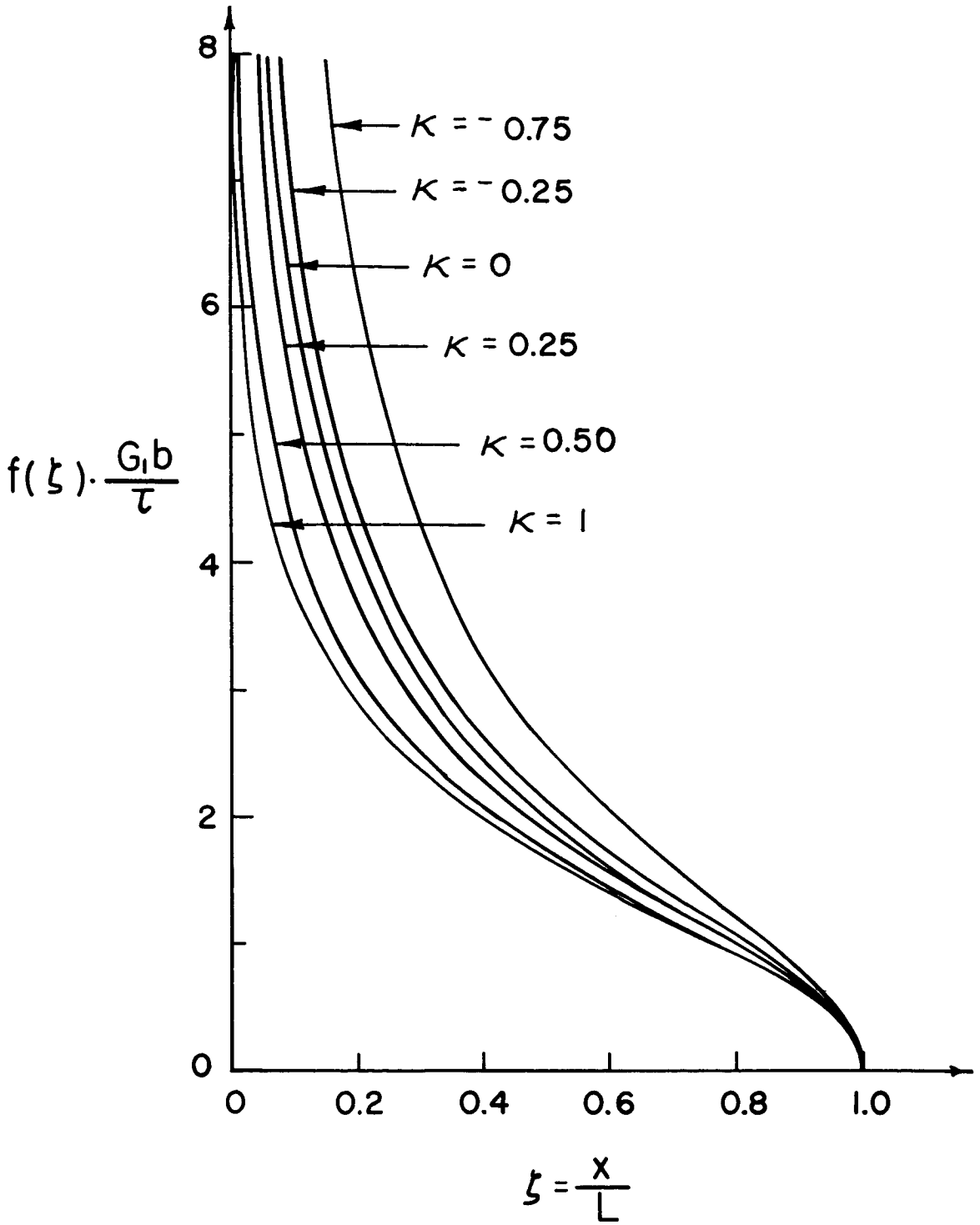

Figure III-2: $f(\zeta)$, the dislocation distribution function, versus $\zeta = x/L$ for different relative rigidity ratios (κ).

The number, N, of dislocations in the pileup is given by

$$\frac{2\pi\tau}{G_1 b}\frac{L}{N} = \frac{\pi}{2}\frac{\sqrt{1-\kappa^2}}{\sin^{-1}\sqrt{\frac{1-\kappa}{2}}} \quad . \qquad \text{(III.1-8)}$$

Chou[33] had predicted that in the range $0 \leq \kappa \leq 1$

$$\left(\frac{2\pi\tau}{G_1 b}\right)\frac{L}{N} = 2 + (\pi-2)\kappa \quad . \qquad \text{(III.1-9)}$$

Both Eqs. (III.1-8) and (III.1-9) are plotted in Figure III-3, and, indeed, the linear relation of Chou does not differ any more than about 1% from the exact relation when $0 \leq \kappa \leq 1$. For $\kappa < 0$, however, the linear relation is not valid.

One notes that when $G_2 = 0$ (i.e., when $x = 0$ represents a free surface), $\kappa = -1$, the distribution function becomes

$$f(t) = \frac{2\tau}{G_1 b}\frac{\sqrt{L^2-t^2}}{t} \quad , \qquad \text{(III.1-10)}$$

and N becomes infinite. The distribution function given by (III.1-10) is characterized by a strong singularity at $t = 0$ and thus is not an admissible solution to (III.1-2).

2. The Pileup Stress Field

The stress field of the pileup (excluding the applied stress) is calculated from the superposition integrals

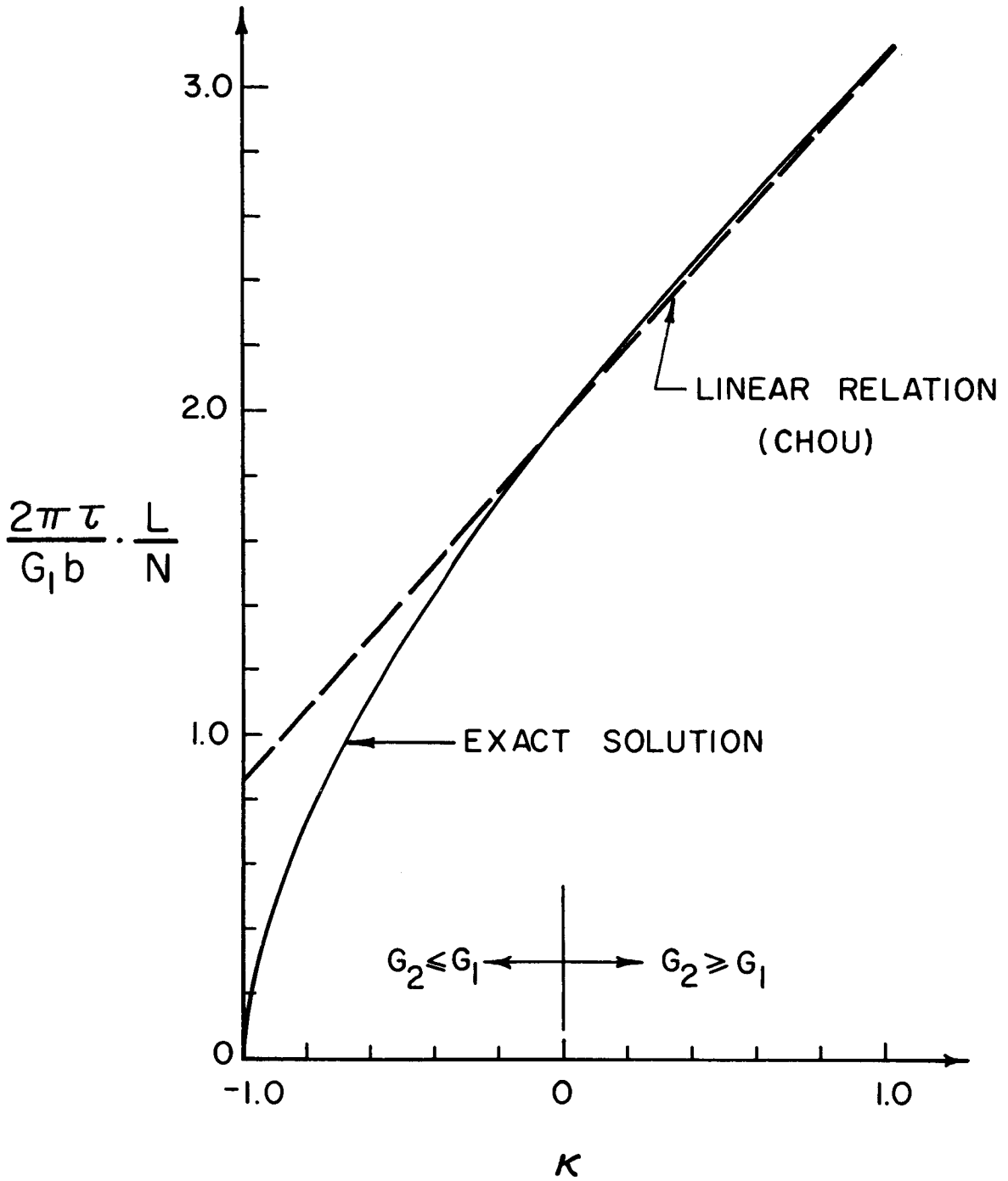

Figure III-3: $\frac{2\pi\tau}{G_1 b} \cdot \frac{L}{N}$ as a function of κ. The linear relation predicted by Chou when $0 \leq \kappa \leq 1$ is shown as a dashed line.

$$\tau_{ij}(x,y) = \int_0^L \tau_{ij}(x,y,t)\, f(t)\, dt \ . \qquad \text{(III.2-1)}$$

Making the substitution $v = \cosh^{-1}(L/t)$ and performing the necessary contour integrations in the complex $v = w + i\Omega$ plane, it is possible to obtain closed form expressions for the stresses (Appendix E). In the second phase $(x < 0)$:

$$\left.\begin{aligned} \tau_{xz} &= -\tau \frac{\sqrt{2(1+\kappa)}}{1-\kappa} \operatorname{sgn}(y) \sinh g\omega_0 \sin g\Omega_0 \\ \tau_{yz} &= -\tau \frac{\sqrt{2(1+\kappa)}}{1-\kappa} \{\cosh g\omega_0 \cos g\Omega_0 - \cos \tfrac{g\pi}{2}\} \\ &= -\tau \frac{\sqrt{2(1+\kappa)}}{1-\kappa} \cosh g\omega_0 \cos g\Omega_0 + \frac{G_2}{G_1}\tau \ , \end{aligned}\right\} \qquad \text{(III.2-2)}$$

where

$$\sinh^2 \omega_0 = \frac{1}{2}\left\{\left(\frac{L}{\rho}\right)^2 - 1 + \sqrt{\left\langle\left(\frac{L}{\rho}\right)^2 - 1\right\rangle^2 + \left\langle\frac{2L}{\rho}\sin\varphi\right\rangle^2}\right\} \qquad \text{(III.2-3)}$$

$$\sin^2 \Omega_0 = \frac{1}{2}\left\{1 - \left(\frac{L}{\rho}\right)^2 + \sqrt{\left\langle\left(\frac{L}{\rho}\right)^2 - 1\right\rangle^2 + \left\langle\frac{2L}{\rho}\sin\varphi\right\rangle^2}\right\} .$$

ρ and φ are polar coordinates relative to the pileup tip in the second phase (Figure III-4). One notes that the term $(G_2/G_1)\tau$ in τ_{yz} cancels the stress in $x < 0$ due to the applied shear (Eqs. (III.1-3)). For $\kappa \neq 1$ and $L/\rho \gg 1$ (close to the pileup tip), the net stresses in $x < 0$ are approximately

$$\left.\begin{aligned} \tau_{xz} &\approx -\tau \sqrt{\frac{1+\kappa}{2}} \frac{1}{1-\kappa} \left(\frac{2L}{\rho}\right)^g \sin g\varphi \\ \tau_{yz} &\approx -\tau \sqrt{\frac{1+\kappa}{2}} \frac{1}{1-\kappa} \left(\frac{2L}{\rho}\right)^g \cos g\varphi \ . \end{aligned}\right\} \qquad \text{(III.2-4)}$$

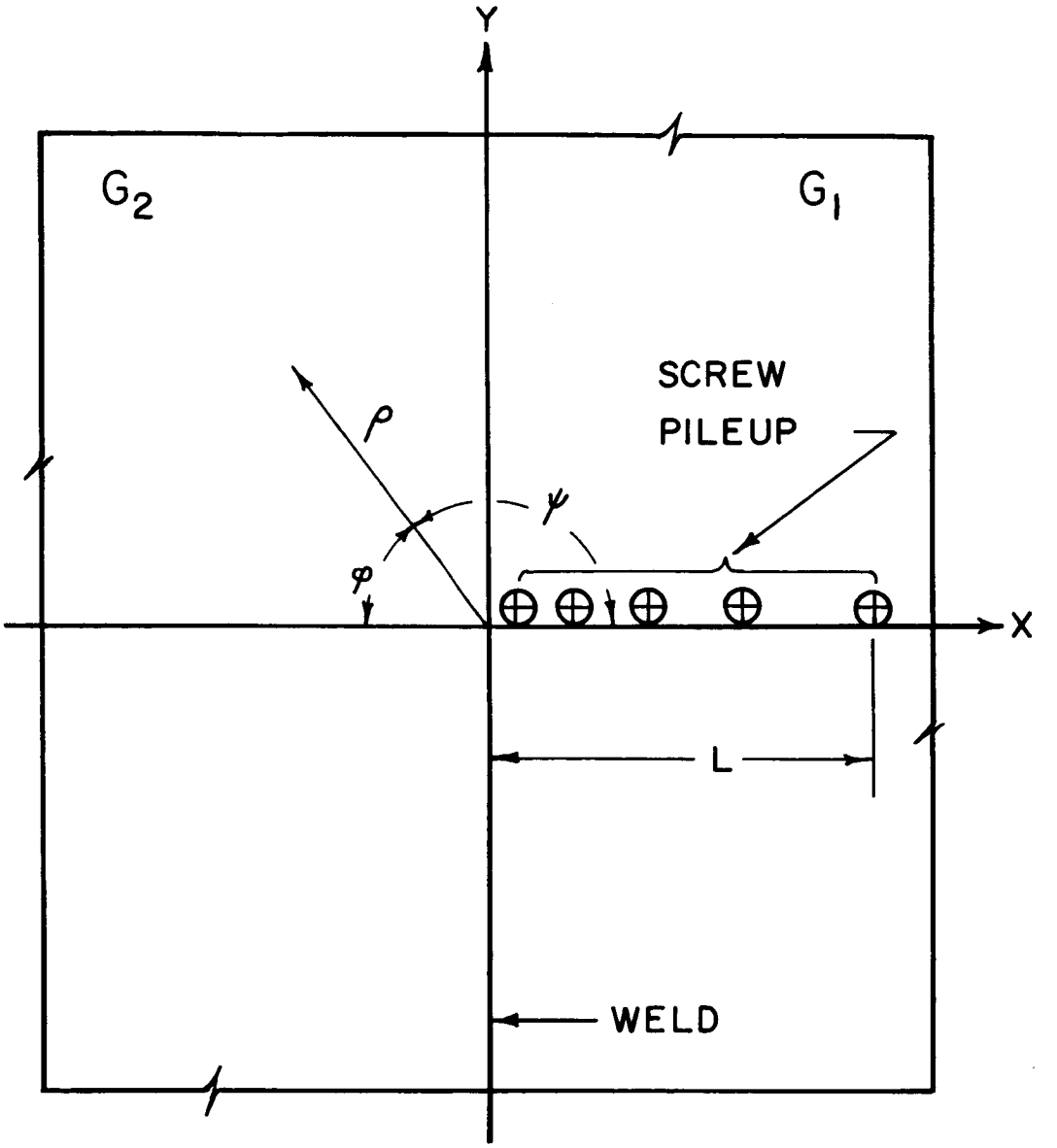

Figure III-4: The co-ordinate system used to express the stress field generated by a screw array at an elastic half-plane of finite rigidity.

When $\kappa = 1$ the stresses in the second phase diverge logarithmically as $\rho \to 0$. As an example the shear stress τ_{yz} on the slip plane $y = 0$ in the second phase is shown in Figure III-5 for several values of κ.

In the matrix $(x > 0)$ the pileup stress field is

$$\left.\begin{aligned} \tau_{xz} &= -\tau \sqrt{\frac{2}{1-\kappa}}\ \operatorname{sgn}(y) \sinh g\omega_0 \cos g\Omega_0 \\ \tau_{yz} &= -\tau \sqrt{\frac{2}{1-\kappa}}\ \cosh g\omega_0 \sin g\Omega_0 + \tau\ . \end{aligned}\right\} \qquad \text{(III.2-5)}$$

Again the term $+\tau$ in τ_{yz} just cancels the applied shear in $x > 0$. Close to the pileup tip in $x > 0$ the net stress field is approximately

$$\left.\begin{aligned} \tau_{xz} &\approx -\tau \operatorname{sgn}(y) \frac{1}{\sqrt{2(1-\kappa)}} \left(\frac{2L}{\rho}\right)^g \left|\cos g(\pi-\varphi)\right| \\ \tau_{yz} &\approx -\tau \frac{1}{\sqrt{2(1-\kappa)}} \left(\frac{2L}{\rho}\right)^g \left|\sin g(\pi-\varphi)\right|. \end{aligned}\right\} \qquad \text{(III.2-6)}$$

Thus, when $0 \leq \kappa < 1$ (i.e., the dislocation pileup is in the softer phase) then $0 < g \leq 1/2$ (eq. III.1-6). When $-1 < \kappa \leq 0$, the dislocation pileup is in the harder phase, and $1/2 \leq g < 1$. The stresses near the pileup tip will evidence the familiar inverse square root singularity[19] ($\tau_{ij} \sim \tau \sqrt{L/\rho}$) only if the medium is perfectly homogeneous ($\kappa = 0$). g as a function of κ is shown in Figure III-6. The presence of a second phase ahead of the dislocation slip band changes the form of the local stresses (Figure III-5), primarily because

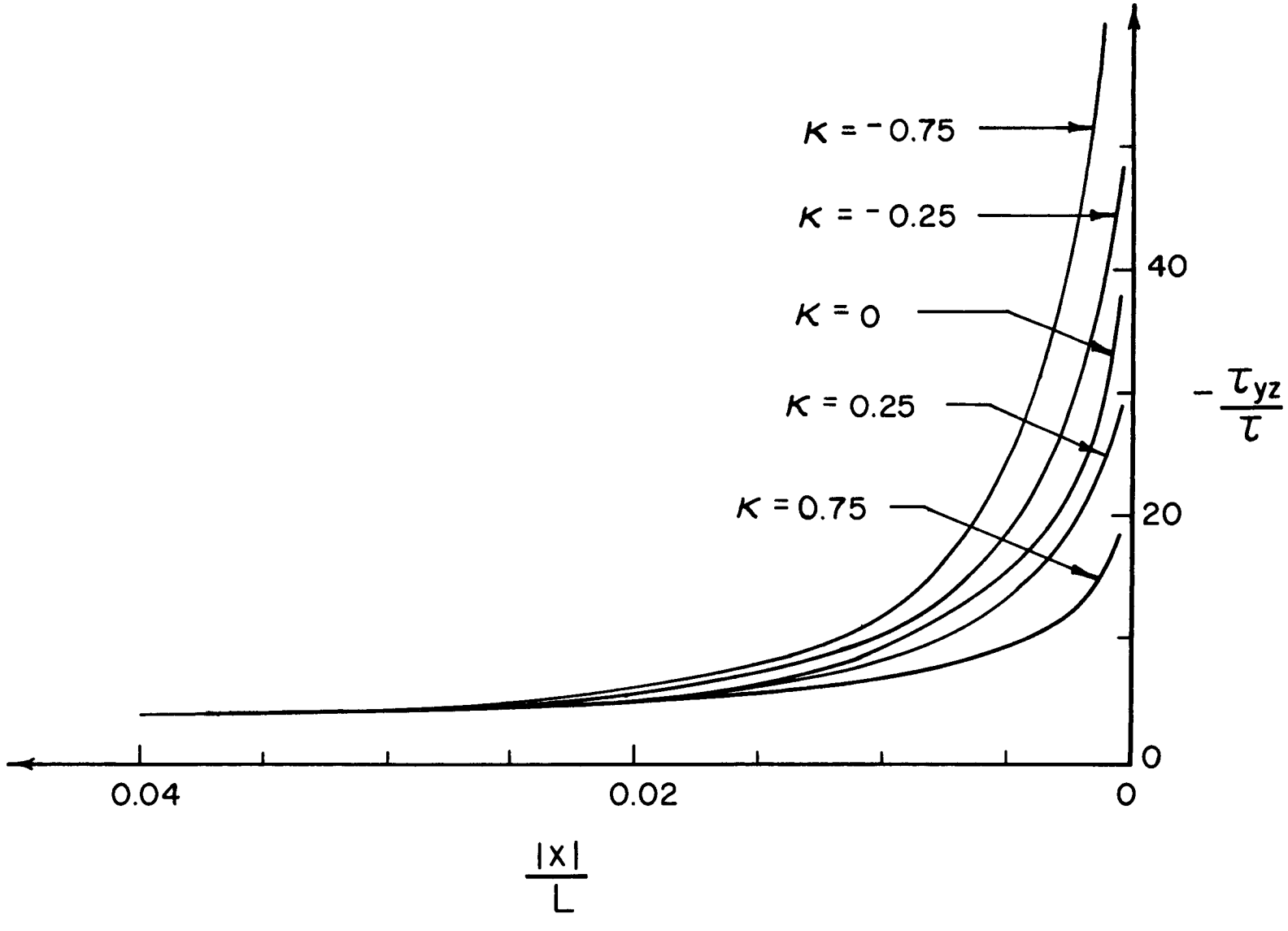

Figure III-5: The shear stress τ_{yz} on the slip plane $y = 0$ inside the second phase for different values of κ.

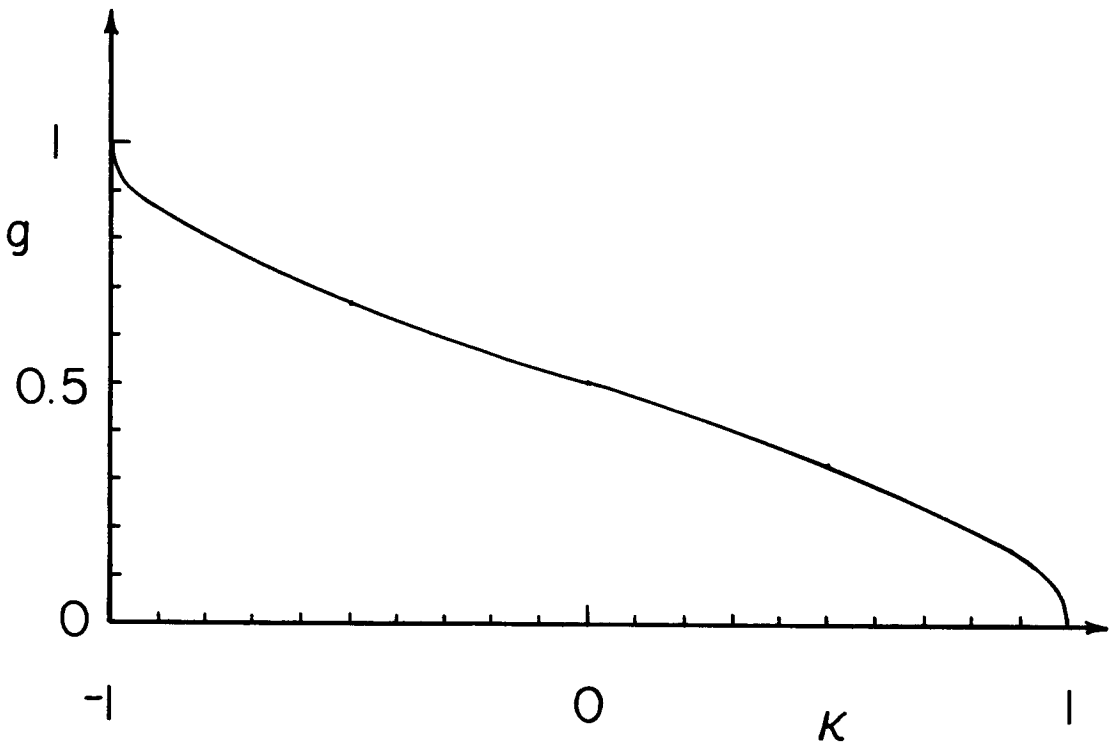

Figure III-6: g, the strength of the pileup tip stress singularity, as a function of κ.

image dislocation forces introduced by the inhomogeneity affect the dislocation configuration near the weld (Figure III-2). Equations (III.2-4) and (III.2-6) are consistent with results reported by Zak and Williams[35] for stress intensification in a bimetallic medium as treated by ordinary continuum elasticity methods.

Because of the form of Eqs. (III.2-4) and (III.2-6) any attempt to discuss crack initiation in a second phase ahead of a blocked slip band via a Griffith-Irwin[36] or Stroh approach encounters immediate difficulty. Both approaches are based upon the inverse square root stress singularity at the pileup tip. The effect of inhomogeneities segregated near grain boundaries might also alter the derivation of a Petch-type equation describing the grain size dependence of the yield stress for such a material, i.e.,

$$\sigma_y = \sigma_i + k_y d^{-1/2} , \qquad \text{(III.2-7)}$$

where

σ_y = yield stress

d = mean grain size

σ_i, k_y are constants .

The classical Petch relation is derived by considering local stresses ahead of a blocked slip band in a single phase medium. A similar derivation based upon the above analysis would replace the Petch relation by

$$\sigma_y = \sigma_i + k'_y d^{-g} , \qquad 0 < g < 1 . \qquad \text{(III.2-8)}$$

CHAPTER IV

A SCREW DISLOCATION PILEUP AT A CIRCULAR INCLUSION OF FINITE RIGIDITY

1. Formulation of the Problem

We are now in a position to remove the restriction of infinite inclusion rigidity imposed in Chapter II, thus allowing a study of the simultaneous effects of inclusion size and rigidity upon the local stresses ahead of a blocked slip band. The size effect will appear through variations of the parameter

$$\beta = \frac{L}{R} + 1 , \qquad \text{(IV.1-1)}$$

where L is the slip line length and R is the inclusion radius. The rigidity effect will appear through variations of the parameter

$$\kappa = \frac{G_2 - G_1}{G_2 + G_1} , \qquad \text{(IV.1-2)}$$

where G_2 and G_1 are the inclusion and matrix shear moduli, respectively.

When the relative rigidity G_2/G_1 can assume all values such that $-1 \leq \kappa \leq 1$, the static equilibrium condition describing a linear array of length L of N right-hand screw dislocations piled up against the inclusion under the application of a shear $\tau_{yz} = -\tau(x)$ (Figure IV-1a) is

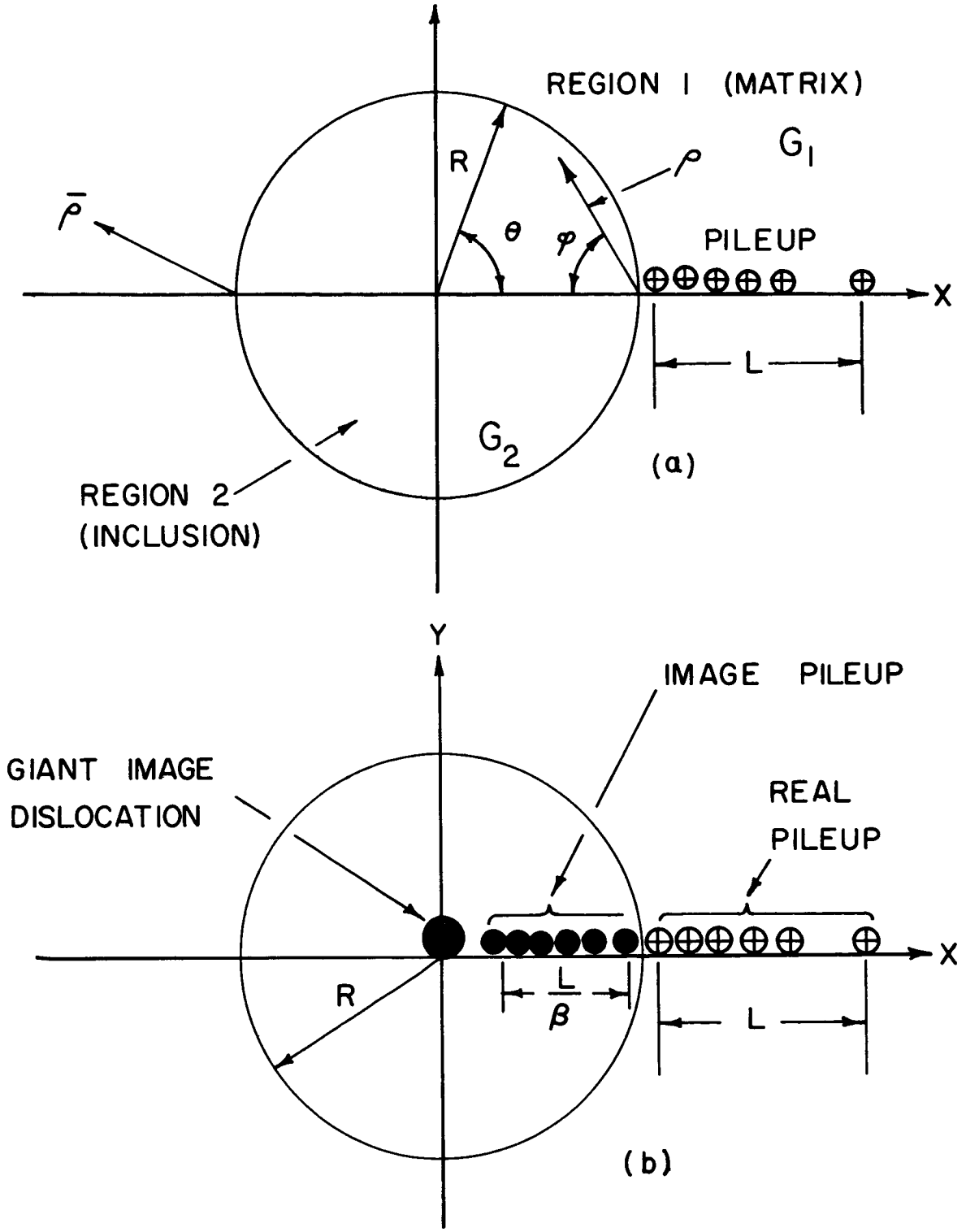

Figure IV-1: (a) Schematic illustration of a screw dislocation pileup against a circular inclusion. (b) Schematic illustration showing the equivalent image dislocation system used to describe the pileup stress field.

$$\frac{G_1 b}{2\pi}\left\{\sum_{\substack{j=1\\ j\neq i}}^{N}\frac{1}{x_i - x_j} + \kappa\sum_{j=1}^{N}\frac{1}{x_i - R^2/x_j} - \frac{\kappa N}{x_i}\right\} = \tau(x_i),\ i = 1,2,\ldots,N\ . \qquad \text{(IV.1-3)}$$

Equation (IV.1-3) may be interpreted in terms of image dislocations as follows (Figure IV-1b). Considering an infinite single phase medium of shear modulus G_1, the first sum on the left side of (IV.1-3) represents the stress at x_i due to the other N-1 dislocations in the real pileup; the second sum represents the stress at x_i due to a pile-up of N image dislocations, each of strength κb, at positions $(R^2/x_j,\ 0)$ inside the inclusion; the third term, the stress at x_i due to a giant image dislocation of Burgers' vector $-\kappa N b$ at the origin. Defining the set of dimensionless parameters $\lambda_i = x_i/R$, and using the continuous distribution approximation, Eq. (IV.1-3) is recast as

$$\int_1^\beta \frac{f(\zeta)\,d\zeta}{\lambda - \zeta} + \kappa\int_1^\beta \frac{f(\zeta)\,d\zeta}{\lambda - \frac{1}{\zeta}} = \frac{\kappa N}{\lambda} + \frac{2\pi R}{G_1 b}\tau(\lambda)\ . \qquad \text{(IV.1-4)}$$

The end conditions on $f(\zeta)$, the dislocation distribution function, are

$$\begin{aligned} &f(\beta) = 0 \\ &f(1)\ \text{unbounded with a weak singularity}\ . \end{aligned} \qquad \text{(IV.1-5)}$$

It will be shown that when $\kappa = -1$ (i.e., the case in which the second phase is a circular hole), the distribution function will vanish at both ends of the array. Discussion of this special case will be deferred until later.

As mentioned in Chapter II, we may consider $\tau(\lambda)$ as being of either of two forms

$$\tau(\lambda) = \tau, \text{ the yield stress--a constant, (pseudo elastic-plastic model)} \qquad \text{(IV.1-6a)}$$

or

$$\tau(\lambda) = \tau\left\{1 - \frac{K}{\lambda^2}\right\}, \quad \text{(purely elastic model)} \; . \qquad \text{(IV.1-6b)}$$

It will be seen that the choice of $\tau(\lambda)$ affects the distribution function, $f(\zeta)$, only through multiplicative constants but does not alter the functional form of $f(\zeta)$. For the present let us choose $\tau(\lambda) = \tau$. We shall indicate later the form of $f(\zeta)$ appropriate to the choice (IV.1-6b).

2. Solution of the Integral Equation for $f(\zeta)$.

Knowing the form of the distribution function obtained by Chou[33] and the results of the preceding two chapters, it is possible to guess the <u>exact</u> solution to (IV.1-4). As a first trial let us guess a solution $f_0(\zeta)$ of the form:

$$f_0(\zeta) = A\left(1 + \frac{1}{\zeta^2}\right) \sinh\left\{g \cosh^{-1}\left[\left(\frac{\beta-1}{\beta+1}\right)\left(\frac{\zeta+1}{\zeta-1}\right)\right]\right\}$$

$$+ B\left(1 - \frac{1}{\zeta^2}\right) \sinh\left\{w \cosh^{-1}\left[\left(\frac{\beta-1}{\beta+1}\right)\left(\frac{\zeta+1}{\zeta-1}\right)\right]\right\} \; . \qquad \text{(IV.2-1)}$$

This particular form is chosen for the following reasons. The distribution function found by Chou[33] and the distribution functions of the two preceding chapters were of the form:

$$f(\zeta) = a_0 \cosh^{-1}\left(\frac{L}{\zeta}\right) \qquad \text{(Chou: } \kappa = 1, \quad \beta = 1\text{)} \qquad \text{(IV.2-2a)}$$

$$f(\zeta) = b_0 \sinh\left\{g \cosh^{-1}\left(\frac{L}{\zeta}\right)\right\} \qquad \text{(Chapter III: } \beta = 1, \ -1 < \kappa \leq 1\text{)} \qquad \text{(IV.2-2b)}$$

$$f(\zeta) = c_0\left(1 + \frac{1}{\zeta^2}\right) \cosh^{-1}\left[\left(\frac{\beta-1}{\beta+1}\right)\left(\frac{\zeta+1}{\zeta-1}\right)\right]$$

$$+ d_0\left(1 - \frac{1}{\zeta^2}\right) \sinh\left\{\cosh^{-1}\left[\left(\frac{\beta-1}{\beta+1}\right)\left(\frac{\zeta+1}{\zeta-1}\right)\right]\right\}$$

$$\text{(Chapter II: } \kappa = 1, \ 1 \leq \beta \leq \infty\text{)} \ . \qquad \text{(IV.2-2c)}$$

[Note: The second term in (IV.2-2c) arises from the first term in Eq. (II.1-15), since

$$\left(1 - \frac{1}{\zeta^2}\right) \sinh\left\{\cosh^{-1}\left[\left(\frac{\beta-1}{\beta+1}\right)\left(\frac{\zeta+1}{\zeta-1}\right)\right]\right\} = \frac{2\sqrt{\beta}}{\beta+1}\left(\frac{1}{\zeta} + \frac{1}{\zeta^2}\right)\sqrt{(\beta-\zeta)(\zeta - 1/\beta)} \ .$$

(IV.2-3)

Thus, the forms of (IV.2-2a) and (IV.2-2b) lead one to generate the trial function in (IV.2-1) from (IV.2-2c). The constants A, B, g, and w in (IV.2-1) are as yet undetermined.

Making the substitution $u = \cosh^{-1}\left[\left(\frac{\beta-1}{\beta+1}\right)\left(\frac{\zeta+1}{\zeta-1}\right)\right]$

$$\left\{\begin{array}{l} \int_1^\beta \frac{f_0(\zeta)\, d\zeta}{\lambda-\zeta} \\ \int_1^\beta \frac{f_0(\zeta)\, d\zeta}{\lambda-\frac{1}{\zeta}} \end{array}\right\}$$

$$= 2A\left(\frac{\beta+1}{\beta-1}\right) \int_{-\infty}^{\infty} \left[\frac{\sinh gu \sinh u\, du}{[(\beta+1/\beta-1)\cosh u \pm 1]} \left[1 + \frac{2}{[(\beta+1/\beta-1)^2 \cosh^2 u - 1]}\right] \right.$$

$$\left. \times \frac{1}{(\beta+1/\beta-1)(\lambda-1)\cosh u \mp (1+\lambda)} \right]$$

$$+ 4B\left(\frac{\beta+1}{\beta-1}\right)^2 \int_{-\infty}^{\infty} \left[\frac{\sinh wu \sinh u \cosh u\, du}{[(\beta+1/\beta-1)\cosh u \pm 1]^2 [(\beta+1/\beta-1)\cosh u \mp 1]} \right.$$

$$\left. \times \frac{1}{(\beta+1/\beta-1)(\lambda-1)\cosh u \mp (1+\lambda)} \right]$$

$$= \left\{\begin{array}{l} \int_{-\infty}^{\infty} I_1(u,\lambda)\, du \\ \int_{-\infty}^{\infty} I_2(u,\lambda)\, du \end{array}\right\} \quad . \qquad \text{(IV.2-4)}$$

Considering

$$\oint_C I_1(u,\lambda)\, du \,, \qquad \text{(IV.2-5)}$$

where C is the indented rectangle in the complex $u = v + i\Omega$ plane (Figure IV-2), letting $v_0 \to \infty$, $\epsilon \to 0$, and applying the Cauchy residue theorem, one finds that if we let (see Appendix F)

$$\left.\begin{aligned} g &= \frac{2}{\pi} \sin^{-1} \sqrt{\frac{1-\kappa}{2}} \,, \\ w &= \frac{2}{\pi} \sin^{-1} \sqrt{\frac{1+\kappa}{2}} = 1-g \,, \\ \gamma_0 &= \cos^{-1} \frac{\beta-1}{\beta+1} \,, \qquad 0 \le \gamma_0 \le \frac{\pi}{2} \,, \\ A &= \frac{2R\tau}{G_1 b} \frac{\sin w(\pi-\gamma_0)}{\sqrt{1-\kappa^2}\ \sin \gamma_0} \,, \\ B &= \frac{2R\tau}{G_1 b} \frac{\sin g(\pi-\gamma_0)}{\sqrt{1-\kappa^2}\ \sin \gamma_0} \,, \end{aligned}\right\} \qquad \text{(IV.2-6)}$$

then $f_0(\zeta)$ satisfies the integral equation

$$\int_1^\beta \frac{f_0(\zeta)\, d\zeta}{\lambda-\zeta} + \kappa \int_1^\beta \frac{f_0(\zeta)\, d\zeta}{\lambda-\frac{1}{\zeta}} = \frac{\kappa N_0}{\lambda} + \frac{2\pi R\tau}{G_1 b} - \frac{\alpha_0}{\lambda} \qquad \text{(IV.2-7)}$$

where

$$N_0 = \int_1^\beta f_0(\zeta)\, d\zeta \,, \qquad \text{(IV.2-8)}$$

and

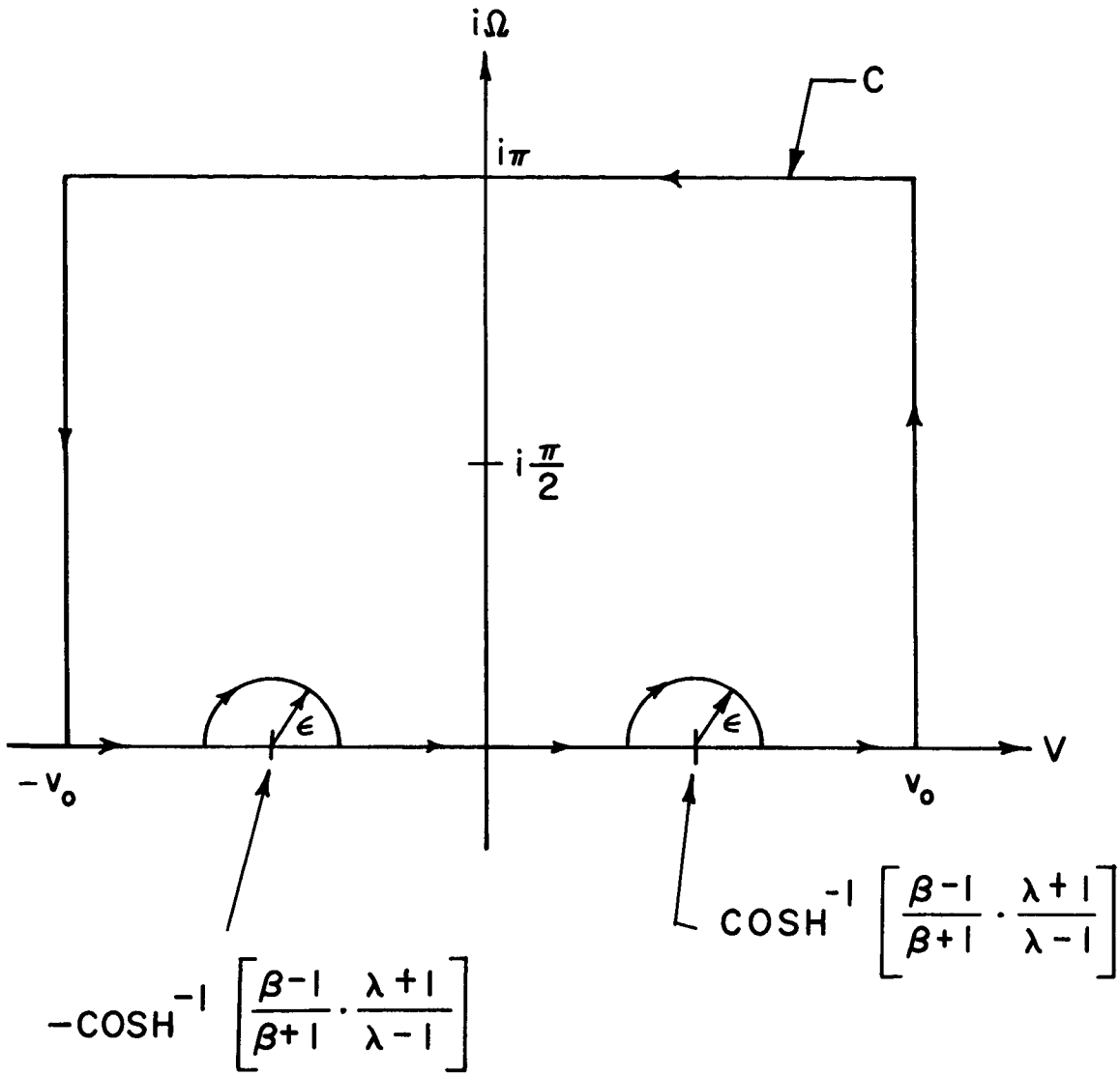

Figure IV-2: The contour C in the complex $u = v + i\Omega$ plane used to solve the integral equation for the dislocation distribution function.

$$\alpha_0 = \kappa N_0 - \frac{2\pi}{\sin \gamma_0} \frac{\beta-1}{\beta+1} \{gA \cos g(\pi-\gamma_0) - wB \cos w(\pi-\gamma_0)\} . \quad \text{(IV.2-9)}$$

If α_0 were identically zero, then $f_0(\zeta)$ would be a solution to (IV.1-4). This is not the case, so we must find a distribution function $f_1(\zeta)$ satisfying

$$\int_1^\beta \frac{f_1(\zeta)\, d\zeta}{\lambda-\zeta} + \kappa \int_1^\beta \frac{f_1(\zeta)\, d\zeta}{\lambda-\frac{1}{\zeta}} = \frac{\kappa N_1}{\lambda} + \frac{\alpha_0}{\lambda} , \quad \text{(IV.2-10)}$$

where

$$N_1 = \int_1^\beta f_1(\zeta)\, d\zeta . \quad \text{(IV.2-11)}$$

Then $f_0(\zeta) + f_1(\zeta)$ will be the required solution to (IV.1-4).

A suitable guess for $f_1(\zeta)$ is

$$f_1(\zeta) = \frac{C}{\zeta} \sinh \left\{ g \cosh^{-1} \left[\left(\frac{\beta-1}{\beta+1}\right)\left(\frac{\zeta+1}{\zeta-1}\right) \right] \right\} . \quad \text{(IV.2-12)}$$

Again making the substitution $u = \cosh^{-1}[(\beta-1/\beta+1)(\zeta+1/\zeta-1)]$ and using the technique illustrated in (IV.2-4), $f_1(\zeta)$ is a solution to (IV.2-10) if

$$C = - \frac{2}{\sin \gamma_0} \frac{\cos \gamma_0}{\cos g\gamma_0} \{gA \sin g\gamma_0 - wB \sin w\gamma_0\} . \quad \text{(IV.2-13)}$$

Thus, in dimensionless form, the exact distribution function is

$$f(\zeta) = \frac{2R\tau}{G_1 b} \frac{1}{\sqrt{1-\kappa^2}} \frac{1}{\sin \gamma_0}$$

$$\times \left\{ \left(1 + \frac{1}{\zeta^2}\right) \sin w(\pi-\gamma_0) \sinh g\eta_0 + \left(1 - \frac{1}{\zeta^2}\right) \sin g(\pi-\gamma_0) \sinh w\eta_0 \right.$$

$$- \frac{2}{\sin \gamma_0} \frac{\cos \gamma_0}{\cos g\gamma_0} \left[g \sqrt{1-\kappa^2} \sin \gamma_0 - \sin g(\pi-\gamma_0) \sin w\gamma_0 \right]$$

$$\left. \times \frac{1}{\zeta} \sinh g\eta_0 \right\}, \qquad \text{(IV.2-14)}$$

where

$$\left.\begin{aligned} \eta_0 &= \cosh^{-1}\left[\left(\frac{\beta-1}{\beta+1}\right)\left(\frac{\zeta+1}{\zeta-1}\right)\right] \\ 0 \le \gamma_0 &= \cos^{-1}\frac{\beta-1}{\beta+1} \le \frac{\pi}{2} \\ g &= \frac{2}{\pi} \sin^{-1}\sqrt{\frac{1-\kappa}{2}} = 1-w \ . \end{aligned}\right\} \qquad \text{(IV.2-15)}$$

The number of dislocations in the pileup is then given by

$$N = \frac{\pi\tau L}{G_1 b} \frac{1}{\sqrt{1-\kappa^2}} \frac{\beta+1}{\beta} \frac{1}{\cos g\gamma_0} \left[g \sin w(\pi-\gamma_0) + w \sin g(\pi-\gamma_0) \cos \gamma_0 \right] .$$

(IV.2-16)

The limiting cases $\kappa \to 1$, 0 and $\beta \to 1$, ∞ check all previous solutions. One should note that the true distribution function on the interval [R, L+R] is

$$f(\zeta)_{true} = \frac{1}{R} f(\zeta) . \qquad \text{(IV.2-17)}$$

Figures (IV-3), (IV-4), and (IV-5) show the true distribution function plotted as a function of $\zeta_0 = \rho_0/L$ (for fixed κ and variable β, and vice-versa), where ρ_0 is the distance from the leading edge of the pileup to any point in the array. The relation between ζ and ζ_0 is

$$\zeta = 1 + (\beta-1)\,\zeta_0 \qquad (0 \le \zeta_0 \le 1)\ . \qquad \text{(IV.2-18)}$$

Figure (IV-6) is a three-dimensional view of the surface $\tau L/G_1 bN$ as a function of inclusion size (β) and rigidity (κ). As particle size decreases (i.e., as β becomes large), the $\tau L/G_1 bN$ surface approaches the plane $\tau L/G_1 bN = 1/\pi$, independent of the value of κ. Figures (IV-7) and (IV-8) represent sections through the surface at constant β and constant κ.

When we take the pure elastic form for $\tau(\lambda)$, Eq. (IV.1-6b), the only difference in the distribution function obtained is in the constants A and B (Eq. (IV.2-13) is still valid for C in terms of A and B). For $\tau(\lambda) = \tau\{1 - \kappa/\lambda^2\}$,

$$A = \frac{\cos w\gamma_0}{\sin \gamma_0}\,\frac{2R\tau}{G_1 b}$$

$$B = \frac{\cos g\gamma_0}{\sin \gamma_0}\,\frac{2R\tau}{G_1 b} \qquad \text{(IV.2-19)}$$

$$C = -\frac{2R\tau}{G_1 b}\,\frac{2}{\sin^2 \gamma_0}\,\frac{\cos \gamma_0}{\cos g\gamma_0}\,[g \sin \gamma_0 - \cos g\gamma_0 \sin w\gamma_0]\ .$$

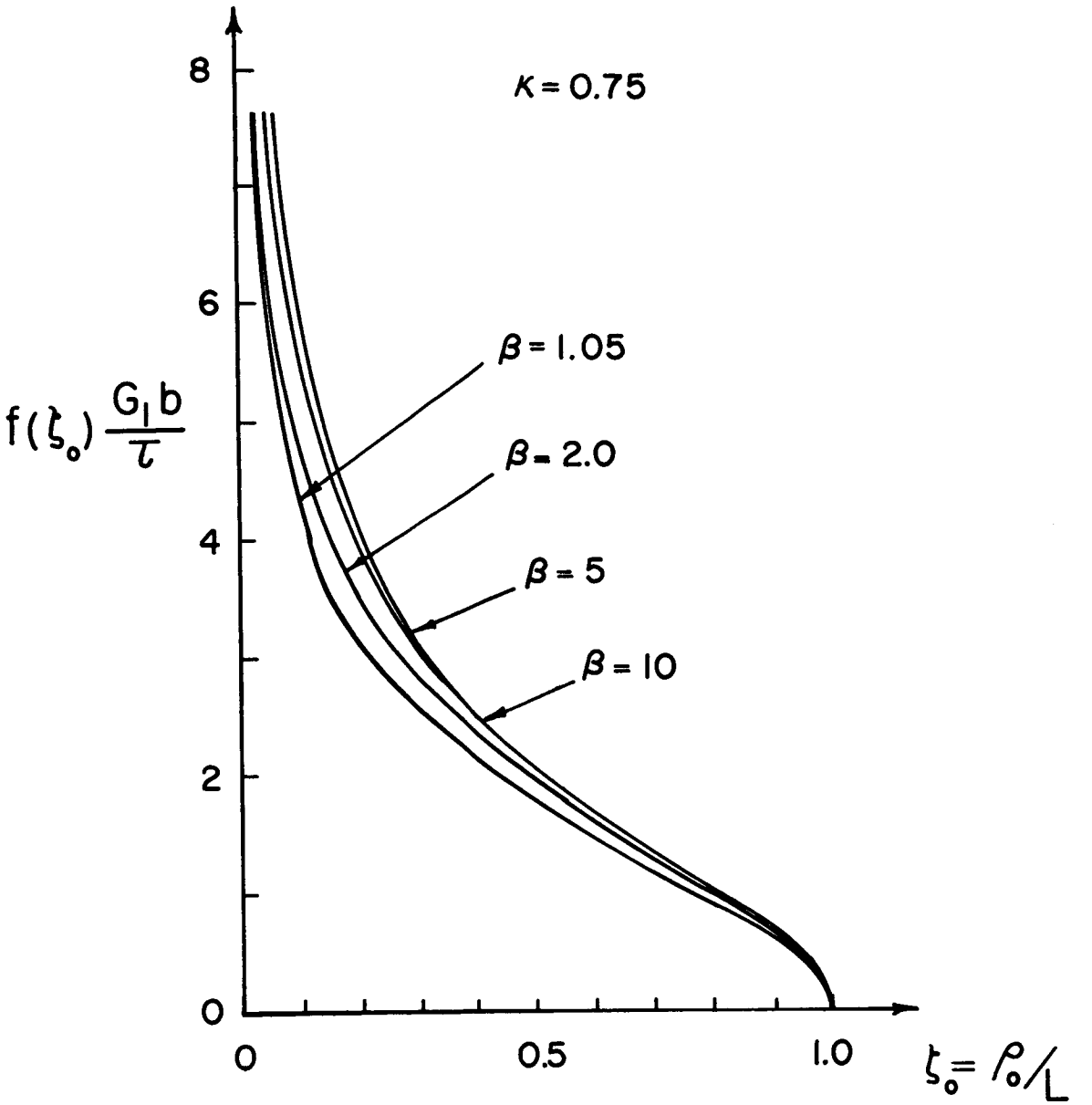

Figure IV-3: $f(\zeta_0)$, the dislocation distribution function, vs. ζ_0 for a fixed relative rigidity (κ) and various L/R ratios. The pileup is in the softer phase ($G_2 > G_1$). ρ_0 is the distance from the leading edge of the pileup to any point in the array.

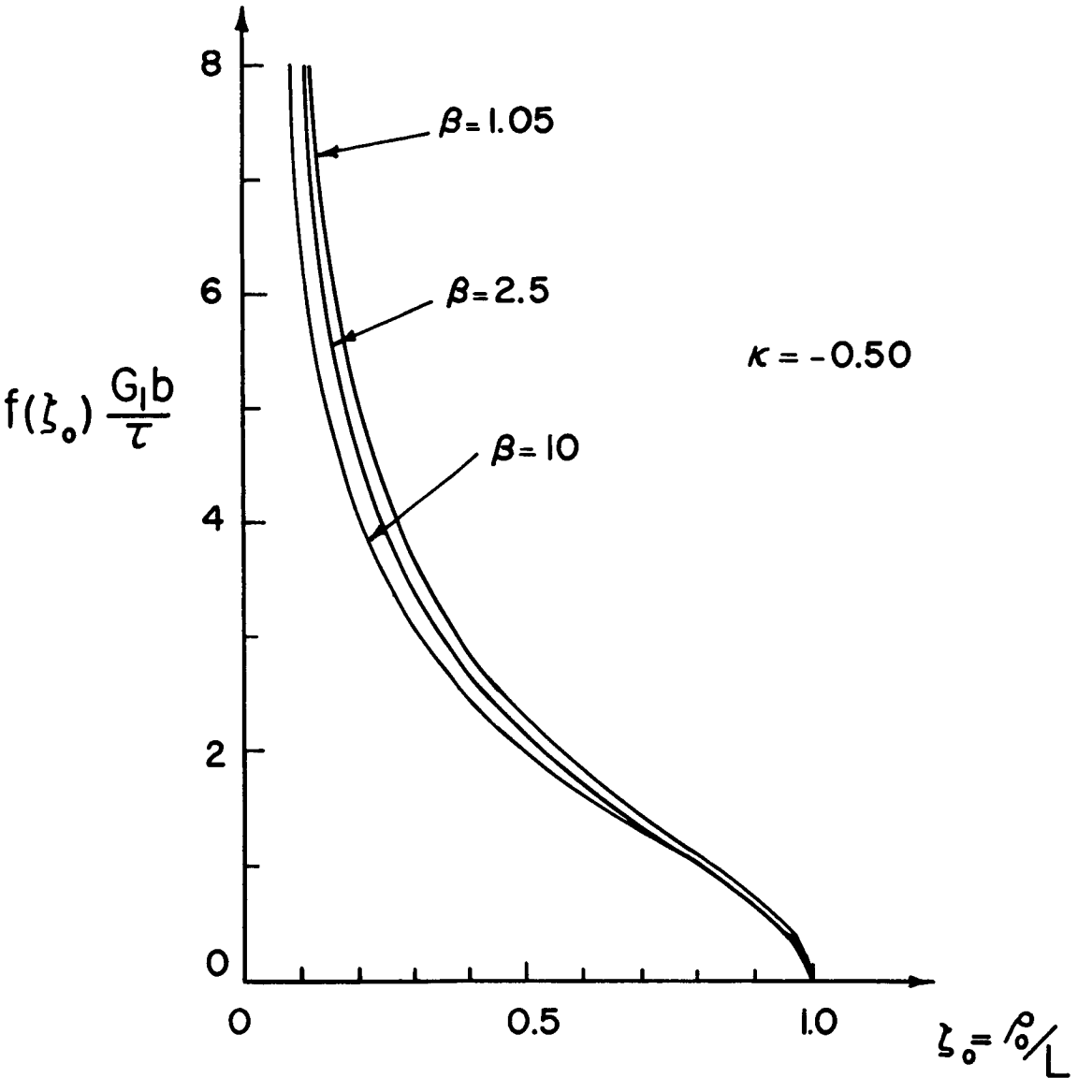

Figure IV-4: $f(\zeta_0)$, the dislocation distribution function, vs. ζ_0 for a fixed relative rigidity (κ) and various L/R ratios. The pileup is in the harder phase ($G_2 < G_1$).

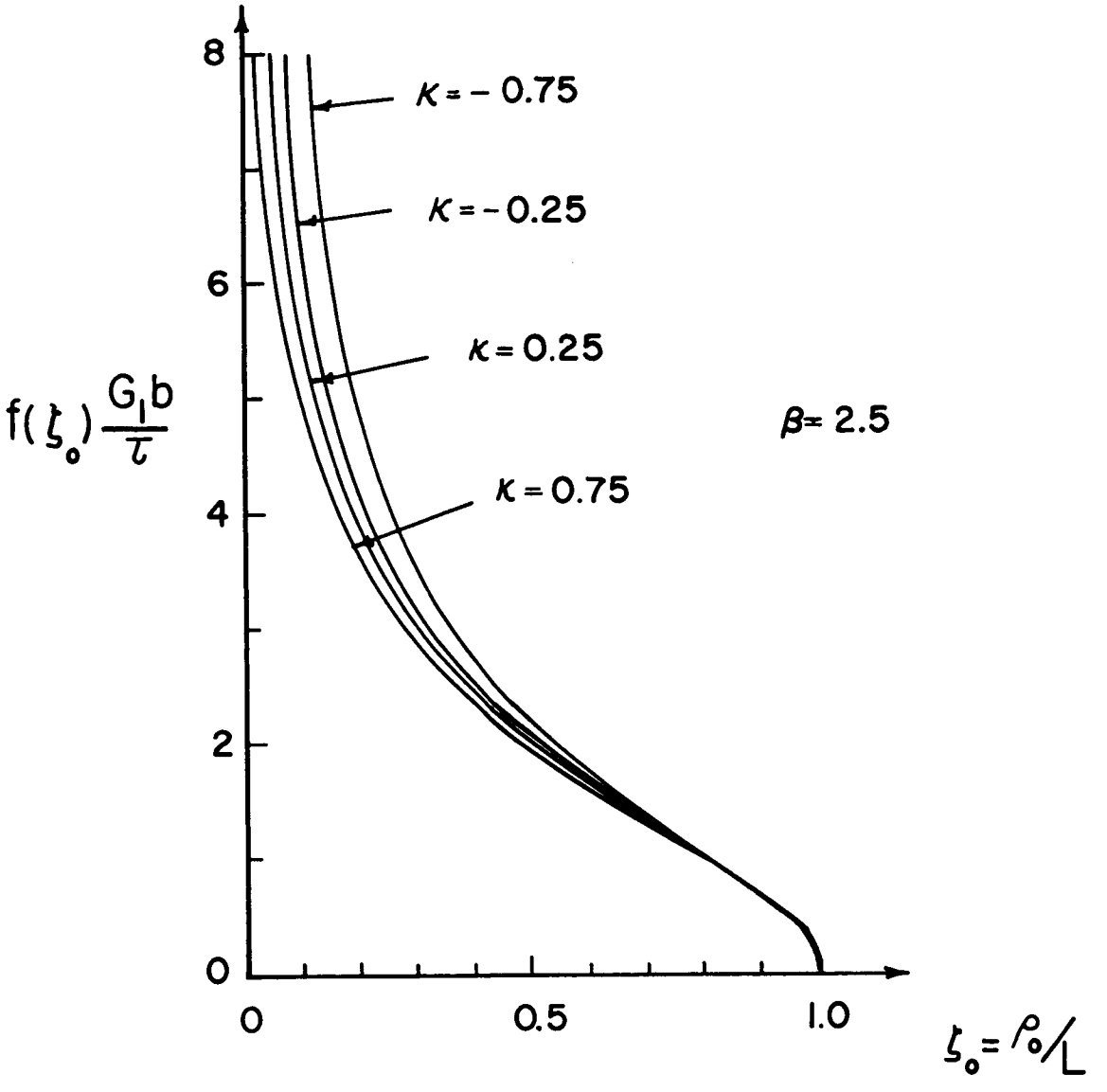

Figure IV-5: $f(\zeta_0)$, the dislocation distribution function, vs. ζ_0 for a fixed L/R ratio and various values of relative rigidity (κ).

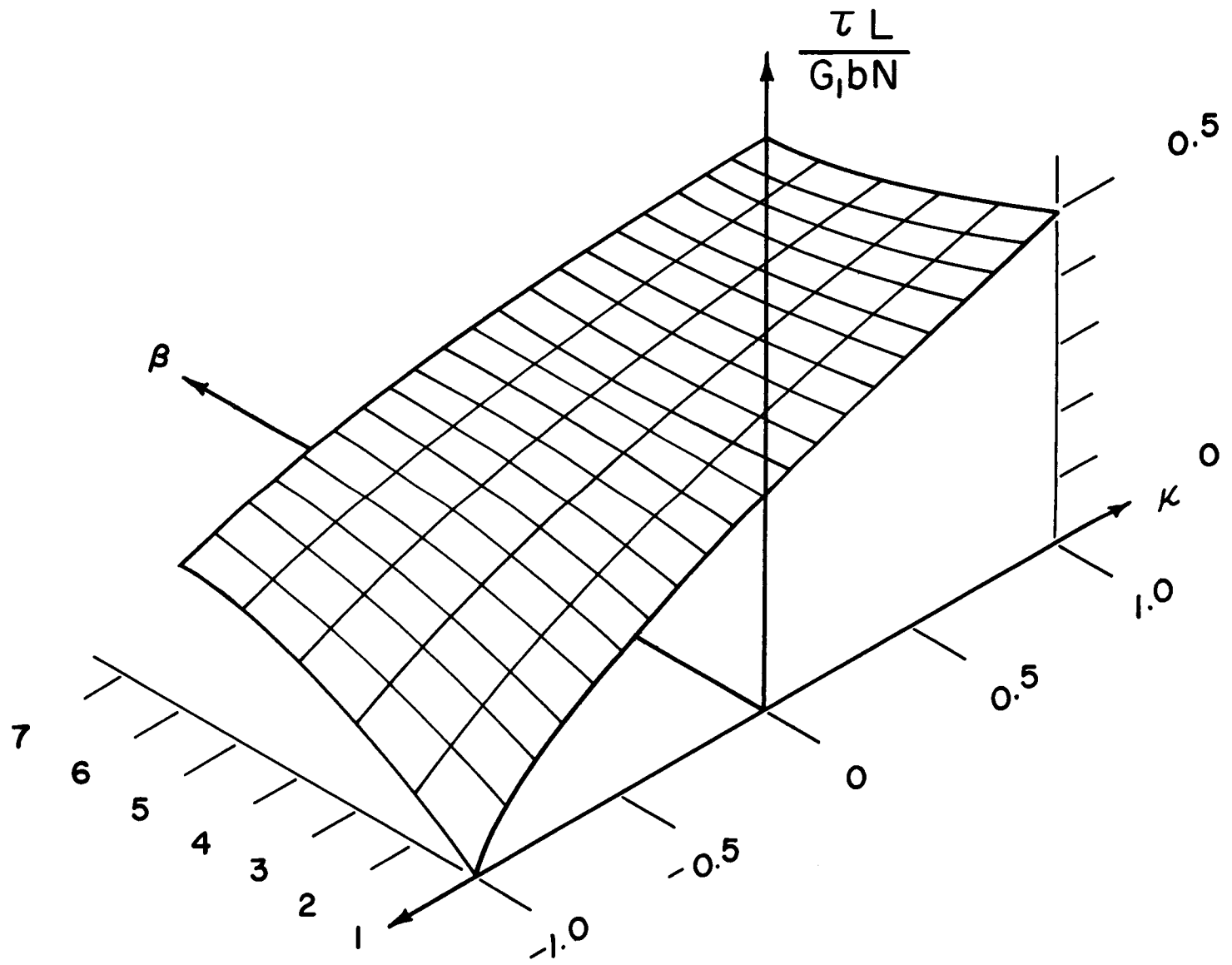

Figure IV-6: The 3-dimensional surface $\tau L/G_1 bN$, where N is the number of pileup dislocations, as a function of β and κ.

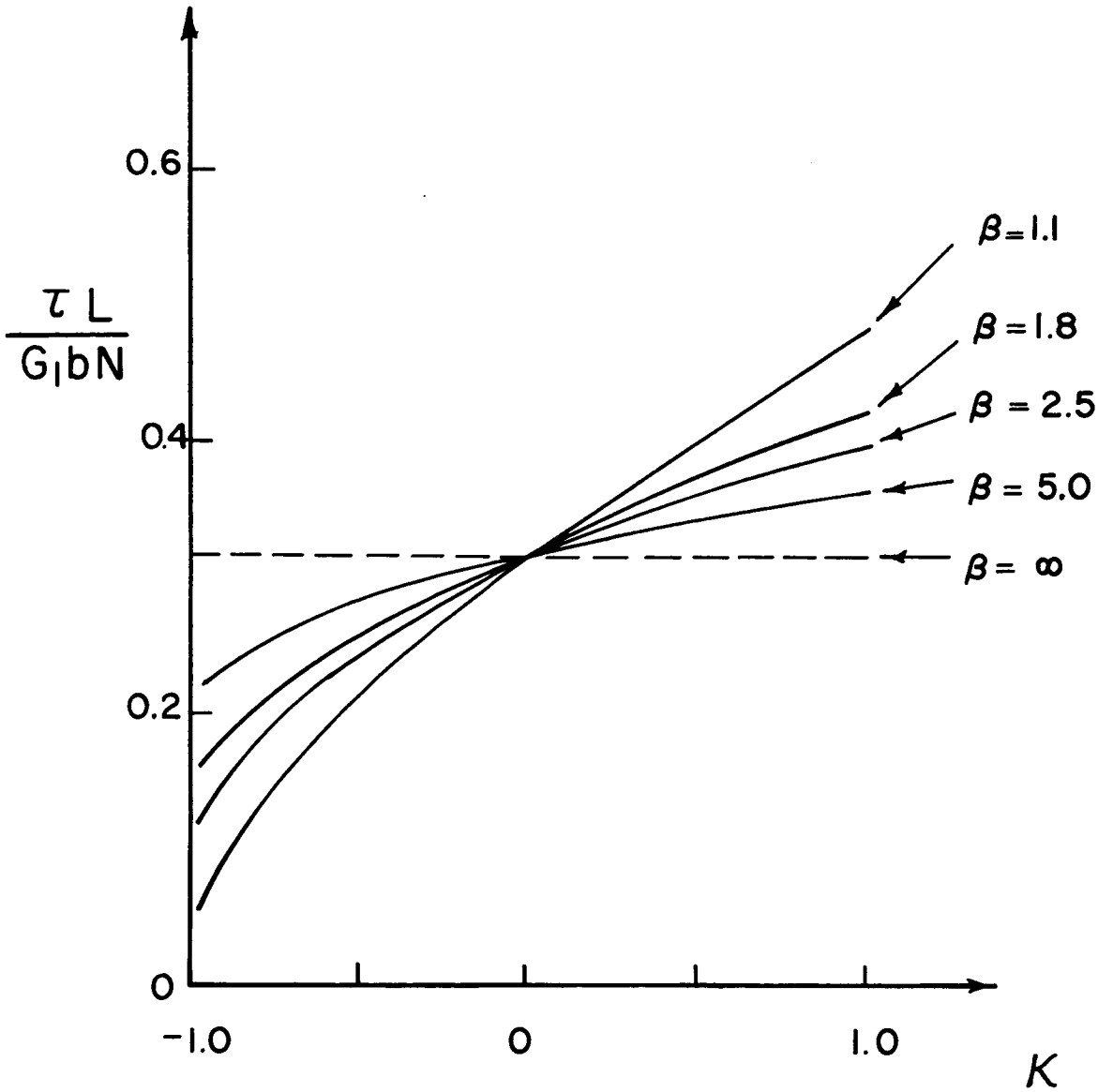

Figure IV-7: $\tau L/G_1 bN$ as a function of relative rigidity (κ) for various L/R ratios.

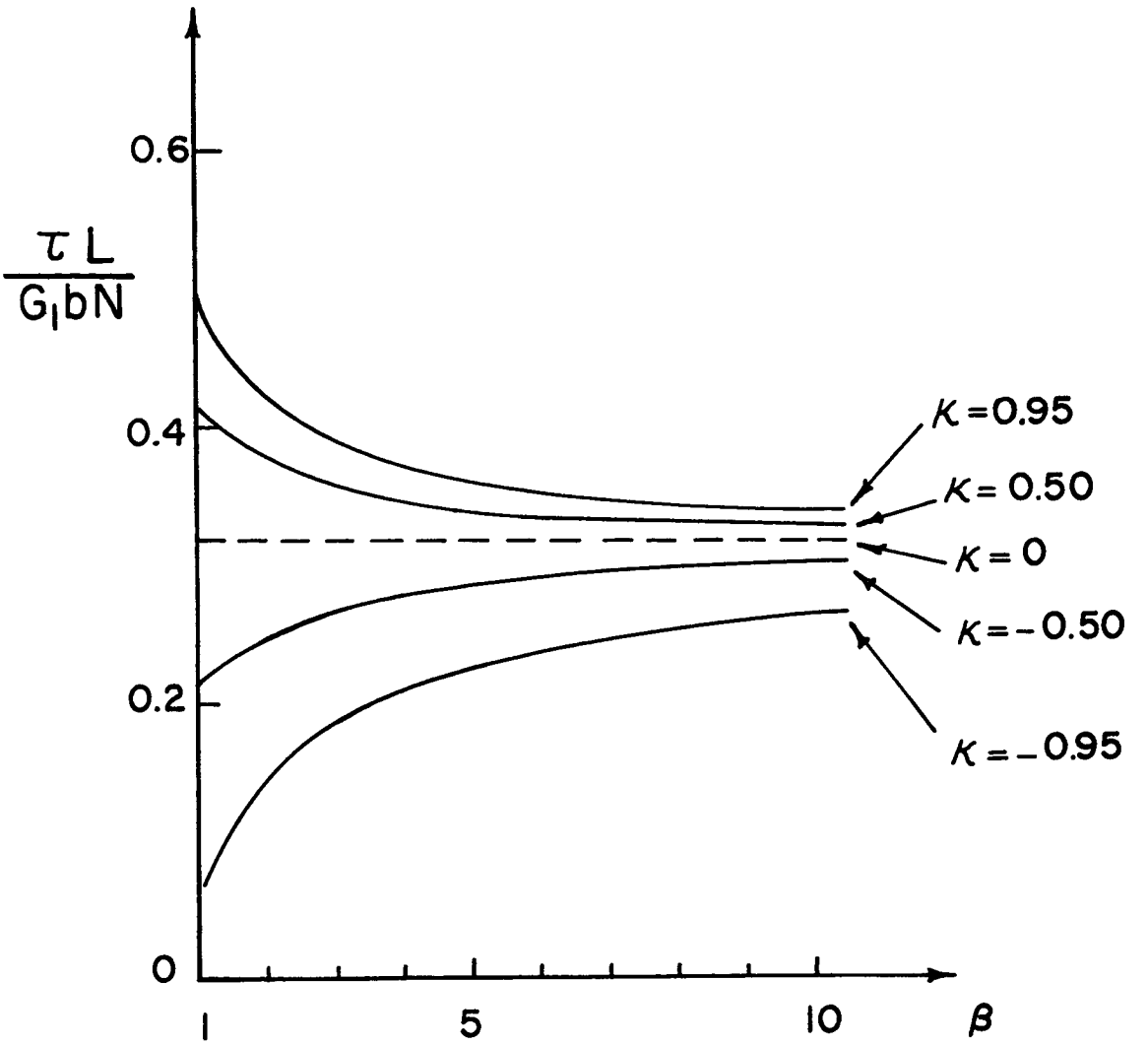

Figure IV-8: $\tau L/G_1 bN$ as a function of β for various values of relative rigidity (κ).

Hence, we obtain the solution for the pure elastic form of $\tau(\lambda)$ by letting

$$\frac{\sin w(\pi-\gamma_0)}{\sqrt{1-\kappa^2}} \to \cos w\gamma_0 \qquad \text{and} \qquad \frac{\sin g(\pi-\gamma_0)}{\sqrt{1-\kappa^2}} \to \cos g\gamma_0 \quad \text{(IV.2-20)}$$

in Eq. (IV.2-14). N, the number of dislocations in the pileup is then given by

$$N = \frac{\pi\tau L}{G_1 b} \frac{\beta+1}{\beta} \frac{1}{\cos g\gamma_0} [g \cos w\gamma_0 + w \cos g\gamma_0 \cos \gamma_0] \,. \quad \text{(IV.2-21)}$$

3. The Pileup Stress Field

The substitution $u = \cosh^{-1}\left[\frac{\beta+1}{\beta-1} \cdot \frac{\zeta+1}{\zeta-1}\right]$ permits an evaluation of the superposition integrals

$$\tau_{ij}(x,y) = \int_R^{L+R} \tau_{ij}(x,y,\zeta)\, f(\zeta)\, d\zeta \qquad \text{(IV.3-1)}$$

by means of contour integration in the complex $u = \omega + i\Omega$ plane. Expressions for special cases of the stress field are presented below (for the choice $\tau(\lambda) = \tau$).

(a) The shear stress τ_{rz} along the inclusion interface:

$$\tau_{rz} = -\frac{\tau}{\sin\gamma_0}\sqrt{\frac{2}{1-\kappa}}$$

$$\times\Big\{\sin w(\pi-\gamma_0)\,[(\sinh g\nu_0)\cos\theta + \sin g(\tfrac{\pi}{2}-\gamma_0)\sin\theta]$$

$$+ \sin g(\pi-\gamma_0)\sin\theta[\cosh w\nu_0 - \cos w(\tfrac{\pi}{2}-\gamma_0)]$$

$$-\frac{\cos\gamma_0}{\sin\gamma_0\cos g\gamma_0}\Big[\,g\sqrt{1-\kappa^2}\sin\gamma_0 - \sin g(\pi-\gamma_0)\sin w\gamma_0\Big]$$

$$\times\sinh g\nu_0\Big\}, \qquad \text{(IV.3-2)}$$

where

$$\nu_0 = \sinh^{-1}\{(\tfrac{\beta-1}{\beta+1})\cot\tfrac{\theta}{2}\}, \qquad \text{(IV.3-3)}$$

and θ is the polar angle measured from the center of the inclusion (Figure IV-1a).

(b) The shear stress τ_{yz} on the slip plane $y = 0$ inside the inclusion:

When $1/\beta \le \lambda = x/R \le 1$,

$$\tau_{yz} = \frac{\tau}{(1-\kappa)\sin\gamma_0}$$

$$\times\Big\{(1+\frac{\kappa}{\lambda^2})\sin\gamma_0 + \frac{2\cos\gamma_0}{\lambda\cos g\gamma_0\sin\gamma_0}$$

$$\times\Big[\,g\sqrt{1-\kappa^2}\sin\gamma_0 - \sin g(\pi-\gamma_0)\sin w\gamma_0\,\Big]\cosh g\eta_1$$

$$-[\sin w(\pi-\gamma_0)(1+\frac{1}{\lambda^2})\cosh g\eta_1$$

$$+\sin g(\pi-\gamma_0)(1-\frac{1}{\lambda^2})\cosh w\eta_1]\Big\}, \qquad \text{(IV.3-4)}$$

where

$$\eta_1 = \cosh^{-1}\{(\frac{\beta-1}{\beta+1})(\frac{\lambda+1}{1-\lambda})\} \quad . \qquad \text{(IV.3-5)}$$

For $-1 \leq \lambda = x/R \leq 1/\beta$, the same equation is valid with $\cosh g\eta_1$ and $\cosh w\eta_1$ replaced by $\cos g\eta_2$ and $\cos w\eta_2$, respectively, where

$$0 \leq \eta_2 = \cos^{-1}\{(\frac{\beta-1}{\beta+1})(\frac{\lambda+1}{1-\lambda})\} \leq \frac{\pi}{2} \quad . \qquad \text{(IV.3-6)}$$

Figure (IV-9) shows a three dimensional view of this stress near the pileup tip as a function of $\rho/L = (1-\lambda)/(\beta-1)$ (see Figure (IV-1a)) and inclusion size β. Each of the three stress surfaces shown corresponds to a different value of relative rigidity (κ). Figure (IV-10) shows a section taken through Figure (IV-9) at constant β.

(c) <u>The shear stress τ_{yz} on the slip plane $y = 0$ outside the inclusion</u> ($\lambda = x/R \leq -1$):

$$\tau_{yz} = \frac{\tau}{\sqrt{1-\kappa^2}\,\sin\gamma_0}$$

$$\times\left\{\sqrt{1-\kappa^2}\,\sin\gamma_0 + \frac{2}{\lambda}\,\frac{\cos\gamma_0}{\cos g\gamma_0\,\sin\gamma_0}\right.$$

$$\times\left[g\sqrt{1-\kappa^2}\,\sin\gamma_0 - \sin g(\pi-\gamma_0)\,\sin w\gamma_0\right]\sin g\sigma_0$$

$$-\left[(1+\frac{1}{\lambda^2})\,\sin w(\pi-\gamma_0)\,\sin g\sigma_0\right.$$

$$\left.\left.+\,(1-\frac{1}{\lambda^2})\,\sin g(\pi-\gamma_0)\,\sin w\sigma_0\right]\right\}, \qquad \text{(IV.3-7)}$$

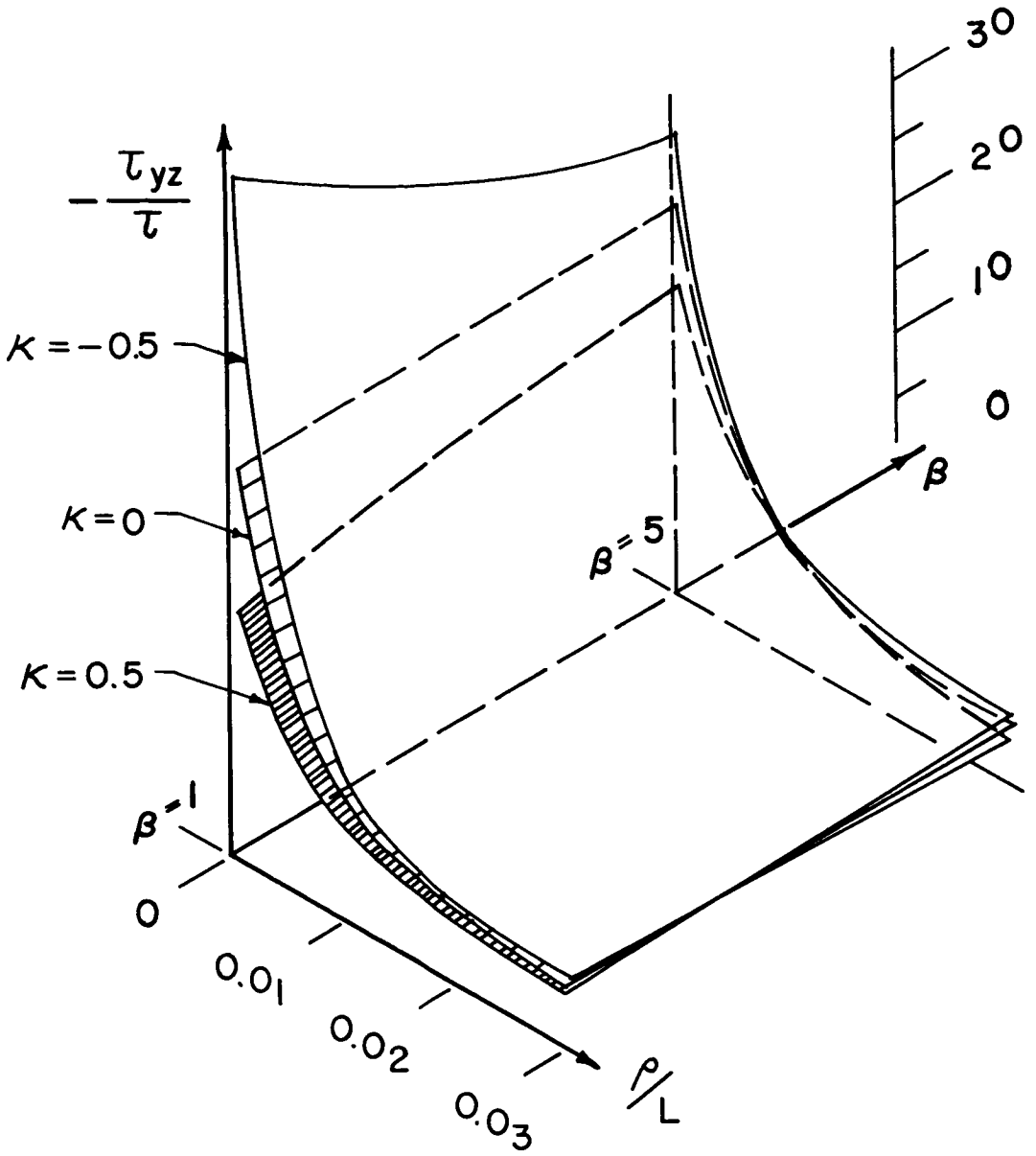

Figure IV-9: 3-dimensional surfaces showing the shear stress τ_{yz} on the slip plane $y = 0$ inside the inclusion close to the pileup tip as a function of β and ρ/L. Each surface represents a different value of relative rigidity (κ).

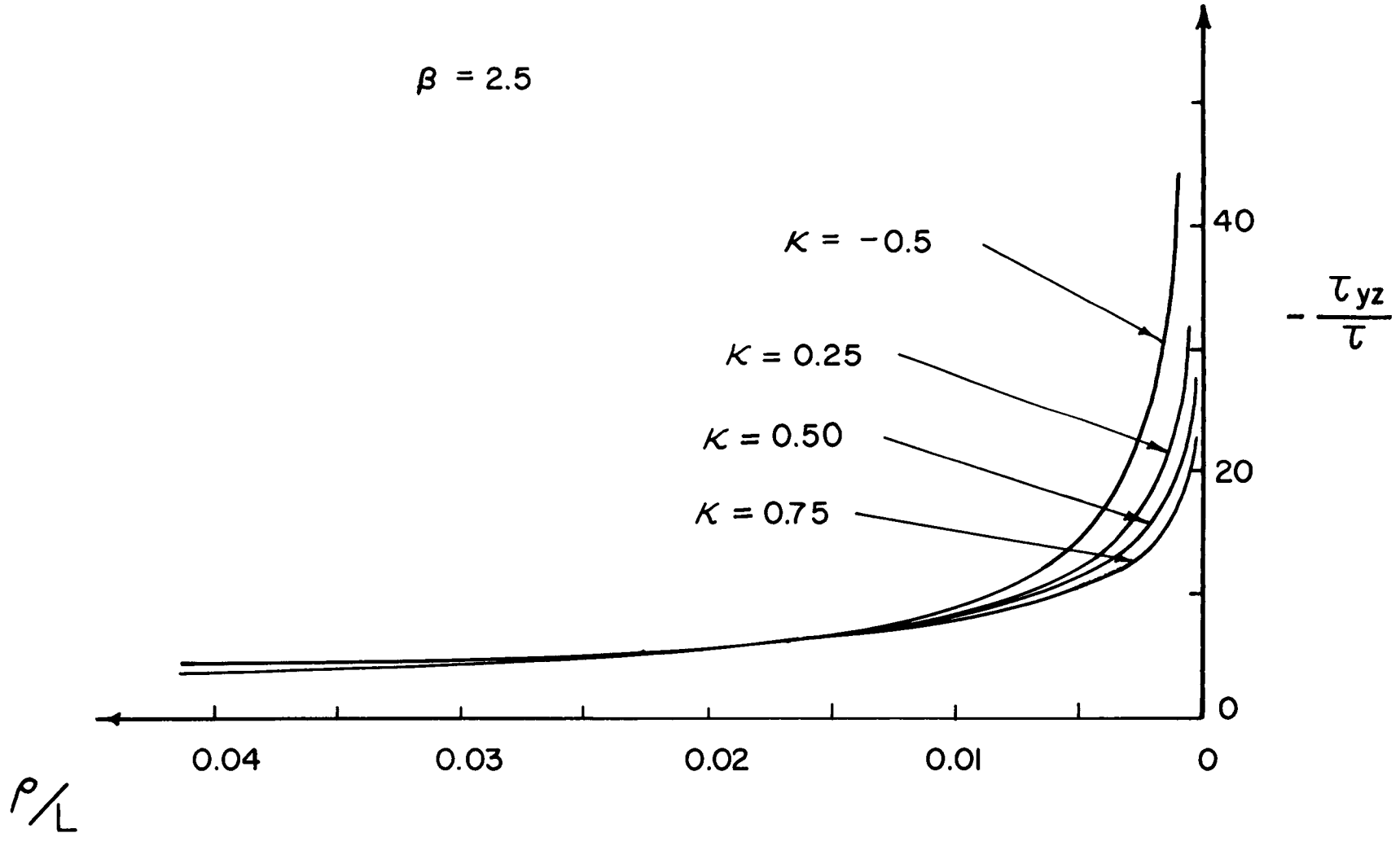

Figure IV-10: τ_{yz} (y = 0) inside the inclusion close to the pileup tip for a fixed L/R ratio and various relative rigidity values (κ).

where

$$0 \leq \sigma_0 = \cos^{-1}\left\{\left(\frac{\beta-1}{\beta+1}\right)\frac{|\lambda|-1}{|\lambda|+1}\right\} \leq \frac{\pi}{2} . \qquad \text{(IV.3-8)}$$

When $\tau(\lambda)$ is taken to be $\tau\{1 - \kappa/\lambda^2\}$, Eqs. (IV.3-2), (IV.3-4) and (IV.3-7) hold provided the substitutions given in Eq. (IV.2-20) are made.

One readily notes that the expressions for the special stresses given in (IV.3-2), (IV.3-4), and (IV.3-7) are extremely cumbersome, and it is useful to have approximate expressions for the stresses close to the pileup tip. Consider first the local stresses inside the inclusion ($x^2 + y^2 \leq R^2$). For $\kappa \neq 1$ ($\kappa = 1$ was treated in Chapter II), provided that the conditions

$$\frac{2R}{\rho} \geq 1 \qquad \text{(IV.3-9a)}$$

$$g \ln\left\{\frac{4}{\beta+1}\ \frac{L}{\rho}\right\} > 1.5 \qquad \text{(IV.3-9b)}$$

are satisfied, these local stresses are found to be

$$\left.\begin{aligned} \frac{\tau_{xz}}{\tau} &\approx -A(\kappa,\beta)\left\{\frac{4}{\beta+1}\ \frac{L}{\rho}\right\}^g \frac{\beta+1}{2\sqrt{\beta}} \sin g\varphi , \\ \frac{\tau_{yz}}{\tau} &\approx -A(\kappa,\beta)\left\{\frac{4}{\beta+1}\ \frac{L}{\rho}\right\}^g \frac{\beta+1}{2\sqrt{\beta}} \cos g\varphi , \end{aligned}\right\} \qquad \text{(IV.3-10)}$$

where

$$A(\kappa,\beta) = \frac{\sin w(\pi-\gamma_0)\,\sin w\gamma_0 + w\sqrt{1-\kappa^2}\,\cos\gamma_0\,\sin\gamma_0}{(1-\kappa)\,\sin\gamma_0\,\cos g\gamma_0} \quad \text{if} \quad \tau(\lambda) = \tau\ ; \tag{IV.3-11a}$$

$$A(\kappa,\beta) = \sqrt{\frac{1+\kappa}{1-\kappa}}\ \frac{\cos w\gamma_0\,\sin w\gamma_0 + w\,\sin\gamma_0\,\cos\gamma_0}{\sin\gamma_0\,\cos g\gamma_0}$$

$$\text{if} \quad \tau(\lambda) = \tau\{1 - \kappa/\lambda^2\} \quad . \tag{IV.3-11b}$$

φ is the polar angle in the second phase relative to the pileup tip, and ρ is the associated radius vector (Figure IV-1a). As $\kappa \to 1$, the stresses diverge logarithmically.

Now let us examine Eqs. (IV.3-10) for cases in which the inclusion diameter $2R$ is much greater and much less than the slip line length L. Since

$$\frac{4}{\beta+1}\,\frac{L}{\rho} = \frac{4R}{L+2R}\,\frac{L}{\rho}\ , \tag{IV.3-12}$$

$$\frac{4}{\beta+1}\,\frac{L}{\rho} \approx \frac{2L}{\rho} \quad \text{when} \quad \frac{L}{R} < 2,$$

and (IV.3-13)

$$\frac{4}{\beta+1}\,\frac{L}{\rho} \approx \frac{4R}{\rho} \quad \text{when} \quad \frac{L}{R} > 2\ .$$

Hence, when conditions (IV.3-9a) and (IV.3-9b) are satisfied, inside the inclusion

$$\left.\begin{aligned} \frac{\tau_{xz}}{\tau} &\approx -A(\kappa,\beta)\left(\frac{2L}{\rho}\right)^g \sin g\varphi \\ \frac{\tau_{yz}}{\tau} &\approx -A(\kappa,\beta)\left(\frac{2L}{\rho}\right)^g \cos g\varphi \end{aligned}\right\} \quad \frac{L}{R} < 2 \tag{IV.3-14}$$

or

$$\left.\begin{aligned}
\frac{\tau_{xz}}{\tau} &\approx -A(\kappa,\beta)\sqrt{\frac{L}{4R}}\left\{\frac{4R}{\rho}\right\}^{g}\sin g\varphi \\
&\approx -A(\kappa,\beta)\sqrt{\frac{L}{\rho}}\left\{\frac{4R}{\rho}\right\}^{g-1/2}\sin g\varphi \\
&\qquad\qquad\qquad\qquad \frac{L}{R} > 2 \\
\frac{\tau_{yz}}{\tau} &\approx -A(\kappa,\beta)\sqrt{\frac{L}{4R}}\left\{\frac{4R}{\rho}\right\}^{g}\cos g\varphi \\
&\approx -A(\kappa,\beta)\sqrt{\frac{L}{\rho}}\left\{\frac{4R}{\rho}\right\}^{g-1/2}\cos g\varphi
\end{aligned}\right\} \qquad \text{(IV.3-15)}$$

where

$$0 < g = \frac{2}{\pi}\sin^{-1}\sqrt{\frac{1-\kappa}{2}} < 1 \,. \qquad \text{(IV.3-16)}$$

One notes that

(a) The exponent g is independent of particle size and depends only upon the ratio G_2/G_1.

(b) In the case of particles which are large relative to the slip line length, particle size affects stresses only through the constant $A(\kappa,\beta)$. The relevant term in the expression for local stress intensification is $(2L/\rho)^g$, and this is the same term which would appear if the second phase were semi-infinite. This is physically reasonable since when $L/R \ll 2$, the second phase is extremely planar near the pileup tip, and the leading dislocations in the pileup do not sense the finite size of the inclusion.

(c) In the case of particles which are small relative to the slip line length, the relevant term in the expression for the local stresses is

$$\sqrt{\frac{L}{R}}\ \left(\frac{4R}{\rho}\right)^{g} = \sqrt{\frac{L}{\rho}}\left\{\frac{4R}{\rho}\right\}^{g-1/2} \quad . \qquad \text{(IV.3-17)}$$

The factor $\sqrt{L/\rho}$ is the same term which appears in the calculations based upon a single phase medium (no inclusion present), so that the term $(4R/\rho)^{g-1/2}$ may be viewed as a correction term introduced by the finite size and rigidity of the second phase. When $L/R \ggg 2$, $\beta \to \infty$, and $\gamma_0 \to 0$ so that

$$A(\kappa,\beta) \approx 2\sqrt{\frac{1+\kappa}{1-\kappa}}\ w = \frac{4}{\pi}\sqrt{\frac{1+\kappa}{1-\kappa}}\ \sin^{-1}\sqrt{\frac{1+\kappa}{2}} \qquad \text{(IV.3-18)}$$

for inclusions whose diameters are much smaller than the slip line length.

We can use Eqs. (IV.3-14) and (IV.3-15) to illustrate size and rigidity effects upon the local stresses by two sample calculations which will be compared with similar calculations assuming the absence of the inclusion. We shall, of course, neglect any effects of plastic relaxation of the pileup stresses. Since the maximum shear stress acting along any plane occurs upon the slip plane $y = 0$, we shall concern ourselves with the stress $\tau_{yz}|_{y=0}$.

Case 1. $L \approx 10^{-4}$ cm, $R \approx 2 \times 10^{-4}$ cm (a typical cermet)

(i) $\frac{G_2}{G_1} = 5, \quad \kappa = \frac{2}{3}$

$$\frac{\tau_{yz}}{\tau} \approx -\left\{ \begin{matrix} 17.5 \\ 7.2 \\ 4.5 \end{matrix} \right\} \quad \text{for} \quad \rho = \left\{ \begin{matrix} 10^{-7} \\ 10^{-6} \\ 10^{-5} \end{matrix} \right\} \text{ cm} .$$

(ii) $\kappa = 0$ (no inclusion)

$$\frac{\tau_{yz}}{\tau} \approx -\left\{ \begin{matrix} 45 \\ 14 \\ 4.5 \end{matrix} \right\} \quad \text{for} \quad \rho = \left\{ \begin{matrix} 10^{-7} \\ 10^{-6} \\ 10^{-5} \end{matrix} \right\} \text{ cm} .$$

Thus, when $\kappa > 0$, the local stresses in large particles may be lower than those predicted by homogeneous elasticity calculations by a factor of 2 or 3 when $\rho \geq 10\text{Å}$. This is essentially a rigidity effect, since R, the particle size, has little effect upon the local stresses when $L/R < 2$. We shall not consider $\kappa < 0$ in this calculation.

Case 2. $L \geq \approx 10^{-5}$ cm, $R \leq 5 \times 10^{-6}$ cm

The essential difference between the local stress field in the inclusion and that in a homogeneous single phase medium is given by the correction factor $(4R/\rho)^{g-1/2}$ in Eq. (IV.3-15). This correction factor is plotted in Figure (IV-11) for two different size particles and two different relative rigidities. The correction factor becomes appreciable at distances ρ from the pileup tip which are less than

10Å. However, it is doubtful that much physical significance can be attached to this range of ρ values. At distances from the pileup tip which are physically significant ($\rho \geq 25$Å), when $\kappa > 0$, the correction factor may vary from about $1/2$ to $1/3$, so that the local stresses in the inclusion are about 2 or 3 times lower than those predicted by homogeneous elasticity calculations.

When discussing the stress field off the slip plane, there is an additional correction from homogeneous elasticity theory due to the angular functions $\sin g\varphi$ and $\cos g\varphi$. (Note: when $\kappa = 0$, $g = 1/2$, and when $\kappa > 0$, $g < 1/2$.) One also notes that the constant $A(\kappa,\beta)$ given by (IV.3-11a) or (IV.3-11b) and (IV.3-18) becomes large when $\kappa \to 1$. However, as $\kappa \to 1$, $g \to 0$ and the condition (IV.3-9b) will be satisfied only for values of ρ which are too small to be of physical importance (i.e., $\rho <$ 10Å). When $L/R \ggg 2$, for example, as $\kappa \to 1$ the values of ρ for which (IV.3-9b) is satisfied yield a correction factor $(4R/\rho)^{g-1/2}$ whose magnitude is small enough to offset the contribution of $A(\kappa,\beta)$ as given by (IV.3-18). In other words one may say that the contribution of the singular terms to the stresses in the inclusion is appreciable only over a distance ρ^* given by

$$\frac{2}{\pi} \sin^{-1} \sqrt{\frac{1-\kappa}{2}} \ln \left\{ \frac{4}{\beta+1} \frac{L}{\rho^*} \right\} \approx 1.5 \ . \qquad \text{(IV.3-19)}$$

Hence, as the inclusion becomes more rigid relative to the matrix, κ increases, and ρ^*, the distance over which the singular stresses are important, decreases.

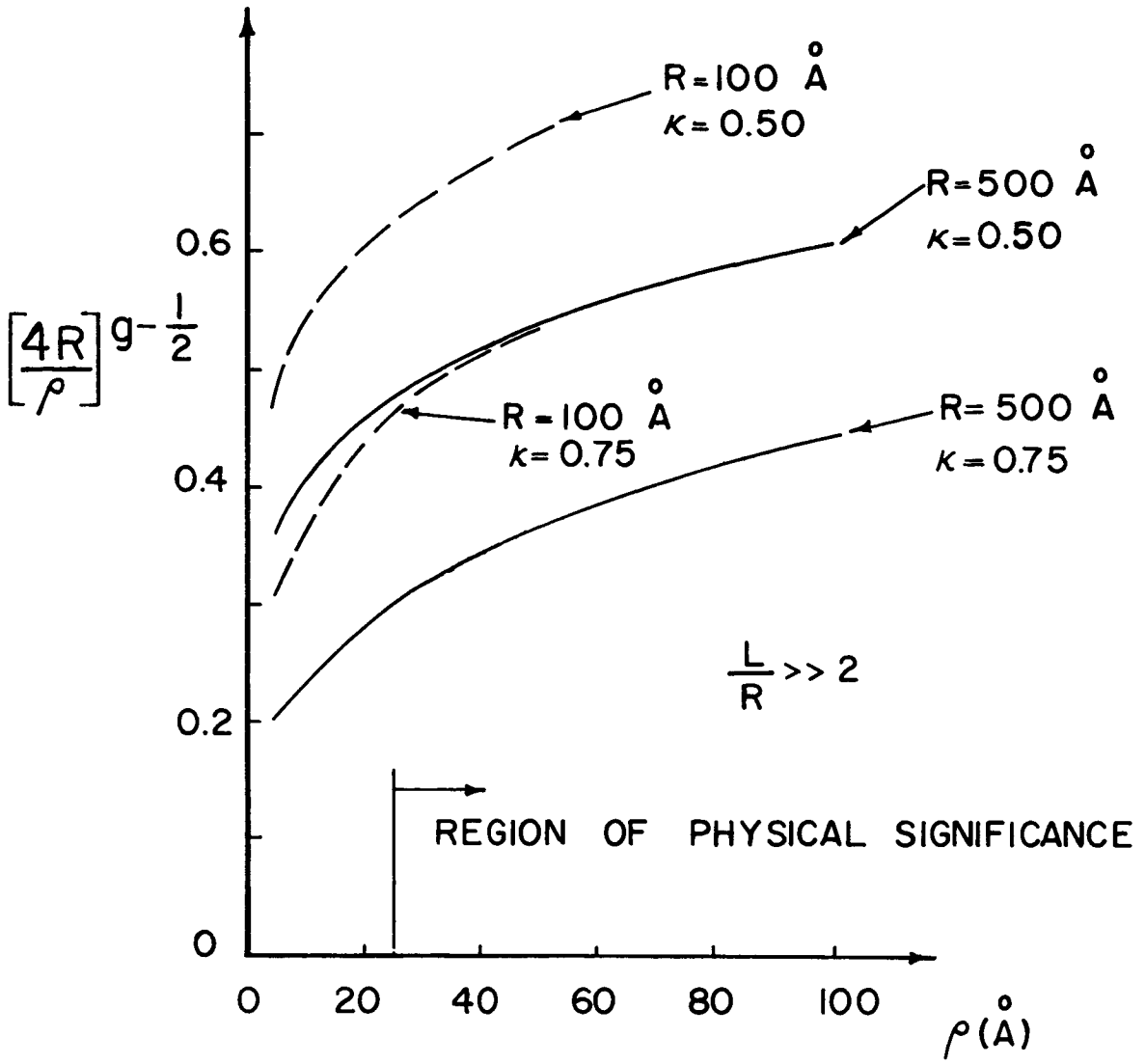

Figure IV-11: The "correction factor" for the local stresses in the second phase as a function of ρ for two particles of different size and different relative rigidities.

Proceeding in a similar manner and neglecting any effects of plastic relaxation, one may also deduce expressions for the local stresses in the matrix. Defining the constant $B(\kappa,\beta)$ by

$$B(\kappa,\beta) = \frac{\sin w(\pi-\gamma_0)\,\sin w\gamma_0 + \sqrt{1-\kappa^2}\; w\cos\gamma_0\,\sin\gamma_0}{\sqrt{1-\kappa^2}\;\sin\gamma_0\cos g\gamma_0} \qquad \text{(IV.3-20a)}$$

$$\text{if } \tau(\lambda) = \tau;$$

$$B(\kappa,\beta) = \frac{\cos w\gamma_0\,\sin w\gamma_0 + w\cos\gamma_0\,\sin\gamma_0}{\sin\gamma_0\cos g\gamma_0}$$

$$\text{if } \tau(\lambda) = \tau\{1 - \kappa/\lambda^2\}\,, \qquad \text{(IV.3-20b)}$$

the local stresses in the matrix are

$$\left.\begin{aligned} \frac{\tau_{xz}}{\tau} &\approx -\,B(\kappa,\beta)\left\{\frac{2L}{\rho}\right\}^g \operatorname{sgn}(y)\,|\cos g(\pi-\varphi)| \\ \frac{\tau_{yz}}{\tau} &\approx -\,B(\kappa,\beta)\left\{\frac{2L}{\rho}\right\}^g |\sin g(\pi-\varphi)| \end{aligned}\right\} \quad \frac{L}{R} < 2 \qquad \text{(IV.3-21)}$$

or

$$\left.\begin{aligned} \frac{\tau_{xz}}{\tau} &\approx -B(\kappa,\beta)\sqrt{\frac{L}{4R}}\left\{2\left(1+\frac{2R}{\rho}\right)\right\}^g \operatorname{sgn}(y)\,|\cos g(\pi-\varphi)| \\ \frac{\tau_{yz}}{\tau} &\approx -\,B(\kappa,\beta)\sqrt{\frac{L}{4R}}\left\{2\left(1+\frac{2R}{\rho}\right)\right\}^g |\sin g(\pi-\varphi)|\,. \end{aligned}\right\} \quad \frac{L}{R} > 2$$

(IV.3-22)

The effects of relative inclusion rigidity and inclusion size upon the local stresses near the pileup tip are best understood by invoking the concept of image dislocation forces. When $\kappa > 0$, decreasing the inclusion size effectively decreases the repulsive image forces near the pileup tip by allowing the giant image dislocation at the origin (Figure IV-1b) to partially cancel out the effect of the image pileup. Thus, the distribution of dislocations near the pileup tip is increased, and local stresses in the second phase increase as inclusion size decreases. When $\kappa < 0$, decreasing the particle size decreases the attractive image forces near the pileup tip, and the same reasoning allows us to conclude that the local stresses should decrease with decreasing particle size. These conclusions are borne out by Figure (IV-9). The effect of relative rigidity (κ) is explained in the same fashion. Local stresses always decrease as the second phase rigidity increases. An increase in κ

(1) increases the repulsive image forces near the pileup tip when $\kappa > 0$

(2) decreases the attractive image forces near the pileup tip when $\kappa < 0$.

In both cases the net effect of an increase in rigidity is to decrease the distribution of pileup dislocations near the inclusion-matrix interface and thus lower the local stresses generated by the array.

4. The Circular Hole ($\kappa = -1$)

When $\kappa = -1$, the second phase becomes a circular hole. Using L'Hospital's rule in Eq. (IV.2-14), the true distribution function for the hole becomes

$$f(\zeta) = \frac{2\tau}{\pi G_1 b} \frac{\zeta-1}{\zeta^2} \left\{ \left[\frac{\pi}{2} + \sin^{-1} \frac{\beta-1}{\beta+1} \right] \sqrt{(\beta-\zeta)(\zeta - 1/\beta)} \right.$$

$$\left. + (\zeta-1) \cosh^{-1} \left[\left(\frac{\beta-1}{\beta+1}\right)\left(\frac{\zeta+1}{\zeta-1}\right) \right] \right\}$$

$$\text{if} \quad \tau(\lambda) = \tau \; ; \qquad \text{(IV.4-1)}$$

$$f(\zeta) = \frac{2\tau}{G_1 b} \frac{\zeta-1}{\zeta^2} \sqrt{(\beta-\zeta)(\zeta - 1/\beta)} \; , \quad \text{if} \quad \tau(\lambda) = \tau\{1 - 1/\lambda^2\} \; . \qquad \text{(IV.4-2)}$$

The distribution function corresponding to (IV.4-1) is shown in Figure (IV-12) for different L/R ratios, and one notes that for the hole the distribution function is bounded at both ends of the array. As $\beta \to 1$ (i.e., $R \to \infty$ and the interface becomes a free surface) the distribution function becomes zero. In reality the integral equation (IV.1-4) does not appear to have an admissible solution for $\kappa = -1$, $R \to \infty$ (see also Chapter III, Eq. (III.1-10)).

The shear stress on the slip plane $y = 0$ outside the hole ($\lambda = x/R \leq -1$) is

$$\tau_{yz} = \tau \left\{ 1 + \frac{\lambda-1}{\lambda^2} \frac{\pi-\gamma_0}{\pi} \sqrt{(\beta-\lambda)\,(1/\beta - \lambda)} - \left(1 - \frac{1}{\lambda^2}\right) \frac{\sigma_0}{\pi} \right\} , \qquad \text{(IV.4-3)}$$

where σ_0 is defined by (IV.3-8). This stress is shown in Figure (IV-13).

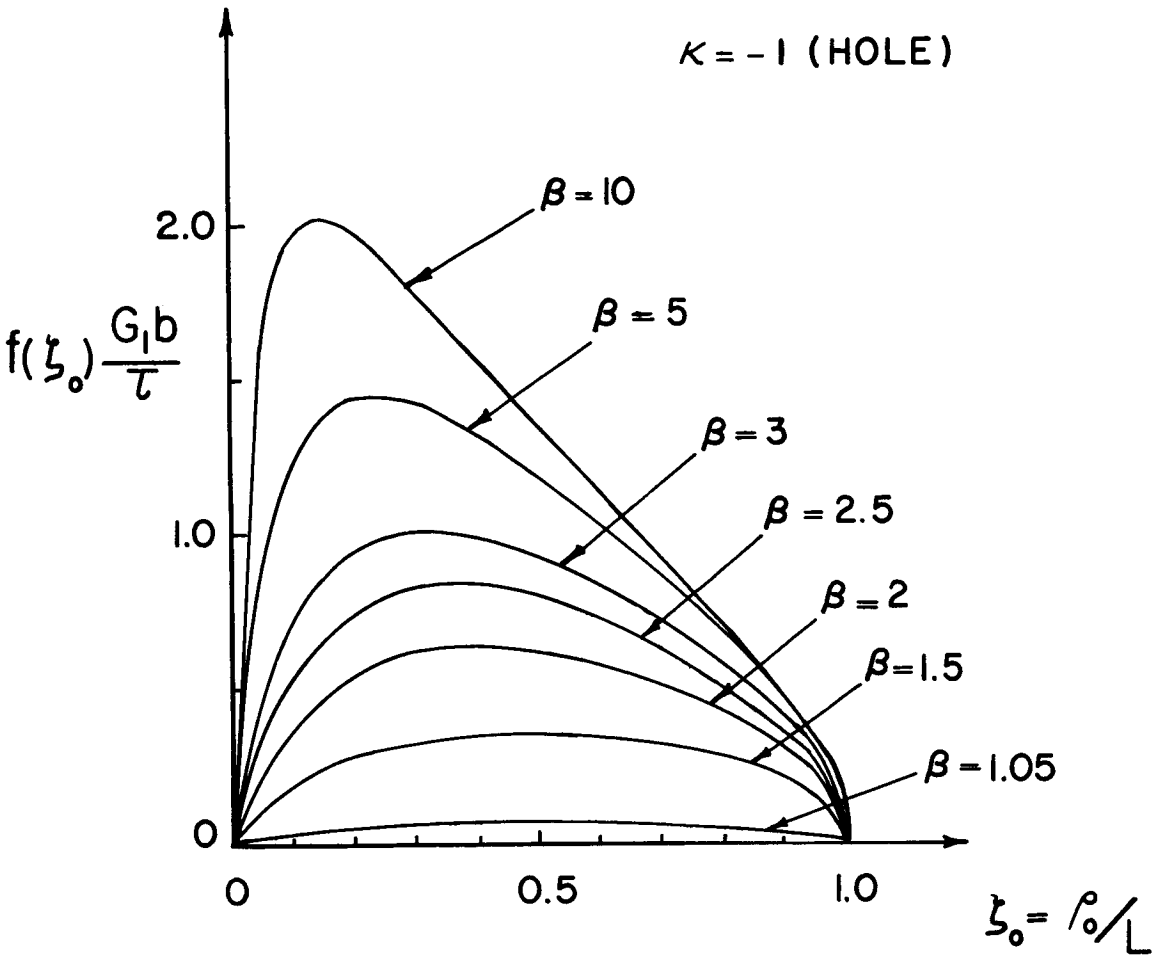

IV-12: $f(\zeta_0)$, the dislocation distribution function for a circular hole, vs. ζ_0 for various values of L/R.

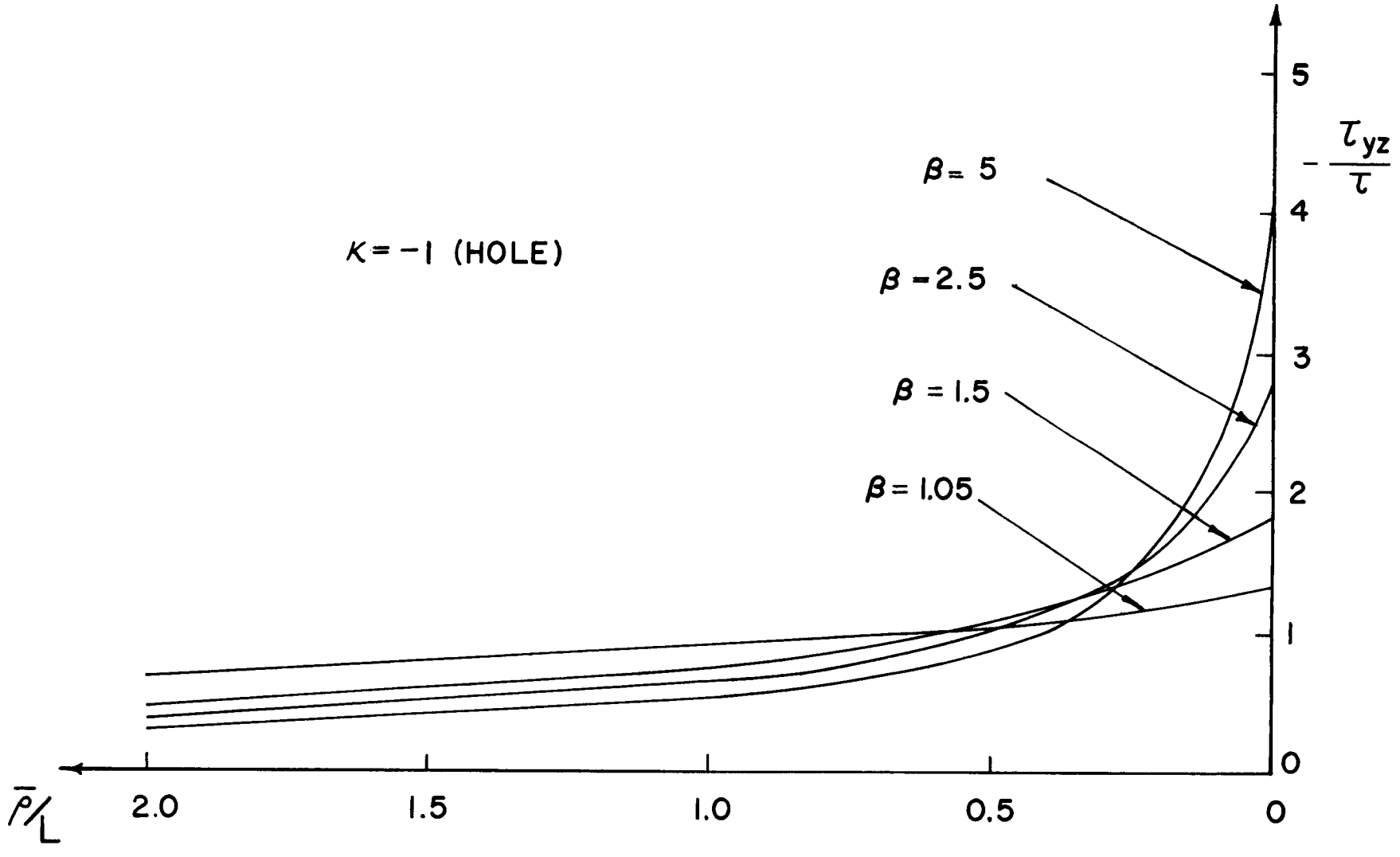

Figure IV-13: The shear stress τ_{yz} on the slip plane $y = 0$ outside a hole. $\bar{\rho}$ is the distance measure along the slip plane from the point $(-R,0)$.

CHAPTER V

AN INFINITE SEQUENCE OF PARALLEL SCREW DISLOCATION ARRAYS PILED UP AGAINST AN ELASTIC HALF-PLANE OF FINITE RIGIDITY

1. Analysis

We again focus our attention upon the bimetallic medium discussed in Chapter III, i.e., two elastic half planes of different shear moduli welded together at $x = 0$. However, instead of restricting ourselves to a single slip band on the plane $y = 0$ (in $x > 0$), we envisage an infinite sequence of linear screw dislocation arrays lying on the planes $y = \pm nh$, where $n = 0, \pm 1, \pm 2, \ldots$ (Figure V-1). Each array is of length L and contains N right-hand screw dislocations of Burgers' vector b. The effective applied shear stress causing the arrays to pile up against the weld is $\tau_{yz} = -\tau$. Since each array induces an image array in $x < 0$ of N screws of strength Kb distributed over $[-L, 0)$, the stress field in the matrix $(x > 0)$ is equivalent to that of the real arrays and the image system depicted in Figure V-1.

Because the situation is translationally invariant with respect to the transformation $y' = y \pm sh$, where s is an integer (i.e., the distribution of dislocations in any one slip band is the same on all slip planes), we need only consider the static equilibrium condition for one array. For convenience we choose the slip plane $y = 0$.

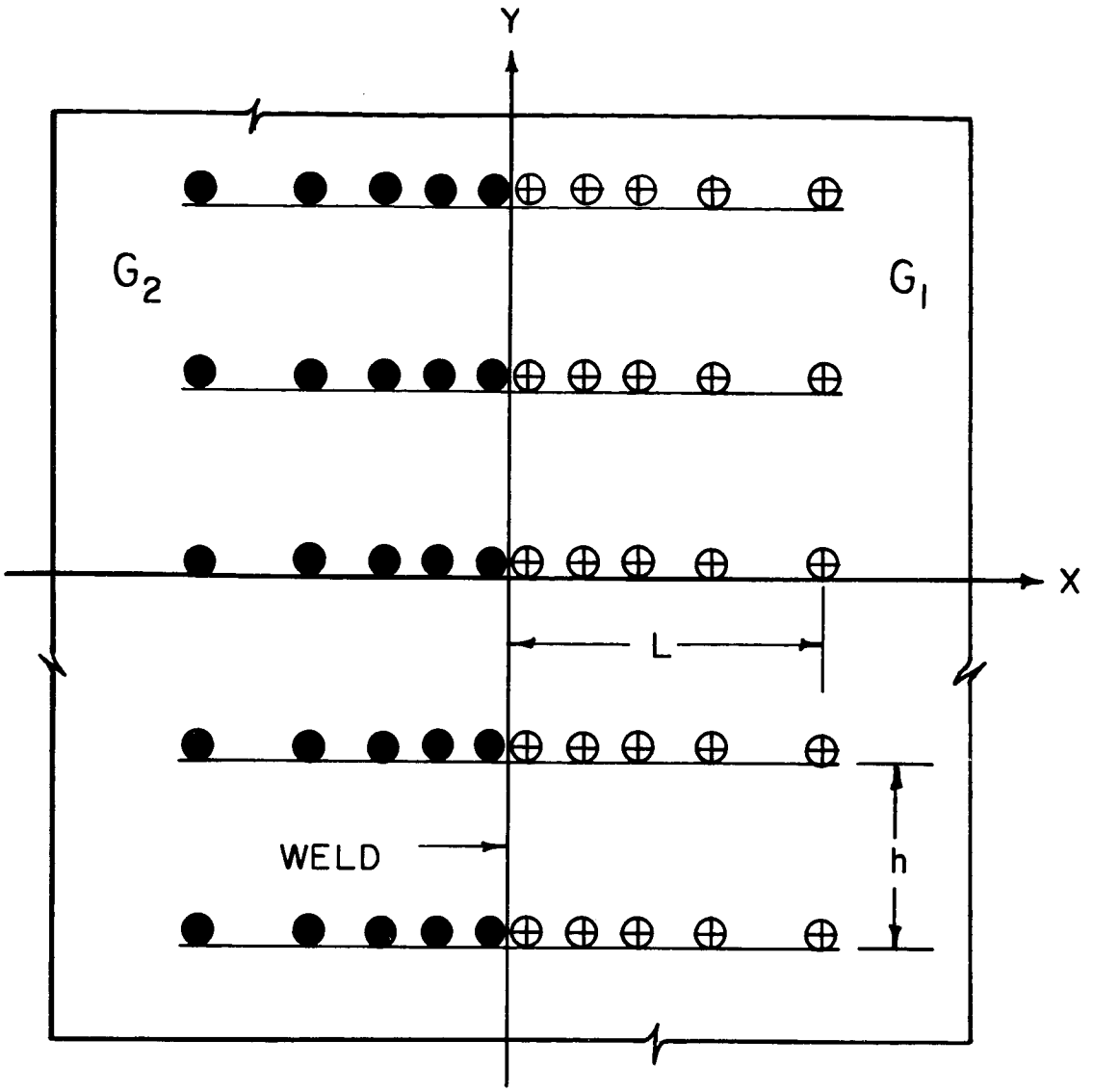

⊕ REAL SCREW DISLOCATION OF STRENGTH b

● IMAGE SCREW OF STRENGTH Kb

Figure V-1: An infinite sequence of parallel screw slip bands stacked against an elastic half-plane of finite rigidity. The induced image arrays are also depicted.

Invoking the approximation of continuously distributed dislocations, the dislocation distribution function on any slip plane must satisfy

$$\frac{G_1 b}{2\pi}\left\{\sum_{n=-\infty}^{\infty}\int_0^L \frac{f(t)\,(x-t)\,dt}{(x-t)^2+n^2h^2}+\kappa\sum_{n=-\infty}^{\infty}\int_0^L \frac{f(t)\,dt\,(x+t)}{(x+t)^2+n^2h^2}\right\}=\tau. \quad (V.1\text{-}1)$$

Defining the dimensionless parameters

$$\lambda=\frac{x}{L}, \qquad \zeta=\frac{t}{L}, \qquad H=\frac{h}{L},$$

and interchanging the operations of summation and integration, we must solve

$$\int_0^1 f(\zeta)\,d\zeta\left(\lambda-\zeta\right)\sum_{n=-\infty}^{\infty}\frac{1}{(\lambda-\zeta)^2+n^2H^2}$$

$$+\kappa\int_0^1 f(\zeta)\,d\zeta\left(\lambda+\zeta\right)\sum_{n=-\infty}^{\infty}\frac{1}{(\lambda+\zeta)^2+n^2H^2}=\frac{2\pi\tau}{G_1 b}. \quad (V.1\text{-}2)$$

But[37]

$$\left(\lambda\pm\zeta\right)\sum_{n=-\infty}^{\infty}\frac{1}{(\lambda\pm\zeta)^2+n^2H^2}=\frac{\pi}{H}\frac{\sinh(2\pi(\lambda\pm\zeta)/H)}{\cosh(2\pi(\lambda\pm\zeta)/H)-1}$$

$$=\frac{\pi}{H}\frac{\cosh(\pi(\lambda\pm\zeta)/H)}{\sinh(\pi(\lambda\pm\zeta)/H)}. \quad (V.1\text{-}3)$$

Further manipulation shows that Eq. (V.1-2) can be rewritten as

$$\int_0^1 f(\zeta)\, d\zeta \, \frac{1 - \tanh(\pi\lambda/H)\tanh(\pi\zeta/H)}{\tanh(\pi\lambda/H) - \tanh(\pi\zeta/H)}$$

$$+ \kappa \int_0^1 f(\zeta)\, d\zeta \, \frac{1 + \tanh(\pi\lambda/H)\tanh(\pi\zeta/H)}{\tanh(\pi\lambda/H) + \tanh(\pi\zeta/H)} = \frac{2H\tau}{G_1 b} \quad . \qquad \text{(V.1-4)}$$

The end conditions on $f(\zeta)$ are

$$\left.\begin{array}{l} f(0) \text{ unbounded with a weak singularity} \\ f(1) = 0 \quad . \end{array}\right\} \qquad \text{(V.1-5)}$$

The solution to Eq. (V.1-4) is (see Appendix G)

$$f(\zeta) = \frac{2\tau}{G_1 b}\sqrt{\frac{2}{1-\kappa}}\, \sec\left\{g \sin^{-1}\left\langle \tanh\frac{\pi}{H}\right\rangle\right\}$$

$$\times \sinh\left\{g \cosh^{-1}\left\langle \frac{\tanh \pi/H}{\tanh \pi\zeta/H}\right\rangle\right\} \quad , \qquad \text{(V.1-6)}$$

where

$$g = \frac{2}{\pi} \sin^{-1}\sqrt{\frac{1-\kappa}{2}} \quad . \qquad \text{(V.1-7)}$$

One notes that as $H = h/L \to \infty$,

$$\frac{\tanh \pi/H}{\tanh \pi\zeta/H} \to \frac{1}{\zeta} \, ,$$

$$\sec\{g \sin^{-1}\langle \tanh\frac{\pi}{H}\rangle\} \to 1,$$

and we recover the single slip band solution (Chapter III). Figure (V-2) shows the distribution function for various values of $H = h/L$ at constant relative rigidity κ .

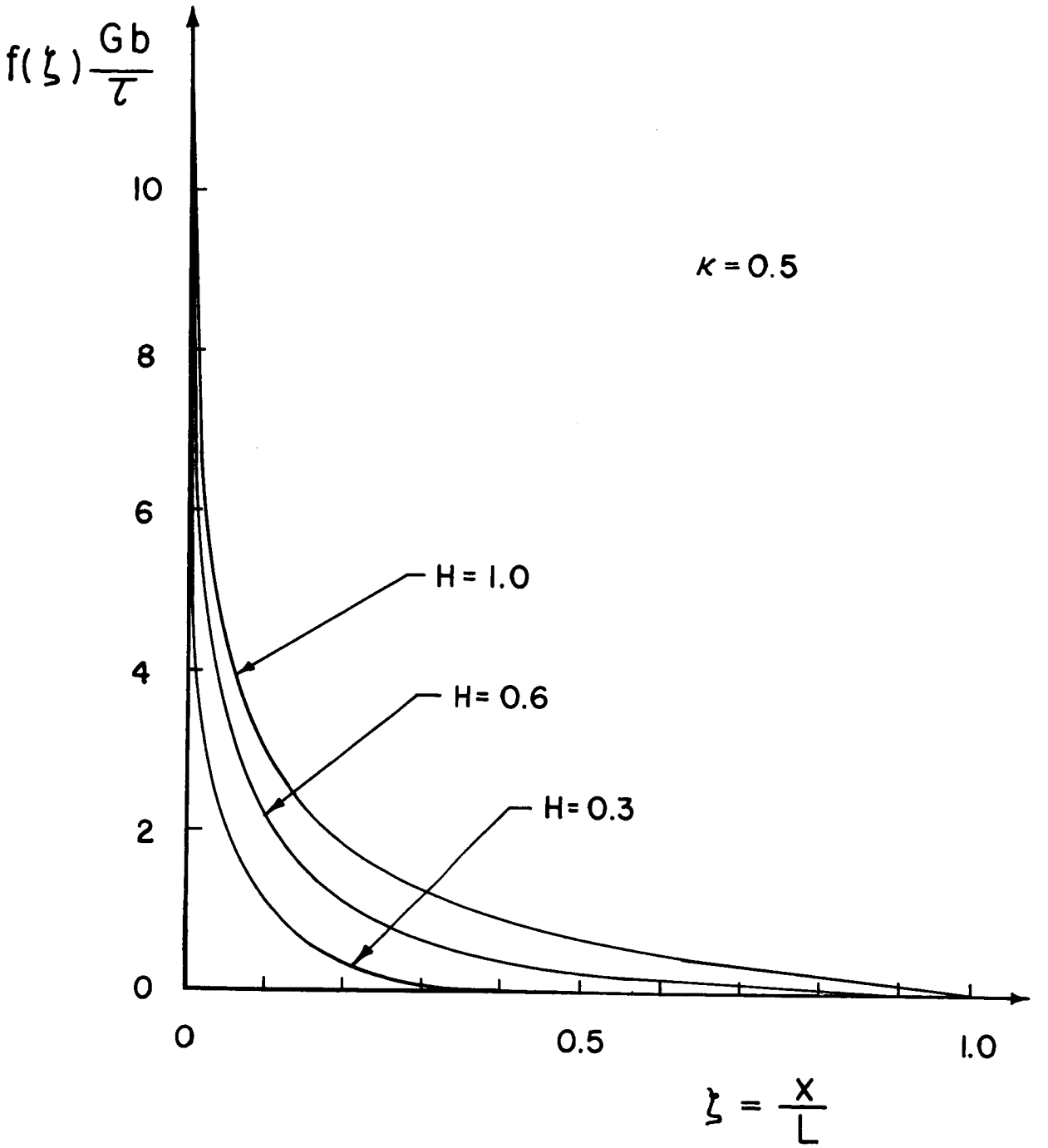

Figure V-2: $f(\zeta)$, the dislocation distribution function, vs. ζ for a fixed relative rigidity and varying slip band separation.

N, the number of dislocations in the pileup, is given by

$$\frac{N}{L} = \frac{2\tau H}{G_1 b} \frac{\tan\{g \sin^{-1}\langle \tanh \pi/H\rangle\}}{\sqrt{1-\kappa^2}} . \qquad \text{(V.1-8)}$$

N as a function of $H = h/L$ for different values of κ is shown in Figure (V-3). Upon examining Eq. (V.1-8), one notes that

(1) when $H = h/L < 2$ (i.e., the slip band separation is less than twice the slip line length),

$$\tanh \frac{\pi}{H} \approx 1 ,$$

so that

$$N \approx \frac{2\tau h}{G_1 b} \cdot \frac{1}{1+\kappa} . \qquad \text{(V.1-9)}$$

Thus, the number of dislocations in each array is proportional to h, <u>not</u> L; since $h < 2L$, the slip band interaction has <u>reduced</u> the number of dislocations in each array (as compared to the single slip band case).

(2) when $H = h/L > 5$,

$$\tanh \frac{\pi}{H} \approx \frac{\pi}{H}$$

so that

$$N \approx \frac{4\tau L}{G_1 b} \frac{\sin^{-1}\sqrt{\frac{1-\kappa}{2}}}{\sqrt{1-\kappa^2}} \qquad \text{(V.1-10)}$$

just as in the case of a single slip band (Chapter III).

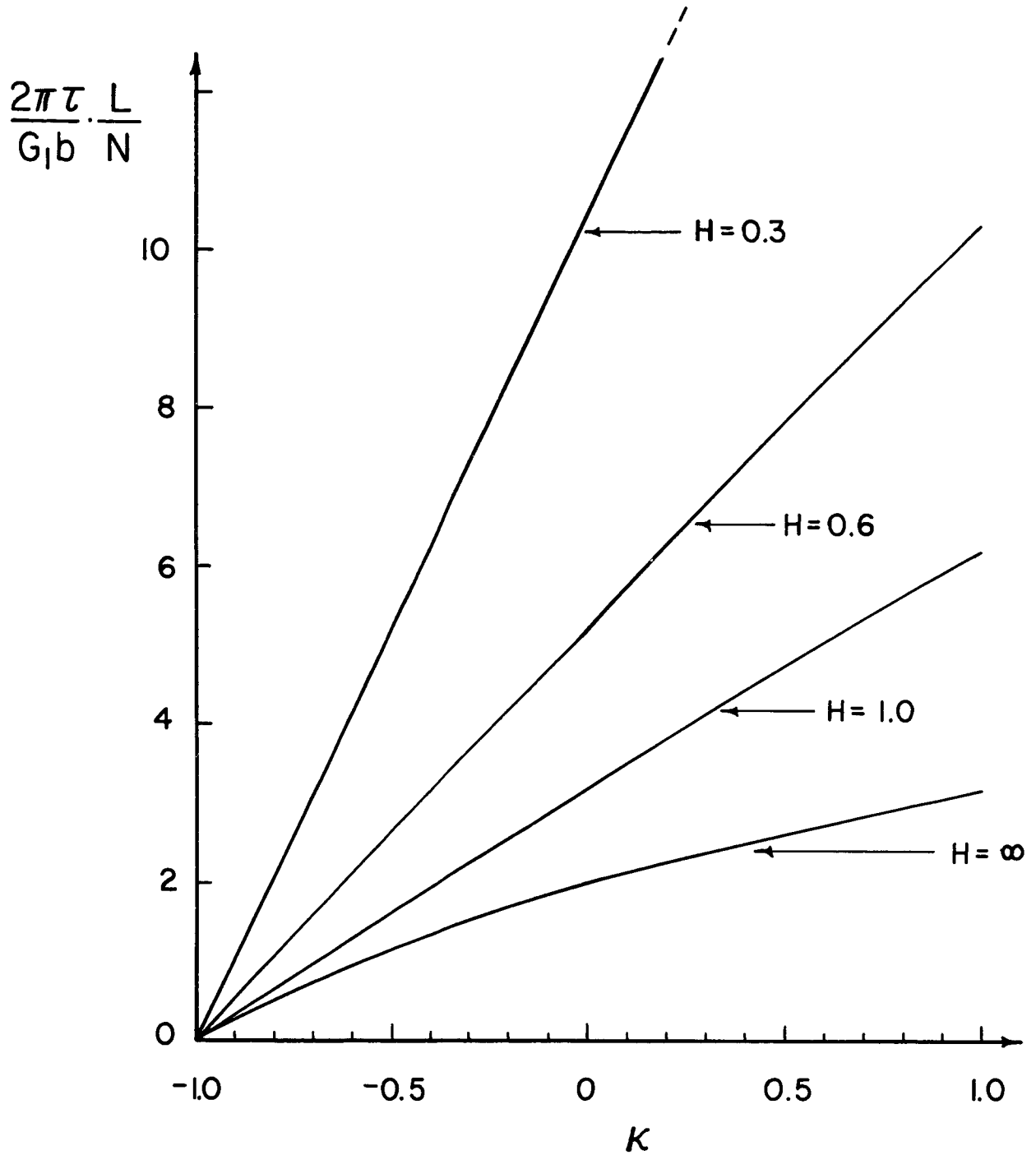

Figure V-3: $\frac{2\pi\tau}{G_1 b} \cdot \frac{L}{N}$ as a function of κ for different slip band separations.

2. The Pileup Stress Field

The calculation of the general stress field is rather difficult. However, the salient features of the effect of slip band interaction upon the stresses generated by the arrays may be deduced from an examination of

(1) the shear stress τ_{yz} on any plane $y = nh$ in the second phase ($x < 0$). For convenience we may choose $y = 0$.

(2) the interfacial shear $\tau_{xz}|_{x=0}$. Translational invariance with respect to the transformation $y' = y + sh$ allows us to restrict our attentions to either the interval $-h/2 \leq y \leq h/2$ or $0 \leq y \leq h$. Considerations of symmetry and translational invariance demand that

$$\tau_{xz}(x,\ y = (2n+1)\frac{h}{2}) = 0, \qquad n = 0, \pm 1, \pm 2, \ldots$$

$$\tau_{xz}(x \neq 0,\ y = nh) = 0\ , \qquad n = 0, \pm 1, \pm 2, \ldots$$

(a) <u>The slip plane shear stress $\tau_{yz}|_{y=0}$ in the second phase</u> ($\lambda = -x/L > 0$): When $\lambda \leq 1$,

$$\tau_{yz}|_{y=0} = \frac{G_2}{G_1}\tau - \tau\,\frac{\sqrt{2(1+\kappa)}}{1-\kappa}\,\sec\{g\,\sin^{-1}\langle\tanh\tfrac{\pi}{H}\rangle\}$$

$$\times \cosh\left\{g\,\cosh^{-1}\left\langle\frac{\tanh\,\pi/H}{\tanh\,\pi\lambda/H}\right\rangle\right\}. \qquad \text{(V.2-1)}$$

For $\lambda \geq 1$, the same expression is valid if

$$\cosh\left\{g\,\cosh^{-1}\left\langle\frac{\tanh\,\pi/H}{\tanh\,\pi\lambda/H}\right\rangle\right\}$$

is replaced by

$$\cos\left\{g\,\cos^{-1}\left\langle\frac{\tanh\,\pi/H}{\tanh\,\pi\lambda/H}\right\rangle\right\}\quad .$$

The term $(G_2/G_1)\tau$ cancels out the stress $-(G_2/G_1)\tau$ induced in $x < 0$ by the applied shear $\tau_{yz} = -\tau$ in $x > 0$ (see Eqs. (III.1-3)).

(b) <u>The interfacial shear</u> τ_{xz} $(x = 0)$: Defining the dimensionless parameter

$$\eta = \frac{y}{L}\ ,$$

$$\tau_{xz}\big|_{x=0} = -\tau\sqrt{\frac{1+\kappa}{1-\kappa}}\ \sec\left\{g\,\sin^{-1}\left\langle\tanh\,\frac{\pi}{H}\right\rangle\right\}$$

$$\times\ \sinh\left\{g\,\sinh^{-1}\left\langle\frac{\tanh\,\pi/H}{\tan\,\pi\eta/H}\right\rangle\right\}\quad . \qquad \text{(V.2-2)}$$

When

$$g\,\ln\left\{\frac{2\,\tanh\,\pi/H}{\tanh\,\pi\lambda/H}\right\} > 1.5$$

and (V.2-3)

$$g\,\ln\left\{\frac{2\,\tanh\,\pi/H}{\tan\,\pi|\eta|/H}\right\} > 1.5\ ;\ |\eta| < \frac{H}{2}\ ,$$

then

$$\left.\begin{aligned}\tau_{yz}\big|_{y=0} &\approx -\frac{\tau}{1-\kappa}\left\{\frac{2h}{\pi\lambda}\right\}^g\\ \tau_{xz}\big|_{x=0} &\approx -\frac{\tau}{\sqrt{2}}\,\frac{\mathrm{sgn}(\eta)}{1-\kappa}\left\{\frac{2h}{\pi|\eta|}\right\}^g\end{aligned}\right\}\ H = \frac{h}{L} < 2 \qquad \text{(V.2-4)}$$

$$\left.\begin{aligned} \tau_{yz}|_{y=0} &\approx -\tau \sqrt{\frac{1+\kappa}{2}}\ \frac{1}{1-\kappa}\left\{\frac{2L}{\lambda}\right\}^{g} \\ \tau_{xz}|_{x=0} &\approx -\frac{\tau}{2}\sqrt{\frac{1+\kappa}{1-\kappa}}\ \mathrm{sgn}(\eta)\left\{\frac{2L}{|\eta|}\right\}^{g} \end{aligned}\right\} \quad H = \frac{h}{L} > 5 \ . \qquad \text{(V.2-5)}$$

The general stress field close to the pileup tip will be such that

$$\left.\begin{aligned} \tau_{ij} &\propto \tau\left\{\frac{2h}{\pi\rho}\right\}^{g} ; \qquad H = \frac{h}{L} < 2 \\ \tau_{ij} &\propto \tau\left\{\frac{2L}{\rho}\right\}^{g} ; \qquad H = \frac{h}{L} > 5 \end{aligned}\right\} \qquad \text{(V.2-6)}$$

where ρ is the radius vector from the pileup tip. Equations (V.2-5) are reminiscent of the single slip band solution, and this seems reasonable, for when $H = h/L > 5$ slip band interaction is rather negligible. However, when the slip bands are more closely spaced $(h/L < 2)$, the interaction becomes important, and stress intensification depends on h, the slip band separation, rather than L, the slip line length. These conclusions are supported by Eqs. (V.1-9) and (V.1-10)

Equations (V.2-6) show that the stress concentration about the pileup tips decreases as the slip band separation decreases. At first glance this may seem unreasonable, since, for a given distribution of array dislocations, a decrease in h brings the singularities closer together and intensifies the local stresses. One must remember, however, that as h decreases, slip band interaction changes the distribution of dislocations in the arrays (Figure V-2). When $h < 2L$, an appreciable number of dislocations is distributed only over a slip

line length $L' \approx h/2 < L$, so that stress intensification is related to L' (and thus h) rather than to L. When $h \ll L$, the value of N given by eq. (V.1-9) will be too small for the continuous distribution approximation to apply. Since the minimum value of N is unity, when $\tau \approx 10^{-3}$ to $10^{-2}\, G_1$, $b \approx 2 \times 10^{-8}$ cm, we must certainly require that h be greater than 10^{-5} to 10^{-6} cm if the continuous distribution approximation is to be valid.

The above model may be taken as a rough approximation to a work-hardening material in which the plasticity is not restricted to a single slip band. When the individual slip bands in a broadened glide band are closely spaced, the interfacial shear is short range (i.e., $\tau_{xz|\,x=0}$ is zero at $y = \pm (2n+1)\, h/2$). Thus, closely spaced slip bands may promote the formation of a series of fine cracks in the second phase, rather than interfacial fracture. Of course, in a real material the sequence of slip bands will be finite, so that somewhat larger stresses can occur near the tips of the top and bottom arrays. Unfortunately, the finite sequence of slip bands cannot be treated in closed form by the continuous distribution approximation.

CHAPTER VI

AN EDGE DISLOCATION PILEUP AGAINST AN ELASTIC HALF-PLANE

1. Analysis

Although the general problem of an edge dislocation array piled up against an elastic half-plane has not been treated in closed form, it is of interest to formulate the problem via the continuous distribution approach and to note the differences between the edge array and the screw array problem (Chapter III). We consider the identical problem discussed in Chapter III, with the array of right-hand screw dislocations replaced by an array of positive edge dislocations. Using the stress functions of Dundurs and Sendeckyj,[12] the continuous dislocation distribution formulation of the static equilibrium condition requires that the dislocation distribution function, $f(t)$ satisfy

$$\int_0^L \frac{f(t)\,dt}{x-t} + \frac{3A-B}{2}\int_0^L \frac{f(t)\,dt}{x+t} + 2A\left\{3x\frac{d}{dx} + x^2\frac{d^2}{dx^2}\right\}\int_0^1 \frac{f(t)\,dt}{x+t}$$

$$= \frac{2\pi(1-\nu_1)\tau}{G_1 b}\,; \qquad \text{(VI.1-1)}$$

$f(0)$ unbounded with a weak singularity;

$f(L) = 0$;

where

$$A = \frac{1 - \Gamma}{1 + \Gamma K_1}$$

$$B = \frac{K_2 - \Gamma K_1}{K_2 + \Gamma}$$

$$\Gamma = \frac{G_2}{G_1}$$

$$K_i = 3 - 4\nu_i , \qquad i = 1, 2, \qquad \text{(VI.1-2)}$$

ν_i = Poisson's ratio of the ith phase

$\tau = -\tau_{xy}$ (applied) = constant.

The first term on the left side of (VI.1-1) is the usual term which appears in single phase calculations; the last three terms effectively represent image arrays of edge monopoles, dipoles and quadrupoles, respectively, distributed on $[-L, 0)$.

Equation (VI.1-1) is a singular integro-differential equation for the distribution function $f(t)$. Its solution is readily apparent for only one special case, that being when $G_2 = G_1$. If $G_2 = G_1$, $\Gamma = 1$ and $A = 0$, so that (VI.1-1) reduces to

$$\int_0^L \frac{f(t)\,dt}{x-t} + \frac{1}{2}\left\{\frac{1-\nu_1}{1-\nu_2} - 1\right\} \int_0^L \frac{f(t)\,dt}{x+t} = \frac{2\pi(1-\nu_1)\tau}{G_1 b} . \qquad \text{(VI.1-3)}$$

Using the results of Chapter III, the solution to (VI.1-3) is given by Eq. (III.1-4) with κ replaced by $\{(1-\nu_1)/(1-\nu_2) - 1\}/2$ and τ

replaced by $(1-\nu_1)\tau$. The parameter g, which dictates the strength of the stress singularity at the pileup tip, is then given by

$$g = \frac{2}{\pi} \sin^{-1} \left\langle \frac{1}{2} \sqrt{3 - \frac{1-\nu_1}{1-\nu_2}} \right\rangle . \qquad \text{(VI.1-4)}$$

Since $g = 1/2$ only if $\nu_1 = \nu_2$ (perfectly identical half-planes), even if $G_2 = G_1$, the pileup tip stress singularity cannot be of the inverse square root type[19] when $\nu_1 \neq \nu_2$.

For $A \neq 0$ $(G_2 \neq G_1)$ the author offers the following as a possible method of attacking Eq. (VI.1-1). By defining

$$\left.\begin{aligned} f(t) &= \frac{2\pi(1-\nu_1)}{G_1 b} f_0(t) , \\ \lambda &= \frac{x}{L} , \\ \zeta &= \frac{t}{L} , \end{aligned}\right\} \qquad \text{(VI.1-5)}$$

the edge problem will be solved if a function $f_0(\zeta)$ can be found satisfying

$$\int_0^1 \frac{f_0(\zeta)\, d\zeta}{\lambda-\zeta} + \left\{ \frac{3A-B}{2} + \frac{2A}{\lambda} \frac{d}{d\lambda} \left(\lambda^3 \frac{d}{d\lambda}\right) \right\} \int_0^1 \frac{f_0(\zeta)\, d\zeta}{\lambda+\zeta} = 1 . \qquad \text{(VI.1-6)}$$

Now we can rewrite (VI.1-6) as

$$\mathcal{L} \left\{ \int_0^1 \frac{f_0(\zeta)\, d\zeta}{\lambda+\zeta} \right\} = \frac{\lambda}{2A} \left\{ 1 - \int_0^1 \frac{f_0(\zeta)\, d\zeta}{\lambda-\zeta} \right\} , \qquad \text{(VI.1-7)}$$

where $\mathcal{L}$ is the self-adjoint linear differential operator

$$\mathcal{L} = \frac{d}{d\lambda}\left(\lambda^3 \frac{d}{d\lambda}\right) + \frac{3A-B}{4A}\lambda \ . \qquad \text{(VI.1-8)}$$

If we now construct the Green's function $G(\lambda; \lambda')$ for $\mathcal{L}$ subject to the end conditions

$G(0; \lambda')$ may be unbounded with a weak singularity

$G(1; \lambda') = 0$

and if

$$\lim_{\lambda \to 1} G(\lambda;\lambda') \frac{d}{d\lambda} \int_0^1 \frac{f_0(\zeta)\, d\zeta}{\lambda+\zeta} = 0 \ ,$$

then

$$\int_0^1 \frac{f_0(\zeta)\, d\zeta}{\lambda'+\zeta} + I(1) \left\{\frac{dG(\lambda;\lambda')}{d\lambda}\right\}_{\lambda=1} + \frac{1}{2A} \int_0^1 \lambda G(\lambda;\lambda')\, d\lambda$$

$$= \frac{1}{2A} \int_0^1 \lambda G(\lambda;\lambda')\, d\lambda \int_0^1 \frac{f_0(\zeta)\, d\zeta}{\lambda-\zeta} \qquad \text{(VI.1-9)}$$

where

$$I(1) = \int_0^1 \frac{f_0(\zeta)\, d\zeta}{1+\zeta} = \text{constant} \ . \qquad \text{(VI.1-10)}$$

Now when the respective elastic constants are such that $-1 < B/A < 3$ (one may note that B/A is always > 0 when G_2/G_1 lies outside the interval $[K_2/K_1, 1]$), the appropriate Green's function, $G(\lambda;\lambda')$ is

$$G(\lambda;\lambda') = \frac{1}{2\mu}\lambda^{-1+\mu}\{\lambda'^{-1-\mu} - \lambda'^{-1+\mu}\} \quad ; \quad \lambda < \lambda'$$

$$= \frac{1}{2\mu}\lambda'^{-1+\mu}\{\lambda^{-1-\mu} - \lambda^{-1+\mu}\} \quad ; \quad \lambda > \lambda' \qquad \text{(VI.1-11)}$$

where

$$\mu = \frac{1}{2}\sqrt{1 + B/A}\ , \qquad \text{(VI.1-12)}$$

so that

$$\left\{\frac{dG(\lambda;\lambda')}{d\lambda}\right\}_{\lambda=1} = -\lambda'^{-1+\mu}$$

$$\int_0^1 \lambda G(\lambda;\lambda')\, d\lambda = \frac{1}{1-\mu^2}\{\lambda'^{-1+\mu} - 1\}. \qquad \text{(VI.1-13)}$$

Thus, Eq. (VI.1-9) may be written as

$$\int_0^1 \frac{f_0(\zeta)\, d\zeta}{\lambda+\zeta} - I(1)\,\lambda^{-1+\mu} + \frac{1}{2A}\,\frac{1}{1-\mu^2}\{\lambda^{-1+\mu} - 1\}$$

$$= \frac{1}{2A}\int_0^1 \lambda' G(\lambda;\lambda')\, d\lambda' \int_0^1 \frac{f_0(\zeta)\, d\zeta}{\lambda'-\zeta}\ . \qquad \text{(VI.1-14)}$$

Now since $G(\lambda;\lambda')$ behaves as $\lambda^{-1+\mu}$ as $\lambda \to 0$, Eq. (VI.1-14) leads us to suspect that

$$\int_0^1 \frac{f_0(\zeta)\, d\zeta}{\lambda+\zeta} \sim \lambda^{-1+\mu} \quad \text{as} \quad \lambda \to 0\ . \qquad \text{(VI.1-15)}$$

If the above argument is valid, then, based upon the results obtained for the corresponding screw array problem, one might intuitively

expect that the stress field in the vicinity of the pileup tip is of the form

$$\tau_{ij} \sim \left(\frac{L}{\rho}\right)^{1-\mu} , \qquad -1 < B/A < 3 . \qquad \text{(VI.1-16)}$$

No rigorous proof of the above statements can be given at this time. It is hoped that the above analysis has lent some insight into the complicated plane strain dislocation array problem. If (VI.1-16) is true, it illustrates the power of the continuously distributed dislocation approach, since the stress field near the pileup tip can be surmised without effecting an actual solution for $f(\zeta)$. We note two special cases:

(1) $G_2/G_1 = 0$ ($x = 0$ a free surface)

$$1 - \mu = 1 - \frac{1}{\sqrt{2}} \approx 0.293 .$$

(2) $G_2/G_1 \to \infty$ (rigid second phase)

$$1 - \mu = 1 - \frac{1}{2}\sqrt{1 + K_1^2} ,$$

so that if $\nu_1 \approx 1/3$,

$$1 - \mu \approx 0.03 .$$

When $B/A \gg 3$ (i.e., when $G_2 \approx G_1$), A is close to zero, so that the image multipole forces are small relative to the image monopole forces. Thus, the stress singularity at the pileup tip should be dictated approximately by Eq. (VI.1-4).

2. The Pileup Stress Field

Provided that one can solve for $f_0(\zeta)$, the pileup stress field can be expressed in terms of only two integrals and their derivatives:

$$\left.\begin{aligned} I_1(\lambda,\eta) &= \int_0^1 \frac{f_0(\zeta)\, d\zeta}{(\lambda-\zeta)^2 + \eta^2} \\ \text{and} \qquad & \\ I_2(\lambda,\eta) &= \int_0^1 \frac{(\lambda-\zeta)\, f_0(\zeta)\, d\zeta}{(\lambda-\zeta^2) + \eta^2} \,, \end{aligned}\right\} \qquad \text{(VI.2-1)}$$

where λ and η are the dimensionless coordinates

$$\lambda = \frac{x}{L} \,, \qquad \eta = \frac{y}{L} \,. \qquad \text{(VI.2-2)}$$

Apart from simple multiplicative constants the exact stress field in the second phase ($\lambda < 0$) can be expressed as:

$$\sigma_{xx}(\lambda,\eta) \sim \left\{ - [(1+A)K_1 + (1+B)]\eta - \frac{2}{\Gamma}(B-A)\eta \left[2 + \lambda \frac{\partial}{\partial\lambda} + \eta \frac{\partial}{\partial\eta}\right] - \frac{2}{\Gamma}(1-B)\eta\left[1 + \eta \frac{\partial}{\partial\eta}\right] \right\} I_1(\lambda,\eta) \,. \qquad \text{(VI.2-3)}$$

$$\sigma_{yy}(\lambda,\eta) \sim \left\{ [-(1-A)K_1 + 1 - B]\eta - \frac{2}{\Gamma}(B-A)\eta \left[2 + \lambda \frac{\partial}{\partial\lambda} + \eta \frac{\partial}{\partial\eta}\right] + \frac{2}{\Gamma}(1-B)\eta \left[2 + \eta \frac{\partial}{\partial\eta}\right] \right\} I_1(\lambda,\eta) \,. \qquad \text{(VI.2-4)}$$

$$\tau_{xy} \sim \left\{ 2[(A\kappa_1 + 1) + \frac{2}{\Gamma}(B-A)]\, I_2(\lambda,\eta) \right.$$
$$\left. - \frac{4}{\Gamma}(B-A)\left[\lambda + \lambda\eta\frac{\partial}{\partial\eta} - \eta^2\frac{\partial}{\partial\lambda}\right] I_1(\lambda,\eta) \right\} . \qquad \text{(VI.2-5)}$$

One can deduce similar expressions for the stresses in the matrix ($\lambda > 0$) which involve not only $I_1(\lambda,\eta)$ and $I_2(\lambda,\eta)$, but also $I_1(-\lambda,\eta)$ and $I_2(-\lambda,\eta)$.

CHAPTER VII

DISCUSSION

1. The Hall-Petch Relation

Numerous investigators have reported that the grain size dependence of the yield stress of a polycrystal obeys a Hall-Petch[38,39] relation, i.e.,

$$\tau_y = \tau_i + k_y d^{-1/2} , \qquad \text{(VII.1-1)}$$

where

τ_y = flow stress of the polycrystal

τ_i = flow stress extrapolated to infinite grain size

d = average grain diameter

k_y = an "unpinning" parameter or measure of the dislocation locking.

A simple derivation of the Hall-Petch relation is as follows. Consider that yielding has occurred in one grain of a polycrystal, such that slip dislocations have piled up at the grain boundary. If slip is to occur in the grain adjacent to the pileup, one argues that the local stresses generated by the pileup must be high enough to activate dislocation sources in the neighboring grain. If these sources are located a mean distance r^* from the pileup tip, and if τ^* is the critical shear stress at which a source becomes operative, then, using the

expressions for the local stresses about a screw or edge dislocation pileup in a single phase material, the condition for continued slip becomes

$$(\tau - \tau_i)\sqrt{\frac{L}{r^*}} = \tau^* \ . \qquad \text{(VII.1-2)}$$

The effective shear stress creating the original pileup of length L is taken to be the difference between τ, the applied shear, and τ_i, the lattice friction stress resisting dislocation motion. Rearrangement gives

$$\tau = \tau_i + (\tau^* \sqrt{r^*})\, L^{-1/2} \ . \qquad \text{(VII.1-3)}$$

Assuming L to be proportional to the mean grain diameter (say $L \approx d/2$) and identifying

$$k_y \propto \tau^* \sqrt{r^*} \ , \qquad \text{(VII.1-4)}$$

one arrives at the Hall-Petch relation.

Gay, Hirsch, and Kelly[40] and Embury, Keh, and Fischer[41] have shown that a Hall-Petch equation may apply to materials exhibiting a substructure, if one interprets d as the mean spacing of substructural barriers. Gay, et al. proposed that the pileup model for source activation is still valid, but that the sources are activated in the vicinity of the barrier, whereas Embury, et al., questioned the validity of the EFN pileup calculations when the specific nature of the barrier was not taken into account.

The treatments presented in this dissertation have made allowances for particular types of barriers. Consider the same model for yielding of a polycrystal used to develop (VII.1-3) with the exception that, because of orientation differences, the grain adjacent to the pileup is assigned a shear modulus G_2 which differs from that of the yielded grain, G_1. Approximating the two grain configuration by the bimetal discussed in Chapter III, and using the local stresses associated with a linear screw array in the bimetal, one predicts yielding to occur when

$$\tau = \tau_i + \left\{ \sqrt{\frac{2}{1+K}} (1-K)\ \tau^* \right\} \left(\frac{r^*}{L}\right)^g , \qquad \text{(VII.1-5)}$$

where

$$K = \frac{G_2 - G_1}{G_2 + G_1} , \qquad \text{(VII.1-6)}$$

$$0 < g = \frac{2}{\pi} \sin^{-1} \sqrt{\frac{1-K}{2}} < 1 .$$

Identifying L as some fraction of the grain size leads to a d^{-g} dependence of the yield stress, with

$$k_y \propto \sqrt{\frac{2}{1+K}}\ (1-K)\ \tau^* (r^*)^g . \qquad \text{(VII.1-7)}$$

A proper treatment of this problem should account for the statistical nature of the two-grain configuration. That is to say, if the initially yielded grain is oriented most favorably for slip, what,

on the average, is a suitable value for the shear modulus, G_2, of the adjacent grain? The parameters g and κ must then be characterized by $\bar{g}$ and $\bar{\kappa}$, their average values obtained from a proper statistical treatment of the problem. Because of scatter common to data plotted on Petch diagrams, it seems doubtful that macroscopic flow stress measurements alone can ever resolve the correct grain size power law.

When considering the appropriate Hall-Petch relation for materials of high stacking fault energy or materials deforming at temperatures high enough to permit dislocation cross slip to occur, the single pileup configuration may be a poor approximation to the dislocation distribution actually present. Replacing the single pileup model for yielding by the broadened glide band model of Chapter V (parallel screw slip bands separated by a distance $h < 2L$), one arrives at the relation

$$\tau = \tau_i + (1-\kappa)\, \tau^* \left\{\frac{\pi r^*}{2h}\right\}^g . \qquad \text{(VII.1-8)}$$

Because the local stresses of the broadened glide band are short range when $h < 2L$, r^* must be small if (VII.1-8) is to apply (i.e., only grain boundary sources may be operated). Since h, the slip band separation should be independent of grain size, the yield stress will depend upon grain size through τ^*, the stress required to operate a grain boundary source, and r^* (since grain size may dictate the number and spacing of the grain boundary sources).

Metallographic studies of many multi-phase materials reveal second phase particles or inclusions segregated at grain boundaries. If we approximate the segregated second phases as being of circular cross section (radius $R < L/2$) and of shear modulus G_2 (assume all grains are of shear modulus G_1), and if we imagine the operative sources to be associated with either the grain boundaries and/or the segregated particles, then the local stresses derived in Chapter IV imply a Hall-Petch type relation of the form

$$\tau = \tau_i + \frac{\tau^*}{B(\kappa,\beta)} \left\{ 2 \left\langle 1 + \frac{2R}{r^*} \right\rangle \right\}^{-g} \sqrt{\frac{4R}{L}} \quad . \qquad \text{(VII.1-9)}$$

$B(\kappa,\beta)$ is the size rigidity factor given by either Eq. (IV.3-20a) or (IV.3-20b). Thus,

$$\tau - \tau_i \propto \tau^* \sqrt{\frac{4R}{L}} \quad . \qquad \text{(VII.1-10)}$$

The grain size dependence of the yield stress is then dependent upon the τ^*-R-L-d relationship.

(1) τ^*, of course, will depend upon the mechanistic aspects of source activation at the grain boundary (grain boundary ledges or sources associated with the particle-matrix interface).

(2) R, the average size of the segregated second phases, is dependent upon the type of heat treatment used to produce the material configuration and upon the kinetics of nucleation and growth of second phases at the grain boundaries. R may depend upon d if diffusion is important during segregation.

(3) L, the slip line length, is certainly limited by the grain size d, but may be more closely associated with smaller substructural barriers such as λ_0, the mean spacing of small particles dispersed within the grains.

At the present time good experimental data indicating the proper connections between R and L and substructural variables such as d or λ_0 is lacking.

It is of interest to compare the values of k_y predicted by Eq. (VII.1-3), the conventional Petch relation, and Eq. (VII.1-9). Assuming that the entire grain size dependence of the yield stress is contained in $L^{-1/2}$, one finds that when $L/R > 2$,

$$\frac{k_y(\text{conventional})}{k_y(\text{two phase})} = B(\kappa,\beta)\left\{2\left(1+\frac{2R}{r_2^*}\right)\right\}^g\sqrt{\frac{r_1^*}{4R}} \quad , \qquad \text{(VII.1-11)}$$

where r_1^* and r_2^* are the distances from the pileup tips to the dislocation sources in the single phase and the two phase materials, respectively. If the sources are grain boundary sources, so that $r_1^* \approx r_2^* < 4R$,

$$\frac{k_y(\text{conventional})}{k_y(\text{two phase})} \approx 2(1-g)\left(\frac{4R}{r^*}\right)^{g-1/2} . \qquad \text{(VII.1-12)}$$

Figure (IV-11) shows that $\{4R/r^*\}^{g-1/2}$ typically varies between 1/2 and 1/3 when $20\text{A}^\circ < r^* < 100\text{A}^\circ$, so that hard second phases segregated at grain boundaries should raise k_y by a factor of about 2 or 3.

If r_2^* is associated with a grain boundary source or a particle source, and r_1^* is associated with a source away from the grain boundary, then

$$\frac{k_y(\text{conventional})}{k_y(\text{two phase})} \approx 2(1-g)\left(\frac{4R}{r_2^*}\right)^{g-1/2}\left(\frac{r_1^*}{r_2^*}\right)^{1/2} . \qquad \text{(VII.1-13)}$$

If $r_2^* \approx 10 - 20\text{Å}$ and $r_1^* \approx 100 - 200\text{Å}$, (r_1^*/r_2^*) may be on the order of 3-5, so that k_y would be unchanged or slightly lowered by segregation effects.

Chou[42] has considered yet another type barrier for the pileup model. A modified EFN calculation considering an edge dislocation slip band blocked by an edge dislocation whose Burgers' vector differs from that of the slip dislocations coupled with a consideration of the forces exerted on the locking dislocation yield a Hall-Petch type relation with a k_y value which may be substantially different from that normally predicted.

The Hall-Petch yield stress-substructural size relation is attractive because of its apparent simplicity. Because of the variety of possibilities for such relations, however, one must exercise caution when attempting to extract meaningful quantitative interpretations from such an analysis. Absolute or relative k_y values can be meaningful only if the relation between the mechanistics of yielding and the important substructural variables is known.

2. Relaxation of the Pileup Stresses by Fracture or Cross-slip

We now consider three possible modes of relaxing the stresses generated by dislocation pileups at second phase particles or inclusions:

(1) Initiation of fracture in the second phase ahead of the pileup.

(2) Fracture of the second phase-matrix interface.

(3) Cross slip of the leading pileup dislocations around the second phase.

Relaxation by yielding inside the second phase will not be considered. In most multiphase materials of technological importance the second phases present are of a higher modulus and have a higher yield stress than the matrix in which they are dispersed. Thus, if we associate either a high yield stress or a low mobile dislocation density with second phases which are more rigid than the matrix, relaxation by particle or inclusion yielding need not be a primary consideration. We will also confine our attentions to second phases which are large enough to be incoherent with the matrix, for it has been shown that small coherent precipitates (particles whose mean radius R is less than about 75Å) may be sheared by single dislocations,[43] thus invalidating a pileup model at the outset.

It must be stated that what follows is essentially an "ex post facto" argument, since relaxation during pileup formation has not been considered (the mathematics is too complex without this restriction). A second feature to note is that the following discussion will consider the formulation of static criteria for the occurrence of relaxation.

In reality the dominant relaxation mode may be dependent on dynamic considerations. That is to say, the true relaxation mode may not be that mode which is most favorable in terms of static stress or energetic considerations, but may be that mode which can best relieve the pileup stresses in the shortest time interval. Although the existing dynamical dislocation theory, generally attributed to Gilman, has enjoyed some success when applied to macroscopic yielding phenomena, the author is skeptical of applying the theory to the internal stress problems to be discussed here.

The question of relaxation by fracture of either the second phase or the second phase-matrix interface is complicated by the fact that once the pileup tip touches the second phase the stress singularity is no longer of the inverse square root variety, i.e.,

$$\tau_{ij} \propto \tau\rho^{-g} , \qquad 0 < g < 1 , \qquad \text{(VII.2-1)}$$

where ρ is the radius vector from the pileup tip to any point in the second phase. Smith[36,44] has examined crack nucleation ahead of a slip band in a single phase material by using Irwin's stationary energy criterion. This criterion effectively allows one to express the condition for stationary values of the total energy associated with an elastic crack solely from a knowledge of local conditions near the crack tip. Consider the nucleation of a crack of length δc on the plane $y = 0$ in the region $x < 0$ (shear modulus G_2) ahead of a screw pileup in $x > 0$ (shear modulus G_1) as depicted in Figure (VII-1). The pileup has formed under the application of an

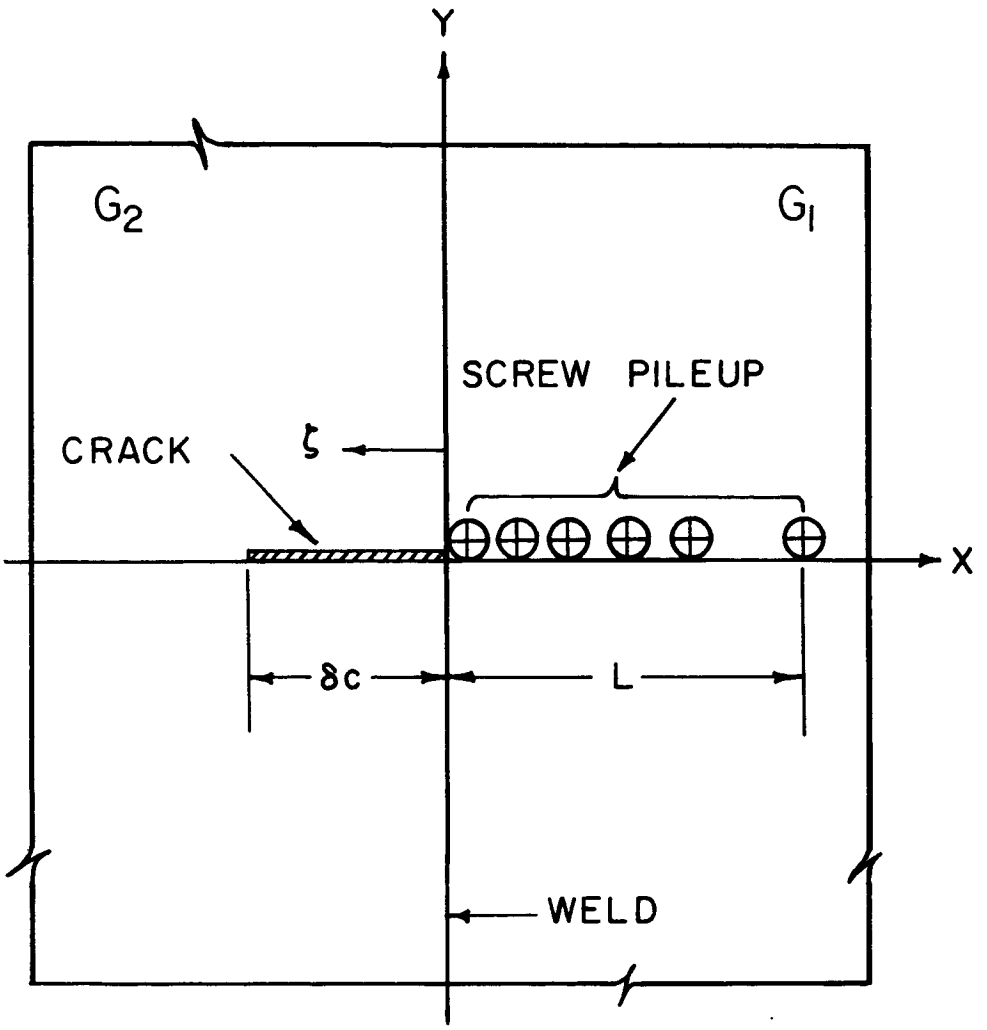

Figure VII-1: Schematic illustration of microcrack initiation ahead of a screw dislocation pileup in a bimetallic medium.

effective longitudinal shear $\tau_{yz} = -(\tau - \tau_i)$, where τ is the applied shear and τ_i is the lattice friction stress. The Irwin criterion is obtained by considering the limit as $\delta c \to 0$ of the following expression:

$$2\int_0^{\delta c} \gamma \, d\zeta = -\frac{1}{2}\int_0^{\delta c} \tau_{yz}(\zeta,0)\, w^*(\zeta,0)\, d\zeta \,. \qquad \text{(VII.2-2)}$$

γ is the effective surface energy of the plane $y = 0$ in the second phase, $\tau_{yz}(\zeta,0)$ is the slip plane shear stress in the second phase before nucleation of the crack, and $w^*(\zeta,0)$ is the relative displacement of the free crack faces. One does not know $w^*(\zeta,0)$ unless the elasticity solution for the slip band-nucleated crack configuration is known. A continuous dislocation distribution approach to such a problem leads to a set of complex dual singular integral equations which have been treated only for the case when $G_2 = G_1$ (Smith[36,44]); to the author's knowledge no solution (distributed dislocation approach or otherwise) to this problem is available at present.

Suppose, however, that we imagine the crack to be nucleated by the penetration of the original leading pileup dislocations into the second phase. If the penetrating dislocations initially retain the same distribution they occupied in the region $x > 0$, then (integrating the second of Eqs. (III.2-6))

$$w^*(\zeta,0) = \frac{\tau - \tau_i}{gG_1} \frac{1}{\sqrt{2(1-\kappa)}} (2L)^g (\delta c - \zeta)^{1-g} \,. \qquad \text{(VII.2-3)}$$

$\tau_{yz}(\zeta,0)$, as given by Eq. (III.2-4), is

$$\tau_{yz}(\zeta,0) = -(\tau-\tau_i)\sqrt{\frac{1+\kappa}{2}}\,\frac{1}{1-\kappa}\left(\frac{2L}{\zeta}\right)^{g}, \qquad \text{(VII.2-4)}$$

so that Eq. (VII.2-2) yields

$$4\gamma\delta c = \frac{(\tau-\tau_i)^2}{2gG_1}\left\{\frac{1+\kappa}{(1-\kappa)^3}\right\}^{1/2}(2L)^{2g}\,\bar{B}(1-g,\,2-g)(\delta c)^{2-2g}, \qquad \text{(VII.2-5)}$$

where $\bar{B}$ is the beta function. Examining (VII.2-5) as δc tends to zero, one notes that:

(1) when $G_2 > G_1$, $0 < g < 1/2$, and the right side of (VII.2-5) is an infinitesimal in δc greater than first order. Since the left side of (VII.2-5) is first order in δc, one predicts that a crack cannot nucleate when $G_2 > G_1$.

(2) when $G_2 < G_1$, $1/2 < g < 1$, and $(\delta c)^{2-2g}$ is less than first order in δc, so that crack initiation should always be possible if $G_2 < G_1$.

(3) when $G_2 = G_1$, both sides of (VII.2-5) are linear in δc. Crack nucleation can occur provided

$$\tau - \tau_i \geq \sqrt{\frac{4G_1\gamma}{\pi L}}, \qquad \text{(VII.2-6)}$$

in agreement with the calculation of Stroh.[18]

Results (1) and (2) are not entirely reasonable. Intuitively we might expect fracture initiation to be more probable in a harder second phase (since one usually associates a low γ and brittle behavior with hard second phases), and experimental evidence supports this contention. Neglecting relaxation by plastic flow in the second phase when $G_2 < G_1$ may negate the model used to obtain result (2), but, as stated previously, this should not be a serious omission when $G_2 > G_1$. Smith has argued that the problem of slip-nucleated cracking must be approached by applying the Irwin criterion using the appropriate local stresses and displacements for the slip band-nucleated crack configuration. This technique assumes from the outset that nucleation is feasible and then examines the stability of the nucleated crack, so that, in a sense, one still has not dealt rigorously with the nucleation problem. It would appear that the discontinuous nature of slip-nucleated cracking at a second phase boundary must be taken into account.

One might try to circumvent the complications arising from taking the limit as $\delta c \to 0$ in Eq. (VII.2-5) by either of the following arguments:

(1) We should really let $\delta c \to \approx b$, the Burgers' vector, rather than let $\delta c \to 0$. The rationalization here is that (a) this type of limiting process recognizes the inapplicability of a continuum calculation near $\delta c \to 0$, and that (b) crack nucleation at a two-phase interface is a discontinuous and irreversible process, so that the limit $\delta c \to 0$ is unrealistic.

(2) Alternatively, one may argue that Eq. (VII.2-5) was obtained by integrating (VII.2-2) assuming that γ, the effective surface energy, was a constant. Since γ is a measure of the work required to create the new crack surface, it is probably a complex function of the non-linear force laws describing atomic bonding in the vicinity of the interface. To obtain a Griffith-Stroh type fracture initiation criterion from Eq. (VII.2-2), one need only assume that $\gamma = \gamma(\zeta)$ such that

$$\int_0^{\delta c} \gamma(\zeta)\, d\zeta = \gamma_s b \left\{ \frac{\delta c}{b} \right\}^{2-2g} . \qquad \text{(VII.2-7)}$$

This could be achieved by choosing any one of an infinitude of functional forms for $\gamma(\zeta)$, e.g.,

$$\left.\begin{aligned} \frac{\gamma(\zeta)}{\gamma_s} &\sim \left(\frac{\zeta}{b} \right)^{1-2g} \\ &\sim \left(\frac{\zeta}{b} \right)^{1-2g} \sin\left(\frac{\zeta}{\delta c} \right) \\ &\sim \left(\frac{\zeta}{b} \right)^{1/2-g} \left(\frac{\delta c - \zeta}{b} \right)^{1/2-g} . \end{aligned}\right\} \qquad \text{(VII.2-8)}$$

Either of the above arguments will yield the same fracture initiation criterion, with γ_s representing an effective surface energy for crack nucleation. The dependence of $\gamma(\zeta)$ upon g (and hence upon G_2/G_1) is not too unrealistic, since the atomic bonding in the vicinity of the interface could be related to G_2/G_1.

Using the above rationalization, the condition for fracture nucleation in a semi-infinite second phase is obtained by letting $\delta c = b$ in Eq. (VII.2-5) (one should note that the same analysis applies in the case of a circular inclusion when $L/R < 2$). Noting that

$$\left\{ \frac{(1-\kappa)^3}{1+\kappa} \right\}^{3/2} = \tan^2 \frac{g\pi}{2} \sin g\pi \ ,$$

the fracture initiation stress τ_F is given by

$$\tau_F - \tau_i = \sqrt{\frac{4G_1\gamma_s}{\pi L} \mu(g) \left(\frac{2L}{b}\right)^{1-2g}} \ , \qquad \text{(VII.2-9)}$$

where

$$\mu(g) = \pi g \frac{\tan^2(g\pi/2) \sin g\pi}{\bar{B}(1-g, 2-g)} \ . \qquad \text{(VII.2-10)}$$

Using a similar procedure, when $L/R > 2$ the fracture initiation criterion becomes

$$\tau_F - \tau_i \geq \sqrt{\frac{4G_1\gamma_s}{\pi L} \alpha(g) \left(\frac{4R}{b}\right)^{1-2g}} \ , \qquad \text{(VII.2-11)}$$

where

$$\alpha(g) = \frac{\pi g \tan(g\pi/2)}{4(1-g)^2 \bar{B}(1-g, 2-g)} \ . \qquad \text{(VII.2-12)}$$

Now let us define

$$\tau_{SP} = \sqrt{\frac{4G_1\gamma_s}{\pi L}} \ , \qquad \text{(VII.2-13)}$$

so that τ_{SP} is the stress required to nucleate fracture by slip in a single phase medium of shear modulus G_1 and effective surface energy γ_s. Then the criteria for fracture initiation in the second phase may be written as:

$$\left.\begin{aligned} \tau_F - \tau_i &= \sqrt{\frac{2\pi g \tan(g\pi/2)}{\bar{B}(1-g,\ 2-g)}}\ \sin\frac{g\pi}{2}\ \tau_{SP}\left(\frac{2L}{b}\right)^{1/2-g}, \\ &\qquad \frac{L}{R} < 2\ ; \\ \tau_F - \tau_i &= \sqrt{\frac{\pi g \tan(g\pi/2)}{\bar{B}(1-g,\ 2-g)}}\ \frac{\tau_{SP}}{2(1-g)}\ \left(\frac{4R}{b}\right)^{1/2-g}, \\ &\qquad \frac{L}{R} > 2\ . \end{aligned}\right\} \quad \text{(VII.2-14)}$$

To illustrate the effect of the presence of a second phase, consider the case of $G_2 = 3G_1$, so that $g = 1/3$. Equations (VII.2-14) become

$$\tau_F - \tau_i \approx 0.495\ \tau_{SP}\left\{\frac{2L}{b}\right\}^{1/6}, \quad \frac{L}{R} < 2\ .$$

$$\tau_F - \tau_i \approx 0.525\ \tau_{SP}\left\{\frac{4R}{b}\right\}^{1/6}, \quad \frac{L}{R} > 2\ .$$

Taking $L \approx 10^{-4}$ cm, $b \approx 2 \times 10^{-8}$ cm, fracture initiation in the second phase requires that

$$\begin{aligned} \tau_F - \tau_i &= 1.13\ \tau_{SP} \quad \text{if} \quad R \approx 50\text{Å} \\ &= 1.65\ \tau_{SP} \quad \text{if} \quad R \approx 500\text{Å} \\ &= 2.30\ \tau_{SP} \quad \text{if} \quad R \geq 5000\text{Å}\ . \end{aligned}$$

For $G_1 \approx 10^{12}$ dynes/cm^2 and $\gamma_s \approx 10^3$ ergs/cm^2, τ_{SP} is about 50,000 psi. One notes that the fracture initiation stresses predicted above are higher than τ_{SP}, the nucleation stress in a single phase material, and that the fracture initiation stress increases with increasing particle radius. This is to be expected, since when $G_2 > G_1$, the local stresses about the tip of a pileup at a circular inclusion (a) are about 2-3 times lower than those predicted by single phase elasticity calculations, and (b) are larger when the inclusion size is smaller.

The above analysis has neglected the effect of plastic relaxation of the pileup stresses by cross-slip of the leading pileup dislocations around the second phase. Hence, although equations (VII.2-14) predict that fracture initiation is easier in smaller particles (when $G_2 > G_1$), it may be that plastic relaxation by cross-slip may also occur more easily when the particles are smaller. We shall investigate the cross slip problem after remarking about the problem of interfacial fracture initiation.

Initiation of interfacial fracture cannot be analyzed rigorously in the same manner used to discuss particle fracture. Since a nucleated interfacial crack would form obliquely to the original slip band, one should not suppose that $w^*(\zeta,0)$, the displacement field of the "penetrating dislocations" nucleating the crack, is known from the calculations of Chapters III and IV. If one does assume that the penetrating dislocations retain their initial distribution, the interfacial fracture criteria are the same as Eqs. (VII.2-14) with

$$\tan \frac{g\pi}{2} \quad \text{replaced by} \quad \sec \frac{g\pi}{2}$$

and

$$\tau_{SP} \quad \text{replaced by} \quad \sqrt{\frac{\gamma_i}{\gamma_s}}\ \tau_{SP} \ ,$$

where γ_i is the interfacial surface energy. γ_i should be dependent on the interfacial "roughness" and the interfacial atomic bonding. One would then expect interfacial cracking rather than particle cracking when $\gamma_i \csc(g\pi/2) < \gamma_s$, and vice-versa.

We now examine the problem of relaxation by cross slip of the leading pileup dislocations around a second phase particle or inclusion. Li[45] has examined cross slip of a single screw dislocation induced by the presence of a locked screw dislocation, and we shall employ a similar technique to discuss cross slip induced by the presence of a second phase. Problems of this type are closely akin to "scattering problems". The essential difference between Li's problem and that to be treated here is the following. Since image dislocation forces are generated by the presence of a second phase in the vicinity of a dislocation, as the real dislocation moves, the scattering centers (i.e., the image dislocations) also move; Li's scattering center was a fixed dislocation.

Let us first consider the cross slip of a single screw dislocation around an inclusion of circular cross section of radius R (Figure VII-2). Consider the applied shear at infinity to be $\tau_{yz} = -\tau$, so that the elastic stress field in the matrix $(r > R)$ due to the applied shear is

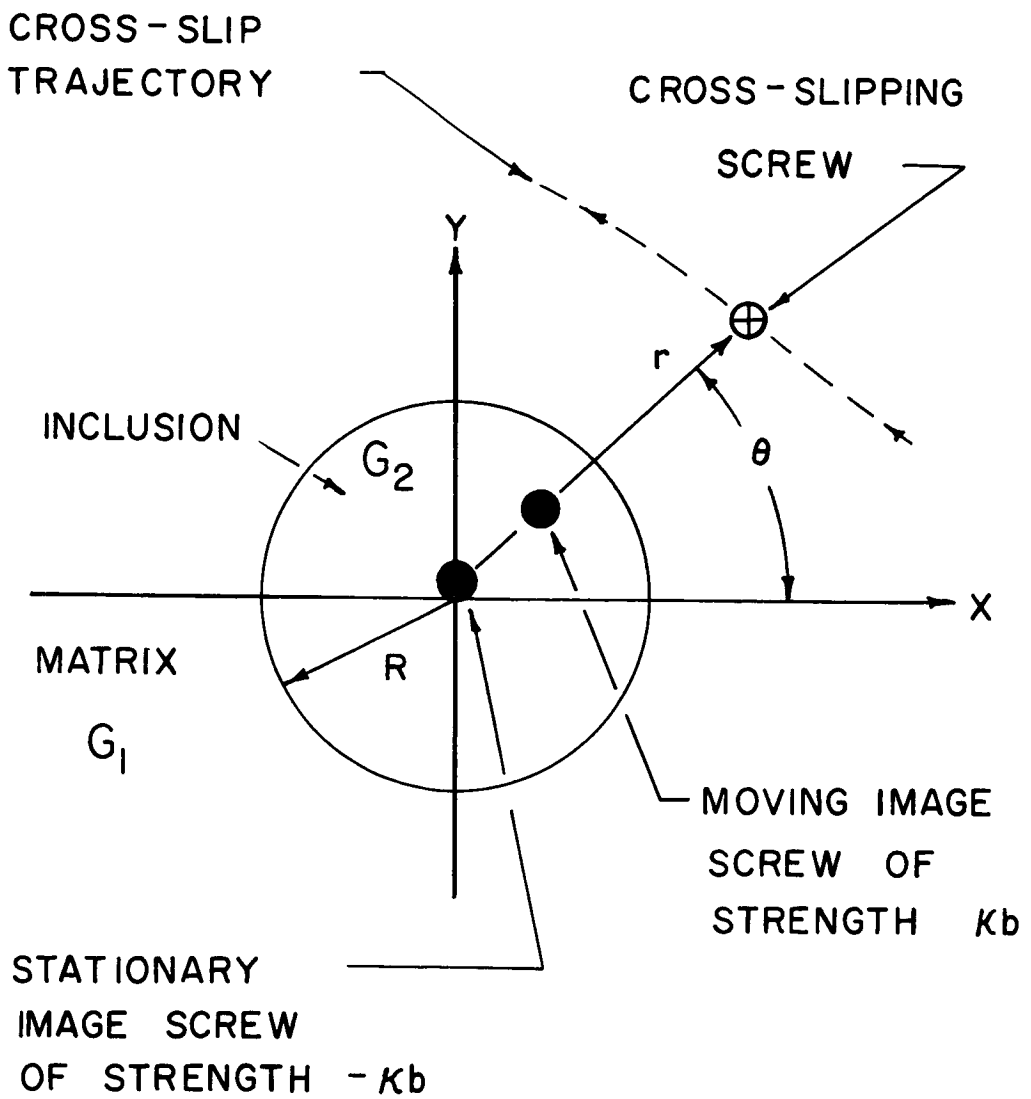

Figure VII-2: Schematic illustration depicting screw cross-slip induced by the presence of a second phase particle.

$$\left.\begin{aligned} \tau_{rz} &= -\tau\left\{1 + \frac{\kappa R^2}{r^2}\right\}\sin\theta \\ \tau_{\theta z} &= -\tau\left\{1 - \frac{\kappa R^2}{r^2}\right\}\cos\theta \end{aligned}\right\} \qquad \text{(VII.2-15)}$$

where $\kappa = (G_2-G_1)/(G_2+G_1)$. If we now introduce a single right hand screw dislocation into the matrix at (r,θ), two image dislocations are induced at the origin and at $(R^2/r,\ \theta)$. The image stress acting at the position of the real dislocation is

$$\tau_{\theta z} = \frac{G_1 b\kappa}{2\pi}\ \frac{R^2}{r(r^2-R^2)}\ . \qquad \text{(VII.2-16)}$$

Defining the dimensionless polar radius vector

$$r_0 = \frac{r}{R}\ , \qquad 1 < r_0 < \infty\ , \qquad \text{(VII.2-17)}$$

the radial and tangential forces on the real dislocation are given by

$$\left.\begin{aligned} \frac{F_r}{\tau b} &= -\left(1 - \frac{\kappa}{r_0^2}\right)\cos\theta + \frac{a}{r_0(r_0^2-1)} \\ \frac{F_\theta}{\tau b} &= \left(1 + \frac{\kappa}{r_0^2}\right)\sin\theta \\ a &= \frac{G_1 b\kappa}{2\pi R\tau}\ . \end{aligned}\right\} \qquad \text{(VII.2-18)}$$

If, following Li, we say that the dislocation moves in the direction of the net force upon it at any point, then its trajectory $r_0 = r_0(\theta)$ is determined by

$$r_0 \frac{d\theta}{dr_0} = \frac{(1 + \kappa/r_0^2) \sin \theta}{-(1 - \kappa/r_0^2) \cos \theta + a/(r_0(r_0^2-1))} . \qquad \text{(VII.2-19)}$$

One may numerically construct the trajectories appropriate for different values of κ and a. The trajectories are most easily constructed by first considering the curve defined by $F_r = 0$. The "flow field" is shown in Figure (VII-3) for $\kappa = 1/2$, $R = 700b$, $\tau \approx 10^{-3} G_1$ (i.e., $a \approx 0.125$). The shaded area between the curve $F_r = 0$ and the second phase ($r_0 = 1$) defines a region which is inaccessible to the real dislocation when $\kappa > 0$.

An examination of Figure (VII-3) shows that if $\kappa > 0$, a right hand screw initially moving on the plane $y = 0$ in the negative x-direction toward the second phase is attracted to the second phase until it reaches an equilibrium position at $x_0 = x/R$ given by

$$(1 - \frac{\kappa}{x_0^2}) = \frac{a}{x_0(x_0^2 - 1)} . \qquad \text{(VII.2-20)}$$

(When $\kappa < 0$, no such equilibrium position exists, and the screw is always attracted to the particle.) For the values of κ and a used in Figure (VII-3), $x_0 \approx 1.1$. If local perturbations in the internal stress field or temperature fluctuations force the dislocation off the slip plane $y = 0$, the dislocation will move (approximately) along the

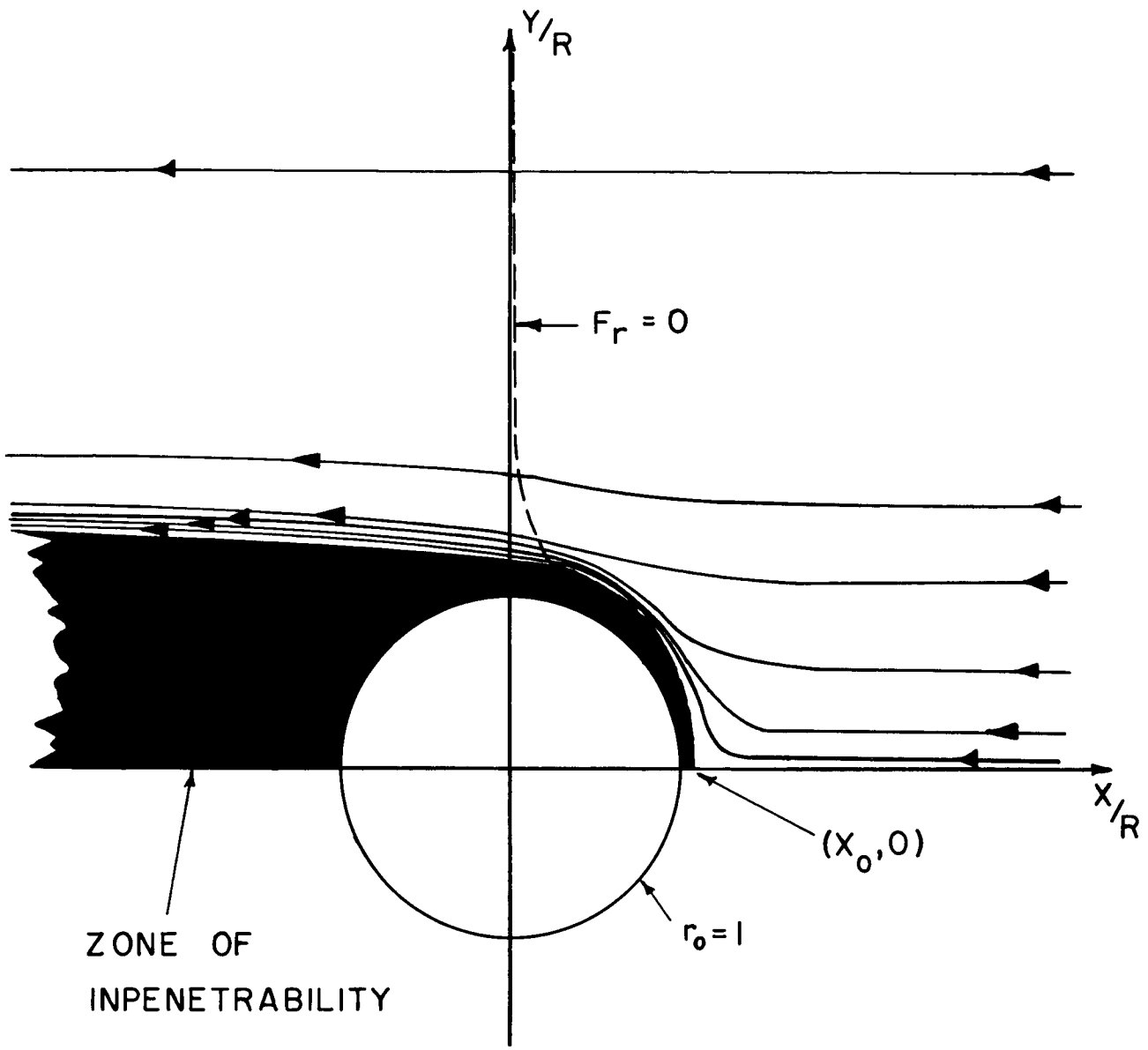

Figure VII-3: Screw dislocation cross-slip trajectories around a circular second phase. A screw originally moving from right to left on the slip plane $y = 0$ cross-slips along the outer boundary of the darkened "zone of inpenetrability".

trajectory defined by $F_r = 0$ until it has cross slipped through an angle $\theta \approx 75°$ and then continue moving along a straight line parallel to its original slip plane (i.e., the cross slip path is the boundary of the zone of impenetrability). If τ, the applied shear is decreased, and all other parameters held constant, a decreases and x_0 increases, so that the curve $F_r = 0$ is shifted away from the second phase. The area of the "inaccessible zone" is increased, and, therefore, the cross slipping screw must travel a longer path to move around the particle. To a good approximation the cross slip trajectory of a dislocation initially on the plane $y = 0$ is a quarter arc of a circle of radius Rx_0 over $0 < |\theta| < \pi/2$ and then the straight line $y = \pm x_0$. Of course, the above analysis is valid only when no lattice frictional stress resists dislocation motion along the cross slip path. When a retarding friction stress exists, the stress τ_{rz} due to the applied shear is not sufficient to cause cross slip over the initial portion of the path defined by $F_r = 0$.

Let us now consider the cross slip of a dislocation near the leading edge of a screw dislocation pileup of length L blocked by a circular inclusion of radius $R < L/2$ (Figure VII-4). We now assume the screw array was created by an effective applied shear $\tau - \tau_i$, where τ_i is the lattice friction stress on $y = 0$, and that the stress aiding cross slip is the applied stress field plus the stress field of the dislocation pileup. As a pileup dislocation cross slips off the plane $y = 0$, its image likewise moves off the plane $y = 0$ inside the second phase. Using the expressions for the local stresses of the

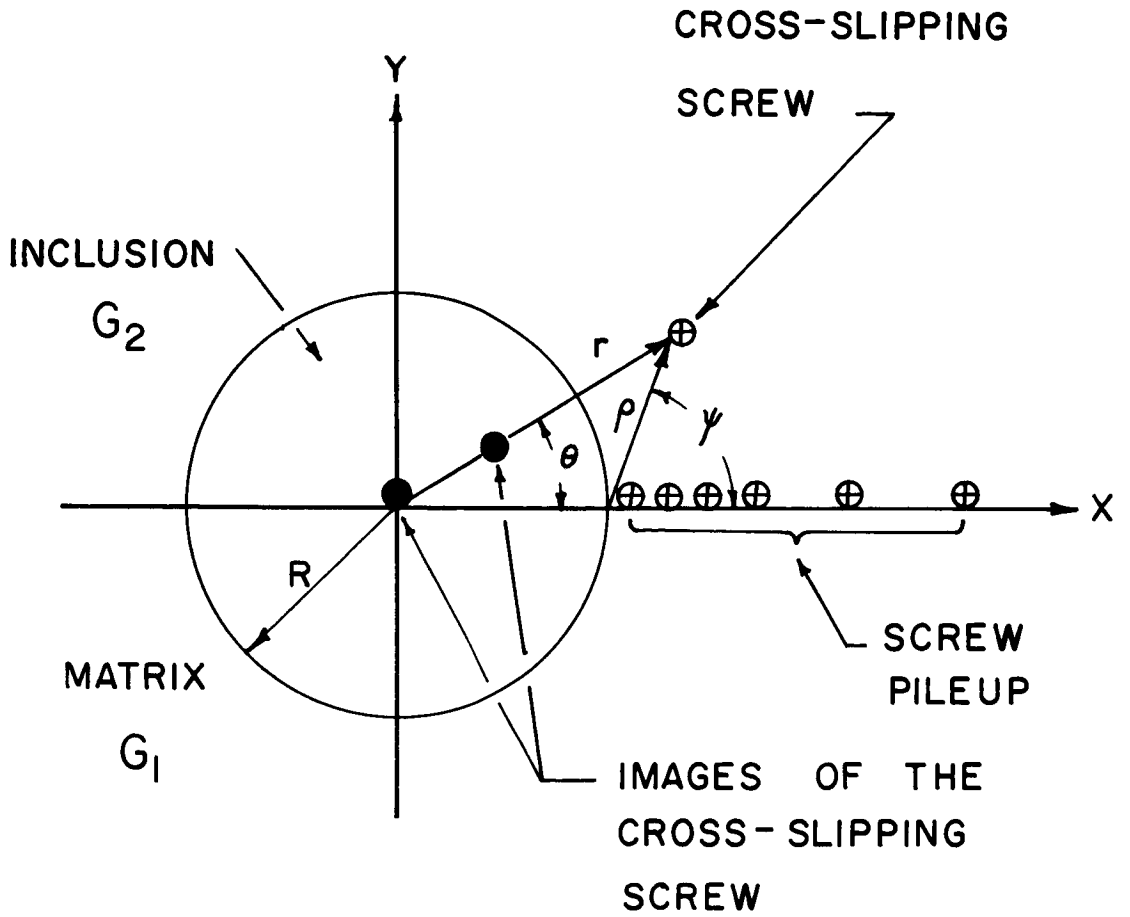

Figure VII-4: Schematic illustration depicting cross-slip of a screw dislocation out of a screw pileup against a circular inclusion.

pileup derived in Chapter IV (we assume that these remain unchanged when one dislocation and its image leave the slip plane $y = 0$) the trajectory of the cross-slipping screw is determined by

$$r \frac{dr}{d\theta}$$

$$\approx \frac{B(\kappa,\beta)(\tau-\tau_i) \sqrt{\frac{L}{4R}} \{2 \langle 1 + \frac{2R}{\rho} \rangle\}^g \cos(\theta - g\psi) \operatorname{sgn}(\theta)}{\left\{ B(\kappa,\beta)(\tau-\tau_i)\sqrt{\frac{L}{4R}} \{2 \langle 1 + \frac{2R}{\rho} \rangle\}^g \sin(\theta-g\psi) + \frac{G_1 b\kappa}{2\pi} \frac{R^2}{r(r^2-R^2)} \right\}} \quad . \tag{VII.2-21}$$

The stresses due to the applied shear (Eq. VII.2-15) do not appear in (VII.2-21); it can be shown that the pileup stresses contain terms which exactly cancel the applied stress field. Equation (VII.2-21) is an extremely complex differential equation, since the polar coordinates relative to the pileup tip, ρ and ψ, are related to the polar coordinates relative to the origin, r and θ, by

$$\rho^2 = r^2 + R^2 - 2rR \cos\theta \ ,$$
$$\rho \sin\psi = r \sin\theta \ . \tag{VII.2-22}$$

If we reason in a manner similar to that in the preceding paragraph, then we expect the cross slipping screw to initially closely follow the path defined by $F_r = 0$, where F_r is the net radial force on the dislocation. The screw can cross slip around the second phase provided that the tangential shear τ_{rz} can overcome the retarding friction stress, i.e., that

$$B(\kappa,\beta)(\tau-\tau_i)\sqrt{\frac{L}{4R}}\left\{2\left(1+\frac{2R}{\rho}\right)\right\}^{g}\cos(\theta-g\psi)\geq\tau_i', \quad 0<\theta<\pi/2\ , \tag{VII.2-23}$$

where τ_i' is the lattice friction stress resisting dislocation motion along the cross slip path. If the inequality (VII.2-23) is not satisfied at some point ρ^*, θ^*, $\psi^*(\theta^*)$, then the cross slipping screw comes to rest. For a dislocation which was initially very close to the leading edge of the pileup, when $22° < \theta^* < 90°$, the factor $2\{(1+2R/\rho^*)\}^g$ is about 2 or 3. Hence, as a conservative estimate, we predict that a single screw dislocation initially near the leading edge of a pileup can cross slip around the second phase provided

$$(\tau-\tau_i)\sqrt{\frac{L}{4R}}\geq\frac{\tau_i'}{2}\ \frac{1}{B(\kappa,\beta)}\ . \tag{VII.2-24}$$

When $L/R > 2$, $B(\kappa,\beta)$, as given by either (IV.3-20a) or (IV.3-20b) can be well approximated by

$$B(\kappa,\beta)\approx 2(1-g)\ , \tag{VII.2-25}$$

so that the cross slip criterion becomes

$$(\tau-\tau_i)\ \sqrt{\frac{L}{R}}\geq\frac{\tau_i'}{2(1-g)}\ . \tag{VII.2-26}$$

If we use (VII.2-26) as the condition for relaxing the pileup stresses by cross slip, we are adopting a somewhat conservative criterion. Essentially we are saying that if a single pileup dislocation cannot cross slip around the second phase, then cross slip will not be an effective mode of relaxation. Of course, if many dislocations near

the pileup tip cross slip simultaneously, then

(1) the trailing dislocations in the cross slip array exert forces on the leading cross slipping screws which may aid the relaxation process, and

(2) the local stresses of the pileup diminish (unless new dislocations are rapidly supplied to the slip band by its source), thus hindering the cross slip process.

Since (1) and (2) act in opposition to one another, (VII.2-26) may be a good approximation to the real cross slip criterion. A more rigorous calculation should include a consideration of both source and cross slip dynamics. Equation (VII.2-26) predicts that cross slip becomes a less effective mode of relaxation as the second phase size increases.

When $L/R < 2$, the second phase-matrix interface is almost perpendicular to the screw array, so that the cross slip path is almost parallel to the interface. A pileup dislocation must now cross slip a vertical distance ρ^* above the pileup. Using Eqs. (III.2-6) we see that ρ^* must be less than L (and consequently less than R) if the stress concentration factor $(2L/\rho^*)^g$ is to be sufficient to overcome the cross slip frictional stress. Cross slip associated with second phases which are large relative to the slip line length will tend to spread out the initial pileup dislocations into several slip bands (whose separation is less than the slip line length) which remain blocked by the second phase.

Let us now examine the conditions which favor particle fracture rather than cross-slip as the mode for relaxing the pileup stresses. Consider first the case of $L > 2R$. Using Eqs. (VII.2-26) and (VII.2-14), we see that second phase fracture cannot possibly occur unless

$$\tau_i' \sqrt{\frac{R}{L}} > \sqrt{\frac{\pi g \tan(g\pi/2)}{\bar{B}(1-g,\ 2-g)}} \sqrt{\frac{4G_1\gamma_s}{\pi L}} \left(\frac{4R}{b}\right)^{\frac{1}{2}-g} . \qquad \text{(VII.2-27)}$$

Cancelling $L^{-1/2}$, which appears on both sides of the inequality, we can rewrite (VII.2-27) as

$$\tau_i' \left(\frac{4R}{b}\right)^{g} > 2 \sqrt{\frac{\pi g \tan(g\pi/2)}{\bar{B}(1-g,\ 2-g)}} \sqrt{\frac{4G_1\gamma_s}{\pi b}} , \qquad \text{(VII.2-28)}$$

an expression which is independent of L (of course R must be $< L/2$). For $G_1 \approx 10^{12}$ dynes/cm^2, $\gamma_s \approx 10^3$ dynes/cm, $b \approx 2 \times 10^{-8}$ cm, we see that relaxation by fracture initiation in the second phase requires that

$$\tau_i' \left(\frac{4R}{b}\right)^{g} > 7.4 \times 10^3 \sqrt{\frac{\pi g \tan(g\pi/2)}{\bar{B}(1-g,\ 2-g)}} , \qquad \text{(VII.2-29)}$$

where τ_i' is in units of ksi. Let us set an upper limit of about 150 ksi for τ_F; this is a reasonable value for medium strength materials. In such materials τ_i typically varies from 10 ksi (high temperatures) to 50 ksi (low temperatures) so that the maximum

difference between τ_F and τ_i is about 100 ksi. The friction stress resisting cross-slip, τ_i', should not be very much different from τ_i, so that it seems reasonable to expect that τ_i' is less than about 50 ksi.

Let us choose the most favorable set of conditions for which a low value of τ_i' satisfies (VII.2-29), i.e., R large (but < L/2) and g close to 1/2. Even if we take L to be as large as 10^{-2} cm, $R \approx 10^{-3}$ cm (10 microns), and $G_2 = 2G_1$, we find that (VII.2-29) is satisfied only if $\tau_i' > 55$ ksi.

Because we cannot satisfy (VII.2-29) for reasonable values of R, L, and τ_i', we are forced to conclude that particle fracture is not possible when the particle diameter is less than the slip line length. This is tantamount to saying that cross-slip is a much more effective mode of relaxation than fracture initiation when $L > 2R$. Noting that

$$\sqrt{2}\,\tau_{SP}\left(\frac{2L}{b}\right)^{\frac{1}{2}-g} = 2\sqrt{\frac{4G_1\gamma_s}{\pi b}}\left(\frac{b}{2L}\right)^{g}, \qquad \text{(VII.2-30)}$$

when $L < 2R$ the fracture initiation criterion is

$$\frac{\tau_F-\tau_i}{\sqrt{\frac{4G_1\gamma_s}{\pi b}}} = 2\sin\frac{g\pi}{2}\sqrt{\frac{\pi g\tan(g\pi/2)}{\bar{B}(1-g,\,2-g)}}\left(\frac{b}{2L}\right)^{g}. \qquad \text{(VII.2-31)}$$

A plot of

$$\ln\left\{\frac{\tau_F-\tau_i}{\sqrt{\frac{4G_1\gamma_s}{\pi b}}}\right\} \text{ vs. } \ln\left(\frac{2L}{b}\right)$$

is linear with slope -g and is depicted in Figure VII-5 for three values of g.

One should note that since

$$\sqrt{\frac{4G_1\gamma_s}{\pi b}} \approx 1 - 3.7 \times 10^6 \text{ psi} ,$$

L must be greater than about $3 - 5 \times 10^{-5}$ cm if $\tau_F - \tau_i$ is to be on the order of 100 ksi (Figure VIII-5). Since the fracture criterion (VII.2-31) is valid only when $L < 2R$, we conclude that fracture can be initiated only in particles whose diameters are greater than about 1-2 microns (a typical cermet).

The conditions favoring fracture initiation in the second phase and relaxation by cross-slip may be summarized as follows:

Relaxation by particle fracture can occur when

$$\left.\begin{aligned} &(1)\quad L < 2R, \text{ and} \\ &(2)\quad \frac{\tau_F - \tau_i}{\sqrt{\frac{4G_1\gamma_s}{\pi b}}} = 2 \sin\frac{g\pi}{2} \sqrt{\frac{\pi g \tan(g\pi/2)}{\bar{B}(1-g,\ 2-g)}} \left(\frac{b}{2L}\right)^g . \end{aligned}\right\} \quad \text{(VII.2-32)}$$

Relaxation by cross-slip can occur when

$$\left.\begin{aligned} &(1)\quad L > 2R, \text{ and} \\ &(2)\quad (\tau - \tau_i)\sqrt{\frac{L}{R}} > \frac{\tau_i}{2(1-g)} . \end{aligned}\right\} \quad \text{(VII.2-33)}$$

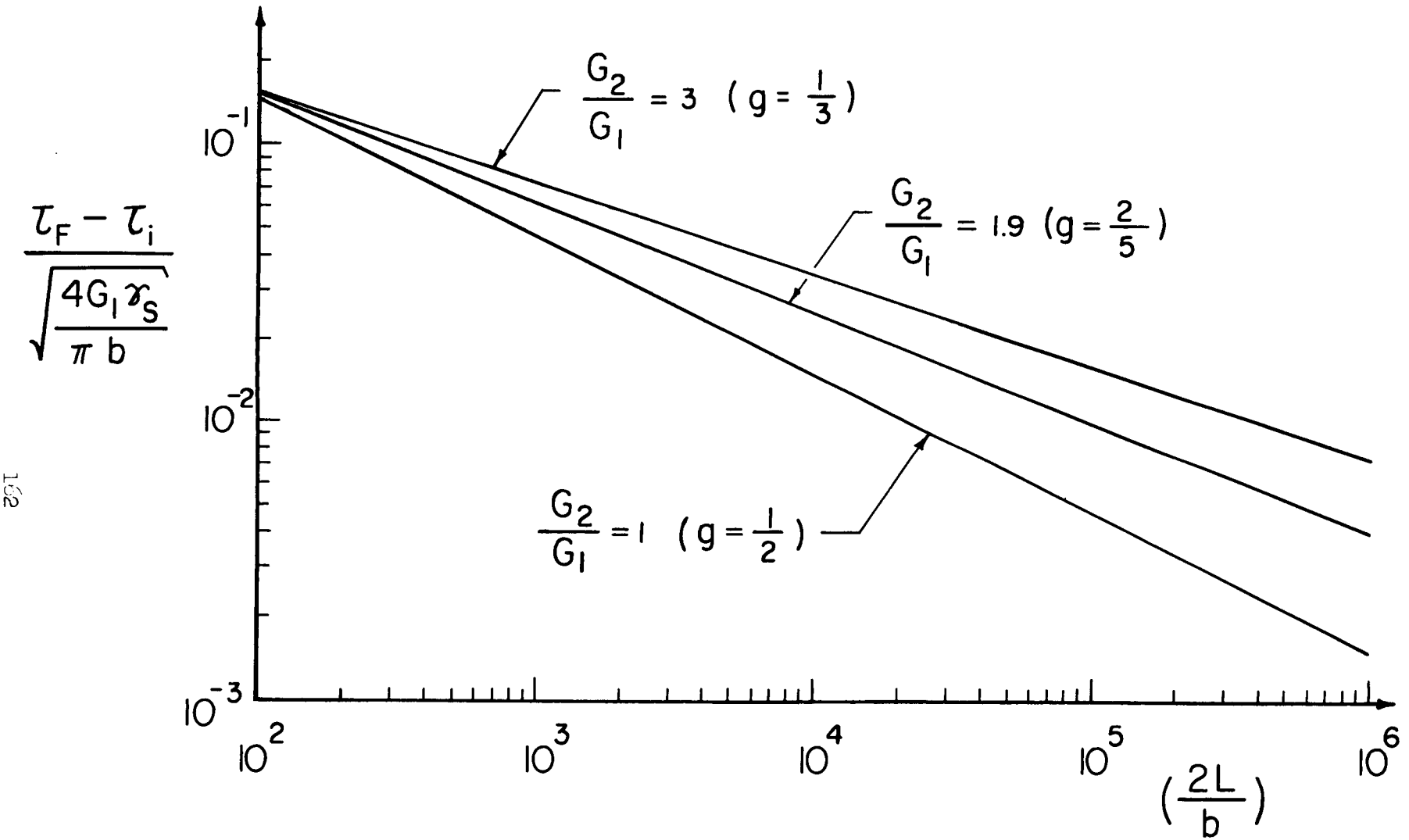

Figure VII-5: τ_F, the stress required to initiate fracture in a second phase ahead of a slip band, as a function of 2L/b when L, the slip line length, is less than the inclusion diameter, 2R.

One should remember that the fracture initiation criterion was derived by letting the incremental crack extension, δc, tend to b, not zero, as a limit. A rigorous justification of this modification is not given here. The analysis was presented as a means of circumventing difficulties inherent in the discontinuous nature of the fracture initiation problem. The legitimacy of invoking atomistic arguments to modify the continuum Griffith-Irwin criterion may be questionable; nevertheless, until a more rigorous calculation can be performed, an appeal to atomistics does not seem wholly unwarranted.

3. Concluding Remarks

A summary of the solutions obtained for the stresses generated by linear screw dislocation arrays (pileups) near second phases will not be given here; these have been presented and discussed at length in Chapters II through V. It has been shown that the method of continuously distributed dislocations provides both a natural and an effective technique for treating slip band stress concentrations in two phase media. In particular the influence of second phase size and relative rigidity upon the local pileup stresses has been examined. The effect of parallel slip band interaction was also studied for the special multi-array configuration of Chapter V. The technique is particularly appealing because it affords a straightforward formulation of such problems which has incorporated within it the appropriate continuity conditions at the matrix-second phase interface. In addition the concept of image dislocation forces permits one to develop reasonably simple physical interpretations of the results obtained. Inevitably

one must solve a singular integral equation for the dislocation distribution function; fortunately, the problems presented in this dissertation could be treated in closed form. This may not be the case when more complex second phase geometries (e.g., an inclusion of elliptical cross-section) are chosen.

One may argue, quite correctly, that the anti-plane strain elasticity problems discussed here could have been treated by more standard techniques of potential theory, since such problems require solving $\nabla^2 w = 0$ with appropriate continuity conditions on w (the z-displacement) and its derivatives at the matrix-second phase interface. The author attempted such an approach, with little success, to several of the problems presented in this dissertation. This should not be construed as an effort to claim the superiority of the dislocation approach; in all probability it is a reflection of the author's own deficiencies. The real justification for or defense of the utility of the distributed dislocation technique is the fact that solutions were obtained in a logical, straightforward fashion. Ultimately, of course the choice of technique is a matter of individual taste.

From the discussion presented in the previous section it is apparent that more attention should be given to the question of relaxation of the pileup stresses. A realistic treatment of relaxation by either cross-slip or plastic flow must

(1) allow relaxation to occur during pileup formation, and

(2) consider the dynamics of dislocation motion.

It is very probable that these considerations will necessitate the use of numerical methods.

BIBLIOGRAPHY

1. F. R. N. Nabarro, Advances in Physics, 1, 3, 271 (July, 1952).

2. J. D. Eshelby, Phil. Trans. A, 244, 101 (1951).

3. L. M. Milne-Thomson, Theoretical Hydrodynamics, MacMillan, New York, 1963.

4. A. K. Head, Phil. Mag., 44, 92 (1953).

5. J. H. Jeans, The Mathematical Theory of Electricity and Magnetism, Cambridge University Press (1911).

6. J. Dundurs, private communication (1965).

7. Y. T. Chou, Screw Dislocations in and Near Lamellar Inclusions, E. C. Bain Laboratory Report No. 1276 (May, 1966).

8. D. M. Barnett, unpublished.

9. Y. T. Chou, Acta Metallurgica, 13, 1131 (1965).

10. H. S. Carslaw and J. C. Jaeger, Conduction of Heat in Solids, Oxford at the Clarendon Press (1959).

11. A. K. Head, Proc. Phys. Soc. London, 66B, 793 (1953).

12. J. Dundurs and G. P. Sendeckyj, J. Applied Phys., 36, 10, 3353 (1965).

13. J. Dundurs and T. Mura, J. Mech. Phys. Solids, 12, 177 (1964).

14. J. Dundurs and G. P. Sendeckyj, J. Mech. Phys. Solids, 13, 141 (1965).

15. J. D. Eshelby, F. C. Frank and F. R. N. Nabarro, Phil. Mag., 42, 351 (1951).

16. T. J. Stieltjes, Acta Mathematica, 6, 321 (1885).

17. W. V. Houston, Principles of Quantum Mechanics, Dover, New York (1959).

18. A. N. Stroh, Proc. Roy. Soc., A223, 404 (1954).

19. P. C. Paris and G. C. M. Sih, Fracture Toughness Testing and Applications, 30-81, ASTM, Philadelphia (1965).

20. G. Leibfried, Zeitschrift fur Physik, Bd. 130, 214 (1951).

21. B. A. Bilby, R. Bullough, and E. Smith, Proc. Roy. Soc., A231, 263 (1955).

22. A. D. Brailsford, private communication (1966).

23. L. D. Webster and H. H. Johnson, J. Applied Phys., 36, 6, 1927 (1965).

24. H. H. Johnson, J. Applied Phys. 37, 4, 1763 (1966).

25. N. I. Muskhelishvili, Singular Integral Equations, P. Noordhoff, Ltd., Groningen, the Netherlands (1953).

26. A. K. Head, Australian J. Phys., 13, 3, 613 (1960).

27. N. Louat, Phil. Mag., 8, 1219 (1963).

28. A. K. Head and N. Louat, Australian J. Phys., 8, 1, 1 (1955).

29. E. Smith, The Opening of Parallel Cracks by an Applied Tensile Stress, Central Electricity Research Laboratories Report No. RD/L/R 1283 (May, 1965).

30. E. Smith, Proc. Roy. Soc., A282, 422 (1964).

31. B. A. Bilby, A. H. Cottrell, and K. H. Swinden, Proc. Roy. Soc. A272, 304 (1963).

32. J. Weertman, Theory of Infinitesimal Dislocations Distributed on a Plane Applied to Discontinuous Yield Phenomena, presented at the Conference on Deformation of Crystalline Solids, Ottawa (August, 1966).

33. Y. T. Chou, Acta Metallurgica, 13, 779 (1965).

34. D. M. Barnett and A. S. Tetelman, J. Mech. Phys. Solids, 14, 329 (1966).

35. A. R. Zak and M. L. Williams, Trans. ASME, 142 (March, 1963).

36. E. Smith, Acta Metallurgica, 14, 985 (1966).

37. L. W. B. Jolley, Summation of Series, Dover, New York (1961).

38. E. O. Hall, Proc. Phys. Soc. London, B.64, 747 (1951).

39. N. J. Petch, J. Iron and Steel Inst., 174, 25 (1953).

40. P. Gay, P. B. Hirsch, and A. Kelly, Acta Cryst., 7, 41 (1954).

41. J. D. Embury, A. S. Keh, and R. M. Fisher, Trans. Met. Soc. AIME, 236, 1252 (1966).

42. Y. T. Chou, Dislocation Pileups and the Hall-Petch Relation, presented at the Conference on Deformation of Crystalline Solids, Ottawa (August, 1966).

43. A. Kelly and R. B. Nicholson, Precipitation Hardening, Progress in Materials Science, 10, 3, Pergamon Press, Macmillan, New York (1963).

44. E. Smith, Acta Metallurgica, 14, 991 (1966).

45. J. C. M. Li, J. Applied Phys., 32, 4, 593 (1961).

46. S. G. Mikhlin, Integral Equations, Macmillan, New York (1957).

47. R. V. Churchill, Complex Variables and Applications, McGraw-Hill New York (1960).

48. N. I. Muskhelishvili, Some Basic Problems of the Mathematical Theory of Elasticity, P. Noordhoff, Ltd., Groningen, the Netherlands (1963).

APPENDIX A

THE SCREW DISLOCATION INSIDE A CIRCULAR INCLUSION

Consider the two complex planes depicted in Figure A-I. The $\alpha = x + iy$ plane may be conformally mapped into the $\zeta = \lambda + i\eta$ plane by the transformation $\zeta = R^2/\alpha$. R is the radius of the circular inclusion of shear modulus G_2 in the α-plane. The region $|\alpha| > R$ is the matrix of shear modulus G_1. Under the above mapping, points inside the inclusion in the α-plane are mapped into the matrix in the ζ-plane and points in the α-plane matrix are mapped inside the inclusion in the ζ-plane.

Let $u = v + iw$ represent the complex potential describing the screw dislocation exterior to the circular inclusion in the α-plane. Thus, w will be the displacement field of the screw, and v will be the potential for the analogous electrostatic problem. From Eqs. (I.3-5) for the screw situated at $(t',0)$ in the α-plane,

$$u_1 = \frac{b}{2\pi}\{\ln(\alpha-t') + \kappa \ln(\alpha-R^2/t') - \kappa \ln \alpha\}; \quad x^2 + y^2 \geq R^2$$

$$u_2 = \frac{b}{2\pi}\{(1-\kappa) \ln(\alpha-t') + i\pi\kappa\}; \quad x^2 + y^2 \leq R^2 . \tag{A-1}$$

The mapping $\zeta = R^2/\alpha$ transforms the screw at $(t',0)$ in the α-matrix into a screw at $(t,0)$ in the ζ-inclusion, where $t = R^2/t'$. Now in the ζ-plane

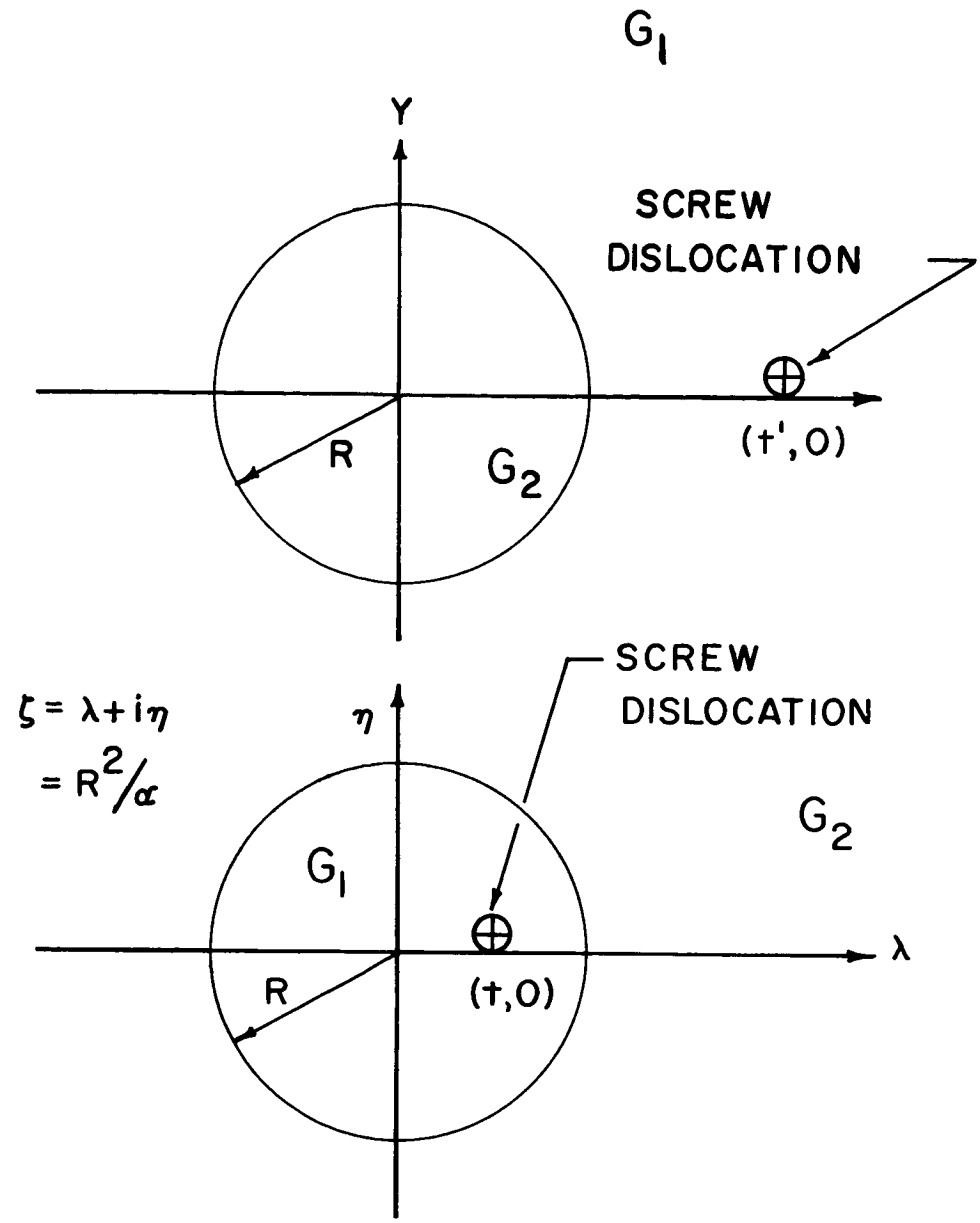

Figure A-1: The complex $\alpha = x + iy$ and $\zeta = \lambda + i\eta$ planes. Under the conformal mapping $\zeta = R^2/\alpha$, a screw dislocation in the α-matrix is mapped into a screw dislocation in the ζ-inclusion, and vice-versa.

$$-\tau_{\lambda z}^{(j)} + i\tau_{\eta z}^{(j)} = G_j \left\{ -\frac{\partial w_j}{\partial \lambda} + i \frac{\partial w_j}{\partial \eta} \right\} . \qquad \text{(A-2)}$$

where j is either 1 or 2. $j = 1$ refers to the α-matrix and the ζ-inclusion; $j = 2$ refers to the α-inclusion and the ζ-matrix. Using the Cauchy-Riemann conditions,

$$-\tau_{\lambda z}^{(j)} + i\tau_{\eta z}^{(j)} = iG_j \frac{du_j}{d\zeta} = -i \frac{R^2}{\zeta^2} G_j \frac{du_j}{d\alpha} . \qquad \text{(A-3)}$$

Considering $j = 2$,

$$-\tau_{\lambda z}^{(2)} + i\tau_{\eta z}^{(2)} = -\frac{R^2}{\zeta^2} G_2(1-\kappa) \frac{b}{2\pi} \frac{i}{\alpha - t'}$$

$$= -\frac{R^2}{\zeta^2} G_2(1-\kappa) \frac{b}{2\pi} \frac{i}{(R^2/\zeta) - (R^2/t)} . \qquad \text{(A-4)}$$

Thus, after some manipulation, one finds that

$$\left.\begin{aligned} \tau_{\lambda z}^{(2)} &= -\frac{G_2 b(1-\kappa)}{2\pi} \left\{ \frac{\eta}{(\lambda - t)^2 + \eta^2} - \frac{\eta}{\lambda^2 + \eta^2} \right\} \\ \tau_{\eta z}^{(2)} &= \frac{G_2 b(1-\kappa)}{2\pi} \left\{ \frac{\lambda - t}{(\lambda - t^2) + \eta^2} - \frac{\lambda}{\lambda^2 + \eta^2} \right\} . \end{aligned}\right\} \qquad \text{(A-5)}$$

These stresses are derivable from the displacement field

$$w^{(2)} = \frac{b}{2\pi} [(1-\kappa)\theta_1 - (1-\kappa)\theta + C_0], \qquad \text{(A-6)}$$

where

$$\theta_1 = \tan^{-1}\frac{\eta}{\lambda - t}, \qquad \theta = \tan^{-1}\frac{\eta}{\lambda}$$

and C_0 is an undetermined constant.

For $j = 1$,

$$-\tau_{\lambda z}^{(1)} + i\tau_{\eta z}^{(1)} = i\,\frac{G_1 b}{2\pi}\left(-\frac{R^2}{\zeta^2}\right)\left\{\frac{1}{\alpha - t'} + \frac{\kappa}{\alpha - (R^2/t')} - \frac{\kappa}{\alpha}\right\}. \qquad \text{(A-7)}$$

Since $\alpha = R^2/\zeta$, $t' = R^2/t$, separation of the terms in (A-7) into real and imaginary parts yields

$$\begin{aligned}
\tau_{\lambda z}^{(1)} &= -\frac{G_1 b}{2\pi}\left\{\frac{\eta}{(\lambda - t)^2 + \eta^2} - \frac{\eta}{\lambda^2 + \eta^2} + \frac{\kappa\eta}{(\lambda - R^2/t)^2 + \eta^2}\right\} \\
\tau_{\eta z}^{(1)} &= \frac{G_1 b}{2\pi}\left\{\frac{\lambda - t}{(\lambda - t)^2 + \eta^2} - \frac{\lambda}{\lambda^2 + \eta^2} + \frac{\kappa(\lambda - R^2/t)}{(\lambda - R^2/t)^2 + \eta^2}\right\}.
\end{aligned} \qquad \text{(A-8)}$$

These stresses are derivable from the displacement field

$$w^{(1)} = \frac{b}{2\pi}\left\{\theta_1 - \theta + \kappa\theta_2\right\}, \qquad \text{(A-9)}$$

where

$$\theta_2 = \tan^{-1}\frac{\eta}{\lambda - R^2/t}.$$

However, we note that the term $-b\theta/2\pi$ in $w^{(1)}$ corresponds to a screw dislocation inside the ζ-inclusion. This is not permissible since the ζ-inclusion contains only the real dislocation at $(t,0)$. Thus, we must add the term $+b\theta/2\pi$ to $w^{(1)}$ and $w^{(2)}$ and we find

$$\left.\begin{aligned} w^{(1)} &= \frac{b}{2\pi}\ \{\theta_1 + \kappa\theta_2\}\ ; \qquad \lambda^2 + \eta^2 \le R^2 \\ w^{(2)} &= \frac{b}{2\pi}\ \{(1-\kappa)\theta_1 + \kappa\theta + C_0\}\ ; \qquad \lambda^2 + \eta^2 \ge R^2 \end{aligned}\right\} \qquad \text{(A-10)}$$

[Note: The addition of the term $b\theta/2\pi$ to both $w^{(1)}$ and $w^{(2)}$ does not affect continuity in tangential shear stress across $\lambda^2 + \eta^2 = R^2$. A screw dislocation at the origin has no τ_{rz} stress associated with it.] Continuity in the displacement field across $\lambda^2 + \eta^2 = R^2$ requires that

$$C_0 = \kappa\pi \ . \qquad \text{(A-11)}$$

The stress fields derived from the displacement field given by (A-10) are then given by Eqs. (I.3-7) in the text. One should note that under the conformal transformation the inclusion in the interior screw problem is of shear modulus G_1 ; the matrix shear modulus is G_2.

APPENDIX B

INVERSION OF A SINGULAR INTEGRAL EQUATION WITH A SIMPLE CAUCHY KERNEL

Head[26] and Chou[33] have given the following lucid, concise summary of the techniques described by Muskhelishvili[25] and Mikhlin[46] for inverting the singular integral equation

$$\int_D \frac{f(t)\,dt}{t-x} = \sigma(x) \ . \qquad \text{(B-1)}$$

If $f(t)$ and $\sigma(x)$ are functions in the Holder classes H^* and H, respectively, in the interval D, and if D consists of p finite segments of which at q of the $2p$ ends $f(t)$ is bounded, then

$$f(x) = -\frac{1}{\pi^2}\left[\frac{R_1(x)}{R_2(x)}\right]^{1/2} \int_D \left[\frac{R_2(t)}{R_1(t)}\right]^{1/2} \frac{\sigma(t)\,dt}{t-x} + \left[\frac{R_1(x)}{R_2(x)}\right]^{1/2} P_{p-q-1}(x) \ , \qquad \text{(B-2)}$$

provided $p-q \geq 0$.

$$R_1(x) = \prod_{i=1}^{q} (x-e_i); \qquad R_2(x) = \prod_{i=q+1}^{2p} (x-e_i) \ . \qquad \text{(B-3)}$$

$P_{p-q-1}(x)$ is an arbitrary polynomial of degree $\leq p-q-1$ with $P_{-1} = 0$; the e_i's are end points. When $p-q < 0$ the same solution is valid with the necessary and sufficient condition

$$\int_D \left[\frac{R_2(x)}{R_1(x)}\right]^{1/2} x^m \sigma(x)\, dx = 0 \; ; \quad m = 0,1,\ldots,q-p-1 \; . \tag{B-4}$$

In the case of the pileup at the rigid cylindrical inclusion one must solve

$$\int_{1/\beta}^{\beta} \frac{f(t)\, dt}{\lambda - t} = \frac{N}{\lambda} + \left\{ \begin{array}{ll} \frac{2\pi R\tau}{G_1 b} \; ; & 1 < \lambda \leq \beta \\ -\frac{2\pi R\tau}{G_1 b\lambda^2} \; ; & \frac{1}{\beta} \leq \lambda < 1 \end{array} \right\} \tag{B-5}$$

The interval D is the single segment $[1/\beta, \beta]$ and since $f(\beta) = f(1/\beta) = 0$ (there are no dislocations at the tail ends of the real and image pileups), $p = 1$, $q = 2$, $q-p-1 = 0$, $p-q < 0$, $R_2(\lambda) = 1$, and $R_1(\lambda) = (\beta-\lambda)(\lambda - 1/\beta)$. (B-5) has a solution if (B-4) is satisfied or if

$$N \int_{1/\beta}^{\beta} \frac{dt}{t\sqrt{(\beta-t)(t-\frac{1}{\beta})}} = \frac{2\pi R\tau}{G_1 b} \int_1^{\beta} \frac{(t-1)\, dt}{\sqrt{(\beta-t)(t-\frac{1}{\beta})}} \; . \tag{B-6}$$

(B-6) yields Eq. (II.1-13) in the text, and $f(t)$ is given by (II.1-15).

APPENDIX C

EVALUATION OF THE STRESS FIELD ABOUT A PILEUP AT A RIGID CIRCULAR INCLUSION

The most difficult integral to evaluate in the superposition integral for the stress field involves

$$I = \int_1^\beta \left(1 + \frac{1}{\zeta^2}\right) \frac{\cosh^{-1}\left(\frac{\beta-1}{\beta+1}\,\frac{\zeta+1}{\zeta-1}\right) d\zeta}{(\lambda-\zeta)^2 + \eta^2} , \qquad \text{(C-1)}$$

where $\lambda = x/R$, $\eta = y/R$, and $\lambda^2 + \eta^2 \leq 1$. Making the transformation

$$u = \cosh^{-1}\left(\frac{\beta-1}{\beta+1} \cdot \frac{\zeta+1}{\zeta-1}\right) ,$$

one finds

$$I = 2\left(\frac{\beta-1}{\beta+1}\right) \frac{1}{\rho^2}(I_1 - 2I_2 + 2I_3) \qquad \text{(C-2)}$$

where

$$\rho^2 = (1-\lambda)^2 + \eta^2 .$$

$$I_1 = \int_{-\infty}^{\infty} \frac{u \sinh u \, du}{B(u)} \qquad \text{(C-3)}$$

$$I_2 = \int_{-\infty}^{\infty} \frac{u \sinh u \, du}{B(u)\, C(u)}$$

$$I_3 = \int_{-\infty}^{\infty} \frac{u \sinh u \, du}{B(u)\, [C(u)]^2}$$

$$B(u) = \left\langle \cosh u + \frac{\beta-1}{\beta+1}\ \frac{1-r^2}{\rho^2} + 2i\ \frac{\beta-1}{\beta+1}\ \frac{\eta}{\rho^2} \right\rangle$$

$$\times \left\langle \cosh u + \frac{\beta-1}{\beta+1}\ \frac{1-r^2}{\rho^2} - 2i\ \frac{\beta-1}{\beta+1}\ \frac{\eta}{\rho^2} \right\rangle$$

$$C(u) = \frac{\beta-1}{\beta+1} \cosh u + 1$$

$$r^2 = \lambda^2 + \eta^2 \ .$$

The integrals are most simply evaluated along the interface $(r = 1)$ or along the slip plane $(\eta = 0)$. Consider $r = 1$ and

$$V = \oint_C \frac{u^2 \sinh u\ du}{\left\{ \cosh^2 u + 4\left(\frac{\beta-1}{\beta+1}\right)^2 \frac{\eta^2}{\rho^4} \right\} \left\{ \frac{\beta+1}{\beta-1} \cosh u + 1 \right\}} \ , \qquad \text{(C-4)}$$

where C is the rectangle in the complex $u = \omega + i\Omega$ plane (Figure C-1). Taking the limit as $u_0 \to \infty$ and applying the Cauchy residue theorem, one finds

$$I_2 = -\frac{1}{2} \sum \text{residues of } \frac{u^2 \sinh u}{\left\{ \cosh^2 u + 4\left(\frac{\beta-1}{\beta+1}\right)^2 \frac{\eta^2}{\rho^4} \right\} \left\{ \frac{\beta+1}{\beta-1} \cosh u + 1 \right\}} \ . \qquad \text{(C-5)}$$

The poles inside the contour C are shown in Figure C-1.

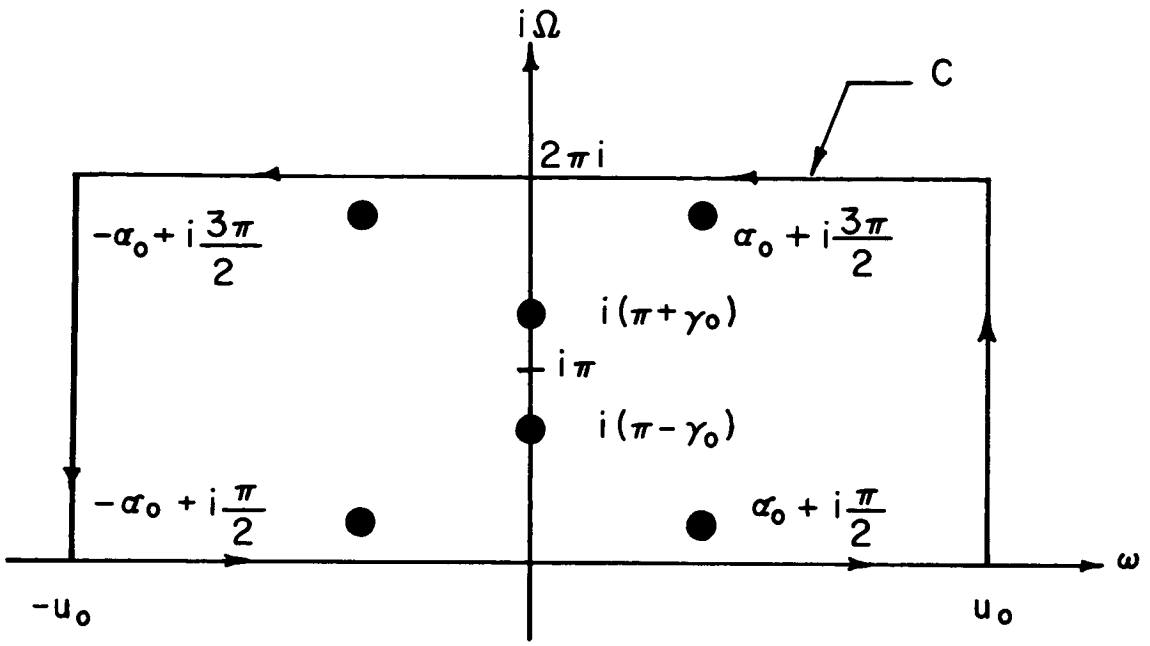

Figure C-1: The contour C in the complex $u = \omega + i\Omega$ plane used to evaluate the stress field generated by a screw pileup at a rigid circular inclusion.

$$\gamma_0 = \cos^{-1}\frac{\beta-1}{\beta+1} \quad , \quad 0 \leq \gamma_0 \leq \frac{\pi}{2}$$

$$\alpha_0 = \sinh^{-1}\left(\frac{\beta-1}{\beta+1}\frac{2|\eta|}{\rho^2}\right) . \tag{C-6}$$

The result is

$$I_2 = \frac{\beta+1}{\beta-1}\frac{1}{1+\frac{4\eta^2}{\rho^4}}\left\{\alpha_0^2 + \frac{\pi\rho^2}{2|\eta|} + \gamma_0^2 - \frac{\pi^2}{4}\right\} .$$

A similar procedure holds for I_1 and I_3, although the integrand in I_3 has poles of order 2 at $i(\pi \pm \gamma_0)$. The residues at the poles of order 2 may be computed according to the method outlined by Churchill.[47] The remaining integrals involving the non-singular portion of the distribution function are evaluated by either the method of partial fractions or by a contour integration following the substitution

$$u = \cosh^{-1}\left(\frac{\beta-1}{\beta+1}\frac{\zeta+1}{\zeta-1}\right) .$$

The above method can be used to calculate the complete stress field in closed form.

APPENDIX D

INVERSION OF THE INTEGRAL EQUATION ASSOCIATED WITH THE SCREW PILEUP AT A HALF-PLANE OF FINITE RIGIDITY

The dislocation distribution function, $f(t)$, must be determined from the integral equation

$$\int_0^L \frac{f(t)\,dt}{x-t} + \kappa \int_0^L \frac{f(t)\,dt}{x+t} = \frac{2\pi\tau}{G_1 b}, \qquad 0 < x \leq L, \tag{D-1}$$

subject to the end conditions

$$\begin{aligned} &f(L) = 0 \\ &f(0) \text{ unbounded with a weak singularity.} \end{aligned} \tag{D-2}$$

Making the substitutions $\lambda = x/L$, $\zeta = t/L$, $\alpha = 1-\kappa$, Eq. (D-1) may be rewritten as

$$\int_0^1 \frac{f(\zeta)\,d\zeta}{\lambda-\zeta} + (1-\alpha) \int_0^1 \frac{f(\zeta)\,d\zeta}{\lambda+\zeta} = \frac{2\pi\tau}{G_1 b}, \qquad 0 < \lambda \leq 1. \tag{D-3}$$

Since $-1 \leq \kappa < 1$, $0 < \alpha < 2$. Developing $f(\zeta)$ in a Neumann series expansion

$$f(\zeta) = \frac{2\pi\tau}{G_1 b} \sum_{n=0}^{\infty} \alpha^n g_n(\zeta), \tag{D-4}$$

substituting into (D-3), and comparing coefficients of α^n requires that

$$\int_0^1 \frac{g_0(\zeta)\, d\zeta}{\lambda-\zeta} + \int_0^1 \frac{g_0(\zeta)\, d\zeta}{\lambda+\zeta} = 1 \qquad \text{(D-5)}$$

$$\int_0^1 \frac{g_n(\zeta)\, d\zeta}{\lambda-\zeta} + \int_0^1 \frac{g_n(\zeta)\, d\zeta}{\lambda+\zeta} = \int_0^1 \frac{g_{n-1}(\zeta)\, d\zeta}{\lambda+\zeta}, \quad n \geq 1 . \qquad \text{(D-6)}$$

Equation (D-5) is essentially the equation Chou[33] solved for the rigid half-plane problem, and its solution is

$$g_0(\zeta) = \frac{2}{\pi^2} \cosh^{-1}\left(\frac{1}{\zeta}\right) . \qquad \text{(D-7)}$$

Combining terms on the left side of (D-6) and making the substitution $\zeta = \sqrt{\omega}$ leads to

$$\lambda \int_0^1 \frac{g_n(\sqrt{\omega})\, d\omega}{\sqrt{\omega}\,(\lambda^2-\omega)} = \int_0^1 \frac{g_{n-1}(\zeta)\, d\zeta}{\lambda+\zeta}, \quad n \geq 1 . \qquad \text{(D-8)}$$

(D-8) may be inverted according to techniques outlined by Muskhelishvili[25] and Mikhlin[46] (Appendix B) to yield the recursion relation

$$g_n(\zeta) = \frac{1}{\pi^2} \sqrt{1-\zeta^2} \int_0^1 \frac{2\beta}{\sqrt{1-\beta^2}} \frac{d\beta}{\beta^2-\zeta^2} \int_0^1 \frac{g_{n-1}(s)\, ds}{\beta+s}, \quad n \geq 1 . \qquad \text{(D-9)}$$

In inverting (D-5) and (D-6) we have assumed that $g_0(\zeta)$ and $g_n(\zeta)$ satisfy the same end conditions as $f(\zeta)$ (Eq. (D-2)).

Taking $n = 1$ and letting $\eta_0 = \cosh^{-1}(1/\zeta)$, one finds

$$g_1(\zeta) = \frac{g_0(\zeta)}{3}\left\{\frac{\eta_0^2}{\pi^2} + \frac{1}{4}\right\} . \qquad \text{(D-10)}$$

Further use of the recursion formula (D-9) yields

$$g_2(\zeta) = \frac{2^2}{5!}\, g_0(\zeta) \left\{ \frac{\eta_0^2}{\pi^2} + \frac{1}{4} \right\} \left\{ \frac{\eta_0^2}{\pi^2} + \frac{9}{4} \right\}$$

$$g_3(\zeta) = \frac{2^3}{7!}\, g_0(\zeta) \left\{ \frac{\eta_0^2}{\pi^2} + \frac{1}{4} \right\} \left\{ \frac{\eta_0^2}{\pi^2} + \frac{9}{4} \right\} \left\{ \frac{\eta_0^2}{\pi^2} + \frac{25}{4} \right\} . \qquad \text{(D-11)}$$

The calculations leading to Eqs. (D-10) and (D-11) are extremely lengthy and, therefore, are not reproduced here.

Thus, it appears that the general term in the Neumann expansion is

$$g_n(\zeta) = \frac{2^n}{(2n+1)!}\, g_0(\zeta) \prod_{j=1}^{n} \left\{ \frac{\eta_0^2}{\pi^2} + \frac{(2j-1)^2}{4} \right\} , \quad n \geq 1 . \qquad \text{(D-12)}$$

Assuming (D-12) is true (the solution will be verified later),

$$\frac{G_1 b}{2\pi\tau}\, f(\zeta) = \frac{2\eta_0}{\pi^2} \left\{ 1 + \sum_{n=1}^{\infty} \frac{1}{(2n+1)!} \left(\frac{\alpha}{2}\right)^n \prod_{j=0}^{n-1} \left[\left(\frac{2\eta_0}{\pi} \right)^2 + (2j+1)^2 \right] \right\} . \qquad \text{(D-13)}$$

Using No. 839 in Jolley,[37] one may deduce that

$$1 + \sum_{n=1}^{\infty} \frac{\theta^{2n}}{(2n+1)!} \prod_{j=0}^{n-1} \left\{ \sigma^2 + (2j+1)^2 \right\} = \frac{\sinh(\sigma \sin^{-1}\theta)}{\sigma\theta} , \qquad \text{(D-14)}$$

so that when $0 \leq \sqrt{\alpha/2} < 1$,

$$f(\zeta) = \frac{2\tau}{G_1 b} \sqrt{\frac{2}{\alpha}} \sinh \left\{ \left(\frac{2}{\pi} \sin^{-1} \sqrt{\frac{\alpha}{2}} \right) \cosh^{-1}\left(\frac{1}{\zeta}\right) \right\} . \qquad \text{(D-15)}$$

In order to verify that (D-15) is indeed a solution to (D-3), one notes that under the transformation $v = \cosh^{-1}(1/\zeta)$

$$\int_0^1 \frac{f(\zeta)\, d\zeta}{\lambda-\zeta} = \frac{\tau}{G_1 b}\sqrt{\frac{2}{\alpha}} \int_{-\infty}^{\infty} \frac{\sinh gv \sinh v\, dv}{\cosh v(\lambda \cosh v-1)} \tag{D-16a}$$

$$\int_0^1 \frac{f(\zeta)\, d\zeta}{\lambda+\zeta} = \frac{\tau}{G_1 b}\sqrt{\frac{2}{\alpha}} \int_{-\infty}^{\infty} \frac{\sinh gv \sinh v\, dv}{\cosh v(\lambda \cosh v+1)} \tag{D-16b}$$

where

$$g = \frac{2}{\pi} \sin^{-1} \sqrt{\frac{\alpha}{2}} \quad . \tag{D-17}$$

Considering

$$w = \oint_C \frac{\sinh gv \sinh v\, dv}{\cosh v(\lambda \cosh v-1)} \quad , \tag{D-18}$$

where C is the indented rectangle in the complex $v = \omega + i\Omega$ plane (Figure D-1), letting $v_0 \to \infty$, $\epsilon \to 0$, and applying the Cauchy residue theorem,

$$\frac{\tau}{G_1 b}\sqrt{\frac{2}{\alpha}}\left\{\int_{-\infty}^{\infty} \frac{\sinh gv \sinh v\, dv}{\cosh v(\lambda \cosh v-1)} + \cos g\pi \int_{-\infty}^{\infty} \frac{\sinh gv \sinh v\, dv}{\cosh v(\lambda \cosh v+1)}\right\}$$

$$= -\frac{\tau}{G_1 b}\sqrt{\frac{2}{\alpha}}\; 2\pi i \sinh \frac{i\pi g}{2} \quad . \tag{D-19}$$

(Note: Inside C the only pole of the integrand in (D-18) is at $v = i(\pi/2)$.) Since

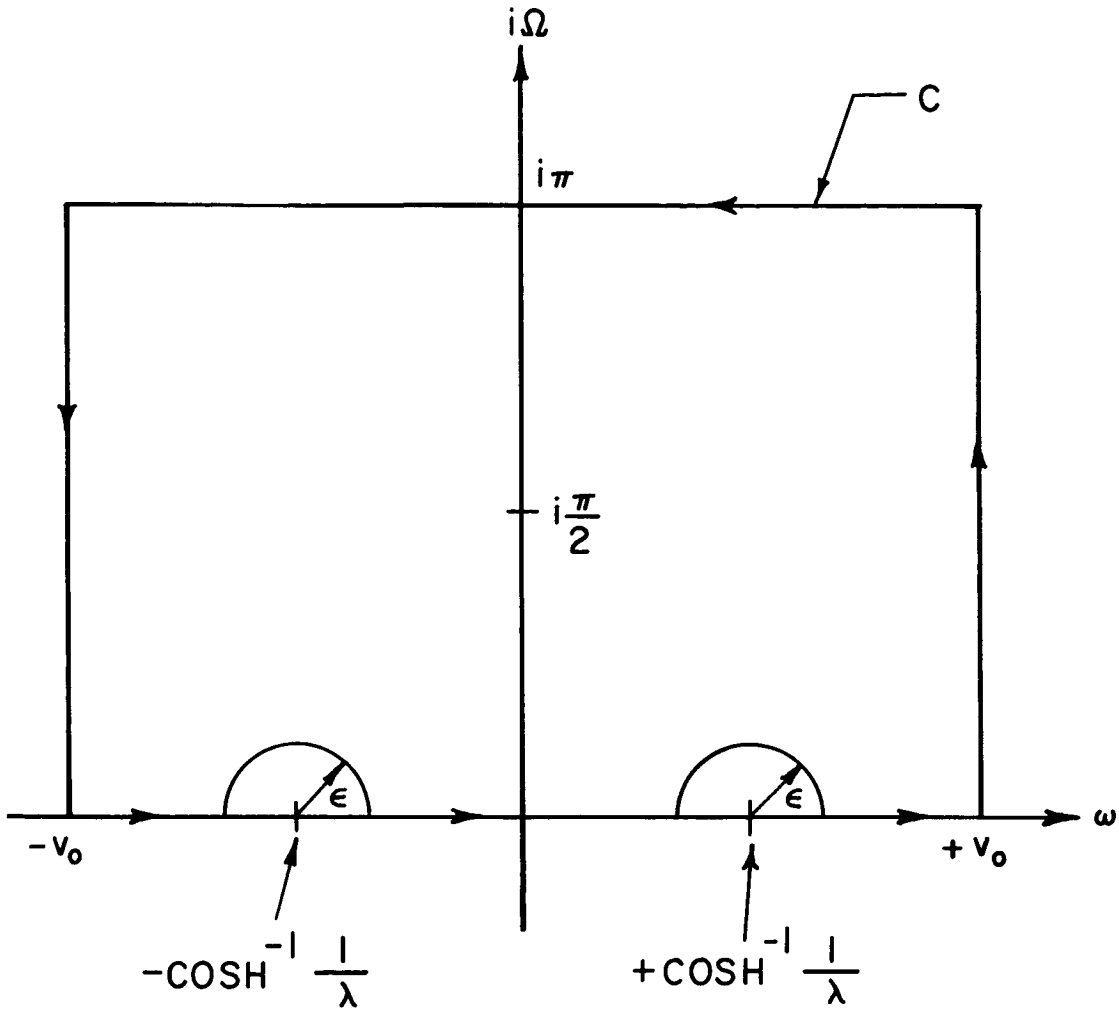

Figure D-1: The indented rectangle C in the complex $v = \omega + i\Omega$ plane used to verify the solution for the dislocation distribution function for a screw pileup against a half-plane of finite rigidity.

$$i \sinh \frac{i\pi g}{2} = - \sin \frac{\pi g}{2} = - \sqrt{\frac{\alpha}{2}}$$

$$\cos g\pi = 1 - \alpha = K \quad , \tag{D-20}$$

eq. (D-19) combined with (D-16a) and (D-16b) yields the original integral equation (D-3) identically.

APPENDIX E

THE STRESSES ABOUT A SCREW PILEUP AT A HALF-PLANE OF FINITE RIGIDITY

The superposition integral for the shear stress τ_{xz} in $x < 0$ is

$$\tau_{xz} = -\frac{\tau}{\pi}\sqrt{\frac{2}{1-\kappa}}\,(1+\kappa)\,y\int_0^L \frac{\sinh(g\,\cosh^{-1}\langle L/t\rangle)\,dt}{(x-t)^2+y^2}\,. \qquad \text{(E-1)}$$

Making the substitutions $v = \cosh^{-1}(L/t)$, $\eta = y/L$, $\lambda = -x/L = |x|/L$, $\rho_0^2 = \lambda^2 + \eta^2 = \rho^2/L^2$, $\rho^2 = x^2 + y^2$, then

$$\tau_{xz}(x,y) = -\frac{\tau}{2\pi}\sqrt{\frac{2}{1-\kappa}}\,(1+\kappa)\,\frac{\eta}{\rho_0^2}\,I_0\,, \qquad \text{(E-2)}$$

where

$$I_0 = \int_{-\infty}^{\infty} \frac{\sinh gv \sinh v\,dv}{\langle\cosh v + (\lambda/\rho_0^2)+i(|\eta|/\rho_0^2)\rangle\langle\cosh v + (\lambda/\rho_0^2)-i(|\eta|/\rho_0^2)\rangle}\,. \qquad \text{(E-3)}$$

Now consider

$$V = \oint_C \frac{\sinh gv \sinh v\,dv}{\langle\cosh v + (\lambda/\rho_0^2)+i(|\eta|/\rho_0^2)\rangle\langle\cosh v + (\lambda/\rho_0^2)-i(|\eta|/\rho_0^2)\rangle}\,, \qquad \text{(E-4)}$$

where C is the rectangle in the complex $v = \omega + i\Omega$ plane (Figure E-1).

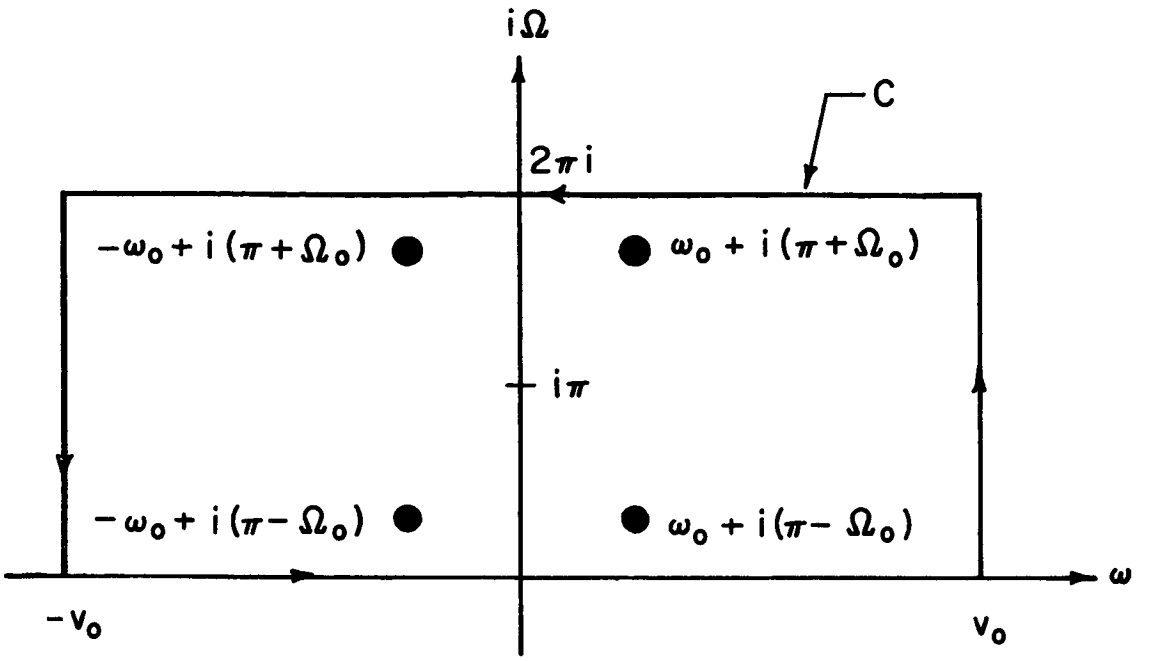

Figure E-1: The contour C in the complex $v = \omega + i\Omega$ plane used to evaluate the stresses in the second phase ahead of a screw pileup at a half-plane of finite rigidity.

Letting $v_0 \to \infty$ and applying the Cauchy residue theorem,

$$I_0 = \frac{\pi i}{\sin^2 \pi g} \sum \text{ residues of}$$

$$\frac{\sinh gv \sinh v \, dv}{\langle \cosh v + (\lambda/\rho_0^2) + i(|\eta|/\rho_0^2)\rangle \langle \cosh v + (\lambda/\rho_0^2) - i(|\eta|/\rho_0^2)\rangle} \, . \tag{E-5}$$

Inside C the poles of the integrand in (E-4) are at

$$\begin{aligned} &v = \omega_0 + i(\pi - \Omega_0), \qquad -\omega_0 + i(\pi - \Omega_0) \\ &-\omega_0 + i(\pi + \Omega_0), \qquad \omega_0 + i(\pi + \Omega_0) \end{aligned} \tag{E-6}$$

where

$$\begin{aligned} \cosh \omega_0 \cos \Omega_0 &= \frac{\lambda}{\rho_0^2} = \frac{L}{\rho} \cos \varphi \\ \sinh \omega_0 \sin \Omega_0 &= \frac{|\eta|}{\rho_0^2} = \frac{L}{\rho} |\sin \varphi| \, . \end{aligned} \tag{E-7}$$

The solution to Eqs. (E-7) is given by Eqs. (III.2-3) in the text. Evaluating the residues in (E-5) yields the first of Eqs. (III.2-2) in the text; the stress τ_{yz} in $x < 0$ is found by a similar technique.

In the matrix $(x > 0)$, the stress τ_{xz} may be expressed as

$$\tau_{xz} = \frac{\tau}{2\pi} \sqrt{\frac{2}{1-\kappa}} \, \frac{\eta}{\rho_0^2} \, \langle I_1 + \kappa I_2 \rangle \, , \tag{E-8}$$

where

$$I_1 = \int_{-\infty}^{\infty} \frac{\sinh gv \sinh v \, dv}{\langle \cosh v - (\lambda/\rho_0^2) + i(|\eta|/\rho_0^2)\rangle\langle \cosh v - (\lambda/\rho_0^2) - i(|\eta|/\rho_0^2)\rangle} \tag{E-9}$$

$$I_2 = \int_{-\infty}^{\infty} \frac{\sinh gv \sinh v \, dv}{\langle \cosh v + (\lambda/\rho_0^2) + i(|\eta|/\rho_0^2)\rangle\langle \cosh v + (\lambda/\rho_0^2) - i(|\eta|/\rho_0^2)\rangle}, \tag{E-10}$$

and $\lambda = |x|/L$.

Considering

$$W = \oint_{C'} \frac{\sinh gv \sinh v \, dv}{\langle \cosh v - (\lambda/\rho_0^2) + i(|\eta|/\rho_0^2)\rangle\langle \cosh v - (\lambda/\rho_0^2) - i(|\eta|/\rho_0^2)\rangle} \tag{E-11}$$

where C' is the rectangle in the complex $v = \omega + i\Omega$ plane in Figure (E-2), letting $v_0 \to \infty$, and applying the Cauchy residue theorem, one finds

$$I_1 + \kappa I_2 = 2\pi i \sum \text{residues of } \frac{\sinh gv \sinh v \, dv}{\langle \cosh v - (\lambda/\rho_0^2) + i(|\eta|/\rho_0^2)\rangle\langle \cosh v - (\lambda/\rho_0^2) - i(|\eta|/\rho_0^2)\rangle}. \tag{E-12}$$

Inside C' the poles of the integrand in (E-11) are at

$$v = \pm \omega_0 + i\Omega_0$$

where

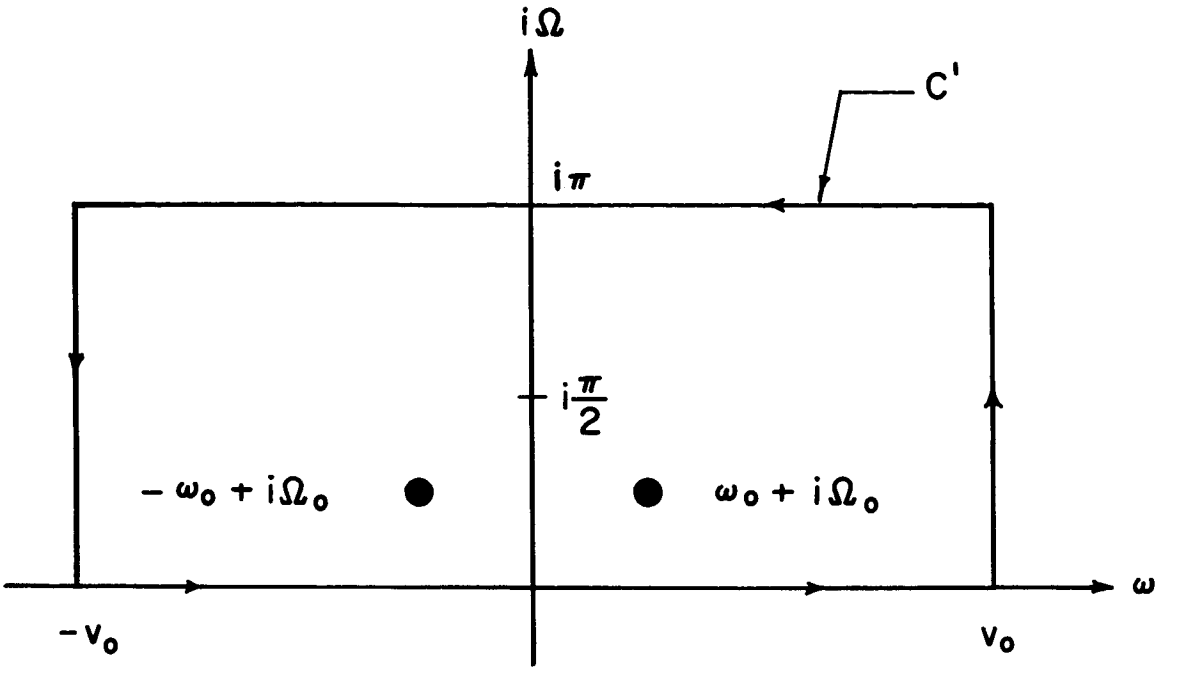

Figure E-2: The contour C' in the complex $v = \omega + i\Omega$ plane used to evaluate the matrix stress field of a screw pileup at a half-plane of finite rigidity.

$$\cosh \omega_0 \cos \Omega_0 = \frac{L}{\rho} \cos \psi = - \frac{L}{\rho} \cos \varphi = \frac{1}{\rho} \cos(\pi-\varphi)$$

$$\sinh \omega_0 \sin \Omega_0 = \frac{L}{\rho} |\sin \psi| = \frac{L}{\rho} |\sin \varphi| = \frac{L}{\rho} |\sin(\pi-\varphi)| \ . \qquad \text{(E-13)}$$

Evaluating (E-12), τ_{xz} is given by (III.2-4) in the text; τ_{yz} $(x > 0)$ is found by a similar procedure.

APPENDIX F

THE DISTRIBUTION FUNCTION FOR THE CIRCULAR INCLUSION OF FINITE RIGIDITY

Consider $\oint_C I_1(u,\lambda)\, du$, where $I_1(u,\lambda)$ is defined by Eq. (IV.2-4) in the text, and C is the indented rectangle in the complex $u = v + i\Omega$ plane (Figure IV-2). If we let $v_0 \to \infty$, $\epsilon \to 0$, apply the Cauchy residue theorem, and choose

$$\kappa = \cos g\pi = - \cos w\pi \tag{F-1}$$

then

$$\oint_C I_1(u,\lambda)\, du = \int_{-\infty}^{\infty} I_1(u,\lambda) + \kappa \int_{-\infty}^{\infty} I_2(u,\lambda)\, du \tag{F-2}$$

$$= 2\pi i \sum (\text{residues of } I_1(u,\lambda) \text{ at the poles contained inside } C), \tag{F-3}$$

where $I_2(u,\lambda)$ is defined by Eq. (IV.2-4) in the text. Evaluating the residues of the integrand, Eqs. (F-2) and (F-3) are equivalent to

$$\int_1^{\beta} \frac{f_0(\zeta)\, d\zeta}{\lambda-\zeta} + \kappa \int_1^{\beta} \frac{f_0(\zeta)\, d\zeta}{\lambda - \frac{1}{\zeta}}$$

$$= \left\{ \pi[A \sin g\gamma_0 + B \sin w\gamma_0] + \pi \left[\frac{A \sin g(\pi-\gamma_0) - B \sin w(\pi-\gamma_0)}{\lambda^2} \right] \right.$$

$$\left. + \frac{2\pi \cot \gamma_0}{\lambda} [gA \cos g(\pi-\gamma_0) - wB \cos w(\pi-\gamma_0)] \right\} \tag{F-4}$$

where

$$0 \leq \gamma_0 = \cos^{-1} \frac{\beta-1}{\beta+1} \leq \frac{\pi}{2} , \qquad \text{(F-5)}$$

and $f_0(\zeta)$ is defined by (IV.2-1).

By comparing Eq. (F-4) with Eq. (IV.1-4) in the text, we then require

$$A \sin g\gamma_0 + B \sin w\gamma_0 = \frac{2R\tau}{G_1 b} , \qquad \text{(F-6)}$$

$$A \sin g(\pi-\gamma_0) - B \sin w(\pi-\gamma_0) = 0 \qquad (\tau(\lambda) = \tau) \qquad \text{(F-7a)}$$

$$= - \frac{2R\tau K}{G_1 b} \qquad (\tau(\lambda)=\tau[1 - \frac{K}{\lambda^2}]) , \qquad \text{(F-7b)}$$

so that A and B are given by

$$\left.\begin{aligned} A &= \frac{2R\tau}{G_1 b} \frac{\sin w(\pi-\gamma_0)}{\sqrt{1-K^2} \sin \gamma_0} \\ B &= \frac{2R\tau}{G_1 b} \frac{\sin g(\pi-\gamma_0)}{\sqrt{1-K^2} \sin \gamma_0} \end{aligned}\right\} \quad \tau(\lambda) = \tau \qquad \text{(F-8a)}$$

or

$$\left.\begin{aligned} A &= \frac{2R\tau}{G_1 b} \frac{\cos w\gamma_0}{\sin \gamma_0} \\ B &= \frac{2R\tau}{G_1 b} \frac{\cos g\gamma_0}{\sin \gamma_0} \end{aligned}\right\} \quad \tau(\lambda) = \tau(1 - \frac{K}{\lambda^2}) \qquad \text{(F-8b)}$$

.

Thus, $f_0(\zeta)$ is a solution to

$$\int_1^\beta \frac{f_0(\zeta)\, d\zeta}{\lambda-\zeta} + \kappa \int_1^\beta \frac{f_0(\zeta)\, d\zeta}{\lambda-\frac{1}{\zeta}} = \frac{\kappa N_0}{\lambda} + \frac{2\pi R}{G_1 b}\, \tau(\lambda) - \frac{\alpha_0}{\lambda} \quad , \qquad \text{(F-9)}$$

where

$$N_0 = \int_1^\beta f_0(\zeta)\, d\zeta$$

$$= \frac{2\pi \cot \gamma_0}{1+\kappa} \{gA[\cos g(\pi-\gamma_0) + \cos g\gamma_0] + wB[\cos w\gamma_0 - \cos w(\pi-\gamma_0)]\} \qquad \text{(F-10)}$$

and

$$\alpha_0 = \kappa N_0 - 2\pi \cot \gamma_0 [gA \cos g(\pi-\gamma_0) - wB \cos w(\pi-\gamma_0)]. \qquad \text{(F-11)}$$

Since $\alpha_0 \neq 0$, the total distribution function must be given by $f_0(\zeta) + f_1(\zeta)$, where $f_1(\zeta)$ is a solution to

$$\int_1^\beta \frac{f_1(\zeta)\, d\zeta}{\lambda-\zeta} + \kappa \int_1^\beta \frac{f_1(\zeta)\, d\zeta}{\lambda-\frac{1}{\zeta}} = \frac{\kappa N_1}{\lambda} + \frac{\alpha_0}{\lambda} \quad , \qquad \text{(F-12)}$$

where

$$N_1 = \int_1^\beta f_1(\zeta)\, d\zeta \quad .$$

Choosing $f_1(\zeta)$ to be given by Eq. (IV.2-12), and using the technique described above, the exact distribution function $f_0(\zeta) + f_1(\zeta)$ is obtained.

APPENDIX G

INVERSION OF THE INTEGRAL EQUATION FOR THE INFINITE SEQUENCE OF PARALLEL SCREW ARRAYS PILED UP AGAINST A HALF-PLANE OF FINITE RIGIDITY

The dislocation distribution function must satisfy

$$\int_0^1 f(\zeta)\, d\zeta \, \frac{1 - \tanh \frac{\pi\lambda}{H} \tanh \frac{\pi\zeta}{H}}{\tanh \frac{\pi\lambda}{H} - \tanh \frac{\pi\zeta}{H}}$$

$$+ \kappa \int_0^1 f(\zeta)\, d\zeta \, \frac{1 + \tanh \frac{\pi\lambda}{H} \tanh \frac{\pi\zeta}{H}}{\tanh \frac{\pi\lambda}{H} + \tanh \frac{\pi\zeta}{H}} = \frac{2H\tau}{G_1 b} \, . \qquad \text{(G-1)}$$

When $\kappa = 1$, one may combine terms on the left side of (G-1), make the substitutions

$$\sqrt{\omega} = \tanh \frac{\pi\zeta}{H} \, , \qquad \sqrt{\alpha} = \tanh \frac{\pi\lambda}{H} \, , \qquad \text{(G-2)}$$

and convert (G-1) into

$$\int_0^{\tanh^2(\pi/h)} \frac{f(\omega)\, d\omega}{\sqrt{\omega}\,(\alpha-\omega)} = \frac{2\pi\tau}{G_1 b \sqrt{\alpha}} \, . \qquad \text{(G-3)}$$

This is a simple equation with only a Cauchy kernel and has as a solution

$$f(\zeta, \kappa=1) = \frac{4\tau}{\pi G_1 b} \cosh^{-1} \left\langle \frac{\tanh(\pi/H)}{\tanh(\pi\zeta/H)} \right\rangle . \qquad \text{(G-4)}$$

Using the results of Chapters III and IV, in order to generate the general solution from the solution for $K = 1$, we assume a distribution function

$$f(\zeta) = A \sinh \left\{ g \cosh^{-1} \left\langle \frac{\tanh(\pi/H)}{\tanh(\pi\zeta/H)} \right\rangle \right\} \quad . \tag{G-5}$$

Under the substitution

$$u = \cosh^{-1} \left\langle \frac{\tanh(\pi/H)}{\tanh(\pi\zeta/H)} \right\rangle \tag{G-6}$$

$$\left\{ \int_0^1 f(\zeta)\, d\zeta \, \frac{1 \mp \tanh(\pi\lambda/H)\, \tanh(\pi\zeta/H)}{\tanh(\pi\lambda/H) \mp \tanh(\pi\zeta/H)} \right\} = \left\{ \begin{array}{c} \int_{-\infty}^{\infty} I_1(u,\lambda)\, du \\ \int_{-\infty}^{\infty} I_2(u,\lambda)\, du \end{array} \right\} \tag{G-7}$$

where

$$\left\{ \begin{array}{c} I_1(u,\lambda) \\ I_2(u,\lambda) \end{array} \right\}$$

$$= \frac{AH}{2\pi} \tanh \frac{\pi}{H} \left\{ \frac{\sinh gu \sinh u}{\tanh(\pi\lambda/H) \mp \tanh(\pi/H)} \; \frac{\cosh v \mp \tanh(\pi/H)\, \tanh(\pi\lambda/H)}{\cosh^2 v - \tanh^2(\pi/H)} \right\} . \tag{G-8}$$

Consider $\oint_C I_1(u,\lambda)\, du$ where C is the indented rectangle in the complex $u = v + i\Omega$ plane (Figure G-1); letting $v_0 \to \infty$, $\epsilon \to 0$ and applying the Cauchy residue theorem,

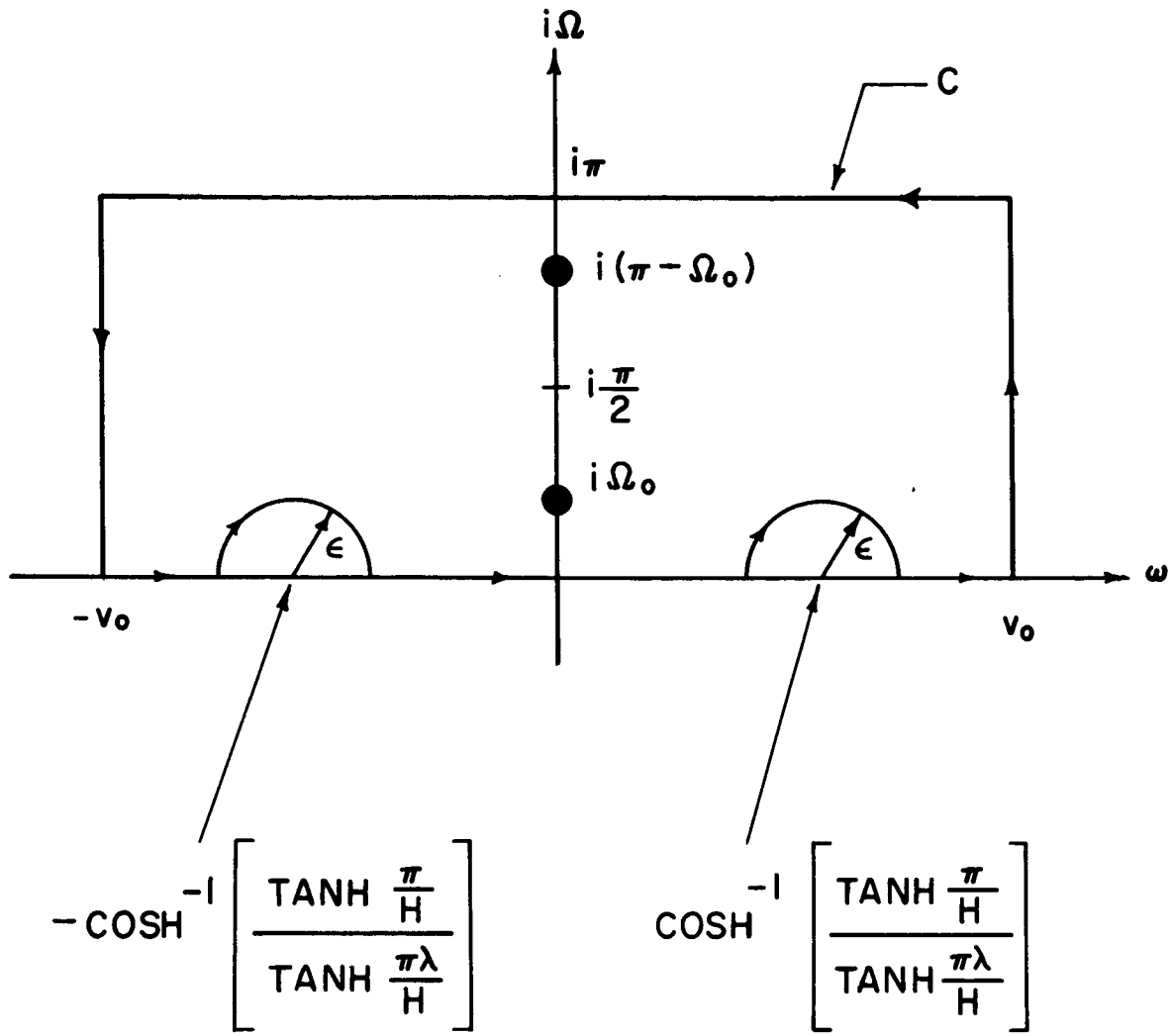

Figure G-1: The indented rectangle C in the complex $v = \omega + i\Omega$ plane used to obtain the dislocation distribution function for an infinite sequence of parallel screw slip bands piled up against a half-plane of finite rigidity.

$$\int_{-\infty}^{\infty} I_1(u,\lambda)\,du + \cos g\pi \int_{-\infty}^{\infty} I_2(u,\lambda)\,du$$

$$= AHi \tanh \frac{\pi}{H} \sum \{\text{residues of } I_1(u,\lambda) \text{ at its poles inside C}\}. \quad (G\text{-}9)$$

Inside C I_1 has only simple poles at

$$v = i\Omega_0, \qquad i(\pi - \Omega_0) \quad (G\text{-}10)$$

where

$$0 \leq \Omega_0 = \cos^{-1}\langle \tanh \frac{\pi}{H} \rangle \leq \frac{\pi}{2} . \quad (G\text{-}11)$$

Choosing

$$\cos g\pi = K \quad (G\text{-}12)$$

and evaluating the residues, (G-5) is a solution to (G-1) if

$$A = \frac{2\tau}{G_1 b} \sqrt{\frac{2}{1-K}} \sec\{g \sin^{-1}\langle \tanh \frac{\pi}{H} \rangle\} . \quad (G\text{-}13)$$